



THE HONG KONG
POLYTECHNIC UNIVERSITY

香港理工大學

Pao Yue-kong Library

包玉剛圖書館

Copyright Undertaking

This thesis is protected by copyright, with all rights reserved.

By reading and using the thesis, the reader understands and agrees to the following terms:

1. The reader will abide by the rules and legal ordinances governing copyright regarding the use of the thesis.
2. The reader will use the thesis for the purpose of research or private study only and not for distribution or further reproduction or any other purpose.
3. The reader agrees to indemnify and hold the University harmless from and against any loss, damage, cost, liability or expenses arising from copyright infringement or unauthorized usage.

IMPORTANT

If you have reasons to believe that any materials in this thesis are deemed not suitable to be distributed in this form, or a copyright owner having difficulty with the material being included in our database, please contact lbsys@polyu.edu.hk providing details. The Library will look into your claim and consider taking remedial action upon receipt of the written requests.

THE HONG KONG POLYTECHNIC UNIVERSITY

INSTITUTE OF TEXTILES AND CLOTHING

**Studies of the Structure and Shape Memory
Effect of Segmented Polyurethane Ionomer**

By ZHU Yong

May 2007

Certificate of Originality

I hereby declare that this thesis is my own work and that, to the best of my knowledge and belief, it reproduces no material previously published or written, nor material that has been accepted for the award of any other degree or diploma, except where due acknowledgement has been made in the text.

_____ (Signed)

ZHU Yong (Name of student)

Abstract

Shape memory polyurethane (SMPU) is composed of the reversible phase and the fixed phase. Thereof, the reversible phase having a melting or glass transition temperature of the soft segments as the transition temperature is used to hold the temporary deformation, whereas the fixed phase is referred to the hard segments covalently coupled to the soft segments and responsible for memorizing the permanent shape. Usually, the hard segment content, the soft segment length and the molecular structure are paramount on controlling the shape memory property in general. However, in some cases, increasing the hard segment content provides an option to alter their inter-connectivity at the expense of the crystallizable soft segment content, and thus lowering the shape fixity ratio. The chemical cross-linking hard segment structure was ever systematically incorporated into SMPU so as to improve its shape memory function. Nevertheless, the advantage of processing ability of this originally thermal plastic SMPU is lost due to the formation of cross-linkage points. Therefore, in this study, the Coulombic force produced by ionic groups within hard segments was considered as an adjustable internal force of the fixed phase, with which the processing ability of thermal plastic segmented PU can be kept. In addition, the introduction of novel functional groups can impart new functions to this kind of smart materials, while the shape memory function can be retained simultaneously. In this way, the application scope of shape memory polymer can be broadened immensely and more practical requirements for

the novel SMP could be satisfied. Therefore, in this research programme, not only the effects of ionic groups within hard segments on shape memory function, but also the novel functions such as antibacterial activity with the choice of suitable ionic groups were studied. Moreover, ionic groups were introduced into shape memory polyurethane fibres to adjust the shape memory properties.

For the above purposes, several series of SMPU anionomers and cationomers with various ionic group contents were synthesized with pre-polymerization. In each series of samples, the soft segment length and hard segment content were fixed so as to solely study the effect of ionic group contents on the morphology and shape memory effect. Considering the huge influence of soft segment crystallization on shape memory effect, the isothermal crystallization kinetic method was conducted with DSC to investigate the crystallization mechanism and process in SMPU ionomers. Microstructure and properties of SMPU ionomers were investigated by using DSC, DMA, FTIR, POM, Instron universal tensile tester. The molecular weight of SMPU ionomers was detected by GPC with DMF or THF as mobile phase.

Result shows that ionic group contents have significant effect on the morphology of SMPU ionomers, accordingly affect the shape memory properties. The ionic groups within hard segments play the two-fold effect: (i) the disruption of the order of hard domain, and (ii) the enhancement of

cohesion among hard segments. The former effect can be detected from the decrease of elastic modulus plateau in temperature higher than transition temperature, subsequently, the recovery ratio presents decreasing trend. The latter effect can be observed from the comparison of DMA results between SMPU ionomers and non-ionomers. Besides, although the ionic groups were located in hard segments, the morphology of the two-phase system in SMPU ionomers was affected significantly. Subsequently, the changes of morphology possibly can give rise to the increasing crystallinity of soft segments in PCL based SMPU ionomers, which was observed to facilitate the fixity of temporary deformation under the specific cyclic SME testing condition. In application of SMPU ionomers, the substrate bonding antibacterial activity was introduced into shape memory materials. At the same time, the rapid fixity ability to the temporary deformation can be achieved. In addition, the tiny ionic groups were introduced into the molecular backbone of SMPU fibres, which behave shape memory function with glass transition point as the switch temperature. The obvious effect from the introduction of ionic groups was found and it offers an effective mean to control shape memory function in SMPU fibres.

The results in this study have offered a reference for the design and application of SMPU ionomer materials. In the part of future work, the theoretical research issues and potential application of these kinds of intelligent materials were suggested.

Publications

Research journal paper:

Y. Zhu, J. L. Hu, K. W. Yeung, H. J. Fan, and Y. Q. Liu, "Shape Memory Effect of PU Ionomer With Ionic Group on Hard-segment," *Chinese Journal of Polymer Science*, vol. 24, pp. 173-186, 2006.

Y. Zhu, J. L. Hu, K. W. Yeung, Y. Q. Liu, and H. M. Liem, "Influence of ionic groups on the crystallization and melting behavior of segmented polyurethane ionomers," *Journal of Applied Polymer Science*, vol. 100, pp. 4603-4613, 2006.

Y. Zhu, J. L. Hu, K. W. Yeung, K. F. Choi, Y. Q. Liu, and H. M. Liem, "Effect of Cationic Group Content on Shape Memory Effect in Segmented Polyurethane Cationomer," *Journal of Applied Polymer Science*, vol. 103, pp. 545-556, 2007.

Y. Zhu, J. L. Hu, L. Y. Yeung, Y. Liu, F. L. Ji, and K. W. Yeung, "Development of Shape Memory Polyurethane Fiber with Complete Shape Recoverability," *Smart Materials & Structures*, vol. 15, pp. 1385-1394, 2006.

Y. Zhu, J. L. Hu, L. Y. Yeung, J. Lu, Q. H. Meng, S. J. Chen, and K. W. Yeung, "Effect of steaming on shape memory polyurethane fibers with various hard segment contents," *Smart Materials & Structures*, vol. 16, pp. 969-981, 2007.

Y. Zhu, J. Hu, K.-f. Choi, K.-w. Yeung, Q. Meng, and S. Chen, "Crystallization and Melting Behavior of Crystalline Soft-segment in Shape Memory Polyurethane Ionomer," *Journal of Applied Polymer Science*, vol. 107, pp. 599-609, 2008.

Y. Zhu, J. Hu, K.-f. Choi, Q. Meng, S. Chen, and K.-w. Yeung, "Shape Memory Effect and Reversible Phase Crystallization Process in SMPU Ionomer," *Polymers for Advanced Technologies*, vol. 19, pp. 328-333, 2007.

Y. Zhu, J. Hu, K.-f. Choi, J. Lu, L. Y. Yeung, and K.-w. Yeung, "Shape Memory Fiber Spun with Segmented Polyurethane Ionomer," *Polymers for Advanced Technologies*, 2008, in press.

Y. Zhu, J. Hu, K.-f. Choi, and K.-w. Yeung, "Effect of Soft-segment Crystallization, hard-segment physical crosslink on Shape Memory Effect in Antibacterizal SMPU Ionomers," 2008, submitted.

- F. L. Ji, Y. Zhu, J. L. Hu, Y. Liu, L.-Y. Yeung, and G. D. Ye, "Smart polymer fibers with shape memory effects," *Smart Materials and Structures*, vol. 15, pp. 1547-1554, 2006.
- S. Mondal, J. L. Hu, and Y. Zhu, "Free volume and water vapor permeability of dense segmented polyurethane membrane," *Journal of Membrane Science*, vol. 280, pp. 427-432, 2006.
- Q. Meng, J. Hu, Y. Zhu, J. Lu, and Y. Liu, "Morphology, phase separation, thermal and mechanical property difference of shape memory fibres prepared by different spinning methods," *Smart Materials & Structures*, vol. 16, pp. 1192-1197, 2007.
- Q. Meng, J. Hu, and Y. Zhu, "Shape-Memory Polyurethane/multi-walled carbon Nanotube fibers," *Journal of Applied Polymer Science*, vol. 106, pp. 837-848, 2007.
- Q. Meng, J. Hu, Y. Zhu, J. Lu, and Y. Liu, "Polycaprolactone-based shape memory segmented polyurethane Fiber," *Journal of Applied Polymer Science*, in press, 2007.
- Y. Q. Liu, J. L. Hu, Y. Zhu, and Z. H. Yang, "Surface modification of cotton fabric by grafting of polyurethane," *Carbohydrate Polymers*, vol. 61, pp. 276-280, 2005.
- S. Chen, J. Hu, Y. Liu, H. Liem, Y. Zhu, and Y. Liu, "Effect of SSL and HSC on morphology and properties of PHA based SMPU synthesized by bulk polymerization method," *Journal of Polymer Science: Part B: Polymer Physics*, vol. 45, pp. 444-454, 2007.
- S. Chen, J. Hu, Y. liu, H. Liem, Y. Zhu, and Q. Meng, "Effect of molecular weight on shape memory behavior in polyurethane films," *Polymer International*, vol. 56, pp. 1128-1134, 2007.
- J. Hu, J. Lu, and Y. Zhu, "New Developments in Elastic Fibers," *Polymer Reviews*, vol. 48, pp. 275, 2008.

Conference paper:

- Y. Zhu, J. Hu, K.-f. Choi, and K.-w. Yeung, "Crystallization Rate of Soft Segment on Shape Memory Effect in Shape Memory Polyurethane Ionomer," in *Annual Technical Conference*. Ohio, Cincinnati, U.S.A.: Society of Plastics Engineers, 2007.
- J. Hu, Y. Zhu, J. Lu, L.-y. Yeung, and K.-w. Yeung, "Uniqueness of shape memory fibers in comparison with existing man-made fibers," in *The 9th Asian Textile Conference*. Taiwan: Federation of Asian Professional Textile Associations, 2007.

J. Hu, J. Lu, Y. Zhu, and L.-y. Yeung, "Effects of Wet Spinning Conditions on Properties of Shape Memory Fibers," in *the 7th Annual Textile Conference by Autex "From Emerging Innovations to Global Business"*. Tampere, Finland, 2007.

Book chapters:

胡金莲, 朱勇, 杨立仁, 第四章, "形状记忆高聚物的微观结构表征及智能透气、机械特性分析", *形状记忆纺织材料*. 北京: 中国纺织出版社, 2006.

J. Hu, Y. Zhu et al., chapter 2, "Preparation of shape memory polymers," in *Shape Memory Polymers and Textiles*. Cambridge: Woodhead Publishing Limited, 2007.

J. Hu and Y. Zhu, chapter 4, "Structure and properties of shape memory polyurethane ionomer," in *Shape Memory Polymers and Textiles*. Cambridge: Woodhead Publishing Limited, 2007.

J. Hu, Y. Zhu et al., chapter 10, "Shape memory textiles," in *Shape Memory Polymers and Textiles*. Cambridge: Woodhead Publishing Limited, 2007

Patent:

J. Hu, Y. Zhu, and G. Ye, "Antibacterial Shape Memory Polyurethane Plate for Orthopedics, Fixing and Rehabilitation, and Preparation Method Thereof." CN1669590 (A), China, 2005.

胡金莲, 朱勇, 刘岩, 吕晶, 丘汉培, "具有形状记忆功能的纺织品及其处理方法," PCT/CN2007/070172, 2007. Pending

J. Hu, Q. Meng, Y. Zhu, J. Lu, and H. Zhuo, "Shape Memory Fibers Prepared via Wet, Reaction, Dry, Melt and Electro Spinning." USA, 2007, pending.

Acknowledgements

First of all, I would like to express my sincere gratitude to the chief supervisor of my PhD programme, Prof. Jinlian Hu. With her valuable direction, wise guidance, continuous encouragement and substantial support, many difficulties in my research working were overcome successfully. Meanwhile, Prof. Hu's profound academic attainments and precise professional integrity continuously inspired me to deepen my academic thought in the last four-year study. This unforgettable research experience under her supervision will be one of the best memories of my life.

The important support and guidance from the co-supervisors of my PhD programme, Prof. Kwok-wing Yeung and Dr. Ka-fai Choi were appreciated sincerely. Their persistent backup and guidance facilitated me to broaden knowledge horizon, subsequently, enriched my research scope.

Besides, I would like to thank Mr. J Yeung of Material Research Centre, The Hong Kong Polytechnic University, Mr. W K Ho of Chemical Lab of ITC, The Hong Kong Polytechnic University, Ms. M N Sun of Fabric Objective Measurements Lab of ITC, The Hong Kong Polytechnic University, Mr. K O Choi of Physical Testing Lab of ITC, The Hong Kong Polytechnic University,

Acknowledgements

for their unselfish help and guidance in using the relevant equipments and guiding safety issue.

I am also very grateful for the help from my colleagues: Dr. Yieqiu Liu, Dr. Subrata Mondal, Dr. Jing Lu, Mr. Baohua Liu, Mr. Fenglong Ji, Ms. Yan Liu, Mr. Lap-yan Yeung, Ms. Yuen-kei Li, Mr. Binjie Xin, Mr. Qinghao Meng, Mr. Shaojun Chen and friends whose names can not be listed here because of the limit of space. The friendship makes my study and life in The Hong Kong Polytechnic University be full of joy and happiness.

In addition, I would like to acknowledge the research facilities of Institute of Textiles and Clothing, The Hong Kong Polytechnic University and the research fund from the projects of The Innovation and Technology Fund (ITF) of Hong Kong, “Development of Shape Memory Fabrics/Garment (ITS/098/02)” and “High Performance Advanced Materials for Textile and Apparel (GHS/088/04)”.

Finally, the endeavor made in this PhD programme also is accompanied with the love, patience and care from my whole family. I am full of gratitude for my entire family and believe their support will keep encouraging me to explore further.

Table of Contents

CERTIFICATE OF ORIGINALITY	I
ABSTRACT.....	I
PUBLICATIONS	IV
ACKNOWLEDGEMENTS.....	VII
TABLE OF CONTENTS	IX
LIST OF FIGURES	XII
LIST OF TABLES	XVII
LIST OF SYMBOLS AND ABBREVIATIONS.....	XIX
CHAPTER 1 INTRODUCTION.....	1
1.1 Shape memory polyurethane and application	1
1.2 Effect of ionic groups on SMPU	5
1.3 Statement of problems.....	7
1.4 Objectives and significance	10
1.5 Methodology	12
1.5.1 Molecular design and synthesis of SMPU ionomers	14
1.5.2 Characterization of micro-structure of SMPU ionomers	14
1.5.3 Investigation of shape memory properties	15
1.5.4 Study of the antibacterial activity of SMPU ionomers	15
1.6 Arrangement of the thesis	16
CHAPTER 2 LITERATURE REVIEW	18
2.1 Development of shape memory polymers.....	18
2.2 Structure-property relationship of SMPU & SMPU Ionomers	23
2.3 Anti—bacterial activity of polyurethane ionomers.....	31
2.4 Shape memory polyurethane fibers.....	33
CHAPTER 3 PREPARATION OF SMPU IONOMERS	35
3.1 Factors affecting shape memory effect in SMPU ionomers	35
3.2 Molecular design for SMPU ionomers	36
3.3 Synthesis routine and sample preparation.....	40
3.3.1 Raw materials for synthesis of SMPU ionomers	40
3.3.2 Synthesis routine and recipe of SMPU ionomers	41

3.3.3 Preparation of SMPU ionomer specimens	49
CHAPTER 4 CHARACTERIZATION TECHNIQUES	51
4.1 Differential scanning calorimetry (DSC).....	51
4.2 Dynamic mechanical analysis (DMA).....	53
4.3 Fourier transform infrared spectroscopy (FTIR).....	55
4.4 Gel permeation chromatography (GPC)	56
4.5 Polarizing microscopy (POM)	58
4.6 Shape memory properties investigation.....	59
4.7 Antibacterial activity testing	64
CHAPTER 5 STRUCTURE AND SME OF SMPU ANIONOMERS	66
5.1 Influence of ionic groups on the crystallization and melting behavior in segmented PU anionomers with different M_w	66
5.1.1 Differential scanning calorimetry measurement	66
5.1.2 Morphology of crystal in SMPU cationomers with different molecular weight.....	69
5.1.3 Analysis of isothermal crystallization kinetics	71
5.1.4 Analysis of crystallization activation energy	75
5.1.5 Equilibrium melting temperature	77
5.2 Effect of ionic group content on SMPU anionomers.....	82
5.2.1 Effect of ionic group content on crystallizability of SMPU ionomers	82
5.2.2 Dynamic Mechanical Analysis	86
5.2.3 IR Analysis.....	91
5.2.4 Cyclic thermo-mechanical investigation.....	94
CHAPTER 6 STRUCTURE AND SME OF SMPU CATIONOMERS	101
6.1 Crystallization and melting behavior of crystallizable soft-segments in SMPU cationomers	101
6.1.1 Differential scanning calorimetry measurement	101
6.1.2 Analysis of isothermal crystallization kinetics	110
6.1.3 Equilibrium melting temperature	118
6.2 Effect of cationic group content on SME in segmented PU cationomers	119
6.2.1 Thermal Properties.....	120
6.2.2 Dynamic Mechanical Analysis	123

6.2.3 Cyclic thermo-mechanical investigation.....	131
CHAPTER 7 APPLICATION OF SMPU IONOMERS	139
7.1 SMPU ionomers with substrate bonding antibacterial activity.....	139
7.1.1 Crystallization and melting behavior	139
7.1.2 Dynamic mechanical analysis	139
7.1.3 IR analysis.....	142
7.1.4 Shape memory properties.....	145
7.1.5 Substrate bonding antibacterial activity	154
7.2 SMPU fibers with ionic groups within hard segments.....	158
7.2.1 Mechanical and dynamic mechanical properties of SMPU ionomer fibers.....	169
7.2.2 Thermal properties	173
7.2.3 Shape memory properties of SMPU ionomer fibers.....	175
CHAPTER 8 CONCLUSIONS AND SUGGESTIONS FOR FUTURE RESEARCH.....	178
8.1 Conclusions	178
8.1.1 Effect of ionic groups on the crystallization of soft segments	178
8.1.2 Effect of ionic groups within hard segments on SME	179
8.1.3 SMPU ionomers with substrate antibacterial activity.....	181
8.1.4 SMPU ionomers used as shape memory fiber materials.....	182
8.2 Future work suggested	183
8.2.1 Influence of chemical structure of ionic groups on SMPU ionomers	183
8.2.2 Effect of ionic groups within soft segments on SMPU ionomers.	184
8.2.3 Crystallization process and SME in SMPU ionomers	185
8.2.4 SMPU ionomers with improved SME	186
8.2.5 Other novel function introduced into SMPU with ionic groups ...	186
8.2.6 Effect of molecular orientation on SME in SMPU fibers.....	187
REFERENCES	188

List of Figures

Figure 1.1 Application: (a) autochoke for engine, (b) intravenous cannula, (c) spoon and fork handles for those unable to grasp objects, (d) sportswear[22]	4
Figure 1.2 Scheme for studies of structure and shape memory effect in segmented SMPU ionomers	13
Figure 2.1 Schematic representation of processing of shape memory effect [1]	19
Figure 2.2 Schematic representation of the molecular mechanism of the thermally induced shape-memory effect for segmented polyurethane. (T_s : T_m of soft segments)	22
Figure 2.3 Polyurethane with micro phase separation structure	24
Figure 3.1 Pre-polymerization to synthesis SMPU ionomers	37
Figure 3.2 wet spinning process for preparing SMPU fibers [31]	50
Figure 4.1 Observance of Maltese cross of isotactic polystyrene from melt[99]	59
Figure 4.2 Schematic representation of the results of the cyclic thermomechanical investigation for two different tests: a) ϵ - σ diagram: ①-stretching to ϵ_m at T_{high} ; ②-cooling to T_{low} while ϵ_m is kept constant; ③-clamp distance is driven back to original distance; ④-at $\epsilon=0\%$ heating up to T_{high} ; ⑤-start of the second cycle. b) ϵ - T - σ diagram: ①-stretching to ϵ_m at T_{high} ; ②-cooling down to T_{low} with cooling rate dT/dt while σ_m is kept constant; ③-clamp distance is reduced until the stress-free state $\sigma=0$ MPa is reached; ④-heating up to T_{high} with a heating rate dT/dt at $\sigma=0$ MPa; ⑤-start of the second cycle.	61
Figure 4.3 Schematic representation of strain recovery test: a) Diagram of preparation procedure of specimens for strain recovery measurements and; b) recovery curves, ϵ - T .	63
Figure 5.1 (a) DSC heating curves (20 °C/min) of PCL-4000 after cooling at 200 °C/min from 120 °C, (b) PU-20N non-ionomer, (c) PU-20I ionomer, (d) PU-58N non-ionomer, (e) PU-58I ionomer, (f) PU-71N non-ionomer, and (g) PU-71I ionomer	68

Figure 5. 2 Polarized optical microscopy images of the crystals for PCL-4000 and PU non-ionomers and ionomers with different molecular weights.....	70
Figure 5.3 Plots of $\ln[-(\ln(1-X(t)))]$ against $\ln t$ for isothermal crystallization with various temperatures.	72
Figure 5.4 Plots of $(1/n)\ln K$ against $1/T_c$ from isothermal crystallization	76
Figure 5.5 Plots of the observed melting temperature T_m against T_c for PU ionomers and non-ionomers with different molecular weights.....	78
Figure 5.6 DSC thermograms of sample PU-58N (upper) and PU-58I (lower) after isothermal crystallization at (a) $T_c=15^\circ\text{C}$, (b) $T_c=18^\circ\text{C}$, (c) $T_c=20^\circ\text{C}$, and (d) $T_c=22^\circ\text{C}$	79
Figure 5.7 Heating scan at $20^\circ\text{C}/\text{min}$ with DSC from 0°C to 240°C for PU non-ionomers and ionomers	84
Figure 5.8 Cooling scan at $20^\circ\text{C}/\text{min}$ with DSC from 0°C to 240°C for PU non-ionomers and ionomers	85
Figure 5.9 Plots of storage modulus E' of PU non-ionomers and the corresponding ionomers	87
Figure 5.10 Comparison of E' at 60°C between PU non-ionomer and ionomer series.....	88
Figure 5.11 Comparison of storage modulus E' of PU non-ionomers and the corresponding ionomers	89
Figure 5.12 Plots of loss modulus E'' of PU non-ionomers and the corresponding ionomers.....	90
Figure 5.13 IR spectrum of PU non-ionomer series and ionomer series	92
Figure 5.14 Comparison of IR spectrum between PU non-ionomers and ionomers	94
Figure 5.15 Comparison of stress at 100% elongation of second tensile cycle between PU non-ionomers and ionomers	95
Figure 5.16 Cyclic tensile test of PU non-ionomers and ionomers.....	96
Figure 5.17 Relaxation time dependence of strain recovery property of sample 60-0	98
Figure 5.18 Strain recovery test of PU non-ionomers and ionomers.....	99
Figure 5.19 Strain recovery ratio of PU non-ionomers and ionomers.....	100
Figure 6.1 DSC cooling scan for SMPU ionomers	103

Figure 6.2 DSC heating scan for SMPU ionomers	104
Figure 6.3 Heating scan after isothermal crystallization at 20°C for various time intervals for the sample 75-0.....	105
Figure 6.4 Heating scan after isothermal crystallization at 20°C for various time intervals for the sample BIN75-6 and BIN75-11	106
Figure 6.5 Heating scan after isothermal crystallization at 20°C for various time intervals for BIN75-6-C8 and BIN75-11-C8	107
Figure 6.6 Heating scan after isothermal crystallization at 20°C for various time intervals (In the first heating to remove the thermal history, the Maximum temperature is 70°C for BIN75-11(graph a), 120°C for BIN75-11(120)(graph b), 240°C for BIN75-11(240)(graph c) respectively).....	108
Figure 6.7 Exothermic curve for isothermal crystallization.....	111
Figure 6.8 Relative crystallinity with time for isothermal crystallization	112
Figure 6.9 Relative crystallinity with various ionic group content for isothermal crystallization at 28°C	113
Figure 6.10 Plots of $\log[-\ln(1-X(t))]$ versus $\log t$ for isothermal crystallization for 75-0, BIN75-6, BIN75-11	114
Figure 6.11 Plots of $\log[-\ln(1-X(t))]$ versus $\log t$ for isothermal crystallization.....	115
Figure 6.12 Plots of the observed melting temperature T_m against T_c for SMPU ionomers.....	118
Figure 6.13 Cooling scan (upper) and reheating scan (lower) of NMDA series SMPU cationomers	121
Figure 6.14 Cooling scan (left) and reheating scan (right) of BIN series SMPU cationomers	122
Figure 6.15 Storage modulus (E') of NMDA and BIN series SMPU cationomers	125
Figure 6.16 Elastic modulus of NMDA and BIN series SMPU cationomers at 20 °C and 70°C	126
Figure 6.17 Comparison of E' between SMPU cationomers and the corresponding non-cationomers	127
Figure 6.18 Loss tangent ($\tan\delta$) of NMDA (a) and BIN (b) series SMPU cationomers	128
Figure 6.19 Loss modulus (E'') of NMDA and BIN series SMPU cationomer	130

Figure 6.20 Cyclic tensile behavior of NMDA series SMPU cationomers	132
Figure 6.21 Cyclic tensile behavior of BIN series SMPU cationomers.....	133
Figure 6.22 Stress at 100% elongation in the tensile cycle of NMDA and BIN series.....	134
Figure 6.23 Fixity ratio and recovery ratio in the tensile cycle of NMDA and BIN series.....	135
Figure 7.1 Elastic modulus (E') of SMPU ionomers with antibacterial activity detected with DMA.....	140
Figure 7.2 Loss tangent for SMPU ionomers	141
Figure 7.3 FTIR spectra of SMPU ionomers and non-ionomers	143
Figure 7.4 FTIR spectra of SMPU ionomers with BIN weight content: 0 wt%, 6 wt%, 10.56 wt%	144
Figure 7.5 Cyclic tensile test for 75-0.....	146
Figure 7.6 Cyclic tensile test for BIN75-6-C8.....	146
Figure 7.7 Cyclic tensile test for BIN75-11-C8.....	147
Figure 7.8 Cyclic tensile test for BIN75-11	147
Figure 7.9 Dependence of fixity ratio (R_f) and recovery ratio (R_r) on cooling time.....	148
Figure 7. 10 Stress of SMPU ionomers at 100% elongation at 70 °C.....	150
Figure 7. 11 Initial tensile modulus of SMPU ionomers at 70°C	150
Figure 7. 12 Effect of cooling time and BIN wt% on R_r , R_f , the stress and the initial modulus.....	151
Figure 7.13 Zone of inhibition and bacterial growth under specimens in AATCC 147.....	156
Figure 7.14 Comparison of elastic modulus between SMPU fibers and various man-made fibers (PU56-120: 56wt% hard segment content; thermal setting at 120°C; PU66-120: 66wt% hard segment content; thermal setting at 120 °C)[28].....	160
Figure 7.15 Thermal shrinkage ratio under periodic stress detected by DMA (PU XX-YY: XX wt% hard segment content with thermal setting at YY°C, such as PU66-120: 66wt% hard segment content; thermal setting at 120°C)[28]	162

Figure 7.16 Thermal shrinkage ratio of original fibers (a) and treated fibers (b) under periodic stress detected by DMA (SMPU XX-O: XX wt% hard segment content without steaming; SMPU XX-S: XXwt% hard segment content with steaming treatment)[58]	163
Figure 7.17 Tan δ value detected by DMA for original (a) and treated SMPU fibers (b).....	167
Figure 7.18 Cyclic tensile test for original SMPU fibers.....	168
Figure 7.19 Cyclic tensile test for treated SMPU fibers	169
Figure 7.20 Tan δ and Storage modulus E' of SMPU ionomer original fibers with 64 wt% hard segment content	170
Figure 7.21 Tan δ and Storage modulus E' of SMPU ionomer steamed fibers with 64wt% hard segment content:	170
Figure 7.22 Tan δ and Storage modulus E' of SMPU ionomer original fibers with 55wt% hard segment content	170
Figure 7.23 Tan δ and Storage modulus E' of SMPU ionomer steamed fibers with 55wt% hard segment content	171
Figure 7.24 DSC heating scan for steamed SMPU ionomer fibers	175
Figure 7.25 Cyclic tensile test for SMPU ionomer fibers.....	176

List of Tables

Table 3.1 Raw materials for the synthesis of SMPU ionomers	40
Table 3.2. Formulae of the synthesis of segmented PU anionomers with different molecular	42
Table 3.3 Formula of the polyurethane synthesis	43
Table 3.4 Formulae of SMPU cationomers for investigating the crystallization and melting behavior of soft segments.....	45
Table 3.5 Formulation of NMDA series PU ionomers	46
Table 3.6 Formulation of BIN series PU ionomers.....	46
Table 3.7 Formulation of SMPU ionomers and non-ionomers.....	47
Table 3.8 Formula of SMPU ionomer fibers	49
Table 4.1 Summary of typical values of modulus at various states of a polymer[90].....	54
Table 4.2 Typical application of PLgel Mixed-C columns (Polymer Laboratories Ltd, USA).....	57
Table 4. 3 Intertek Ltd Testing file about the antibacterial activity of SMPU ionmoer film.....	65
Table 5.1 Thermal properties of PCL and PU samples.....	67
Table 5. 2 The Avrami Parameters n, K, t(0.5) (crystallization half time), and E (activation energy) of the soft segment of PU non-ionomers and ionomers	74
Table 5. 3 Values of the equilibrium melting temperature T_e , the stability parameter Φ , and the low and high apparent melting temperature	81
Table 5. 4 Thermal properties of SMPU non-ionomers and ionomers	86
Table 5.5 Tg of soft segments from dynamic mechanical curves of films	90
Table 6.1 Thermal properties of SMPU ionomers	105
Table 6.2 Parameters of isothermal crystallization	116
Table 6.3 Thermal properties of SMPU cationomers	123
Table 6.4 Tgh of hard segment of BIN series detected from the peak of loss tangent ($\tan\delta$)	124
Table 7. 1 The stress at 100% elongation raio of SMPU ionomers	152

Table 7. 2 ANOVA table of two-factor experiment for the stress	152
Table 7. 3 The initial modulus of SMPU ionomers	154
Table 7. 4 ANOVA table of two-factor experiment for the initial modulus.....	154
Table 7.5 Antibacterial activity testing result according to AATCC 147.....	155
Table 7.6 Antibacterial activity testing result according to ASTM E2149.....	158
Table 7.7 The samples were listed in the following table.....	171
Table 7.8 DSC data for the heating scan of SMPU fibers	175
Table 7.9 Summary of shape fixity ratio (R_f) and shape recovery ratio (R_r)	177

List of Symbols and Abbreviations

<u>Symbol</u>	<u>Definitions</u>
ΔC_p	change in the heat capacity
ΔE	activation energy
AATCC	American Association of Textile Chemists and Colorists
ANOVA	Analysis of Variance
ASTM	American Society for Testing and Materials
BDO	1,4-butanediol
BIN	N, N-bis(2-hydroxyethyl)isonicotinamide
C8I	1-Iodooctane
CPE	chlorinated polyethylenes
df	Degree of freedom
DMA	Dynamic Mechanical Analysis
DMF	N,N-dimethylformamide
DMPA	dimethylolpropionic acid
DSC	Differential Scanning Calorimetry
dT/dt	cooling rate
E'	storage modulus
E''	loss modulus
FTIR	Fourier Infrared Spectra
GPC	Gel permeation chromatography
HAc	Acetic acid
HD	Hexane-diol
HDI	Hexamethylene diisocyanate
IPDI	Isophorone diisocyanate
IR	Infrared Spectra
L^*	critical lamellar thickness
MDI	4,4'-diphenylmethane diisocyanate
MHI	Mitsubishi Heavy Industry
M_n	number average molecular weight
M_w	weight average molecular weight
NMDA	N-methyldiethanolamine)
PBA	poly(butylenes adipate)
PCL	poly(ϵ -caprolactone)
PE	polyethylene
PEA	poly(ethylene adipate)
PEO	Poly Ethylene Oxide
POM	Polarizing Optical Microscope

List of Symbols and Abbreviations

PPG	poly(propylene oxide)
PTMG	poly(tetrahydrofuran)
PU	polyurethane
QAS	quaternary ammonium salts
R	gas constant
R_f	fixity ratio
$R_f(N)$	strain fixity ratio
$R_r(N)$	strain recovery ratio
$R_{r,tot}$	total strain recovery ratio
SEC	size-exclusion chromatography
SME	shape memory effect
SMPU	shape memory polyurethane
$\tan\delta$	loss tangent
T_c	isothermal crystallization temperature
T_{ch}	temperature of hard-segment crystallization
T_{cs}	temperature of soft-segment crystallization
TDI	Toluene diisocyanate
T_e	equilibrium melting point
TEA	Triethylamine
T_g	glass transition
T_{gh}	glass transition temperature of hard segments
T_{gmix}	mixed glass transition temperature
T_{gs}	glass transition temperature of soft segments
THF	tetrahydrofuran
T_{high}	high temperature
T_m	melting temperature
T_{mh}	melting temperature of hard segments
T_{ms}	melting temperature of soft segments
T_{perm}	permanent transition point
TPI	trans-polyisoprene
T_{trans}	transition temperature
UV	ultraviolet
wt%	weight content
$X(t)$	relative crystallinity
γ	the ratio of the lamellar thickness L to the lamellar thickness of the critical nucleus L^* at T_c
ΔH_{ch}	heat of hard-segment crystallization
ΔH_c	heat of crystallization
ΔH_{cs}	heat of soft-segment crystallization
ΔH_{fs}	heat of fusion
ΔH_{mh}	enthalpy of melting hard-segment
ΔH_{ms}	enthalpy of melting soft-segment
ε_m	maximum strain
Φ	stability parameter

CHAPTER 1 INTRODUCTION

1.1 Shape memory polyurethane and application

In recent decades, shape memory polymers as one group of most applicable smart materials were developed widely in not only academic area, but industrial application field as well, which is due to the low cost, good processing ability, high shape recoverability and wide range of shape recovery temperature in comparison with shape memory alloy [1, 2]. So far, a variety of polymers were reported to possess shape memory properties such as *trans*-polyisoprene (TPI), poly(styrene-co-butadiene), polynorbornene, cross-linked polycyclooctene and segmented polyurethane[1, 3]. In particular, segmented shape memory polyurethane (SMPU) has come to much attention since the Nagoya Research and Development Center of Mitsubishi Heavy Industry (MHI) developed the series of functional polymer [4]. Foremost among the reported microscopic structures on segmented SMPU systems, the two-phase heterogeneous structure is the well acceptable picture, consisting of a rigid fixed and a soft reversible phase. According to the mechanism of shape memory effect of segmented polyurethane (PU), the reversible phase having a melting or glass transition temperature of the soft segments as the transition temperature is used to hold the temporary deformation, whereas the fixed phase is referred to the hard segments covalently coupled to the soft segments. Hereinto, the fixed phase inhibits plastic slip of the molecular chains by having physical cross-linkage points among them and can be responsible for memorizing the permanent shape [5-9]. In the linear segmented PU system, the strong inter-molecular force among hard

segments results from their possessing the hydrogen bonding and high polarity due to the presence of urethane and urea units. The shape memory effect (SME) of PU therefore is mainly influenced by the hard segment content and the moiety of its molecular structure[8, 10, 11]. In addition, it is reported that soft segment content, its molecular weight, conformation, and morphological structure play significant roles in affecting the shape memory effect (SME) [9, 12]. Conducting research on SMPU, these parameters are paramount on controlling the shape memory property in general. This in turn, provides a mean to control the measurable shape recovery and shape fixity ratio in particular. Consequently, in lots of research about shape memory polyurethane, the above factors such as hard segment content, length of soft segments, even the molecular structure of hard segments were used to control the shape memory properties, such as shape recovery ratio, shape fixity ratio, to satisfy the various application requirements. Besides, as for the trigger pattern, some researchers have explore a variety of new kinds of shape memory polymer which can response to different external stimulus such as UV (ultraviolet)[13], water immersion[14-18], electricity[19], remote electromagnetic activation[20] and infrared irradiation[21]. Some of these studies were based on the introduction of some novel functional groups within molecular chain of shape memory polymer or introduction of nano-materials into shape memory polymer matrix and have broadened the scope of application of shape memory polymers.

In viewpoint of application of shape memory polyurethane, some progress has been made in the past decades. About 20 years ago, Hayashi of MHI developed shape memory segmented polyurethane copolymer, which has already been the

mostly familiar shape memory polymer. Among various SMPs, the shape memory polyurethanes (PUs) made by Diaplex Company have made great progress because of the following advantages: the forming processes used for other thermoplastic polymers could be utilized directly; the shape recovery temperature could be set at any value within 50 K around the room temperature; there are the large differences of mechanical properties, optical property and water vapor permeability at the temperatures above and below the designed T_g . Based on these advantages, the shape memory PU has been expected to be used as self-repairing, and smart materials or biomaterials. As shown in Figure 1.1, the use area can be divided into the following classes: use of variation in modulus of elasticity; use of shape fixity and shape recoverability; use of variation in moisture permeability, volume expansion and refractive index and high damping[22]. In textile area, the shape memory polyurethane was reported to be used in coating on the fabric surface to offer the temperature dependence of water vapor permeability to improve the comfort sense of fabric[23]. The smart water vapor permeability dependent on temperature arises from the increased free volume in soft segment domains, which allow water vapor molecules with an average diameter of 3.5Å to be easily transmitted through the polymer thin film[24]. Since 2003, the Shape Memory Textile Centre in The Hong Kong Polytechnic University has applied shape memory polyurethane in fiber spinning, fabric finishing, garment finishing with various techniques so as to impart shape memory function into fiber and garment products[25-36]. In these ways, the crease retention and flat appearance of fabric were expected to be improved simultaneously. In biomedical materials area, shape memory function around

human body temperature range together with biocompatibility offer tremendous application potential for use in minimally invasive surgery[37-40]. Through a

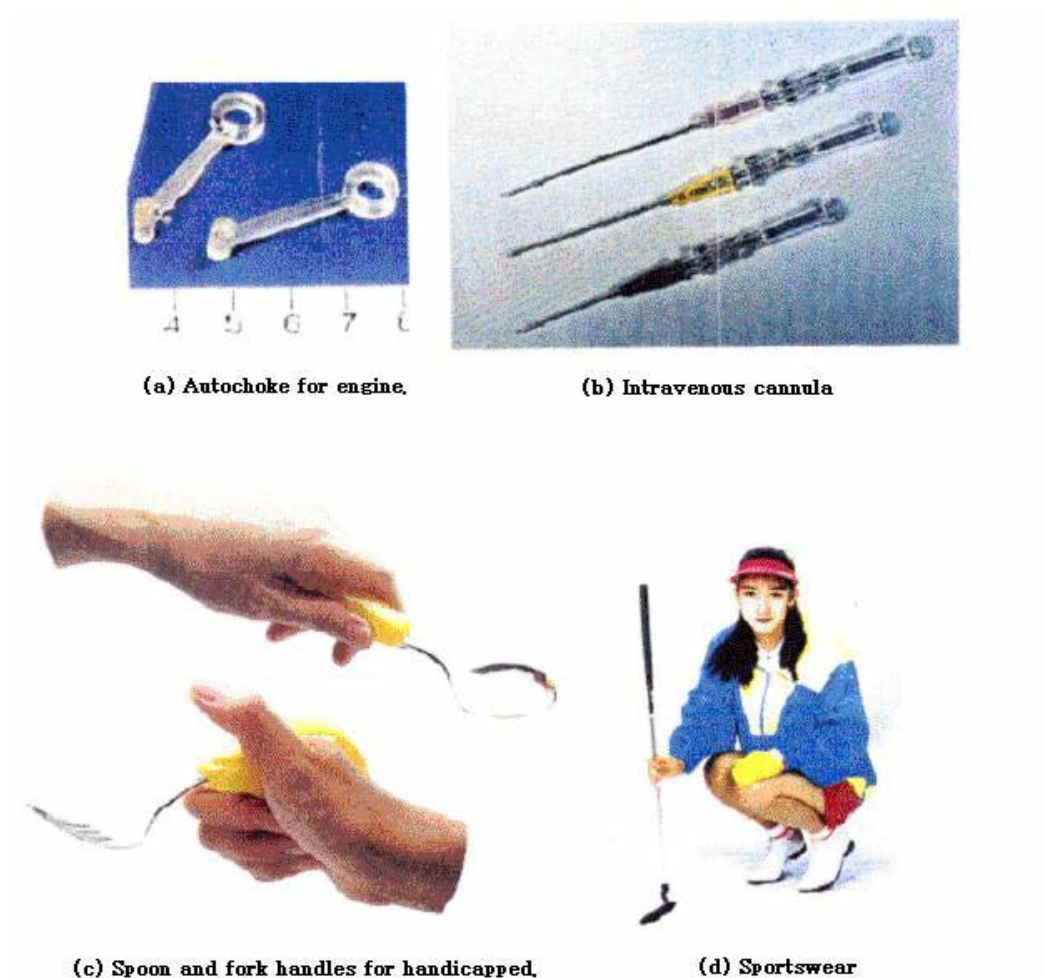


Figure 1.1 Application: (a) autochoke for engine, (b) intravenous cannula, (c) spoon and fork handles for those unable to grasp objects, (d) sportswear[22]

small incision in the human body, degradable implants can be inserted into in a smaller compressed (temporary) shape. When they are placed at the correct position, they obtain their application relevant shape after warming up to body temperature. After a defined time period, the implant is degraded and becomes desorbed. In this case a follow-on surgery to remove the implant is not

necessary[37, 39, 41]. A group of biomaterials potentially used as implant, medical device with shape memory property has been described and developed for biomedical applications[42-44].

Therefore, it can be found that the shape memory polyurethane together with its application has been widely developed in academic scope and industrial field. It is believed to be an important branch of smart materials.

1.2 Effect of ionic groups on SMPU

In recent years, numerous studies on polyurethane ionomers are emerging because of their superior mechanical and thermal properties. For example, tensile strength, modulus, and elongation at fracture, etc., of the PU ionomers in the form of thin films can be increased due to the presence of Coulombic force between the ionic centers within the molecular chain backbone[45-47]. Usually, polyurethane ionomers can be attributed into three categories: (1) cationomers formed by use of a tertiary amine followed by reaction with alkyl halide; (2) anionomers formed by use of a secondary amine following with a reaction with a sultone or lactone or chain extender with carboxyl groups following with the neutralization reaction with neutralization agent; (3) zwitterionomers formed by use of a tertiary amine followed by reaction with a sultone to form a quaternary ammonium sultone[48-53]. The research has revealed that, after ionization, the ionic groups within hard segments play dual effect on the morphology of polyurethane: improved cohesion through ionic interaction and disruption of the order of hard segment domain by ion insertion[48]. But, for different specific

molecular structure, the predominant effect might be different. For example, for the system composed of MDI, NMDA, PTMG with molecular weight 2000, the former effect is dominant, which is indicated by T_{gh} shifts to higher temperature and T_{gs} drops to low temperature. Instead, for the system consisting TDI, NMDA, PTMG with the molecular weight 2000, the latter factor is dominant[48].

For shape memory materials, it was found that PU ionomer species with phase separation morphology also have shape memory effect and especially, in some cases, have some specific tendency in mechanical property and thermal property, such as higher recovery strain, lower residual strain, higher hardness, increased modulus and strength as compared with non-ionomers for the Coulombic force between the ionic centers positioned within the hard domains[46, 47]. Kim *et al.* systematically studied the effect of various soft segments content and lengths on the shape memory effect with cyclic tensile test[47]. Meanwhile, with the comparison of the dynamic mechanical properties and crystallization properties between the PU ionomers and the corresponding non-ionomers, Kim pointed out that the effect of the ionomers on micro-phase separation is two-fold. But, the study about this two-fold effect and this effect on shape memory properties has not yet been done. Jeong *et al.*[46] preliminarily investigated the shape memory properties of shape memory polyurethane ionomers based on poly(ϵ -caprolactone) (PCL), 4,4'-diphenylmethane diisocyanate (MDI), 1,4-butanediol (BDO), dimethylolpropionic acid (DMPA), hexamethylene diisocyanate (HDI), hexamethylene diamine [54] with a range of DMPA content from 1.5% to 4.5% through the cyclic tensile test. It was found that the introduction of DMPA can minimize the fatigue behavior during repeated thermo-mechanical cycles.

Therefore, it can be concluded that ionic moieties in hard segments can influence the shape memory effect significantly.

1.3 Statement of problems

According to the research progress about the microscopic structures on segmented SMPU systems, the two-phase heterogeneous structure is the well acceptable picture, consisting of a rigid fixed and a soft reversible phase. In stretching process, the distance between net-points of fixed phase is increased and the molecular chain becomes oriented with the loss of entropy. Then the reversible phase can fix the deformation in the situation with the temperature lower than transition temperature (T_m or T_g of reversible phase). In the recovery process, when the temperature increase beyond the transition temperature, the networks containing flexible reversible phase component in the form of amorphous chain segments can return to the original shape and gains the entropy loss back. Up until the present time, for some special purpose such as increasing the shape recovery ratio, raising the modulus of rubber state, it is expected to enhance the connection among hard segments in shape memory polyurethane. In some cases, increasing the hard segment content provides an option to alter their inter-connectivity at the expense of the crystallizable soft segment content, and thus lowering the shape fixity ratio[5]. Some researchers also reported that chemical cross-linking hard segment structure could be systematically incorporated into PU so as to improve its shape memory function[27, 55]. However, the advantage of reprocessing ability of this originally thermal plastic SMPU is lost due to the formation of chemical cross-linkage points. Therefore,

the Coulombic force produced by ionic groups within hard segments was considered as an adjustable internal force of reversible phase, with which the processing ability of thermal plastic segmented PU can be kept. Some researchers have studied the mechanism of the effect of ionic groups on micro phase separation in PU. Chen and the coworkers[48] revealed the dual effect of ionization: improved cohesion through ionic interaction and disruption of the order by ion insertion in the study of polyurethane cationomers with NMDA as chain extender. With respect to this dual effect of ionic groups within hard segments, in this study, the ionomer moiety was used to act as a part of chain-extender for hard segments, providing the necessary Coulombic Force to adjust the physical crosslink among hard segments, meanwhile the introduction of ionic groups into hard segments was expected to alter the packing extent in hard domain or increase the micro phase separation, which possibly improve the crystallizability of soft segments. Therefore, this research will give rise to an easy mean to adjust the inter-connectivity between hard domains and crystallizable soft segments in thermal plastic SMPU, providing a systematic step to improve SME in segmented PU.

Besides, so far, there are lots of research relating to the shape memory polymer with multi-function such as biodegradable, elastic shape memory polymer[37, 39], electric conductivity shape memory polyurethane[56], light-induced shape-memory polymer[13], electroactive shape memory polyurethane composites[19]. Therefore, it can be found the introduction of novel functional groups into the traditional shape memory polyurethane can potentially impart new function to this kind of smart materials, while the shape memory function can be retained

simultaneously. In this way, the application scope of shape memory polymer was broadened immensely and more practical requirements for the novel SMP could be satisfied admirably. Therefore, in this research, not only the effects of ionic groups within hard segments on shape memory function, but also the antibacterial activity with the choice of suitable ionic groups will be studied, which will provide an effective mean to fabricate shape memory polymer materials with substrate bonding biocidal properties. As for the fabrication of biomaterials with antibacterial activity, usually, the molecular biocide can be directly added into the matrix materials to kill the microorganism in contact with the substratum and it becomes active by migrating out of the polymer matrix. However, the biocidal activity is dependent on the release of the biocide in the environment and subsequently gives rise to two results: a continuous loss of activity with time and the potential hazard to the environment (biocides are usually highly toxic)[57]. If the biocidal group was bound into the molecular chain through the covalent/ionic bond, which will not be cleaved in the presence of microorganism, the modified polymer will be active by contact with the cell membrane of the microorganisms and the substrate binding biocidal activity will be kept for a long time for the covalent/ionic bond. In that, with choosing the suitable chain extender possessing ionic groups and the corresponding counter-ion, the antibacterial activity might be incorporated to the shape memory polyurethane. On the other hand, as the preliminary exploration relating to the practical application of SMPU ionomers, the SMPU fibers composed of shape memory polyurethane ionomers were spun by wet spinning process. This application of SMPU ionomers necessitates the study on the relations between

the micro structure and properties in the SMPU fibers, which might be different from that of SMPU film.

As a result, although some knowledge gaps in this area have been revealed in literature reported, the following problems need to be tackled to further the study in details:

How does the ionic group within hard segments influence the crystallization and melting behavior of the soft segments in segmented polyurethane ionomers?

What is the effect of the ionic group within hard segments on the shape memory function including shape fixity, shape recovery?

Is it feasible to introduce the substrate bonding antibacterial activity into SMPU ionomers with choosing suitable ionic groups and counter-ion?

Is it possible to adjust SME with ionic groups within hard segments in SMPU ionomer fibers?

1.4 Objectives and significance

Although presently some relations between structure and properties in polyurethane ionomers have been revealed and the T_m type shape memory polyurethane ionomers and non-ionomers with various soft segment length and content has been compared in thermal properties and shape memory investigation,

the knowledge about the effect of ionic groups contents on morphology and shape memory properties are not clarified. Especially, for T_m type shape memory polyurethane ionomers, the crystallization of soft segments which is usually regarded as reversible phase responsible for fixing the temporary deformation need to be deeply studied in SMPU ionomers. On the other hand, considering other novel function introduced by ionic groups such as antibacterial activity, in the part about the application of SMPU ionomers in this thesis, the SMPU ionomers with antibacterial activity and SMPU ionomer fibers are studied respectively. In that, based on the present progress of shape memory polyurethane ionomers, the objectives of this research are listed as follows:

To synthesize shape memory polyurethane ionomers with various ionic groups content by solution polymerization;

To study the influence of ionic groups on the crystallization and melting behavior of soft segments in segmented polyurethane ionomers;

To investigate the influence of ionic groups on shape memory effect of segmented polyurethane ionomers;

To impart substrate bonding antibacterial activity into SMPU with ionic groups;

To adjust shape memory effect of SMPU ionomer fibers with ionic groups within hard segments;

In the application of SMPU ionomers, substrate-bound antibacterial activity was introduced into shape memory polyurethane ionomers to fabricate a kind of multi-functional shape memory materials. In addition, the shape memory fibers composed of segmented polyurethane ionomers will be prepared with wet spinning and the relations between the structure and shape memory effect of this novel functional fibre was planned to be studied preliminarily.

The relations between structure and properties are the eternal topics for academic and application research. In this thesis, the study of structure and shape memory effect in SMPU ionomers is expected to open up a new pathway to understand the effect of ionic groups on morphology of the reversible phase and fixed phase in SMPU ionomers, subsequently, to bridge the gap between micro-structure and shape memory properties, eventually, to offer a new control mean in the design of SMPU ionomers including not only shape memory effect, but other novel function as well.

1.5 Methodology

As shown in Figure 1.2, in this study, the research was divided into two parts: the study on relations between structure and shape memory effect in SMPU cationomers and anionomers; the study on SMPU ionomers with antibacterial activity and SMPU ionomer fibers. In the first part, the effect of ionic group content on shape memory effect was systematically studied together with the investigation about morphology. Meanwhile, the crystallization and melting behavior of the crystallizable soft segments were investigated with isothermal

crystallization kinetic method. Moreover, the cooling induced crystallization process was quantitatively detected so as to reveal the effect of soft segment crystallization on the shape fixity. In the second part, some specific SMPU ionomer molecular structure was designed in the light of practical application. Therefore, the second part is only preliminary and need to be detailed in future working in comparison with the first part in this research. Nevertheless, the influence of asymmetrical chain extender and long chain alkyl neutralization agent on SME and crystallization of soft segments was analyzed. The resultant data will be useful for novel functional shape memory molecular design. For SMPU ionomer fibers, the effect of hard segments, post-treatment with various temperatures on SME, thermal stability, morphology has ever been studied systematically in our previous research working[28, 58]. Therefore, as a preliminary study for this kind of shape memory polymer, only 2 wt% NMDA was introduced into hard segments so as to investigate the influence of ionic groups on SMPU fibers with different hard segment content.

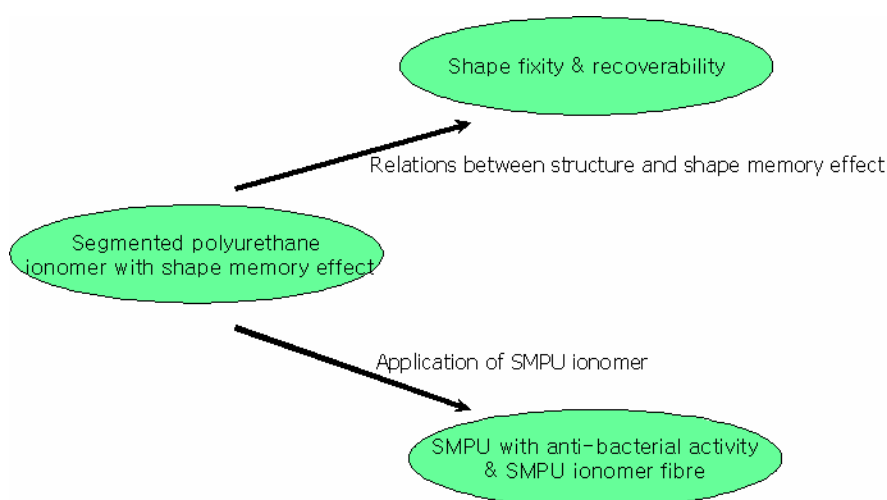


Figure 1. 2 Scheme for studies of structure and shape memory effect in segmented SMPU ionomers

1.5.1 Molecular design and synthesis of SMPU ionomers

In order to make micro phase separated morphology in SMPU ionomers to realize the shape memory function, two or three steps condensation polymerization in solution was applied. Compared with bulk polymerization, solution polymerization has advantages such as the ease to control the reaction rate, diminishing the cross link or branched structure. The most important is that the neutralization reaction must be finished in solution. Through the neutralization, the ionic groups were introduced into the molecular system with the usage of chain extender containing ionic group including anion or cation groups. For the influence of hard segment content and soft segment length has been studied in lots of literature reported, the focus of this study is the effect of the ionic groups category and content on shape memory effect. In the process of polymerization, the ratio of isocyanate and hydroxyl groups was kept to be 1 around to make the molecular chain extended to the maximum.

1.5.2 Characterization of micro-structure of SMPU ionomers

Micro-structure, morphology and thermal properties of shape memory polyurethane ionomers were studied systematically by FTIR, DSC, DMA, and POM. Especially for the comparison between SMPU ionomers and the corresponding SMPU non-ionomers, the mentioned characterization techniques such as FTIR, DSC, DMA were used to investigate the change of crystallization of soft segment phase, micro phase separation and cohesion among hard domains, thereby clarify the effect of ionic groups within hard segments on shape memory function. For the quantitative research on the crystallization of soft segments in

segmented SMPU ionomers, the isothermal crystallization kinetic was conducted to disclose the influence of ionic groups on crystallizable soft segments in SMPU ionomers with different molecular weight, ionic group content and category.

1.5.3 Investigation of shape memory properties

In this study, the cyclic tensile test and/or strain recovery test were used to characterize the shape memory property, namely investigate the shape recovery, shape fixity and switching temperature of the series of SMPU ionomers. Cyclic tensile test was employed by using universal tensile tester with a constant temperature control chamber and a personal computer was used to control testing cycle and record all data; A microscopy (Leitz Wetzlar) with a hot stage (Mettler Toledo FP90 Central Processor & FP82 Hot Stage) and a camera (Pixera PVC 100C) were used to observe and record the strain recovery effect of sample film stretched in the cyclic thermal-mechanical investigation after one cycle, in which the heating rate and temperature range of the recovery measurement were under control with heating system.

1.5.4 Study of the antibacterial activity of SMPU ionomers

ASTM E 2149 is designed to evaluate the resistance of non-leaching antimicrobial treated specimens to the growth of microbes under dynamic contact condition. Meanwhile, the test method AATCC 147 that is directly dependent on the ready leach-ability of the antimicrobial agent from the treated samples is used to detect whether the antibacterial activity is caused by the leaching of biocidal agent or not. Therefore, the aforementioned testing methods combined to test the

substrate-bound antibacterial activity of SMPU ionomers with the suitable chain-extender and counter-ion.

1.6 Arrangement of the thesis

The focus of this thesis is to study the structure and shape memory effect of segmented polyurethane ionomers. Accordingly, the effect of ionic groups on shape memory properties was systematically studied. Besides, SMPU ionomers with substrate bonding antibacterial activity and SMPU ionomer fibers were prepared and the influence of ionic groups was discussed. It comprises 8 chapters described as follows.

Chapter 1 stated the general background of this research, academic and industrial application progress of shape memory polyurethane, the mechanism about the effect of ionic groups on morphology in segmented polyurethane, statement of problems, objectives and significance and research methodology.

Chapter 2 included literature review about the development of shape memory polymer, the structure-property relationship of shape memory polyurethane & shape memory polyurethane ionomers, the antibacterial activity of polyurethane ionomers, shape memory polyurethane fibers.

Chapter 3 contained the preparation of shape memory polyurethane ionomers. The factors affecting shape memory effect, molecular design for SMPU ionomers, synthesis routine and sample preparation, recipes for SMPU ionomers were discussed respectively.

In chapter 4, the characterization techniques used in this study were described in details. Thereof, the specific testing condition chosen for each series specimens was stated.

The study on shape memory polyurethane anionomers was concentrated in chapter 5, in which the influence of ionic groups on the crystallization and melting behavior in SMPU anionomers with different molecular weight was firstly studied, and then the effect of ionic groups on shape memory effect was illustrated in details.

Chapter 6 presented the study about shape memory cationomers. Firstly, the crystallization and melting behavior of crystalline soft segments was studied with isothermal crystallization kinetic method. After that, the study about the effect of cationic groups on shape memory effect was conducted systematically.

In chapter 7, it was illustrated that the ionic groups in SMPU ionomers were used to introduce the substrate bonding antibacterial activity into SMPU and simultaneously to control shape memory effect in SMPU ionomers. Also, the ionic group was introduced into SMPU fibers so as to adjust SME. This chapter was mainly concerned with the application of SMPU ionomers.

Chapter 8 presented the summary of conclusions and potential application of SMPU ionomers. Finally, some future work including theoretical study and applied technology was suggested.

CHAPTER 2 LITERATURE REVIEW

2.1 Development of shape memory polymers

Shape memory materials including shape memory polymer, shape memory gel, shape memory alloy and shape memory ceramics are stimuli-responsive materials, which can change their shape or temporary deformation when stimulated by external trigger such as heating, lighting or PH value change. In recent decades, shape memory polymer was one of the key smart materials developed widely in both academia and industry for their low cost, good processing ability, high shape recoverability, and larger range of shape recovery temperature compared with shape memory alloys[2]. Meanwhile, shape memory behavior can be observed in various polymer systems which are significantly different in molecular structure and morphology. In the investigation of shape memory effect, it is also obvious that the shape memory behavior is not only related to the molecular structure and morphology, but dependent on the applied processing and programming as well[1, 59]. Therefore, for the study of shape memory effect of various shape memory polymer, several kinds of investigating methodology, such as cyclic tensile investigation[5, 47, 60], strain recovery test[7, 61], bending test for the determination of the shape memory effect[8, 9], shrinkage determination of heat-shrinkable products[62], were established so as to satisfy the research and application requirement. Whereas, in the view of principle about shape memory behavior, the following Figure 2.1 is representative and typical one, in which the temporary shape can be fixed for a long time after programming process, and then the permanent shape can be

recovered from temporary shape when triggered by the external stimulus such as heating up to a certain temperature.

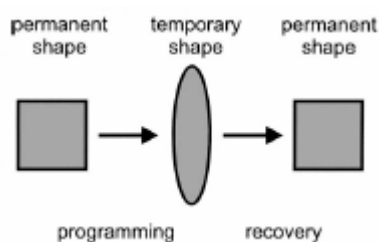


Figure 2.1 Schematic representation of processing of shape memory effect [1]

Several polymer systems have been reported to possess shape memory properties such as cross-linked polyethylene, *trans*-polyisoprene (TPI), poly(styrene-co-butadiene), poly-norbornene, polyethylene/nylon6-graft copolymer and cross-linked polyethylene-poly(vinyl acetate) copolymer etc. Since the 1960s, polyethylene (PE) covalently cross-linked by ionizing radiation has been found to possess shrinkable effect with the heating stimulus and began to be gradually and widely used in electric wire and cable area because it can store large deformation that can be recovered on application of heat[63, 64]. In this case, this smart function of cross-linked PE was explained with the principle of “Memory Effect”. In molecular structure of cross-linked PE, the molecular chains are entangled each other and could be categorized into crystalline regions and amorphous regions. Ionizing radiation can induce the cross-linking structure and formation of the three dimensional network, which was believed to occur preferably in amorphous regions. Crystalline regions appear to retain the deformed temporary shape, when the film is cooled down below the melting point of crystalline regions. Heating up the film above the melting point of crystalline region cleaves the restraint for shape recovery. Then the original

shape will be recovered, which is due to the cross-linking structure and the entropy elasticity. Here, “Memory effect” means that irradiated cross-linking PE is capable of memorizing its original irradiated structure however it is deformed. In the late 1970s, amorphous poly-norbornene with the molecular weight of 3×10^6 was initially used as shape memory polymer[65, 66]. The poly-norbornene containing 70-80 mol% of trans-linked norbornene units has a glass transition (T_g) at 30-40°C used as switching temperature and physical cross-linking network due to entanglement of the high molecular weight chains is regarded as fixed phase. When the stretched sample is cooled down below T_g rapidly enough, the freezing of temporary deformation will be applicable because the relaxation time for disentangle is much longer than that for stretching and cooling process. After that, the shape recovery can be observed with the heating above the switching temperature. Besides, some co-polymer systems such as poly(styrene-co-butadiene)[67], polyethylene-poly(vinyl acetate) copolymers[68], polyethylene/nylon-6-graft copolymer[61], ethylene oxide-ethylene terephthalate segmented copolymer[69] also were found to have shape memory effect for their specific molecular structure. Presently, the most readily available is segmented shape memory polyurethane (SMPU) which aroused much attention since the Nagoya Research and Development Center of Mitsubishi Heavy Industry (MHI) developed a series of functional polymers[4]. Foremost among the reported microscopic structures on segmented SMPU systems, the two-phase heterogeneous structure is the well acceptable picture, consisting of a rigid fixed and a soft reversible phase as shown in Figure 2.2. According to the mechanism of shape memory effect, the reversible phase having a melting or glass transition temperature of the soft segments as the transition

temperature (T_{trans}) is used to hold the temporary deformation, whereas the fixed phase is referred to the hard segments covalently coupled to the soft segments. Thereof, the fixed phase inhibits slippage between the molecular chains by having physical cross-linkage points between them that are responsible for memorizing the permanent shape [5-9]. In the linear segmented polyurethane (PU) system, the strong inter-molecular force among hard segments results from their possessing high polarity and hydrogen bonding among hard segments due to the presence of urethane and urea units. The hard segment phase with the highest thermal transition temperature (T_{perm}) acts as the physical cross-link and controls the permanent shape. Heating above the highest thermal transition point, the physical cross-links among hard segments will be destroyed. The whole molecular chains therefore melt and can be processed with the traditional processing techniques such as extrusion, injection or blow moulding, in which the permanent shape such as some products with specific figure can be formed easily by cooling. So, the process and recycle usage of shape memory polyurethane can be realized easily. As far as the effect of microstructure on shape memory properties is concerned, the shape memory effect (SME) of PU is significantly influenced by the hard segment content and the moiety of its molecular structure. When cooling below T_{perm} and above the glass transition or melting point of soft segments of SMPU, the SMPU is still kept in relative soft status and readily deformed but can not flow for the restraint of physical cross-links. In this process, the temporary deformation can be easily conducted such as stretching or compressing and cause the molecular chains oriented with the loss of entropy. Continuously cooling SMPU deformed below the glass transition or melting point of soft segments, the soft segments under glass status or crystalline

state begin to restrain the movement of molecular chains and keep the materials relative rigid with high modulus at two or three orders higher than that at the previous stage, so as to fix the deformed shape. Reheating above the glass transition or melting point of soft segments but below T_{perm} can give rise to the movability of molecular chain and simultaneously induce the shape recovery due to entropy elasticity. The original shape will be recovered and the entropy lost in deformation process will be gained back[1]. In term of the fixity function of SMPU, it can be found that the soft segment phase enables the fixity of temporary shape as a molecular switch which dominates the variation of transition temperature and the extent of fixity of temporary deformation. In that,

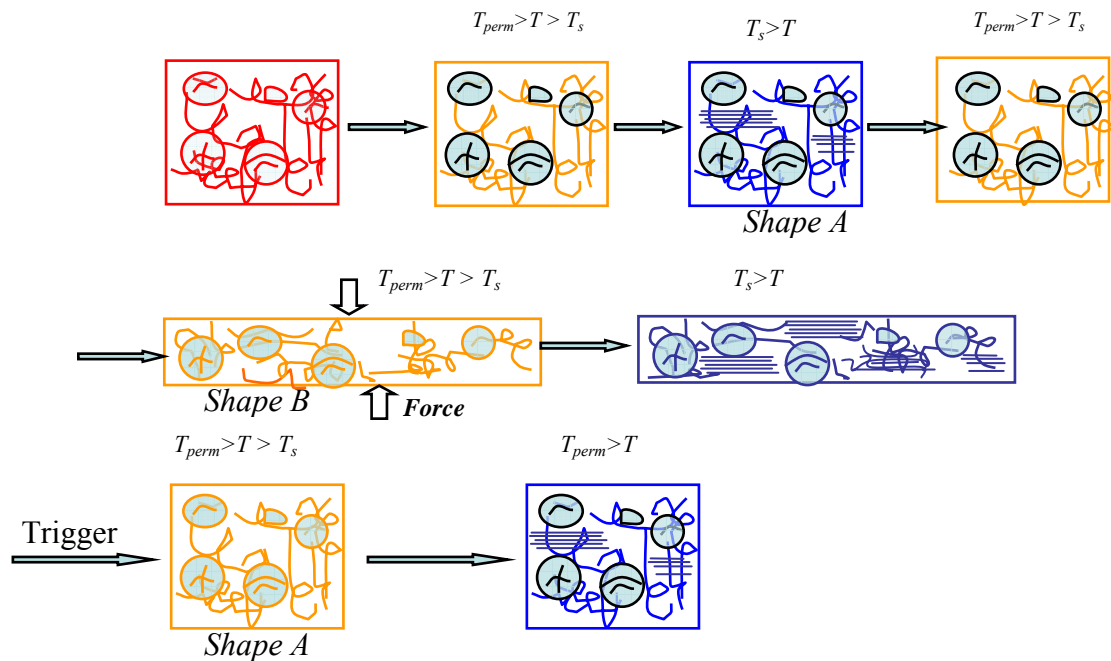


Figure 2.2 Schematic representation of the molecular mechanism of the thermally induced shape-memory effect for segmented polyurethane. (T_s : T_m of soft segments)

soft segment content, its molecular weight, and morphological structure play significant role on the SME [5, 9]. Conducting research on SMPU, these

parameters are paramount on controlling the shape memory property in general. This in turn, provides a mean to control the measurable shape recovery and shape fixity ratio in particular.

2.2 Structure-property relationship of SMPU & SMPU Ionomers

It is totally different from conventional polyurethane elastomer that there is micro phase separation structure in shape memory polyurethane. The mechanism of the thermally induced shape-memory effect of these materials is based on the formation of phase segregated morphology. Moreover, in one of phase, there is a transition temperature in usage temperature range such as melting point or glass transition temperature of soft segments. In addition, the formation of stable hard segment domains acting as physical crosslink above the permanent transition point (T_{perm}) is responsible for the permanent shape. T_{perm} may be melting temperature of hard segments (T_{mh}) or glass transition temperature of hard segments (T_{gh}) according to different molecular structure, such as hard segment content and molecular regularity of hard segments. Above this temperature, the polymer melting occurs and will be not different from conventional one. The transition temperature T_{trans} is either a melting temperature(T_{ms})[47] or a glass transition temperature(T_{gs})[45, 70]. In the case of T_{ms} , a relatively sharp transition can be observed in most cases while T_{gs} (glass transitions temperature of soft segments) always is located in a broad temperature range. Mixed glass transitions temperature $T_{g\ mix}$ between the glass transition of the hard segment and the soft segment may occur in the cases where there is no sufficient phase separation between the hard segment and soft

segment. Mixed glass transition temperature can also act as switching transitions for the thermally induced shape-memory effect[1].

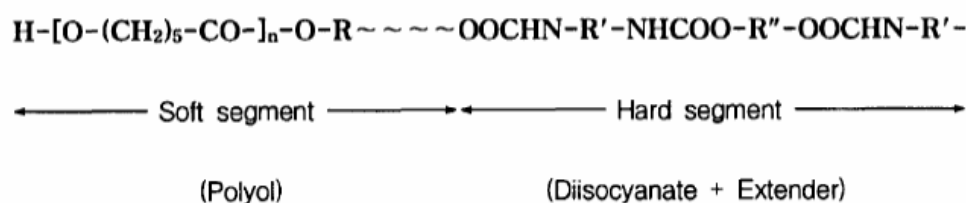


Figure 2.3 Polyurethane with micro phase separation structure

Usually, the linear polyurethane systems are synthesized according to the pre-polymer method. In this process, isocyanate-terminated pre-polymer are obtained by reaction of di-functional, Hydroxy-terminated oligoesters and –ethers with an excess of a low molecular weight diisocyanate. Subsequently, low molecular weight diols or diamines are added as chain extenders to further couple these pre-polymers to form the linear, phase segregated polyurethane- and polyurethane-urea block copolymers. The typical molecular structure of such a kind of PU is shown as Figure 2.3. Through this way, the phase separation morphology will be obtained.

Besides, through introduction of different functional segments and groups in hard segments or soft segments, the shape memory polyurethane will be imparted with other specific properties, for instance high water vapor permeability, biocompatibility, biodegradability which might enlarge the application scope of such kind of smart materials[26, 37, 45, 46]. Meanwhile, the composites, composed of shape memory polyurethane with glass fibers or nano materials

(carbon nanotube, nano CSi) or conducting carbon black, is found that not only the shape memory effect can be retained in such series of materials, but some novel function, such as higher recovery stress, improvement of the mechanical weakness and electric conductivity, can be realized as well[21, 56, 60, 71]. As for the pattern of external stimulus, except for the usually used heating to the switching temperature, there are some novel trigger methods reported, such as remote ultraviolet light activation[13], electro-activation[19], remote activation with infrared irradiation[21], electromagnetic activation[20], water activation[14-18] to activate the shape recovery in the shape memory polymer with specific molecular or configuration design.

Choice of soft segments and hard segments depends on the molecular structure design according to the application requirement such as the melting temperature of soft segments, glass transition temperature of soft segments, mechanical properties of segmented PU, light fastness of such kind of products and so on. Usually, the soft segments can be composed of poly ether (PTMG(poly(tetrahydrofuran)), PPG(poly(propylene oxide))) or poly ester (PEA(poly(ethylene adipate)), PCL(poly(ϵ -caprolactone))) for its low polarity; the hard segment consists of diisocyanate (MDI(4,4'-diphenylmethane diisocyanate), IPDI(Isophorone diisocyanate), TDI(Toluene diisocyanate), HDI(Hexamethylene diisocyanate)) and chain extender (BDO(Butane-diol), HD(Hexane-diol), DMPA(Dimethylol propionic acid), NMDA(N-methyldiethanolamine)) for its high polarity. In some special molecular design, HDI was used to form the part of the soft segment and DMPA or other tiny extender can be introduced into the hard segment[45]. In that it is worth noting

that the difference between the soft segment and hard segment is the polarity. Meanwhile, together with the difference on molecule polarity, strong hydrogen bonding function between carbonyl groups and amine groups on hard segments can induce the phase separation which will cause the formation of soft domain or/and hard domain — the main characteristic of segmented polyurethane. Some literatures have reported the research progress about the relations between properties and structure of shape memory polyurethane as follows:

Mitsubishi Heavy Industries developed shape memory polyurethane with the glass transition point as switching temperature in the 1980s[72]. Hayashi and coworkers reported the research progress including the structure and property, shape memory mechanism and thermo mechanical constitutive modeling of this series of shape memory polyurethane[22, 70, 73, 74]. In the series of PEA(poly(ethylene adipate)) polyurethane systems, the range of switching temperature determined by the glass transition temperature of soft segments(T_{gs}) is from -4.8°C to 48°C with tailoring the molecular chain structure[70]. In the conclusion, the glass transition temperature of the soft segment is noticeably affected by the molecular weight of the soft segment and MDI/PEA/BDO ratio. It also can be found that T_{gs} show increasing trend with the decrease of molecular weight of the soft segment in the same MDI/PEA/BDO ratio system; the increase of hard segment weight content gives rise to the increase of T_{gs} too. The possible composition of the hard segment and the switching soft segment was described in a patent, in which the hard segment could be formed by TDI, MDI HDI and the chain extender: BDO, ethylene glycol, bis(2-hydroxyethyl)hydroquinone, bis(4-hydroxyphenyl)propane and ethylene oxide; the switching soft segment might

consist of PEO($M_n=600$), poly(propylene oxide)($M_n=400, 700, 1000$), PTMG($M_n=400, 700, 850, 1000$) or a combination of biophenol A and propylene oxide and PEA[75]. Besides, Chun et al.[10, 76] ever studies the shape memory polyurethane block copolymers composed of MDI, PTMG ($M_n=1000$) and BDO as chain extender. In the study, the soft segment length was fixed to inspect the effect of hard segment content on the shape memory effect and micro-structure, suggesting that the mechanical properties of polyurethane block copolymers film are influenced by the hard segment content and phase separation; the shape recovery of 80-90% is obtained at the hard segment content of 30-40%, but shape recovery property is not observed with excess or shortage of hard segments. In the research of shape memory polyurethane with the glass transition temperature of soft segments as switching temperature, the mixing of the hard segment and soft segment can not be neglected. Therefore, in the case of less-separation phases, which usually are obtained with the usage of the short soft segment in the segmented polyurethane synthesis, the mixed T_g will form the switching temperature, which will be located between the T_g of pure hard segment phase and soft segment phase. There is an example with mixed T_g , which is composed of MDI, BDO and PTMG as soft segments having the molecular weight of 250 and 650 studied by Chen and the coworkers[8, 9]. The highest thermal transition temperature (T_{perm}) is decided by the melting point of hard segments and in the range between 200 to 240 °C; the corresponding switching temperature could be controlled in the range from 16 to 54 °C for the SMPU with a soft segment of $M_n=250$ (hard segment content between 57 and 95%); from -13 to 38 °C for that with a soft segment of $M_n=650$ (hard segment content between 57 and 95%); and from -36 to 22 °C for that with a soft segment of $M_n=1000$. But, for the SMPU

with the soft segment with $M_n=2000$ or above, a mixed T_g was not observed for the high extent of phase separation. In this study, the switching temperature depends on the hard segment content for the hard segment content can alternate the extent of phase mixing or restrict the mobility of soft segments.

In the case of shape memory polyurethane with the strong crystalline polyester as the soft segments, the melting point of the crystallization of soft segments was used as switching temperature and to be responsible for the fixity of temporary deformation. For PCL based shape memory polyurethane, Li and associates[7, 77] ever systematically studied shape memory behavior of the series of PCL/MDI/BDO segmented polyurethane with strain recovery investigation method. It is reported that a lower limit of PCL molecular weight, below which the PCL segments were not able to crystalline at the usual processing conditions, is in the range of 2000-3000 and exhibits a slight increase with increasing hard-segment content of polyurethanes; the minimum weight content of hard segment domain acting as physical crosslinks in the temperature range above the melting temperature of soft segment crystals is about 10 wt%. Through investigating the segmented PU composed of PCL of 1600-7000 molecular weights and the hard segment of 7.8-27 wt%, the below two prerequisites for a segmented copolymer with shape memory behavior were summarized: the high crystallinity of the soft segment regions and the formation of stable hard segment domains acting as physical crosslinks. The switching temperature for the shape memory effect can be varied between 44 to 55°C with the adjustment of soft segment length and hard segment content. And it also slightly increases in the initial three repeated strain recovery process. This behavior is explained with the destruction of weak

crosslinks among hard segments and the specimens become an ideal elastic network in this treatment. Kim et al.[5] prepared a series of PCL based shape memory polyurethane with various soft segment length ($M_n=2000, 4000, 8000$) and soft segment content (50-90 wt%) and studied the effect of soft segment length and soft segment content on the cyclic tensile properties as well as the dynamic mechanical and mechanical properties, illustrating that the glassy state and rubbery state modulus of PCL based polyurethane strongly depended on the soft segment length and content; the shape memory characteristics of the segmented polyurethanes having crystallizable soft segments are closely related to the temperature-dependent dynamic mechanical properties of the materials. The “cyclic hardening” behavior can be observed from the slope of loading curve in cyclic tensile test and is interpreted by the orientations of PU segments during extension. Meanwhile, the variation of cyclic hardening, residual strain and the shape of stress-strain curve are mostly confined to the first several cycles and no significant change is observed with further cycles.

As far as shape memory PU ionomers is concerned, with the introduction of ionic groups into molecular chain, the relations between properties and structure will be of specific characters and ever described in the literature reported by Kim *et al.* [47]. This series of shape memory PU ionomers composed of 4, 4'-diphenylmethane diisocyanate (MDI), poly (ϵ -caprolactone)(PCL), 1, 4-butanediol (BDO), dimethylolpropionic acid (DMPA), show the different properties compared with the corresponding non-ionomers for the Coulombic force among the ionic groups within hard segments. The ionomers gave higher hardness, modulus and strength and the effects are more pronounced with

increasing hard segment content and at room temperature. Meanwhile, the DSC result indicated that for PCL-4000 ($M_w = 4000$) based PUs with 70 % soft segment content, the PU non-ionomers and ionomers showed similar thermal behavior except that the non-ionomers were of slightly lower ΔH_{cs} (heat of crystallization) and ΔH_{fs} (heat of fusion), implying an enhancement of the microphase separation in the ionomers. However, when the soft segment content is 55 % with the same soft segment length, its crystallization is observed in solely non-ionomers but not in ionomers, suggesting that ionic groups within hard segments in this case hinder the crystallization, decrease the phase separation. Accordingly it is concluded that the two-fold effect of ionic groups within hard segments on microphase separation exists. Kim also reported that for the ionomers and non-ionomers, it can be seen that the ionomers give higher recovery strain and lower residual strain as compare with the non-ionomers, while the strain upon unloading is almost the same. Jeong et al. [46] preliminarily investigated the shape memory properties of SMPU ionomers based on poly (ϵ -caprolactone) (PCL), 4, 4'-diphenylmethane diisocyanate (MDI), 1, 4-butanediol (BDO), dimethylolpropionic acid (DMPA), hexamethylene diisocyanate (HDI), and hexamethylene diamine [54] with DMPA content ranged from 1.5 to 4.5 % using cyclic tensile test. Their result suggested that fatigue of the SME is reduced with the incorporation of ionic moieties into hard segments. It was then evident that ionic moieties on hard segments can influence the SME significantly.

2.3 Anti—bacterial activity of polyurethane ionomers

Bacterial infection remains one of the most serious complications associated with the use of medical devices. An estimated 45% of hospital infections are related to implants and medical devices[78]. Bacteria can adhere to the surface of biomaterials as well as the proteins absorbed to that surface and form the colony or bio-film. Then the bacteria might further the hematogenous spread and colonization. Biocidal coatings are widely used to prevent the growth of microorganisms on the surface of materials. At the present time, the protection is achieved by leaching of bioactive molecules from the coating. However, these molecules are highly toxic to the environment and the protection is short-lived due to the difficulty of controlling the rate of diffusion. Therefore, one effective strategy was developed to kill the microorganism in contact with the substratum, which has given to the deep study of polymer materials containing immobilized biocides.

In polyurethane ionomers, a variety of polyurethane anionomers and cationomers have been found to possess substrate bonding antibacterial activity with choosing the suitable ionic groups and the counter-ion agent. For polyurethane anionomers, for instance, Kim and the associates[79] ever reported that the waterborne polyurethane-urea anionomers composed of isophorone diisocyanate(IPDI), poly(tetramethylene oxide)(PTMG), dimethylol propionic acid(DMPA) and ethylene diamine with the 28:1 mol/mol ammonium hydroxide/cupric hydroxide as counter-ion, has a strong antibacterial halo, which was attributed to the bactericidal power of Cu^{2+} cation itself. In the study of antibacterial activity of cationomers, the polymer bearing quaternary ammonium

salts (QAS) has been studied for QAS possessing at least one alkyl substituent of eight carbon or more atoms are able to kill microorganisms such as bacteria, fungi and moulds by interacting with the cell membrane[57]. It is claimed to cause the death of the cell by destroying the membrane integrity and the process of the lethal action was described as follows[80]: (1) adsorption onto the bacterial cell surface; (2) diffusion through the cell wall; (3) binding to the cytoplasmic membrane; (4) disruption of the cytoplasmic membrane; (5) release of K^+ ion and other cytoplasmic constituents; (6) precipitation of cell contents and death of the cell. Kawabata and Nishigushi[81] observed that the soluble pyridinium-type polymer cationomers showed strong antibacterial activity against gram-positive bacteria, whereas it was less active against gram-negative bacterial. Cooper and the co-workers[82] synthesize and characterize non-leaching biocidal polyurethane with 1-iodooctane and 1-iodooctadecane as neutralization agent, N, N-bis(2-hydroxyethyl)isonicotinamide (BIN) as chain extender, poly(tetramethylene oxide) (PTMG) as the soft segment. The pyridine ring in BIN was quaternized with a variety of alkyl halides to form cationic polyurethes possessing the biocidal activities against *Staphylococcus aureus* and *Escherichia coli* as well as the good mechanical properties in the dry state. Therefore, it can be tentatively conclude that the polyurethane ionomer is an effective way to introduce the substrate bonding antibacterial activity into this series polymeric molecular system.

From the viewpoint of application, shape memory polyurethane is potentially used as bio-medical materials not only for its shape memory function, but for its low cost, easy processing as well. Other function, for instance biodegradable

property, could broaden the usage area of shape memory polyurethane materials immensely. In this way, the smart degradable suture was created to illustrate the potential of these shape memory thermoplastics in biomedical applications[37]. In that, the novel function such as substrate bonding anti-bacterial activity is also expected to satisfy the requirement for such kinds of bio-materials in some areas such as immobilizations materials for the disabled patients. Therefore, the realistic significance of shape memory polyurethane ionomers with anti-bacterial activity can be seen obviously.

2.4 Shape memory polyurethane fibers

Presently, there are few literatures about the study of shape memory polyurethane fibers. But the sparse application and production of the kinds of functional fibers has aroused much attention. In the patent, Hayashi et al.[83] reported that a woven fabric of shape memory polymer which is formed by weaving yarns of shape memory polymer fibers along or by weaving said yarns or ordinary natural or synthetic fibers wherein the shape memory polymer fibers are made of a polyurethane elastomer having a shaped memory property. The switching temperature dependent on the glass transition or melting point of the shape memory fibers used can be set to the temperature higher or lower than room temperature in terms of application requirement such as the need of crease retention or wrinkle free and the handle properties. The raw materials include the TDI (2,4-toluene diisocyanate), MDI (4,4'-diphenylmethane diisocyanate), PBA, PPG, PTMG, PEA, BDO, bis(2-hydroxyethyl)hydroquinone), bisphenol-A plus ethylene oxide. Besides, Chun et al.[10] ever studied the shape memory polyurethane composed of PTMG, BDO, MDI, with the switching temperature

range from -15°C to 1.5°C . Meanwhile, the shape memory fibers made of this series shape memory polyurethane can be prepared with electrospinning with the use of the mixed solvent of DMF(N,N-dimethylformamide) and THF(tetrahydrofuran)[76] when the hard segment is 40 or 50 wt%. The electrospun polyurethane nonwovens with hard segment concentration of 40 and 50 wt% were found to have a shape recovery of more than 80%. Since 2003, the Shape Memory Textile Centre in The Hong Kong Polytechnic University has applied shape memory polyurethane in fiber spinning, fabric finishing, garment finishing with various techniques so as to impart shape memory function into fibers and garment products[25-36]. Hereinto, the effect of hard segment content, post-treatment, thermal setting temperature on morphology and SME were analyzed systematically. Consequently, these factors can be used as a mean to control the properties of SMPU fibers.

CHAPTER 3 PREPARATION OF SMPU IONOMERS

3.1 Factors affecting shape memory effect in SMPU ionomers

Based on the literature review, it can be found the shape memory polyurethane has the unique characteristic molecular structure compared with the ordinary polyurethane. The properties of ordinary polyurethane (e.g., from 1, 6-hexane diisocyanate and 1,4-butane diol) are similar to polyamides. The starting materials can be composed of two components: a) diisocyanate and b) either short chain glycol or long chain polyethers or polyester glycol [84]. The polyurethane consisting of short chain glycol and diisocyanate possesses a large amount of hydrogen bonding [85] between –NH- and –OC- groups. Therefore, it is of high hardness, strength and low degree of solubility. Instead, if the polyurethane synthesized by the reaction of long chain, non-crystalline, unbranched, OH-functional polyethers or polyesters with stoichiometric amounts of diisocyanates contains about 4 to 7 % urethane groups [86], the intermolecular forces for polyethers and polyesters PU are weak van der Waals force and the hardness and strength are comparatively low and the products exhibit rubber-like properties. Both types of products have only one phase and can not restore the temporary deformation and recover to the original shape with external heating trigger. The technical importance of ordinary PU is cross-linked hard products (PU rigid foams, non-textile coatings). In contrast, SMPUs can recover the most of their original length (shape) even after the large amount of deformation through a micro-Brownian movement triggered by heating to the temperature above the transition temperature, which is caused by the entropy elasticity and

the net points among hard segments. Segmented polyurethanes showing shape memory properties are composed of three basic starting materials: a) long chain polyether or polyester polyol; b) diisocyanate and c) diols or diamine (chain extender). Diisocyanate and chain extender are hard segments and the long chain polyol is the soft segment. The properties of segmented polyurethane are dependent on this block copolymer structure and the resulting morphology. Thereof, the micro-phase separation structure is necessary and due to the thermodynamic incompatibility between the hard and soft segment. Hard segments can bind themselves via hydrogen bonding and crystallization, making the segmented polyurethane very stiff below melting temperature of hard segments. Reversible phase transformation of soft segments is reported to be responsible for fixing the temporary deformation and dependent on the molecular weight of the soft segment, mole ratio between hard and soft segments, categories of the soft/hard segment and polymerisation process[70]. As for SMPU ionomers, the category of ionic groups, neutralization reagent, ionic group content also were considered as the factors affecting shape memory effect.

3.2 Molecular design for SMPU ionomers

In order to make micro phase separated morphology in SMPU ionomers to realize the shape memory function, two or three steps condensation polymerization in solution was applied. In the synthesis of pre-polymer, the crystallizable polyols, such as polycaprolactone with molecular weight 4000 or 10000, was reacted with the excess of diisocyanate to produce the pre-polymer capped with isocyanate groups. And then, the stoichiometric chain extender was

added into the reaction system to finish the condensation polymerization. In this

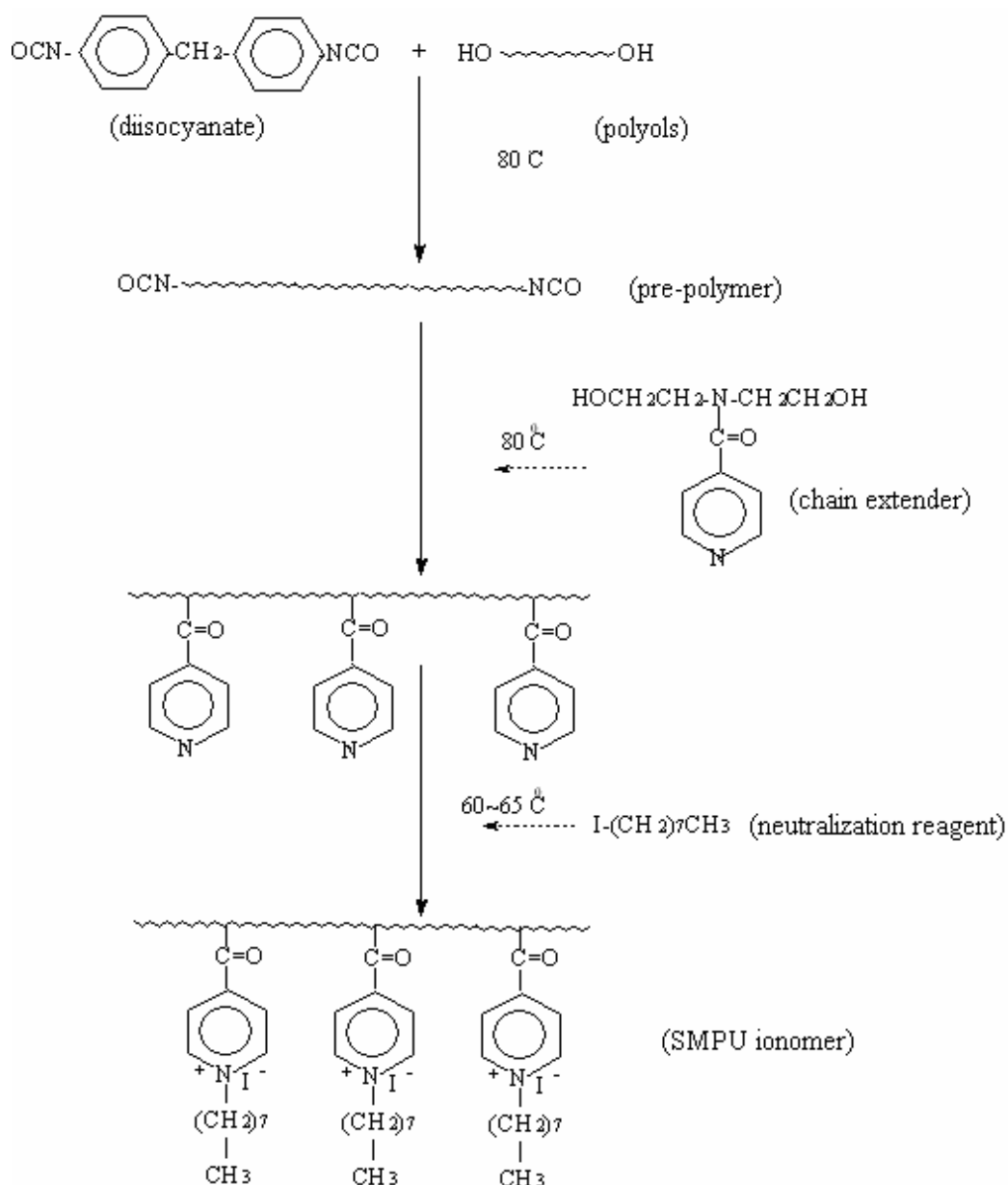


Figure 3.1 Pre-polymerization to synthesis SMPU ionomers

way, the crystallisable soft segment was introduced into the segmented polyurethane to form the reversible phase with T_{ms} (melting point of the soft segment) as switch temperature for shape memory function. Meanwhile, Considering the minimum limitation of hard segment content to form sufficient

physical cross link network and the length of crystallizable soft segments offering the enough fixity ability reported by Li et.al.[7], the polycaprolactone with molecular weight 4000 or 10000 was chosen as the soft segment and the hard segment content was 40wt%, 25wt% or 20wt% to synthesis SMPU anionomers and cationomers respectively.

The samples for the study about segmented PU anionomers include two series specimens. The first series of SMPU anionomer samples with different molecular weight was synthesized for studying the effect of ionic groups within hard segments on the crystallization of soft segments. In this series specimens, the soft segment is PCL with molecular weight 4000 and the hard segment content is 20 wt%. The total molecular weight was controlled by the ratio between isocyanate and hydroxyl groups and the hard segment content was fixed. The other series of SMPU anionomer samples with enough high molecular weight (the ratio NCO/OH was in the range from 1.0 to 1.1.) was synthesized and used in the investigation about the influence of ionic group content on SME. The corresponding length of the soft segment and the hard segment content are also the fixed values: 4000 and 40wt%. As for SMPU cationomers, PCL with molecular weight 10000 was chosen to be the soft segment and the hard segment content is 25 wt% including chain extender and isocyanate. Moreover, based on our previous study for SMPU fibers, the PBA with molecular weight 600 was used in SMPU ionomer synthesis for fiber spinning[28, 31]. In this case, the glass transition temperature of amorphous soft segment rich phase was used as switch temperature in shape memory function. As shown in Figure 3.1, the ionic groups were introduced into the molecular system with the usage of chain

extender containing ionic groups including anion or cation groups. Since the influence of hard segment content and soft segment length have been widely studied in lots of literature reported previously, the focus of this study is the effect of the ionic group category and content on shape memory effect. Therefore, the length of soft segments and the hard segment content were fixed in each series SMPU ionomers and the ionic group content was denoted with the weight content of the chain extender containing ionic groups. The ionic group content was increased from the minimum to the maximum amount, which is dependent on the specific molecular structure. In the process of polymerization, the ratio of isocyanate and hydroxyl groups was kept to be 1.0 around to make the molecular chain extended to the maximum except for SMPU ionomers with M_w controlled purposely by using the ratio between isocyanate and hydroxyl groups. In that, if the stoichiometric chain extender with ionic groups is not enough to react with diisocyanate groups, BDO will be used as a part of chain extenders in this case so as to keep the ratio between isocyanate and hydroxyl groups to be around 1.0.

As far as the neutralization step involving the weak base and the weak acid, such as the triethylamine / carboxyl group and $R_3N/R'COO^-$ is concerned, the acid strength of Acetic acid is stronger than that of R_3NH^+ , and the base strength of R_3N is stronger than that of $R'COO^-$. Therefore, the neutralization reaction should go to completion[48]. According to the published value of $K_a=1.74\times 10^{-5}$ for acetic acid, $K_b=5.25\times 10^{-4}$ for triethylamine and $K_w=1.0\times 10^{-14}$ for water, we can calculate the equilibrium constant for neutralization as $K=K_a\cdot K_b/K_w=9.14\times$

10^5 [87]. The equilibrium conversion of acid or triethylamine calculated from the K value is 99.9%, indicating the nearly complete reaction[88].

3.3 Synthesis routine and sample preparation

3.3.1 Raw materials for synthesis of SMPU ionomers

The specific formulae of the PU samples are shown in the part of 3.3.2 In pretreatment process for chemicals, PCL diols (DAICEL CHEMICAL INDUSTRIES LTD) with molecular weight (M_n) 4000 and 10000 were dried and degassed at 80 °C under 1-2 mmHg for 12 hours prior to PU synthesis.

Table 3.1 Raw materials for the synthesis of SMPU ionomers

Raw materials		Supplier	Pre-treatment
MDI	4, 4'-diphenylmethane diisocyanate	Aldrich Chemical Company, USA	No further treatment
PCL-4000	polycaprolactone diols with molecular weight 4000	Daicel Chemical Industries Ltd, JAPAN	Drying under vacuum
PCL-10000	polycaprolactone diols with molecular weight 10000	Daicel Chemical Industries Ltd, JAPAN	Dehydration under vacuum
PBA-600	poly(butylenes adipate) With molecular weight 600	CHINA	Dehydration under vacuum
BDO	1, 4-butanediol	Acros Organics, USA	Dried by molecular sieves
BIN	N,N-bis(2-hydroxyethyl)isonicotinamide	Aldrich Chemical Company, USA	No further treatment
NMDA	N-Methyldiethanolamine	Advanced Technology & Industrial Company, USA	No further treatment
DMPA	2,2-Bis(hydroxymethyl)propionic acid,	Acros Organics, USA	No further treatment
HAc	Acetic acid glacial	International Laboratory, USA	No further treatment
C8I	1-Iodoctane	International Laboratory, USA	No further treatment
TEA	Triethylamine	International Laboratory, USA	No further treatment
DMF	Dimethylformamide	Ajax Finechem, New Zealand	Dried by molecular sieves

Extra pure grade of MDI (Aldrich Chemical Company, USA), DMPA (Acros Organics, USA), NMDA (Advanced technology & industrial company, USA), BIN (Aldrich Chemical Company, USA) were used without further treatment. BDO (ACROS, ORGANICS) was dried by molecular sieves. Triethylamine (TEA) (International Laboratory, USA), HAc (Acetic acid glacial, INTERNATIONAL LABORATORY, USA), 1-Iodooctane (C8I) (International Laboratory, USA) were used to neutralize the ionic group with stoichiometric amount. Dimethylformamide (DMF) is dehydrated with 4 Å molecular sieves for several days in advance before using as solvent in PU synthesis. All raw materials were listed in Table 3.1.

3.3.2 Synthesis routine and recipe of SMPU ionomers

3.3.2.1 SMPU anionomers

For the study about the influence of ionic groups on the crystallization and melting behavior in segmented PU with different molecular weight, polycaprolactone diols with molecular weight 4000, 4, 4'-diphenylmethane diisocyanate (MDI), 1, 4-butanediol (BD) and dimethylolpropionic acid (DMPA) were used in the synthesis of segmented PU non-ionomers and ionomers. The formulae of the PU samples are shown in Table 3.2. The reaction to prepare the pre-polymer with PCL and MDI was carried out at 80 °C for 2 hours in a 500 ml round-bottom, four-necked flask filled with nitrogen and equipped with a mechanical stirrer, a thermal meter, and a condenser. Following the chain extension process with BDO and/or DMPA for another 2 hours, the neutralization reaction was carried out at 40 °C for 1 hour by adding stoichiometric amount of TEA agent, subsequently. Prior to neutralization

reaction, some of the PU solution was used for film casting of the corresponding PU non-ionomers.

Table 3.2. Formulae of the synthesis of segmented PU anionomers with different molecular

Sample	PCL wt% ^a	DMPA wt% ^b	Soft Segment (mol)	Hard Segment (mol)			M_w	$\frac{M_w}{M_n}$
			PCL-4000	MDI	DMPA	BDO ^c		
PU-20N PU-20I	80.0	5.0	0.34	1	0.63	0.03	20,200	3.2
PU-58N PU-58I	80.0	5.0	0.34	1	0.63	0.03	58,500	4.7
PU-71N PU-71I	80.0	5.0	0.34	1	0.63	0.03	71,600	3.7

^a Mass content of soft segments in PU samples

^b Mass content of DMPA in PU samples

^c BDO content can change slightly to obtain different M_w values

In this project, the content of DMPA, soft segments, and the extent of neutralization in PU ionomer and non-ionomer samples were adjusted to approximately the same values as shown in Table 3.2 to investigate the effect of ionic groups on the crystallization mechanism of PCL-4000 based PU with various M_w values. Molecular weight of the PU was determined by using GPC with THF as the eluting solvent. The series of PU samples is designated as PU-XX, where XX denotes the weight average molecular weight in kg/mol, a letter either representing non-ionomers-“N” or ionomers-“I” is then followed. The soft segment content is calculated by assigning PCL-4000 units to the soft segment.

To investigation the effect of ionic groups content on SMPU anionomers, PCL diols with molecular weight (M_n) 4000, MDI, DMPA, BDO were used to synthesize segmented polyurethane anionomers. The formula of this series of

SMPU anionomers is shown in Table 3.3. Triethylamine (TEA) was chosen to neutralize the carboxyl groups of DMPA with the same mole. The reaction to prepare the pre-polymer with PCL and MDI was carried out at 80 °C for 2 hours in a 500 ml round-bottom, four-necked flask with a mechanical stirrer, nitrogen, thermal meter and condenser, followed the chain extension with BDO and/or DMPA for the same period of time. Thereafter the neutralization reaction is followed at 40 °C for 1 hour by adding stoichiometric amount of TEA agent. Before neutralization, some of PU solution was poured out from the flask for film casting of the corresponding PU non-ionomers. The hard segment content and soft segment length in PU ionomer and non-ionomer samples are controlled to the approximately the same value so as to investigate the effect of ionic group content on the shape memory effect of PCL-4000 based SMPU cationomers.

Table 3.3 Formula of the polyurethane synthesis

Sample Code	PCL (wt%)	DMPA (wt%)	PCL (Mole)	DMPA (Mole)	BDO (Mole)	MDI (Mole)	TEA (Mole)	M_w	$\frac{M_w}{M_n}$
60-0	60	0	1	0	7.1	8.1	0	169520	3.26
60-2I	60	2	1	1	6	8	1	100240	3.58
60-5I	60	5	1	2.5	4.3	7.8	2.5	62700	2.85
60-8I	60	8	1	4	2.6	7.6	4	78010	2.69
60-10I	60	10	1	5	1.5	7.5	5	104640	3.27
60-13I	60	13	1	6.3	0	7.3	6.3	84500	3.25
60-2N	60	2	1	1	6	8	0	100240	3.58
60-5N	60	5	1	2.5	4.3	7.8	0	62700	2.85
60-8N	60	8	1	4	2.6	7.6	0	78010	2.69
60-10N	60	10	1	5	1.5	7.5	0	104640	3.27
60-13N	60	13	1	6.3	0	7.3	0	84500	3.25

This series of samples (non-ionomers and ionomers) are identified by the first number denoting the soft segment content, the second number representing the DMPA weight content and a letter showing the non-ionomers-“N” and ionomers-“I”, such as 60-5I in which “60”, “5” and “I” mean 60wt% soft segment content, 5wt% DMPA content and ionomers neutralized with TEA respectively. The sample 60-0 does not comprise DMPA and just is composed of MDI, BDO and PCL-4000 as comparison with the two series above.

3.3.2.2 SMPU cationomers

In order to investigate the crystallization and melting behavior of crystallizable soft segments of SMPU cationomers, SMPU cationomers were synthesized from polycaprolactone diols (PCL), 4, 4'-diphenylmethane diisocyanate (MDI), 1, 4-butanediol (BDO) and N,N-bis(2-hydroxyethyl)isonicotinamide (BIN). The formulation of the PU samples is shown in Table 3.4. PCL diols with M_w 10000, MDI, BDO, and BIN were used to synthesize the SMPU cationomer samples. Acetic acid (HAc, International Laboratory, USA) and 1-Iodooctane (C8I, International Laboratory, USA) were used to neutralize BIN with the same mole[48, 82]. Dimethylformamide (DMF) is used as solvent in PU synthesis.

The Pre-polymerization with PCL and MDI was carried out at 80 °C for 2 hours in a 500 ml round-bottom, four-necked flask filled with nitrogen and equipped with a mechanical stirrer, a thermal meter, and a condenser, following the chain extension process with BD and/or BIN for another 2 hours, the neutralization reaction was carried out at 40 °C or 65 °C for 2 hour by adding stoichiometric amount of HAc or C8I agent, subsequently[48, 82]. The series of SMPU

ionomers neutralized with HAc are nomenclated by abbreviation of ion chain-extender and followed by 3 numbers as shown in Table 3.4. The first two numbers denote the soft segment contents. The third number represents the BIN weight content. As an example, the sample BIN75-11 contains 75 wt% of soft segments, approximate 11wt% of BIN (10.56 wt% in formula), the default neutralization agent, HAc. The sample 75-0 contains no BIN but only MDI, BDO and PCL-10000 components as the control sample in this study. For the sample neutralized with C8I, the similar denotation to those neutralized with HAc is followed by hyphen and C8, which illustrates that the neutralization agent is 1-Iodoctane, such as BIN75-11-C8.

Table 3.4 Formulae of SMPU cationomers for investigating the crystallization and melting behavior of soft segments

Sample Code	PCL (wt%)	BIN (wt%)	PCL (mole)	BIN (mole)	BDO (mole)	MDI (mole)	HAc (mole)	C8I (mole)	M_w	$\frac{M_w}{M_n}$
75-0	75	0	1	0	9.07	10.07	0	0	98300	5.02
BIN75-6	75	6	1	3.81	3.91	8.71	3.81	0	107200	5.66
BIN75-11	75	10.56	1	6.7	0	7.7	6.7	0	94100	6.55
BIN75-6-C8	75	6	1	3.81	3.91	8.71	0	3.81	97100	6.14
BIN75-11-C8	75	10.56	1	6.7	0	7.7	0	6.7	176500	6.72

The formulae of the SMPU cationomers shown in Table 3.5 and Table 3.6 are designed for comparing the effect of cationic group content on shape memory effect in segmented polyurethane cationomers. PCL with molecular weight (M_n) 10000, MDI, NMDA, BIN, BDO were used in polymerization reaction. HAc was added to neutralize the cationic group with stoichiometric amount. Prepolymer was synthesized by terminating a 10000 g/mol molecular weight PCL with diisocyanate MDI at 80 °C for 2 hours in a four-necked cylindrical

CHAPTER 3 PREPARATION OF SMPU IONOMER

vessel equipped with a mechanical stirrer. Then it was chain-extended with BDO and/or NMDA or BIN for the same period of time. Dimethylformamide (DMF) was used in the PU synthesis as solvent. The neutralization reaction was carried out at 40 °C for 1 hour by adding stoichiometric amount of HAc subsequently. The series of PU copolymers cationomers are nomenclated by abbreviation of ion chain-extender and followed by 3 numbers. The first two numbers denote the soft segment content, the third number represents the ion chain extender weight content, and for some PU non-cationomers, the alphabet

Table 3.5 Formulation of NMDA series PU ionomers

Sample Code	PCL (wt%)	NMDA (wt%)	PCL (mole)	NMDA (mole)	BDO (mole)	MDI (mole)	HAc (mole)	M_w	$\frac{M_w}{M_n}$
75-0	75	0	1	0	9.07	10.07	0	98300	5.02
NMDA 75-2	75	2	1	2.24	6.64	9.88	2.24	61100	4.30
NMDA 75-4	75	4	1	4.48	4.21	9.69	4.48	53300	5.16
NMDA 75-8	75	7.46	1	8.35	0	9.35	8.35	54000	4.5
NMDA 75-4N	75	4	1	4.48	4.21	9.69	0	53800	3.86
NMDA 75-8N	75	7.46	1	8.35	0	9.35	0	55000	4.17

Table 3.6 Formulation of BIN series PU ionomers

Sample Code	PCL (wt%)	BIN (wt%)	PCL (mole)	BIN (mole)	BDO (mole)	MDI (mole)	HAc (mole)	M_w	$\frac{M_w}{M_n}$
75-0	75	0	1	0	9.07	10.07	0	98300	5.02
BIN75-4	75	4	1	2.54	5.63	9.16	2.54	90500	5.60
BIN75-6	75	6	1	3.81	3.91	8.71	3.81	107200	5.66
BIN75-8	75	8	1	5.07	2.19	8.27	5.07	90800	6.4
BIN75-11	75	10.56	1	6.7	0	7.7	6.7	94100	6.55
BIN75-6N	75	6	1	3.81	3.91	8.71	0	113400	8.96
BIN75-11N	75	10.56	1	6.7	0	7.7	0	107500	9.11

“N” in the end indicating that it is the sample without neutralization for the corresponding ionomers. As an example, the sample NMDA75-4 contains 75 wt% of soft segments, approximate 4 wt% of NMDA and its non-ionomers is NMDA75-4N. The sample 75-0 contains no NMDA or BIN but only MDI, BDO and PCL-10000 components as the control sample in this study.

3.3.2.3 SMPU ionomers with antibacterial activity

Cooper and co-workers ever reported the biocidal activities of a series of quaternized polyurethane ionomers against *Staphylococcus aureus* and *Escherichia coli*[82]. Therefore, BIN was incorporated into segmented PCL based polyurethane as chain extender. In this study, the soft segment length and hard segment content were fixed so as to investigate the ionic group content on this series segmented polymer ionomers. As shown in Table 3.7, the PCL with

Table 3.7 Formulation of SMPU ionomers and non-ionomers

Sample Code	PCL (wt%)	BIN (wt%)	PCL (mole)	BIN (mole)	BDO (mole)	MDI (mole)	C8I (mole)	M_w	$\frac{M_w}{M_n}$
75-0	75	0	1	0	9.07	10.07		98300	5.02
BIN75-6N	75	6	1	3.81	3.91	8.71		113400	8.96
BIN75-11N	75	10.56	1	6.7	0	7.7		107500	9.11
BIN75-6-C8	75	6	1	3.81	3.91	8.71	3.81	97100	6.14
BIN75-11-C8	75	10.56	1	6.7	0	7.7	6.7	176500	6.72

molecular weight 10000 was chosen as the soft segment and the soft segment content was 75wt%. Just like the aforementioned synthesis procedures of SMPU cationomers in the part of 3.3.2.2, pre-polymerization method was applied to prepare this series SMPU ionomers. 1-Iodoctane was used as neutralization agent. The sample codes such as BIN75-6-C8 and BIN75-11-C8 have the

similar denotation as the SMPU cationomers shown in Table 3.4. The other two samples BIN75-6N and BIN75-11N mean the corresponding segmented polymer non-ionomers. The used testing cultures for the test of antibacterial activity are limited in *Staphylococcus aureus* and *Klebsiella pneumoniae*. All the testing procedures were conducted strictly according to relevant standards.

3.3.2.4 SMPU ionomer fibers

The polyurethane (PU) with various hard segment content used in this study were synthesized with pre-polymerization method by using poly-diols, diisocyanate and chain extender. PBA (Poly(buthylene-adipate)) diols with molecular weight (M_n) 600 were dried and degassed at 70 °C under 1-2 mmHg for 12 hours prior to PU synthesis. Extra pure grade of MDI (4, 4'-Methylenebis(phenyl isocyanate) (Aldrich Chemical Company, USA) was used without further treatment. BDO (1,4-Butanediol) (ACROS, ORGANICS) was dried by molecular sieves beforehand. Pre-polymerization was conducted by terminating PBA with excess diisocyanate MDI in DMF as solvent at 80 °C for 2 hours in a 500ml four-necked flask equipped with mechanical stirrer, purge gas (nitrogen) inlet, thermometer and condenser. After that it was chain-extended with BDO and NMDA for the same period of time. The neutralization reaction was carried out at 40 °C for 1 hour by adding stoichiometric amount of HAc subsequently. Dimethylformamide (DMF) was used in the PU synthesis as solvent, which was added to the reactants occasionally to control the viscosity of solution and dehydrated with 4 Å molecular sieves for two days prior to be used.

Table 3.8 Formula of SMPU ionomer fibers

Sample code	Hard segment content (wt%)	NMDA content (wt%)	Post treatment	M_w	$\frac{M_w}{M_n}$
SMPU64-0-O	64.1	0	Non	70900	3.32
SMPU64-2-O	64.1	2	Non	95300	2.68
SMPU55-0-O	54.7	0	Non	85600	4.53
SMPU55-2-O	54.7	2	Non	86800	2.79
SMPU64-0-S	64.1	0	Steaming	70900	3.32
SMPU64-2-S	64.1	2	Steaming	95300	2.68
SMPU55-0-S	54.7	0	Steaming	85600	4.53
SMPU55-2-S	54.7	2	Steaming	86800	2.79

3.3.3 Preparation of SMPU ionomer specimens

3.3.3.1 SMPU ionomer film

Segmented PU non-ionomer and ionomer films were prepared by transferring some of the PU solution to Teflon moulds with 8 wt%~15 wt% solid content and allowed them to solidify at 60 °C in air ventilation for 24 hours. To remove the residual DMF, the films were held at 70~75 °C under vacuum of 1-2 mmHg for another 24 hours subsequently. The nominal thickness of the films for cyclic thermo-mechanical investigation and dynamic mechanical analysis was about 0.1~0.5 mm.

3.3.3.2 SMPU ionomer fibers spun with wet spinning

In the preparation of SMPU fibers, the SMPU ionomers used in this study were synthesized with pre-polymerization method beforehand by using poly-diols, diisocyanate, chain extender and neutralization agent. Solid concentration of the final polyurethane solution in DMF was adjusted in the range of 20-30 wt% to meet the requirement for viscosity in wet spinning process, in which the PU

solution is extruded through 30 spinneret capillary holes horizontally in coagulation water bath to diffuse out the solvent with spinning speed of approximate 15 m/min, subsequently to form multi-filaments by coagulation. After passing the water bath, the filaments are taken up to apply subsequent process including water bath to further the removal of residual DMF and drying with hot air of 60°C. Then, the SMPU filaments are wound with a given velocity. Then the original shape memory polyurethane fibers can be obtained. The whole setup was shown in Figure 3.2. In order to release the internal stress caused by the velocity difference among rollers in drying and winding process, the original SMPU fibers with constant length were treated with saturated water vapor under around 180kPa for ten minutes. After that, all fiber specimens underwent conditioning process in room temperature (20°C) and room humidity condition (70%) for at least one week before other testing to balance the fraction of moisture.

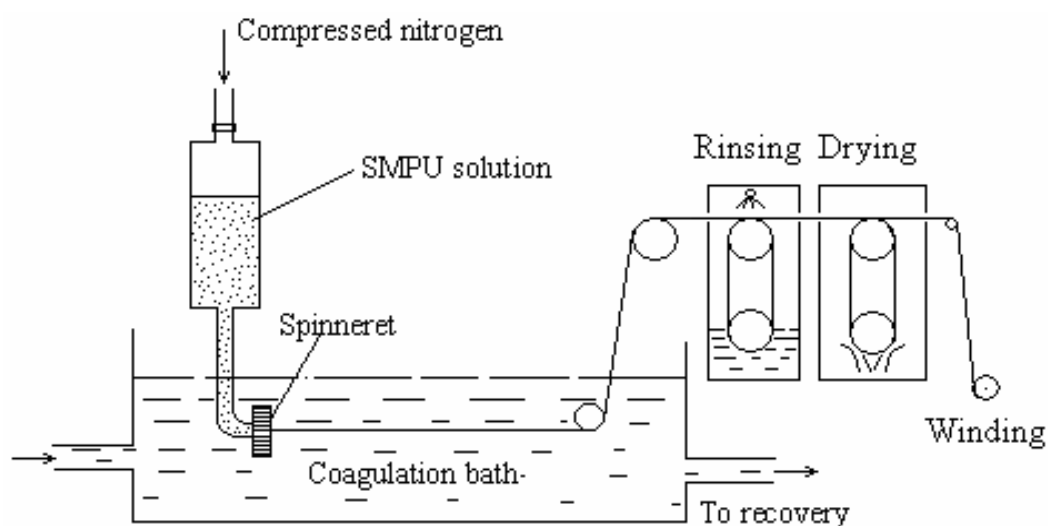


Figure 3.2 wet spinning process for preparing SMPU fibers [31]

CHAPTER 4 CHARACTERIZATION TECHNIQUES

4.1 Differential scanning calorimetry (DSC)

DSC is a technique in which the heat flux (power) compensated to the sample is recorded against time or temperature in a specific atmosphere when the temperature of the sample is programmed such as heating, cooling at given heating/cooling rate. In practice, it is to detect difference in heat flux to a pan containing the sample and an empty pan in the power-compensating DSC. Usually, it is used in polymer research for measuring mainly three parameters[89]:

- Glass-rubber transition temperature (T_g value) determinations
- Melting/re-crystallization temperature and heat determinations
- Measurements on reacting systems (cure measurements)

In this study, the first and second processes were characterized with this technique. The glass transition temperature is non-equilibrium property and is a parameter sensitive to heating rate and the method used[90]. Therefore, T_g obtained differs from one technique to another and is over a range of several degree. The value of T_g is referred to the temperature region at which the amorphous phase of a polymer is transformed from glassy material into a tough rubber-like status and is accompanied by a “step-wise” increase of the heat flow curve. As for melting/recrystallization temperature determinations, usually semi-crystalline polymers generally melt in a quite wide temperature range, which is related to imperfections in the crystallites and non-uniformity in their size: the

smaller and/or less perfectly formed crystallites will melt at lower temperatures. Therefore, in DSC testing process, the melting point represents the measured temperature of the maximum heat flow in the fusion process. The corresponding peak area of melting range is nominated with the melting enthalpy of this crystallization structure. The melting enthalpy can be calculated with the peak area surrounding by the heat flow curve and the baseline. This enthalpy change in this melting process can be determined from the area of the curve peak (A) by using the following relationship[91].

$$\Delta Hm = KA \quad \text{Equation 4.1}$$

Where m is the mass of the polymer specimen and K is a calibration coefficient dependent on the instrument being employed for the measurements.

It is well known that the different thermal histories of specimens, such as the scanning rate of instrument, heating procedure of instrument, and sample weights will have a strong influence on the glass transition and melting process of crystallization structure. Also, some researchers have reported that the micro-phase mixing extent can be analyzed by detecting the glass transition of soft segments in segmented polyurethane[92-95]. The more micro-phase mixing extent will cause the increase of T_g of soft segments in segmented polyurethane. On the other hand, Li and coworkers ever reported that, in segmented polyurethane, the increase of T_g of soft segments can be ascribed to the effects of the soft segment crystallization and hard segment content, in which the later factor was believed to cause the more phase mixing between soft and hard segments[96]. Therefore, in our measurement, the effect of soft segment crystallization was removed by quenching specimens from melting status to

glassy status and in the following heating scan. The T_g of soft segments detected was used to study the effect of ionic groups within hard segments on micro-phase mixing extent. Melting point and enthalpy of SMPU ionomer samples are determined by a Perkin-Elmer Diamond DSC with nitrogen as purge gas. Indium and zinc standards were used for calibration. All samples (~ 5 mg) were heated to 240 °C at 10°C/min beforehand to remove the thermal history and then cooled to -70 °C at a cooling rate of 10°C/min. Subsequently, heating scan up to 240 °C at 10 °C/min was carried out. The soft segment crystallinity of segmented polyurethane ionomer samples was calculated from the enthalpy of 100% crystalline PCL, 32.4cal/g, given by Crescenzi et al[97]. Crystallinity of hard segments in SMPU ionomers was calculated by using the endothermic peak area located at 150°C to 200°C, hard segment content and a value of 36 cal/g for the heat of fusion of MDI/BDO segments determined by Kajiyama and MacKnight[98].

4.2 Dynamic mechanical analysis (DMA)

Dynamic mechanical analysis is a technique in which the elastic and viscous response of a sample under periodical load, are monitored against temperature, time or frequency[89]. In DMA, the stress/strain relationship in heating scan with controlled heating rate was recorded to obtain the information about the relaxation behavior of the test piece.

The dynamic mechanical properties of a polymer are described in terms of a complex dynamic modulus[99]:

$$E^* = \left(\frac{\sigma(t)}{\varepsilon(t)} \right) (\cos \delta + i \sin \delta) = E' + iE'' \quad \text{Equation 4.2}$$

Where E' is called the storage modulus and is a measure of the recoverable strain energy and when loading is small it equals approximately to the Young's modulus. E'' is called the loss modulus and is related to the hysterisial energy dissipation. The phase angle (δ) is given by

$$\tan \delta = E'' / E' \quad \text{Equation 4.3}$$

Table 4.1 Summary of typical values of modulus at various states of a polymer[90]

Phase/transition	Modulus E' (Pa)	Comment
Rigid glass	$10^{10} \sim 10^9$	0 K to T_β
Ductile glass	$\sim 10^9$	Above T_β to T_g ; with 30-50°
Glass-rubber transition	$\sim 10^9 \sim 10^6$	Typically 10-20° in width
Rubber to viscous liquid	$10^6 \sim 10^5$	Typically 50-100° in width and depends on M_w
Viscous liquid to mobile fluid	$10^5 \sim 10^3$	Typically 30-60° in width and depends on M_w

Table 4.1 indicates typical values of the Young's modulus at various states of a polymer and appropriated magnitudes of changes for relaxation transitions[90]. Therefore, DMA is the most commonly used to identify the location of various transitions which often have a significant effect on the modulus values.

In this study, the PU films were prepared by casting in Teflon mould with an area of $5 \times 25 \text{ mm}^2$. The film thickness is about 0.1~0.5 mm and the distance between two clamps is 15mm in the initial testing status. Dynamic mechanical properties of the samples were determined by using a Perkin-Elmer DMA at

frequency of 2 Hz. The heating rate is 2 °C/min and temperature is scanned from -100 to 150 °C. As far as SMPU ionomer fibers are concerned, the length for each fiber sample between crossheads is 15mm and a bunch of 100 fibers was used in each testing process. All the resulting data about the storage modulus was normalized with the linear density of the fiber so as to make the comparison among them. Besides the above heating rate, frequency and heating range for SMPU film testing were used. According to the literature reported, the deformation subjected to periodic stress can be detected to figure out the changes in the dilatation coefficients and expansion coefficient, then to study the various transition regions[100]. Considering the thermal responsive property of shape memory polyurethane fibers studied, there might be inter-stress produced in the spinning process, which will cause a large amount of shrinkage in heating, subsequently lead to the dimensional instability. Therefore, it is necessary to quantitatively investigate the thermal shrinkage extent of various fibers in heating process. So, in this study, dynamic mechanical analysis was used to measure the average strain of the fiber subject to periodic dynamic tensile stress at increasing temperature, then to characterize the extend of heating shrinkage.

4.3 Fourier transform infrared spectroscopy (FTIR)

Fourier-transform infrared (FTIR) spectrometer is a popular method for characterizing polymers. This technique is to probe the chemical bonding vibrations between the atoms of a molecule. An infrared spectrum is obtained by passing an infrared radiation through a sample and determining which fraction of the incident radiation is absorbed at a particular energy. The energy at peaks in

an absorption spectrum corresponds to the frequency of a part of the sample molecule. Therefore, it is a useful tool for identifying a polymer, monitoring the polymerization stage, and characterizing any structural changes under different conditions.

In our experiment, Fourier Infrared Spectra equipped with attenuated total reflectance accessories were determined with 0.5 mm thickness specimen film by using Perkin-Elmer (2000 FT-IR) spectrometer in the region of 700–4000 cm^{-1} at room temperature. Each sample was scanned 30 times at a resolution of 2 cm^{-1} and the scans signals were averaged. The region of carbonyl stretching vibration at 1700~1730 cm^{-1} , the region of amine groups stretching vibration at 3100~3500 cm^{-1} were used to detect changes of the extent of micro phase separation between PU non-ionomers and the corresponding PU ionomers studied. IR spectra can be normalized by using the height of the 1412 cm^{-1} peak, assigned to the C—C stretching mode of the aromatic ring[48]. In the study about SMPU ionomers with substrate bonding antibacterial activity, FTIR was used to detect the neutralization reaction of heterocyclic nitrogen within molecular chain. Besides, the disappearance of NCO absorption at around 2270~2280 cm^{-1} in all segmented PU specimens illustrates that the isocyanate groups can be reacted completely[101-103].

4.4 Gel permeation chromatography (GPC)

GPC, a type of size-exclusion chromatography (SEC), is a technique that employs porous non-ionic gel beads to separated polymers in solution[91].

Beads containing pores of various sizes and distributions are packed into a column in SEC. When a solution containing the polymer of interest is pumped down into this column, the polymers attempt to enter the pores in the packing material. But only sufficiently small polymers can enter the pores, and once they do, they are effectively trapped there until they exit again and return to the flowing solvent. The small polymers are retarded and leave the GPC column last. Various detectors are used to sense when the polymers finally emerge from the column. Fractionation of the polymer sample results as different-sized molecules are eluted at different times. The time it takes a polymer to elute is converted to molecular weight and exactly depends on parameters of GPC. Large molecules cannot permeate the pores and travel rapidly through the void volume. Small molecules travel partly through the porous packing materials and go slower due to hydrodynamic shielding from the flow field. In this measurement, a molecular weight and its distribution of the resulting SMPU ionomers were measured by GPC (HP GPC) together with column (PLgel Mixed-C type, Polymer Laboratories Ltd, USA) and refractive index detector. The M_w linearity range of this column is from 200 to 2,000,000. The typical application of this column is listed in the following Table 4.2:

Table 4.2 Typical application of PLgel Mixed-C columns (Polymer Laboratories Ltd, USA)

Application	Solvent	Temperature
Polystyrene	THF	20-40°C
PVC	THF	40°C
Polycarbonate	CHCL ₃	Ambient
Polyurethane	DMF	80°C
Polysiloxane	Toluene	20-50°C

After testing the solubility of SMPU ionomer samples in DMF and THF at room temperature, the testing temperature is set up to 25°C. The flow rate of mobile phase is 1.0ml/min. Integral method was used to calculate the number-average molecular weight (M_n) and polydispersity (M_w / M_n) of the resulting polymers accordingly. The standard PS samples were tested with the same mobile phase and testing condition.

4.5 Polarizing microscopy (POM)

Polarizing microscopy (POM) is equipped with both a polarizer, positioned in the light path before the specimen, and an analyzer (the second polarizer) placed in the optical pathway between the objective rear aperture and the observation tubes or camera port. The specimen tested in this technique usually is of optically anisotropic character. Transmitted light converts the refractive index difference in such samples to light and dark image regions. Therefore, POM could be used to investigate the morphology of a crystalline polymer. When a crystalline polymer is heated, the birefringence disappears as the crystallites disappear into the polymer melt. Changes in birefringence can be observed with a hot-stage microscopy by using crossed polarizers. The point of disappearance of the last trace of birefringence can be used to determine the crystalline melting point[91]. In crystallizable polymer materials, spherulite crystalline with the size of 0.5 ~100 micron was common characteristic and can be formed during condensing the polymer solution or cooling the polymer melt[99]. Thereof, the spherulite crystalline with the size larger than 5 micron can be observed with the formation of Maltese Cross as shown Figure 4.1 by using POM.



Figure 4.1 Observance of Maltese cross of isotactic polystyrene from melt[99]

In this measurement, a Leica polarizing optical microscope (POM) equipped with a Mettler FP 80 hot stage and a controller was used to observe the morphologies of PCL-4000, segmented polyurethane non-ionomer and ionomer samples with the similar melting-crystallization cycles used in the isothermal crystallization process. The isothermal crystallization temperature in POM study is chosen to be at the room temperature (20 °C) which is approximately the T_c value (crystallization temperature) in the study of isothermal crystallization kinetics.

4.6 Shape memory properties investigation

As for the quantitative study of shape memory effect, the shape memory effect could be quantified by cyclic thermo-mechanical investigations which usually include programming the test piece and recovering its permanent shape in single cycle[1, 73]. Byung Kyu Kim et al[5, 47, 104] ever reported the typical protocol about the programming the test piece as follows: first, the test sample is stretched to the maximum strain ε_m at the high temperature T_{high} above the switching

temperature T_{trans} and below the highest thermal transition temperature T_{perm} which will cause the polymer to melt. Then the sample is cooled down below the transition temperature T_{trans} under a constant strain ε_m to a temperature T_{low} , thus fixing the temporary shape. Retracting the crosshead of tensile tester to the original position causes the sample to bend. When the temperature of sample is increased to T_{high} again, the permanent shape is recovered. The cyclic tensile test is just like the left graph in Figure 4.2. In this test, there are several parameters used to describe the shape memory effect quantitatively as below:

$$R_r(N) = \frac{\varepsilon_m - \varepsilon_p(N)}{\varepsilon_m - \varepsilon_p(N-1)} \quad \text{Equation 4.4}$$

The strain recovery ratio $R_r(N)$ (Equation 4.4) quantifies the ability of the material to memorize its permanent shape and is a measure of how far a strain that was applied in the course of the programming $\varepsilon_m - \varepsilon_p(N-1)$ is recovered in the following shape memory transition. $\varepsilon_p(N-1)$ and $\varepsilon_p(N)$ represent the strain of the sample in two successively passed cycles in the stress free state.

$$R_{r, tot}(N) = \frac{\varepsilon_m - \varepsilon_p(N)}{\varepsilon_m} \quad \text{Equation 4.5}$$

The total strain recovery ratio $R_{r, tot}$ (Equation 4.5) is defined as the strain recovery after N passed cycles based on the original shape of the sample.

$$R_f(N) = \frac{\varepsilon_u(N)}{\varepsilon_m} \quad \text{Equation 4.6}$$

The strain fixity ratio $R_f(N)$ (Equation 4.6) describes how exactly the sample could be fixed in the stretched shape after a deformation to ε_m . Therefore, it could be regarded that the cyclic tensile test is just a part (①-③) of thermal mechanical test as shown in graph b of Figure 4.2.

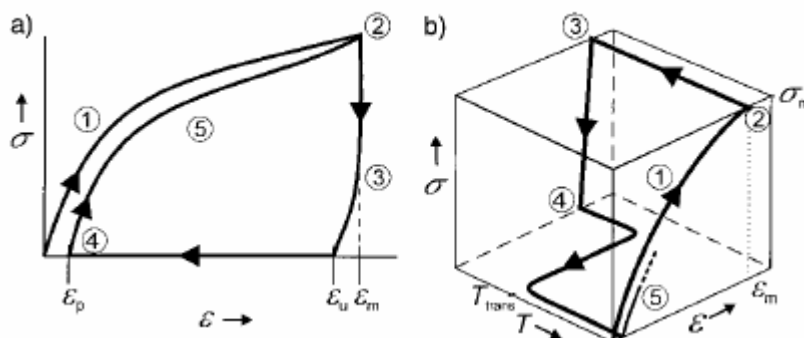


Figure 4.2 Schematic representation of the results of the cyclic thermomechanical investigation for two different tests: a) ϵ - σ diagram: ①-stretching to ϵ_m at T_{high} ; ②-cooling to T_{low} while ϵ_m is kept constant; ③-clamp distance is driven back to original distance; ④-at $\epsilon=0\%$ heating up to T_{high} ; ⑤-start of the second cycle. b) ϵ - T - σ diagram: ①-stretching to ϵ_m at T_{high} ; ②-cooling down to T_{low} with cooling rate dT/dt while σ_m is kept constant; ③-clamp distance is reduced until the stress-free state $\sigma=0$ MPa is reached; ④-heating up to T_{high} with a heating rate dT/dt at $\sigma=0$ MPa; ⑤-start of the second cycle.

In this study, cyclic tensile test was done by using ISTRON 4466 with a constant temperature control chamber and a personal computer was used to control and record all data. First, the sample film with 5mm width, 20mm length and 0.5mm thickness were heated to T_{high} , 60 °C within 600 second. Then the sample was stretched to ϵ_m , 100% elongation at T_{high} , 60 °C with 10 mm/min stretching rate. After that, the cool air will be inputted to the chamber for cooling sample film with constant strain, ϵ_m , to T_{low} , 20 °C, within 900s. Thereafter, the strain was released from ϵ_m to 0 and the recurrent heating for 600s began. That is one cycle among all cyclic tensile test and the cycle for each sample will be repeated four or five times for assessing the shape memory effect. For SMPU ionomers with PCL-10000 as the soft segment, the high temperature (deforming temperature, T_{high}) was set to 70 °C instead of 60 °C for the consideration of higher melting temperature of PCL-10000. In the study of the effect of cooling time on shape

memory properties in SMPU cationomers, the cooling time was chosen in the range from 30 seconds to 900 seconds.

In the cyclic tensile programming, the deformation is usually conducted at temperature higher than the switching temperature and then the deformation can be fixed in the cooling process. The advantage of deformation at higher temperature was explained by the fact that the SMPU film will possess lower elastic modulus and be readily shaped at higher temperature. With respect to the practical application such as the produce of wrinkle or the diminution of crease of the cloth, the fiber might be deformed / stretched at the temperature lower than the switching temperature. Moreover, as far as the effect of deformation temperature on the shape memory properties is concerned, some researchers have reported the related conclusion as follows: Hashimoto et al.[73] studied the shape fixity and recovery with various loading temperature and concluded the shape fixity and recovery ratio at loading temperature (T_g-20K) below the switching temperature are poor compared with that at higher temperature (T_g+20K), but the loading at low temperature has an economical advantage; In our previous work[59], we investigated the dependency of the recovery ratios on the deformation temperature and the results indicated if the deformation occurs at temperature below $T_g-20^\circ\text{C}$ or above $T_g+80^\circ\text{C}$, then the shape memory effect should be far satisfied. Therefore, based on the practical application and the transition temperature of SMPU ionomer fibers prepared in this study, the SMPU ionomer fiber is deformed at room temperature 20°C (T_{low}) and recovered when heated up to 75°C (T_{high}) with cyclic tensile method to quantitatively evaluate the shape memory effect. The elongation ratio in cyclic tensile test for SMPU

ionomer fibers is chosen according to the stretching ratio of human skin reported by Wu and Yu[105]. In the paper of Wu and Yu, the maximum stretching ratios of human skin are 66%~78% in vertical direction and 30%~42% in horizontal direction. In that, 50% was used as the maximum elongation ratio in assessing shape memory effect for SMPU ionomer fibers.

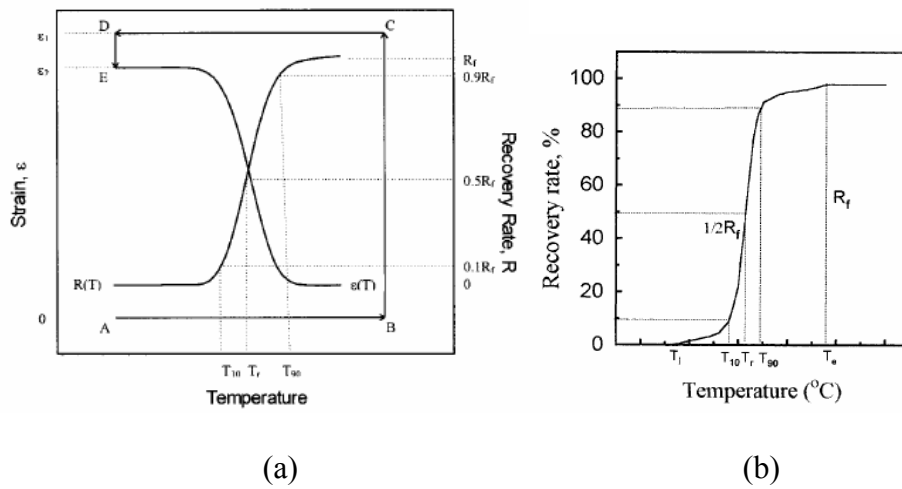


Figure 4.3 Schematic representation of strain recovery test: a) Diagram of preparation procedure of specimens for strain recovery measurements and; b) recovery curves, ϵ - T .

On the other hand, the strain recovery test could be used to test the recovery temperature and recovery rate R_f as shown in the curve ④ of the right graph (b) in Figure 4.2. Li, Mao Xu et al [6, 7, 61, 77, 106] ever investigated the shape memory recovery behavior with the strain recovery test as shown in Figure 4.3. In the strain recovery test, film specimens with uniform thickness were prepared by stretching to different draw ratios at the high temperature T_{high} above the switching temperature T_{trans} and below the highest thermal transition temperature T_{perm} ; subsequently cooling to the low temperature T_{low} under constrained conditions with constant length for a certain time. The strain recovery effect will be measured under microscope equipped with a hot stage. The heating rate will

be fixed and the recovery temperature, recovery rate R_f , which could be calculated by the reversible length divided by total deformed length, ε_2 , after stretching, will be figured as shown in the graph (b) of Figure 4.3.

4.7 Antibacterial activity testing

ASTM E 2149 is designed to evaluate the resistance of non-leaching antimicrobial treated specimens to the growth of microbes under dynamic contact condition. This shake flask test is used to determine the antimicrobial activity of surface bound materials by shaking samples in a concentrated bacterial suspension for a one hour contact time. The number of viable organisms in the suspension is determined and the percent reduction is calculated based on initial counts. Meanwhile, the leachability of antimicrobial materials from the bulk also needs to be considered in the study of SMPU ionomers with substrate bonding antibacterial activity. Therefore, the test method AATCC 147 that is directly dependent on the ready leach-ability of the antimicrobial agent from the treated samples is used to detect whether the antibacterial activity is caused by the leaching of biocidal agent. In the study of SMPU ionomers with substrate bonding antibacterial activity, the aforementioned two testing methods were combined to test the substrate-bound antibacterial activity of SMPU ionomers with choosing the suitable chain-extender and counter-ion. The testing cultures include Gram positive organism *Staphylococcus aureus* and Gram negative organism *Klebsiella pneumoniae*. All the testing procedures were conducted strictly according to ASTM 2149E and AATCC 147 by Intertek Testing Services Hong Kong Ltd. The resultant file was detailed in the Table 4. 3.

CHAPTER 4 CHARACTERIZATION TECHNIQUES

Table 4. 3 Intertek Ltd Testing file about the antibacterial activity of SMPU ionmoer film

Sample code	Standard	Intertek Labtest file number	Testing data
75-0	AATCC147-1998	HJ00402848	Jan 11, 2006
	ASTM E 2149-01	HJ00402848	Jan 11, 2006
BIN75-6-C8	AATCC147-1998	HJ00385844	Nov 15, 2005
	ASTM E 2149-01	HJ00385844	Nov 15, 2005
BIN75-11-C8	AATCC147-1998	HJ00385844	Nov 15, 2005
	ASTM E 2149-01	HJ00385844	Nov 15, 2005

CHAPTER 5 STRUCTURE AND SME of SMPU ANIONOMERS

5.1 Influence of ionic groups on the crystallization and melting behavior in segmented PU anionomers with different M_w

To investigate the influence of ionic groups on the crystallization and melting behavior in segmented PU anionomers with different molecular weight, the series of segmented PU anionomers and non-anionomers with the different molecular weight, same chemical composition and chemical structure were synthesized as shown in Table 3.2 in the part 3.3.2.1. The DMPA weight content was fixed in 5.0 wt% and the soft segment content was 80.0 wt% for all specimens. Molecular weight as one of basic parameters for polymer system was considered in this study and adjusted in the studied range to reveal the various roles played by anionic groups on the morphology of segmented PU anionomers.

5.1.1 Differential scanning calorimetry measurement

As shown in Figure 5.1 and Table 5.1, the glass transition temperature (T_g) of the soft segment increases with increasing the M_w value of the segmented PU samples. It is due to the reason that the more the hard segment dissolves in the soft domain the higher the restriction of soft segment mobility[107-109]. In view of the fact that the SMPU ionomer samples are of the same hard segment content, DMPA content, and molecular structure, the effect of the M_w value on the change of T_g is quite pronounced. It suggests that high molecular weight PU samples

enhance the mixing process of soft and hard segments. It is observed that the change in the heat capacity (ΔC_p) of PCL-4000 is smaller than that of the SMPU ionomer samples which might be due to the existence of non-isothermal crystallization process participating in the cooling process of the PCL-4000. Therefore, the amount of amorphous phase having flexible molecular chain of PCL-4000 is decreased, resulting in smaller ΔC_p . The melting endothermic peak of the DSC curve of PCL-4000 is a signature of the crystallization process. In Table 5.1, it is worth noting that both the T_g and ΔC_p values of the PU ionomers are smaller than that of the corresponding PU non-ionomers. The drop of ΔC_p is direct evidence showing that the Coulombic force between the ionic groups can restrict the soft segment mobility. On the other hand, from the decrease of T_g value after neutralizing the corresponding PU non-ionomers, the improvement of the micro-phase separation especially in high molecular weight PU ionomers is observed. After neutralization of PU samples, for instance, PU-71N and PU-71I,

Table 5.1 Thermal properties of PCL and PU samples

Sample code	T_g [°C]	$T_{(end)}-T_{(onset)}$	ΔC_p [J/g · °C]	$T_{(end)}$ [°C]	$T_{(onset)}$ [°C]
PCL-4000	-65.81	8.94	0.056	-61.18	-70.12
PU-20N	-46.40	15.86	0.303	-39.35	-55.21
PU-20I	-46.71	14.95	0.285	-39.92	-54.87
PU-58N	-41.29	12.32	0.208	-34.95	-47.27
PU-58I	-43.86	13.79	0.176	-37.18	-50.97
PU-71N	-32.00	15.71	0.205	-24.3	-40.01
PU-71I	-39.46	17.32	0.203	-30.64	-47.96

the T_g of the soft segment is decreased substantially with the presence of ionic groups, suggesting that the Coulombic force are responsible for the improvement of micro-phase separation. We conclude in this section that the effect of Coulombic force is different on PU samples with different M_w values – they play

different roles on the crystallization process in PU samples with different molecular weights. It will be shown in the following part that this unique effect manifests itself in the change in Avrami parameters, n and K , in isothermal crystallization.

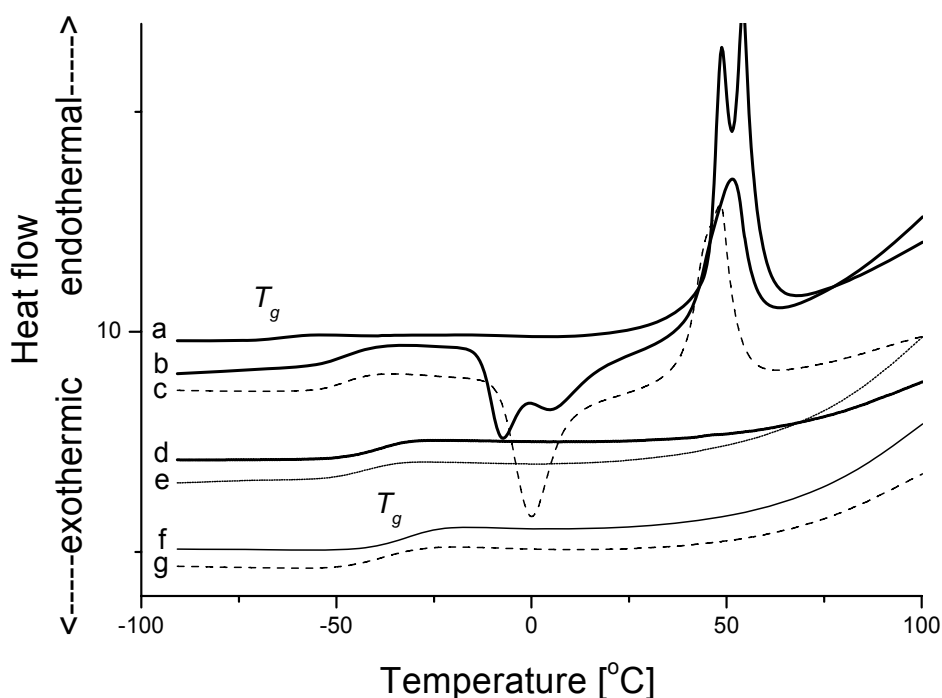


Figure 5.1 (a) DSC heating curves (20 °C/min) of PCL-4000 after cooling at 200 °C/min from 120 °C, (b) PU-20N non-ionomer, (c) PU-20I ionomer, (d) PU-58N non-ionomer, (e) PU-58I ionomer, (f) PU-71N non-ionomer, and (g) PU-71I ionomer .

From the DSC thermograms of PU-20N and PU-20I, there are exothermal crystallization peaks at about -10 °C and 0 °C respectively, and endothermic peaks of crystallization melting of soft segments at about 50 and 45 °C. However, for the thermograms of PU-20N and PU-20I as shown in Figure 5.1 (b) and (c), not only the exothermal crystallization peak position but also the peak shape is

totally different, suggesting that the crystallization rate and crystallization mechanism have been altered by neutralization. As the molecular weight increases, the DSC thermograms in Figure 5.1 (d)-(g) for samples PU-58N, PU-58I, PU-71N, and PU-71I show decreased PU crystallizability, resulting in no significant exothermal crystallization and melting features.

5.1.2 Morphology of crystal in SMPU cationomers with different molecular weight

Figure 5.2 shows the crystal morphologies of PCL-4000. The nominal crystal size shown on the figure is about 30- 50 micron which is consistent with the literature reported[110]. In general, both the average crystal sizes of PU non-ionomers and ionomers decrease with increasing M_w compared with that of PCL-4000. However, the evolution of crystal morphology for each pair of PU non-ionomer and ionomer samples with the same M_w value is different. For instance, in the case of PU-20N/PU-20I which falls into the low M_w regime, the crystal size in PU-20N is smaller whilst the crystal outlook of PU-20I still resembles roughly the morphological details as in PCL-4000. This is illustration of the effect of ionic groups within hard segments on the crystal size and in turn the crystal morphology in PU. The pair of PU samples denoted by PU-58N/PU-58I shares a similar surface morphology. Their crystal sizes in PU are nearly the same but originated from a different morphological transformation. The last pair of samples (PU-71N/PU-71I) has the highest M_w value, but their crystal sizes are the smallest among all the other PU films. In this pair of specimens, ionic moiety causes the obvious decrease of crystal size instead. The difference in morphological transformation suggests the different effects played by the

Coulombic force on the crystallization process. This might open up a new line of research on the perturbation of crystallization kinetics analysis of such copolymer.

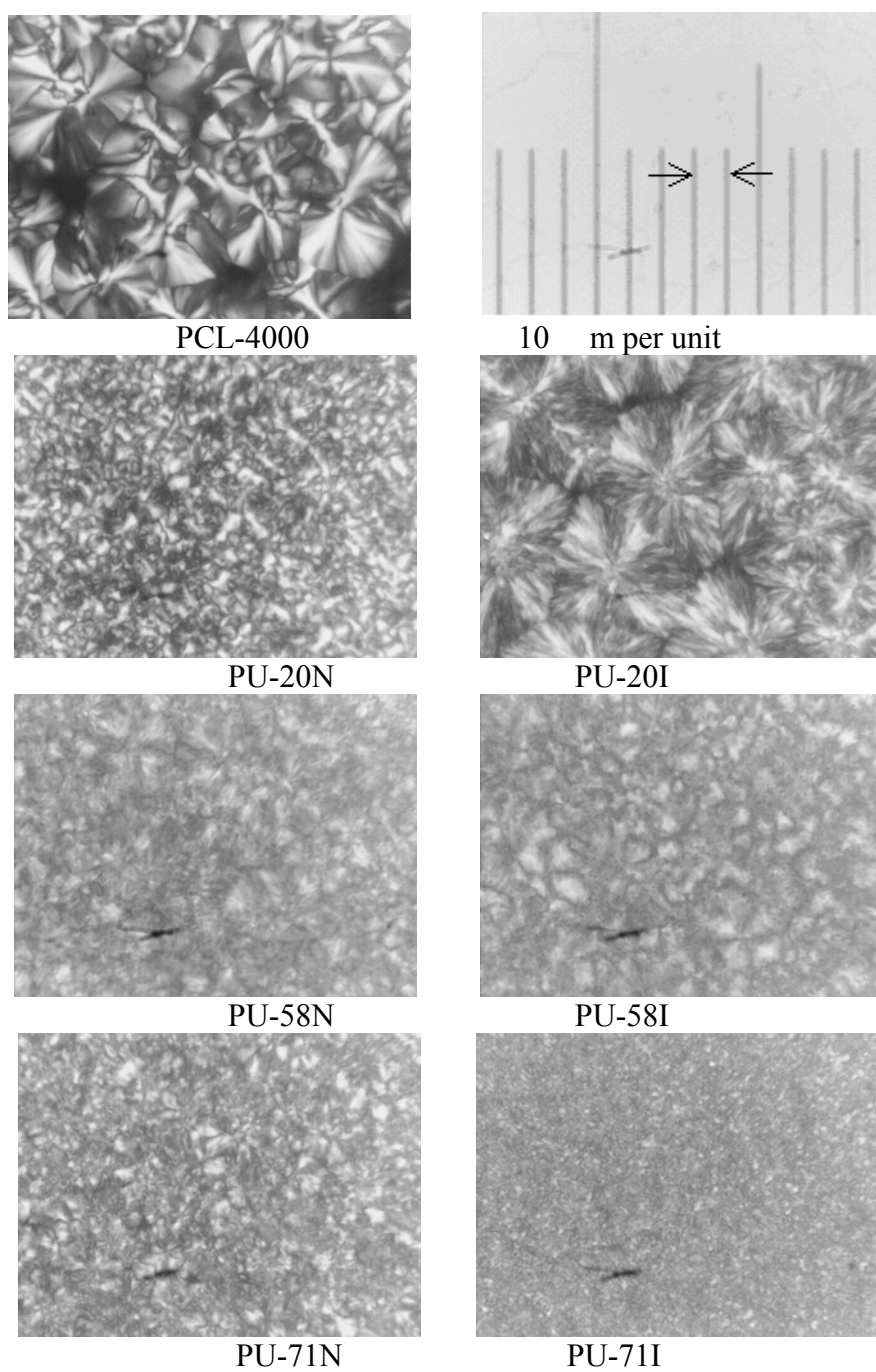


Figure 5. 2 Polarized optical microscopy images of the crystals for PCL-4000 and PU non-ionomers and ionomers with different molecular weights.

5.1.3 Analysis of isothermal crystallization kinetics

The overall kinetics of the isothermal crystallization from the melt can be analyzed on the basis of the Avrami equation[111]. This crystallization theory is widely accepted to describe the physical behavior of a variety of crystallization process, for instance, semi-crystallization in polymer, polymer blends, and copolymers[112-117]. We use the modified Avrami equation called the Ozawa equation to describe the crystallization kinetics:

$$X(t) = 1 - \exp(-Kt^n) \quad \text{Equation 5.1}$$

which can be linearized in the form:

$$\ln[-\ln(1 - X(t))] = n \ln t + \ln K \quad \text{Equation 5.2}$$

where n is the Avrami (Ozawa) exponent whose value depends upon the mechanism of nucleation and on the crystal-growth geometry, K is a rate constant containing the nucleation and the growth parameters. Theoretically, if Equation 5.2 can adequately follow the crystallization process, a plot of $\ln[-\ln(1 - X(t))]$ against $\ln t$ should yield a straight line with slope n and intercept $\ln K$.

The double logarithmic plots of $\ln[-\ln(1 - X(t))]$ against $\ln t$ for PCL-4000, non-ionomers, and ionomers with various temperatures are shown in Figure 5.3. Each plot represents a linear dependence of $\ln[-\ln(1 - X(t))]$ on $\ln t$, but of slightly deviation from the prediction when both parameters are large, indicating the existence of a secondary crystallization of PCL which occurs consecutively with primary. The study of PCL ($M_w = 80,000$) by Kuo *et al.* [118] suggests that the PCL with a higher M_w value has the same tendency at a later stage in the

crystallization process. The deviation is attributed to the secondary crystallization involving fibrillar growth between the primary lamellae of the spherulite, and leading to the occurrence of spherulite impingement.

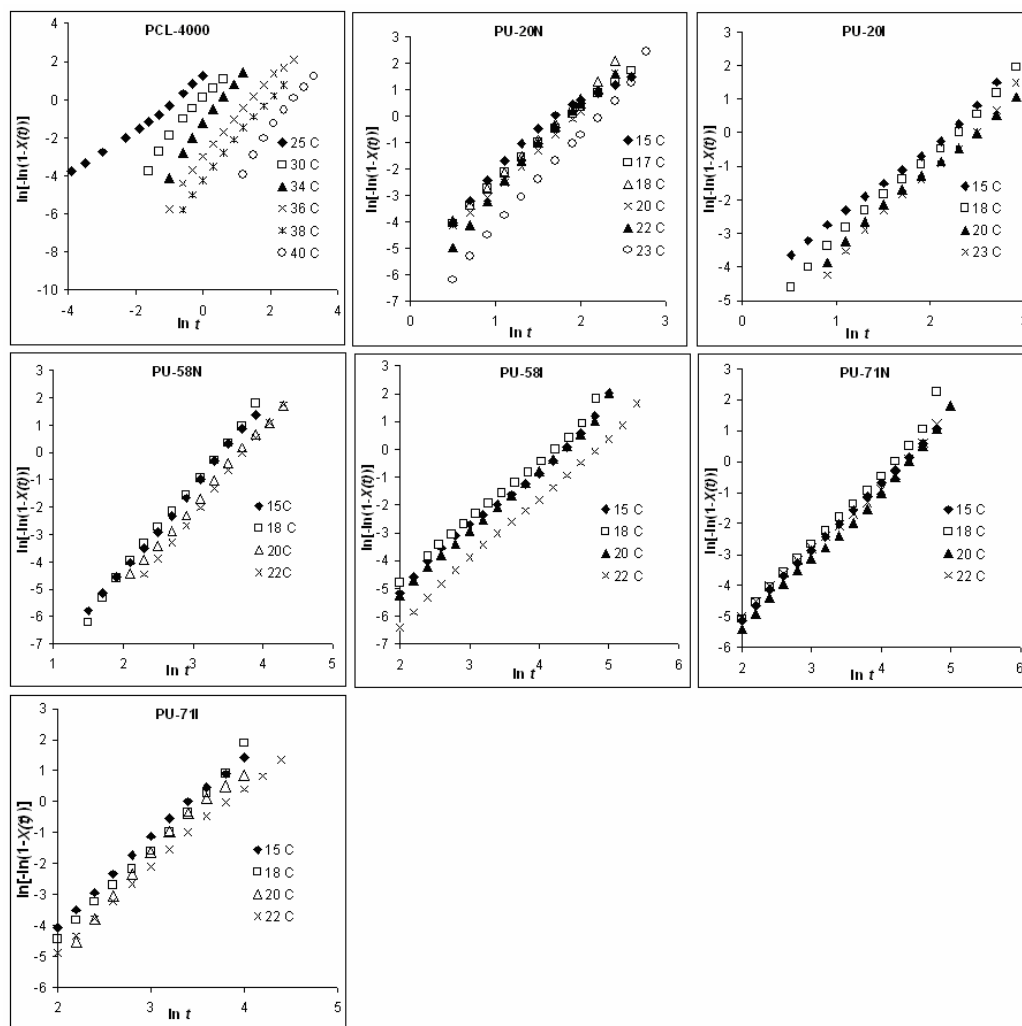


Figure 5.3 Plots of $\ln[-\ln(1-X(t))]$ against $\ln t$ for isothermal crystallization with various temperatures.

The values of n and K for a particular sample can be determined from the initial linear portions of the double logarithmic plots shown in Figure 5.3. The results for different samples are summarized in Table 5.2. The Avrami parameter n of PCL-4000 at 40 °C in our experiment is consistent to that reported by Bogdanow

et al.[119]. For PCL-4000, the Avrami parameter n is approximately ~ 1 to 2 and 3 to 4 at low and high crystallization temperatures, respectively. The isothermal crystallization of PU can be described by the Avrami equation with the exponent n ranging from 2 to 3 at the crystallization temperature chosen in this study. However, it has been observed that ionic groups in hard segments play a significant role on altering the crystallization mechanism in PU films. The Avrami parameter n is decreased from 3 to 2 after neutralization process in PU samples with lower M_w values, such as PU-20I and PU-58I, but is increased from 2 to 3 in samples with higher M_w values such as PU-71I. This is a manifestation of a different crystallization mechanism induced by the ionic groups in PCL-4000 based PU with different M_w values. An understanding of the M_w dependence of the Avrami parameters is slightly more involved. In PU samples with lower M_w , the extent of the soft and hard segment phase mixing is relatively not very high compared with that in high M_w samples. Under this circumstance, the effect of ionic groups in the hard segments on the micro-phase separation is not effective. However, the increased hard segment cohesive force induced by the ionic groups after neutralization may bring about restriction on the physical mobility of soft segments, resulting in the decrease and increase of the Avrami parameters n and K , respectively. In segmented PU samples with higher M_w values, the extent of phase mixing is expected to be higher. The Coulombic forces between ionic groups improve the micro-phase separation significantly. The crystallization mechanism is then altered and can be observed by the reversed change in the Avrami parameters n and K . The half crystallization time $t(0.5)$ is defined as the time at which the crystallinity is equal to 50 %. It is

related to the Avrami parameter K and can be determined from the following expression:

$$K = \ln 2 / [t(0.5)]^n \quad \text{Equation 5.3}$$

Table 5. 2 The Avrami Parameters n , K , $t(0.5)$ (crystallization half time), and E (activation energy) of the soft segment of PU non-ionomers and ionomers

	M_w	T_c [°C]	T_c [K]	N	K	$1/T_c$	$(1/n)\ln K$	ΔE [kJ/mol]	$t(0.5)$ [min]	${}^a K = \ln 2 / [t(0.5)]^n$
PCL -4000	4000	25	298.15	1.28	2.89E+00	3.35E-03	0.83	184.09	0.355	2.61E+00
		30	303.15	2.12	1.04E+00	3.30E-03	0.02		0.760	1.24E+00
		34	307.15	2.46	2.57E-01	3.26E-03	-0.55		1.440	2.83E-01
		36	309.15	2.09	4.42E-02	3.23E-03	-1.49		3.470	5.17E-02
		38	311.15	2.17	1.44E-02	3.21E-03	-1.95		5.960	1.44E-02
		40	313.15	2.42	1.47E-03	3.19E-03	-2.69		11.950	1.71E-03
		42	315.15	4.26	2.90E-06	3.17E-03	-2.99		19.400	2.27E-06
PU -20N	20200	15	288.15	3.29	4.37E-03	3.47E-03	-1.65	36.80	4.650	4.40E-03
		17	290.15	3.01	3.95E-03	3.45E-03	-1.84		5.670	3.74E-03
		18	291.15	3.08	4.07E-03	3.43E-03	-1.79		5.320	4.06E-03
		20	293.15	2.87	3.65E-03	3.41E-03	-1.96		6.120	3.83E-03
		22	295.15	3.75	1.15E-03	3.39E-03	-1.80		5.500	1.15E-03
		23	296.15	3.35	5.90E-04	3.38E-03	-2.22		8.230	5.90E-04
		25	298.15	2.91	1.64E-03	3.35E-03	-2.20		7.900	1.68E-03
PU -20I	20200	15	288.15	2.18	8.41E-03	3.47E-03	-2.20	28.53	7.830	7.87E-03
		18	291.15	2.32	4.77E-03	3.43E-03	-2.30		8.630	4.63E-03
		20	293.15	2.23	3.84E-03	3.41E-03	-2.49		10.500	3.62E-03
		23	296.15	2.42	2.42E-03	3.38E-03	-2.49		10.530	2.33E-03
PU -58N	58500	15	288.15	3.12	2.40E-05	3.47E-03	-3.41	34.02	26.683	2.48E-05
		18	291.15	3.09	2.80E-05	3.43E-03	-3.40		26.490	2.79E-05
		20	293.15	2.92	2.33E-05	3.41E-03	-3.65		33.340	2.48E-05
		22	295.15	3.21	6.62E-06	3.39E-03	-3.71		36.110	6.88E-06
PU -58I	58500	15	288.15	2.00	1.53E-04	3.47E-03	-4.39	39.70	67.890	1.51E-04
		18	291.15	2.07	1.56E-04	3.43E-03	-4.23		58.420	1.52E-04
		20	293.15	2.18	7.43E-05	3.41E-03	-4.36		66.100	7.40E-05
		22	295.15	2.13	3.36E-05	3.39E-03	-4.83		104.97	3.42E-05
PU -71N	71600	15	288.15	2.16	8.62E-05	3.47E-03	-4.33	12.90	63.975	8.63E-05
		18	291.15	2.27	7.36E-05	3.43E-03	-4.19		57.290	7.12E-05
		20	293.15	2.23	5.14E-05	3.41E-03	-4.43		69.900	5.39E-05
		22	295.15	2.03	1.29E-04	3.39E-03	-4.41		68.940	1.28E-04
PU -71I	71600	15	288.15	2.71	8.84E-05	3.47E-03	-3.44	31.13	26.020	1.01E-04
		18	291.15	2.96	3.07E-05	3.43E-03	-3.52		29.790	3.05E-05
		20	293.15	3.48	5.29E-06	3.41E-03	-3.49		30.180	4.91E-06
		22	295.15	2.63	4.41E-05	3.39E-03	-3.81		38.270	4.70E-05

^a The crystallization rate parameter K is derived from equation 5.3

Table 5.2 summarizes the Avrami parameters for the soft segments of PU non-

ionomers and ionomers. The parameter K calculated from equation 5.3 agrees well with that obtained experimentally and is summarized in Table 5.2.

It suggests that the Avrami equation analysis is adequate to describe the crystallization mechanism of PCL-4000 based PU ionomers and non-ionomers[120]. Usually, the rate of crystallization is mathematically defined as the inverse of $t(0.5)$. The values of $t(0.5)$ for different samples are summarized in Table 5.2. It illustrates the fact that in PU samples having low M_w values, such as PU-20 and PU-58, the crystallization rate ($1/t(0.5)$) is decreased by the presence of ionic groups. On the contrary, in PU samples having high M_w values, such as PU-71, the presence of ionic groups promotes the crystallization process. This shows that the role of ionic groups in samples with different M_w values is different.

5.1.4 Analysis of crystallization activation energy

The crystallization process in PCL-4000 or soft segments of PU is assumed to be thermally activated. The Avrami parameter K can then be described by the Arrhenius equation[112, 117]:

$$K^{1/n} = k_o \exp\left(-\frac{\Delta E}{RT_c}\right) \quad \text{Equation 5.4}$$

or

$$(1/n) \ln K = \ln k_o - \frac{\Delta E}{RT_c} \quad \text{Equation 5.5}$$

where k_o is a temperature-independent pre-exponential factor, R is the gas constant, and ΔE is the crystallization activation energy in kJ/mol. The plots of

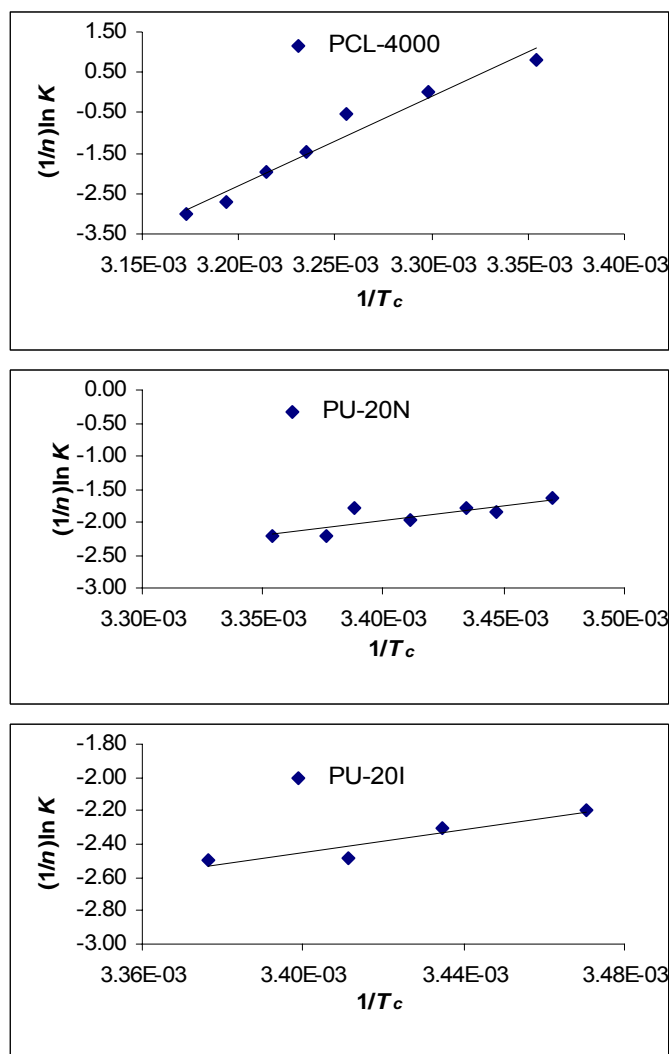


Figure 5.4 Plots of $(1/n)\ln K$ against $1/T_c$ from isothermal crystallization

the parameter $(1/n)\ln K$ against the inverse of the corresponding T_c for the PCL-4000, PU non-ionomer and ionomer samples are shown in Figure 5.4. The activation energy is calculated and summarized in Table 5.2. For PCL-4000, the ΔE for the primary crystallization process is calculated to be -183.09 kJ/mol, while for PU non-ionomer (PU-20N) and ionomer (PU-20I) samples, the ΔE increases significantly to -36.80 and -28.53 kJ/mol, respectively. Comparison of the activation energy for different samples indicates that the ionic groups have less influence on the ΔE in PU samples with low M_w values. On the contrary, for

PU samples having high M_w values such as PU 71I, the ΔE is decreased from -12.9 to -31.13 kJ/mol after neutralization by TEA.

5.1.5 Equilibrium melting temperature

A dominant sharp exothermic peak in the re-heating DSC thermogram of our samples is considered to be the primary melting temperature (T_m). In Figure 5.5, it clearly reveals that T_m increases linearly with T_c . The experimental data can be fitted well by the Hoffman-Weeks equation[121]:

$$T_m = \phi T_c + (1-\phi)T_e \quad \text{Equation 5.6}$$

where T_e is the equilibrium melting point, and $\Phi=1/\gamma$ is the stability parameter depending on the crystal thickness (γ is the ratio of the lamellar thickness L to the lamellar thickness of the critical nucleus L^* at T_c). The Φ in Equation 5.6 can have values between 0 and 1 ($\Phi=0$ and $T_m=T_e$, whereas $\Phi=1$ and $T_m=T_c$). The crystal are the most stable for $\Phi=0$ and unstable for $\Phi=1$. T_e can be calculated from the intersection point between plots of T_m against T_c and lines of $T_m=T_c$. As shown in Figure 5.5, the melting temperature T_m for PCL-4000 and PCL-4000 based PU samples increases with the crystallization temperature T_c as expected. The extrapolation of the observed melting temperatures to the line $T_m=T_c$ has been widely employed to calculate the T_e of different copolymers and homopolymers[107]. However, in the case of the study on segmented poly (ester-urethanes) based on poly (ϵ -caprolactone) by Bogdanow *et al.*[119], linear polyethylene, and random copolymers at low level of crystallinity by Alamo *et al.* [122, 123], this extrapolation method fails to describe the relations between the T_m and T_c . Bogdanow has used different approaches to understand this

scenario[119]. Firstly, the non-isothermal crystallization during cooling to

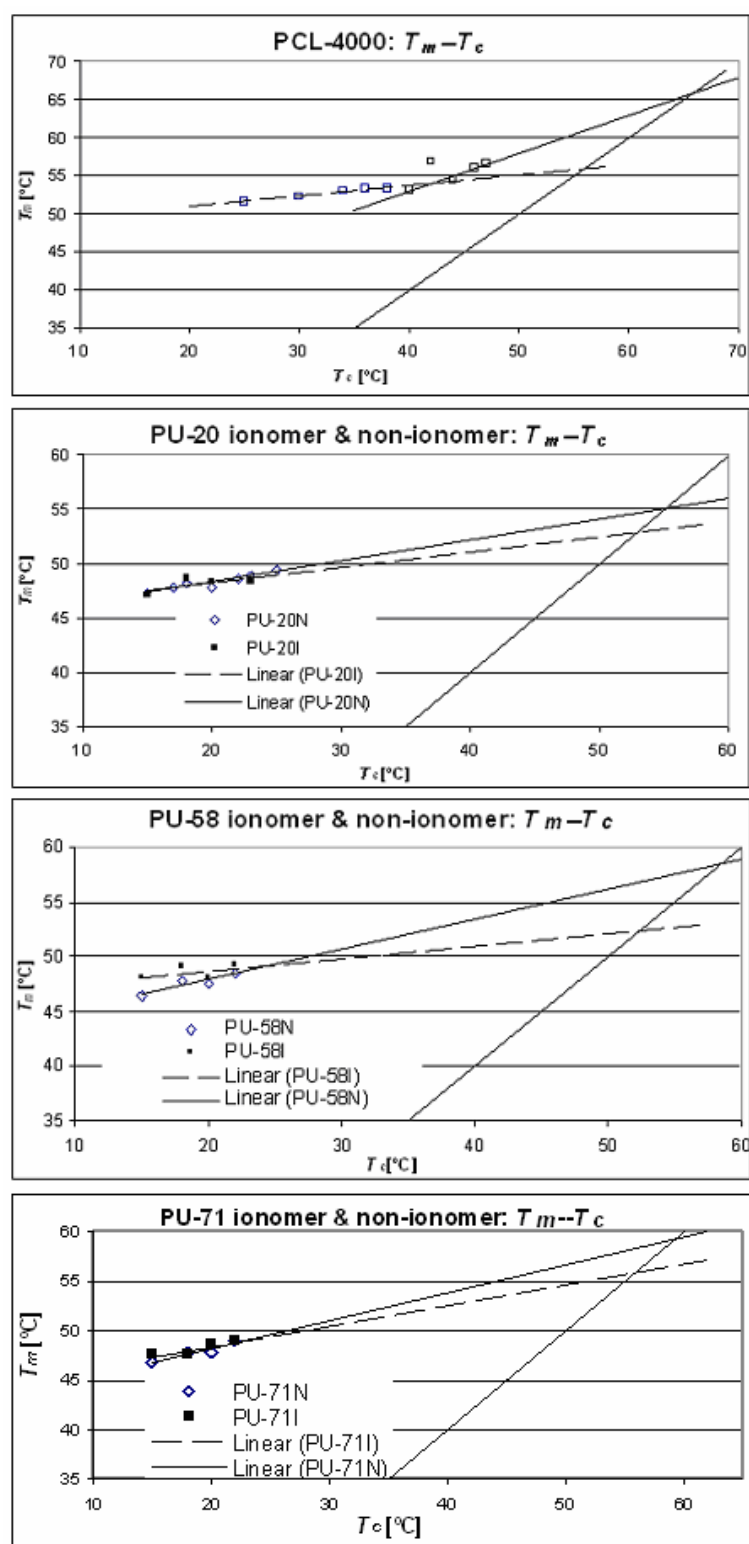


Figure 5.5 Plots of the observed melting temperature T_m against T_c for PU ionomers and non-ionomers with different molecular weights.

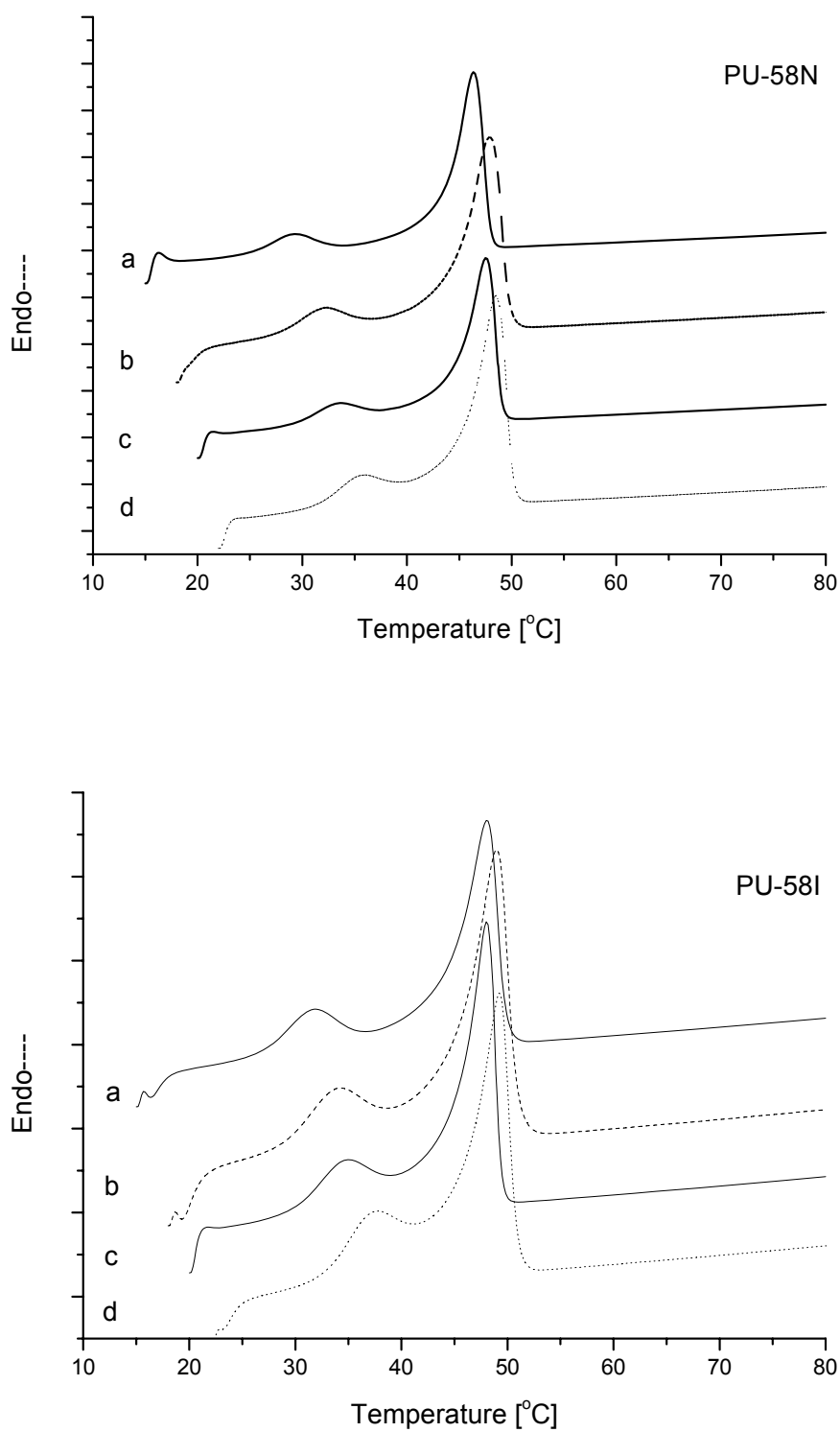


Figure 5.6 DSC thermograms of sample PU-58N (upper) and PU-58I (lower) after isothermal crystallization at (a) $T_c=15^\circ\text{C}$, (b) $T_c=18^\circ\text{C}$, (c) $T_c=20^\circ\text{C}$, and (d) $T_c=22^\circ\text{C}$.

the certain T_c causes the corresponding T_m to increase. Secondly, the observed dependence also arises from annealing during the heating scan which causes the improvement in crystal quality and hence the T_m increases, and the effect is particularly pronounced when T_c is lower. Therefore, in this investigation of T_e of PCL-4000, the equilibrium melting temperature is calculated from the crystallization temperatures range above 38 °C. As a result, T_e for PCL-4000 is 65.89 °C which is in agreement with the literature reported[110, 119].

It is worth noting that there are double-melting features in all the DSC thermograms shown in Figure 5.6. Similar signature was also observed on the 30/70 DGEBA/PCL blend, binary blends of solution-chlorinated polyethylenes (CPE) with polycaprolactone (PCL), and blends of poly(hydroxyl ether of bisphenol A) (Phenoxy) with polycaprolactone (PCL)[124-126]. In the investigation on Phenoxy/PCL by Defieux[125], the isothermal crystallization process was interrupted after different time intervals and DSC melting trace was immediately recorded. The highest melting endotherm reaches a constant area and position on the temperature scale after short isothermal crystallization times (primary crystallization), while the lower melting peak only appears after much longer crystallization time (secondary crystallization). The secondary crystallization is supposed to occur in the amorphous phase segregated during the primary crystallization of PCL, resulting in a slower crystallization process as this happens in the presence of a higher Phenoxy concentration. Therefore, in calculation of the equilibrium melting temperature of PCL-4000 based PU ionomers and non-ionomers, the higher melting temperature corresponding to the primary crystallization was used.

Table 5. 3 Values of the equilibrium melting temperature T_e , the stability parameter Φ , and the low and high apparent melting temperature

Sample code	T_c [°C]	^a T_{m-1} [°C]	^b T_{m-2} [°C]	T_e [°C]	Φ
PCL-4000	25.00		51.62		
	30.00		52.21		
	34.00		53.00		
	36.00		53.31		
	38.00		53.25	65.89	0.50
	40.00		53.05		
	42.00		56.87		
	44.00		54.50		
	46.00		56.03		
PU-20N	15.00	25.49	47.34		
	17.00	28.01	47.83		
	18.00	29.19	48.17		
	20.00	30.86	47.81	55.07	0.19
	22.00	32.52	48.63		
	23.00	33.68	48.94		
	25.00	35.35	49.42		
PU-20I	15.00	26.15	47.16		
	18.00	29.17	48.67		
	20.00	30.34	48.31	52.83	0.14
	23.00	33.00	48.43		
PU-58N	15.00	29.34	46.34		
	18.00	32.34	47.84		
	20.00	33.67	47.50	58.51	0.28
	22.00	36.00	48.50		
PU-58I	15.00	31.84	48.00		
	18.00	34.17	49.00		
	20.00	35.00	48.00	52.36	0.11
	22.00	37.84	49.17		
PU-71N	15.00	32.00	46.84		
	18.00	34.67	47.84		
	20.00	36.67	47.84	59.32	0.28
	22.00	38.84	49.00		
PU-71I	15.00	31.00	47.50		
	18.00	33.17	47.50		
	20.00	36.10	48.53	55.89	0.21
	22.00	38.00	48.84		

^a low peak of melting endotherm; ^b high peak of melting endotherm

Table 5. 3 summarizes the values of equilibrium melting temperature (T_e) of this series of SMPU ionomers. It is interesting to note that the T_e values of samples are lower than that of PCL-4000 and increase with increasing the molecular weight of the PU samples. After neutralization, it is observed that the T_e values of the PU ionomers are decreased. The stability parameter Φ varies within 0.28 to 0.11 in samples, suggesting that the formation of crystals in this series of samples is rather stable. The Φ values of PU ionomers samples are significantly smaller than the corresponding PU non-ionomers, providing clear evidence that

the ionic groups in hard segments improve the stability of the crystallization in soft segments. Last, the Φ value of PCL-4000 is larger than that in all the PU ionomers and non-ionomers, which can be attributed to the relative larger critical lamellar thickness L^* value of PCL-4000.

5.2 Effect of ionic group content on SMPU anionomers

To study the relations between the structure and shape memory effect of SMPU anionomers, SMPU (shape memory polyurethane) non-ionomers and ionomers were synthesized by using poly(ϵ -caprolactone) (PCL, M_n : 4000), 4, 4'-diphenylmethane diisocyanate (MDI), 1,4-butanediol (BDO), dimethylolpropionic acid (DMPA) according to the recipes shown in Table 3.3. In the synthesis of PU samples detailed in the part 3.3.2.1, DMPA as a part of chain extender reagent is introduced into the hard segment of shape memory polyurethane. Through this way, the PU non-ionomers could be synthesized and the corresponding PU ionomers could be obtained by neutralizing all carboxyl groups of DMPA with the same amount of triethylamine (TEA). The DMPA content was gradually increased from 0 wt% to the maximum content, which is related to specific molecular structure, and other parameters about the molecule structure such as the soft segment content and soft segment length were fixed so as to investigate the effect of ionic group content on the properties of such series of materials.

5.2.1 Effect of ionic group content on crystallizability of SMPU ionomers

The thermograms of all the SMPU non-ionomers and the corresponding ionomers studied showed the endothermic melting peak of soft segments in heating scan as shown in Figure 5.7. The data about thermal properties have been shown in Table 5.4. When the DMPA content is low enough such as 60-5I, the endothermic melting peak of hard segments of PU ionomers at around 162 °C could be observed obviously, however, the corresponding PU non-ionomers 60-5N could not show the distinct melting peak of hard segments. The melting of hard segments in all PU non-ionomers and the PU ionomers with the DMPA content higher than 5% was not observed in DSC investigation. It might be because the increased DMPA content on hard segments disrupts the order of hard domain. In comparison with the PU sample without DMPA such as 60-0, the melting point and enthalpy of melting of soft segments of PU non-ionomers and ionomers was increased. Just like the experimental result reported by Ahn and Kim et al [46], with the increase of DMPA content, the enthalpy of soft segments of two series generally increased. Especially for PU ionomers, this trend is more significant and the increase of the melting enthalpy is higher than the corresponding PU non-ionomers, illustrating, in PU ionomers, there's higher crystallinity of soft segments compared with the corresponding PU non-ionomers.

From the Figure 5.8 cooling scan of DSC investigation, in the sample 60-0 without DMPA, the crystallization exothermal peak of the soft segment and the hard segment show up, suggesting that the two phase separation structure does exist. However, the introduction of DMPA on hard segments causes the disappearance of crystallization exothermal peak of the soft segment and hard segment in the light of observation from the cooling curve of PU non-ionomers

series. Instead, for PU ionomer series, when the DMPA content is higher than 10 wt% such as in sample 60-10 I and 60-13 I, the crystallization exothermal peak

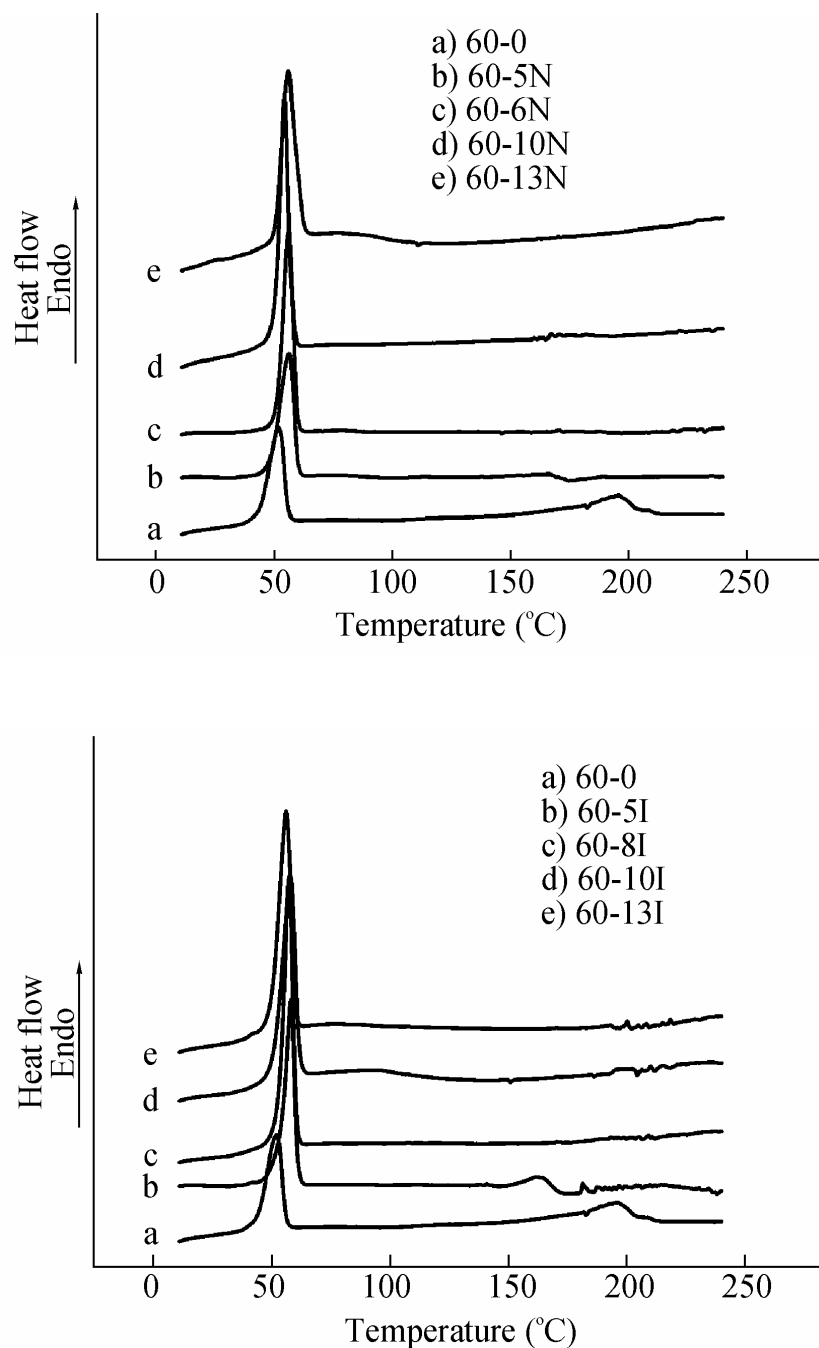


Figure 5.7 Heating scan at 20°C/min with DSC from 0°C to 240°C for PU non-ionomers and ionomers

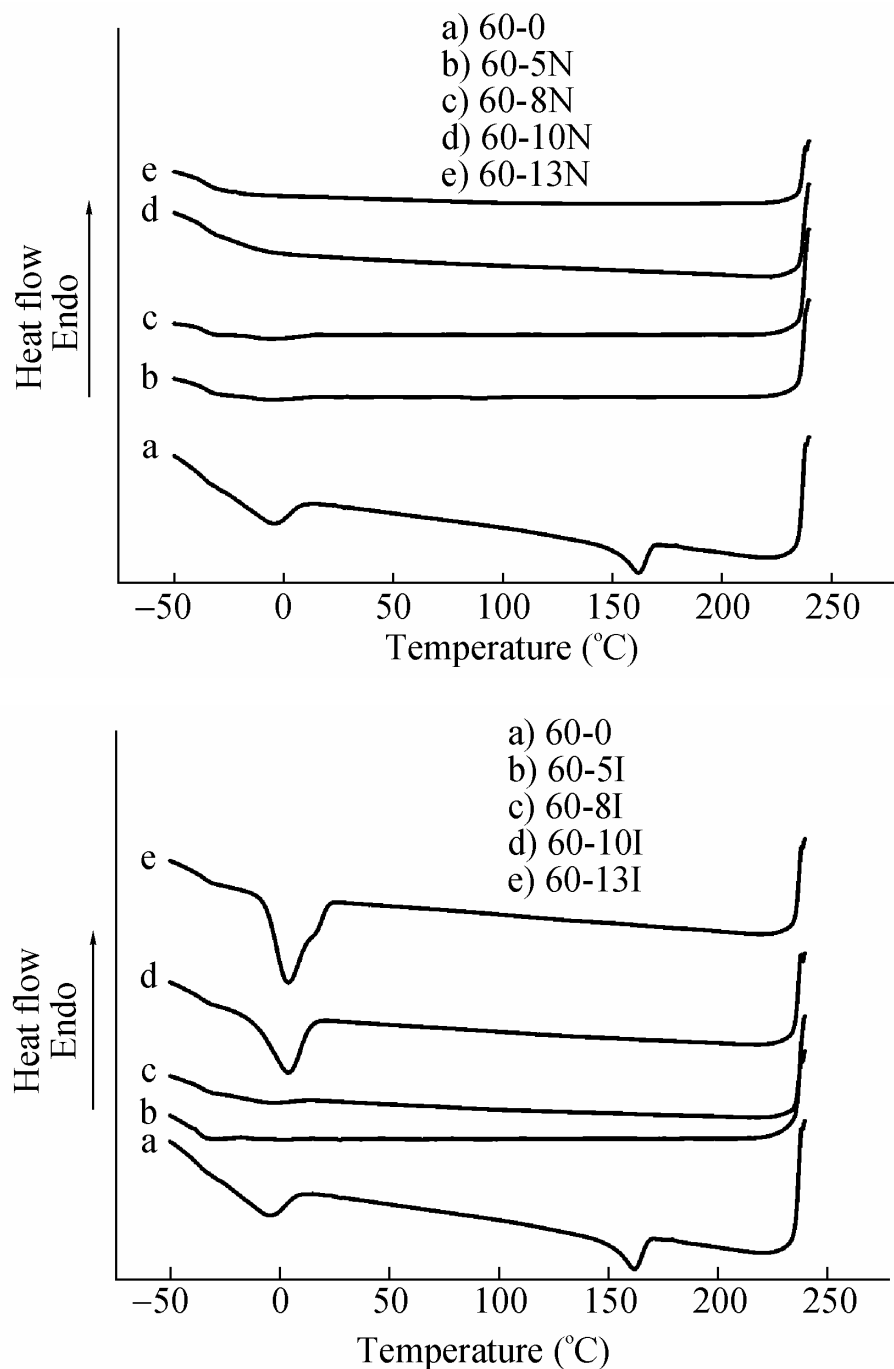


Figure 5.8 Cooling scan at 20°C/min with DSC from 0°C to 240°C for PU non-ionomers and ionomers

of soft segments could be observed, suggesting that the ionic groups with high concentration on hard segments could facilitate the phase separation which increase the crystallizability of soft phase.

Table 5. 4 Thermal properties of SMPU non-ionomers and ionomers

Sample Code	heating at 20 °C/min				cooling at 20 °C/min			
	T_{ms} (°C)	ΔH_{ms} (J/g)	T_{mh} (°C)	ΔH_{mh} (J/g)	T_{cs} (°C)	ΔH_{cs} (J/g)	T_{ch} (°C)	ΔH_{ch} (J/g)
60-0	52	19.86	195.67	14.12	-5.1	12.29	161.9	-8.85
60-5N	56.3	23.4	--	--	--	--	--	--
60-8N	56	27.7	--	--	--	--	--	--
60-10N	54.3	33.7	--	--	--	--	--	--
60-13N	56	31.9	--	--	--	--	--	--
60-5I	58	26.88	162.67	7.23	--	--	--	--
60-8I	57.3	35.64	--	--	--	--	--	--
60-10I	57.7	37.3	--	--	3.93	24.77	--	--
60-13I	56	38.16	--	--	3.93	32.43	--	--

T_{ms} : the melting temperature of the soft-segment; ΔH_{ms} : the enthalpy of melting soft-segment; T_{mh} : the melting temperature of hard-segment; ΔH_{mh} : the enthalpy of melting hard-segment; T_{cs} : the temperature of soft-segment crystallization; ΔH_{cs} : the heat of soft-segment crystallization; T_{ch} : the temperature of hard-segment crystallization; ΔH_{ch} : the heat of hard-segment crystallization

5.2.2 Dynamic Mechanical Analysis

From Figure 5.9 and Figure 5.10 tensile storage modulus E' from dynamic mechanical analysis of PU non-ionomer and ionomer series, it's obviously found that there is a large difference in modulus below and above the transition temperature, which renders a sharp transition to the shape memory materials. The crystallization state of soft domain offers the high modulus at temperature below T_{ms} , whereas the entropy elasticity of molecular chain and physics cross links among hard segments causes the rubbery state modulus when the temperature increase beyond transition temperature. In non-ionomer series, with the increase of DMPA content, the storage modulus E' at the temperature range above T_{ms} is decreased abruptly which might be due to the disruption of the order of hard domain with the introduction of asymmetrical extender. Meanwhile, in ionomer series studied, with the increase of DMPA content, the E' at the

temperature higher than T_{ms} is decreased firstly and subsequently increased when

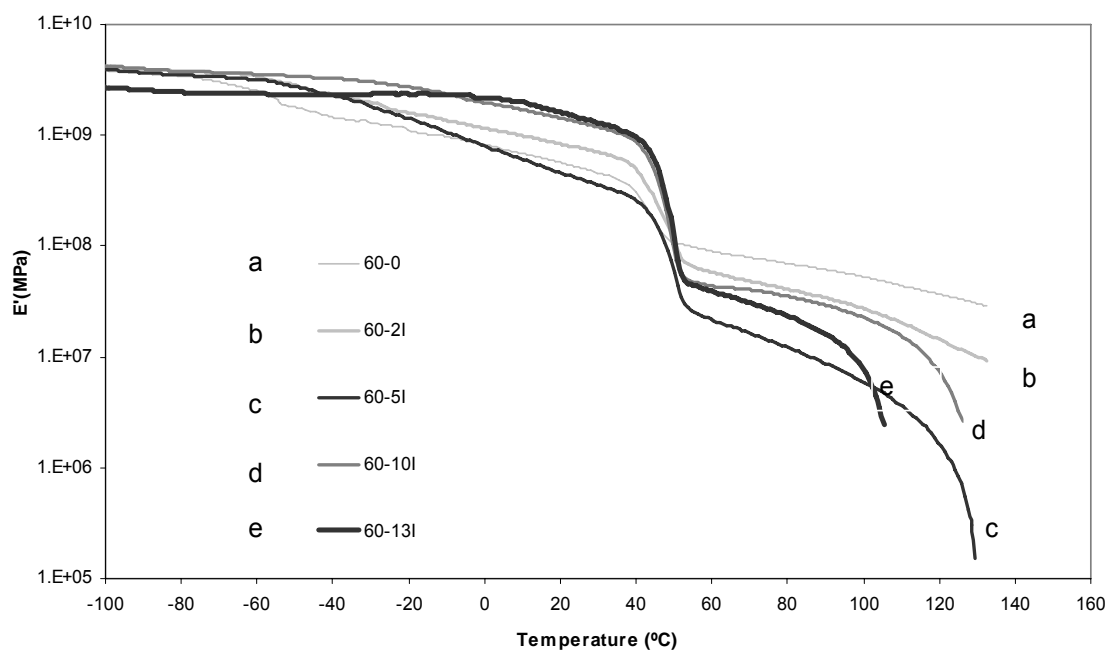
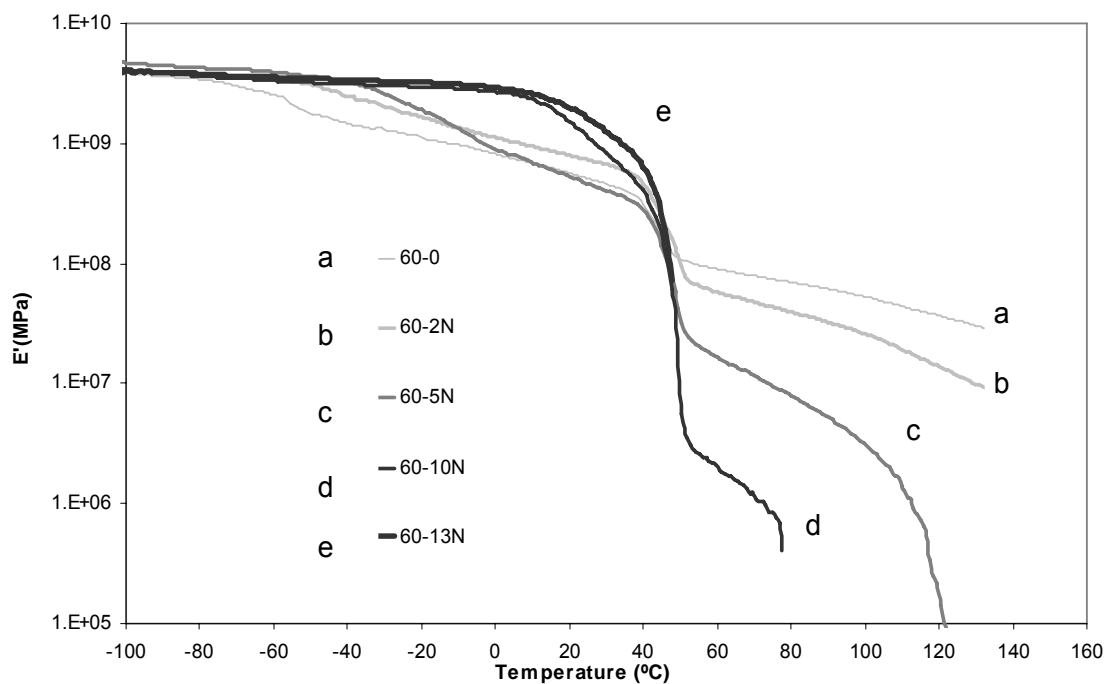


Figure 5.9 Plots of storage modulus E' of PU non-ionomers and the corresponding ionomers

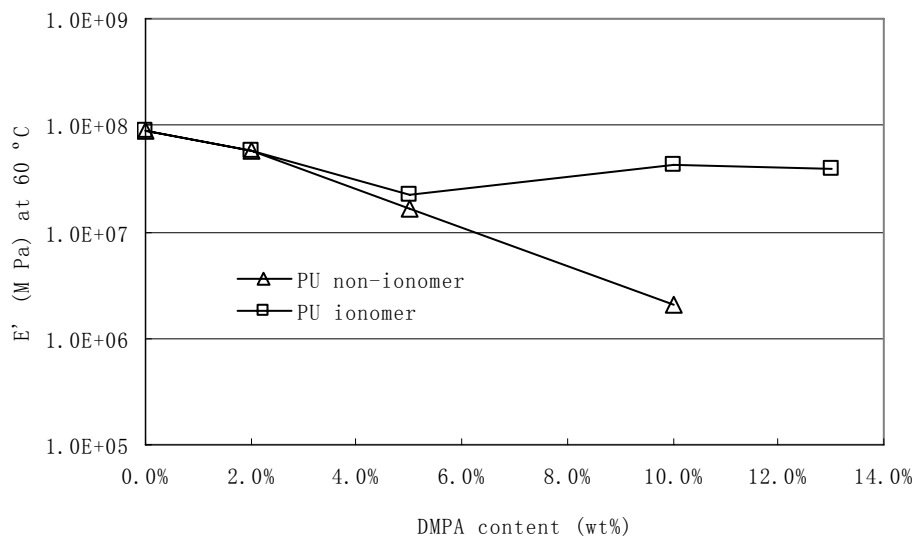


Figure 5.10 Comparison of E' at 60 °C between PU non-ionomer and ionomer series

the DMPA content is higher than 5 wt%, suggesting that charged ionic groups could enhance the cohesion among the hard segments in comparison with the corresponding PU non-ionomers especially in the PU ionomer samples with high ionic group content. The effect of increased cohesion among hard segments could be observed clearly from the comparison between PU non-ionomers and ionomers in Figure 5.11. Therefore, the two fold effect of charged ionic groups within the hard segments could be elucidated just like the literature reported by other researchers [48, 49]. On the one hand, ionic groups in hard segments could cause the disruption of the order of hard domain; on the other hand, the cohesion between hard segments could be increased for the Coulombic force between the ionic groups on hard segments. One of the two factors could be dominant under different specific polyurethane molecular system. The glass transition of soft segments could be determined from the maxima of the loss modulus as shown in

Figure 5.12 and listed in Table 5.5. Glass transition temperature of soft segment (T_{gs}) of the two series exhibited the similar trend.

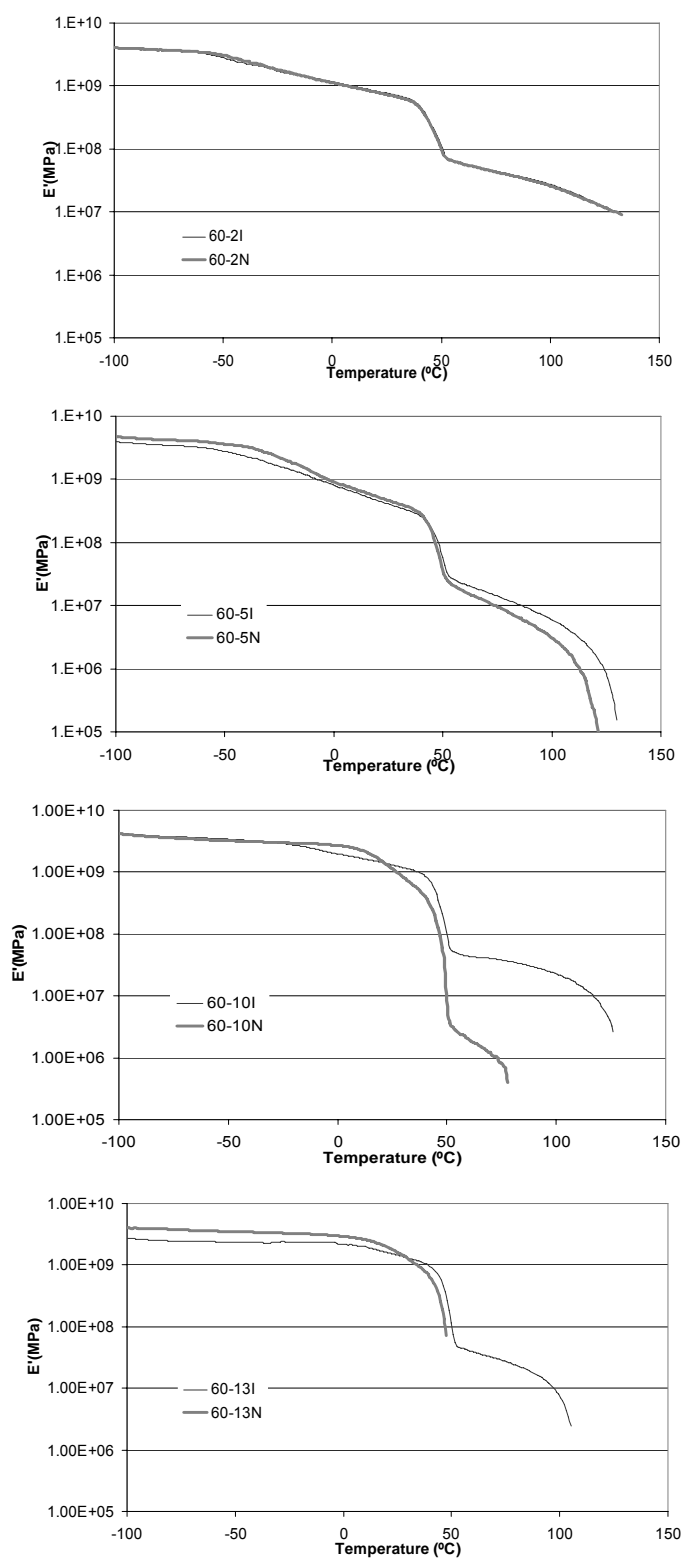


Figure 5.11 Comparison of storage modulus E' of PU non-ionomers and the corresponding ionomers

Table 5.5 T_g of soft segments from dynamic mechanical curves of films

Sample Code	60-0	60-2N	60-5N	60-10N	60-13N
T_g (°C)	-75.0	-52.0	-35.5	10.0	18.0

Sample Code	60-0	60-2I	60-5I	60-10I	60-13I
T_g (°C)	-75.0	-60.0	-58.0	-25.5	2.4

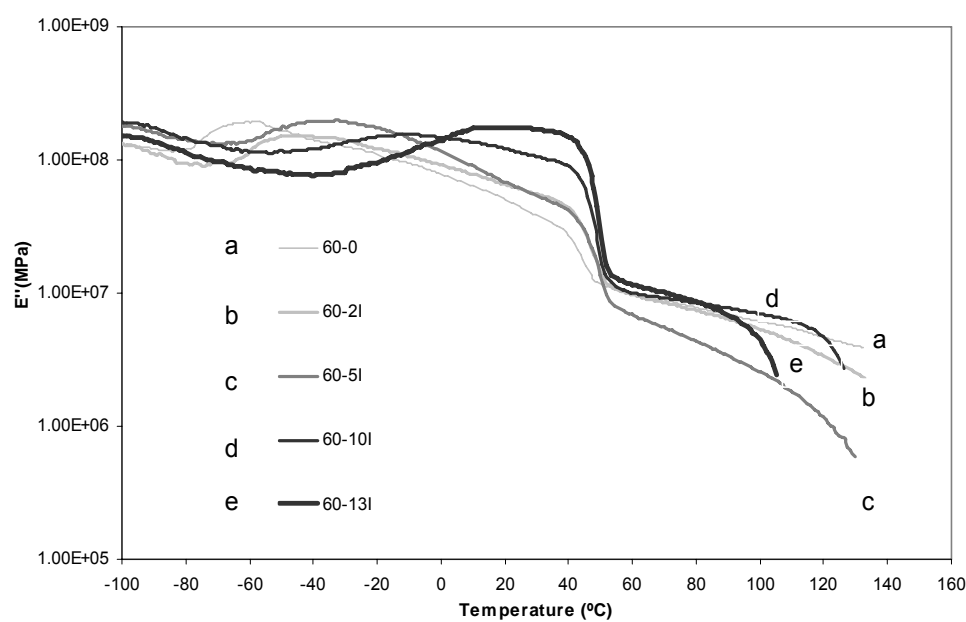
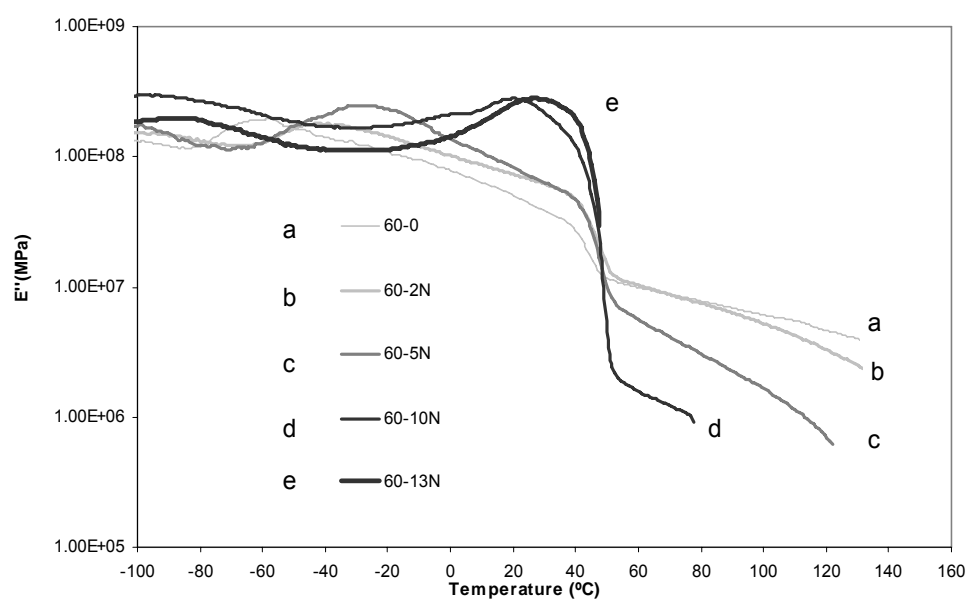


Figure 5.12 Plots of loss modulus E'' of PU non-ionomers and the corresponding ionomers

Table 5.5 shows that the T_{gs} increases with the increase of DMPA content, suggesting the introduction of ionic groups, whether neutralized or not, could disrupt the order of hard domain and cause the more hard-segment dissolved in the soft segment phase. Whereas, T_{gs} of PU ionomers is lower than the corresponding PU non-ionomers. The location of T_{gs} is sometimes used as indicators of phase purity in multi-block polyurethanes. If the copolymer is assumed to behave like a blend of homopolymers, the T_g of the phases in the blend could be compared to those of the neat components to determine the degree of hard/soft segment mixing[109, 127]. Therefore, in terms of the lower T_{gs} of PU ionomers compared with that of corresponding PU non-ionomers, it could be tentatively concluded that there are more hard-segment mixing in soft segment phase in PU non-ionomers in comparison with that of the corresponding ionomers, which suggests charged ionic groups on hard segments could improve the micro phase separation through enhancing the cohesion of hard segments.

5.2.3 IR Analysis

To investigate the effect of charged ionic groups within hard segments on the micro phase separation, infrared spectrum was used to analyze the carbonyl absorption for PU non-ionomers and ionomers. The hydrogen bonding is characterized by a frequency shift of bonded carbonyl groups to values lower than those corresponding to the free carbonyl groups. Xu et al [128] ever reported the IR spectrum of PU synthesized with polycaprolactone (PCL), 4, 4'-diphenylmethane diisocyanate (MDI), 1,4-butanediol (BDO), in which, 1730 cm^{-1} and 1701 cm^{-1} are attributed to free and hydrogen bonded carbonyls of hard segments respectively, meanwhile the corresponding values for that of the soft

segment carbonyl are selected at 1735 cm^{-1} and 1706 cm^{-1} respectively. Kim [79], Ten-Chin Wen et al[129] ever reported the band centered at 1665 cm^{-1} is assigned to the stretching of hydrogen-bonded carboxylic carbonyl groups in PU, which comes from DMPA unit. Therefore, the extent of hydrogen bond could be studied through analysis of carbonyl region ($1650\text{-}1740\text{ cm}^{-1}$) at IR spectrum.

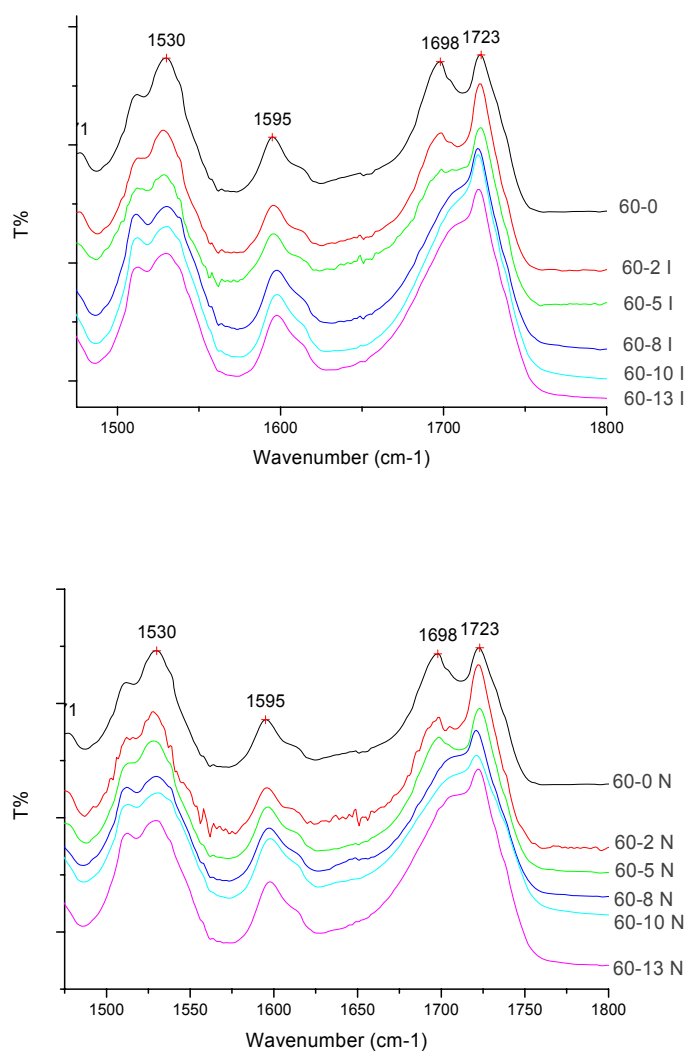


Figure 5.13 IR spectrum of PU non-ionomer series and ionomer series

From Figure 5.13, it could be found the carbonyl stretching vibration is shifted to high frequency with the increase of DMPA content whether in PU non-ionomer

series or PU ionomer series, indicating there might exist two possibilities: (i) the more free carbonyl groups produced; (ii) the reduction of the order of hard domain. According to the analysis above by DMA, in which, it was tentatively concluded that the more phase mixing was produced with adding DMPA, which means the fraction of free carbonyl groups in soft phase is reduced. Therefore, we could presumably consider there is more disordered structure or free carbonyl groups produced in hard phase, which surpass the effect of reduction of the fraction of free carbonyl groups in soft phase in IR spectrum to some extent and caused the shift to high frequency of carbonyl region. It might demonstrate, with the introduction of asymmetrical extender after neutralization or not, the effect of the disruption of the order of hard domain, caused by DMPA is predominant.

Through the comparison between the carbonyl regions at IR spectrum of PU non-ionomers and the corresponding ionomers, the effect of ionic groups on phase separation could be studied. As shown in Figure 5.14, there is not significant difference between PU non-ionomers and the corresponding ionomers when DMPA content is low value (2 wt %) or the highest (12.6 wt %) content. However, when DMPA content is from 5 wt % to 10 wt %, the charged ionic groups cause the obvious shift of the carbonyl group stretching vibration to high frequency. It might be concluded that the fraction of free carbonyl groups are increased after neutralization which might be caused by enhanced phase separation, which agree well with the resulting data about T_{gs} of soft phase with DMA, in which, the T_{gs} of samples with 5 wt % and 10 wt % DMPA content, is decreased significantly after neutralization with TEA. For the samples, 60-13N and 60-13I, it's hard to give a reasonable explanation about the similar IR

spectrum of the non-ionomers and ionomers. It might be the result of counteraction of two opposite factors induced by strong Coulombic Force between ionic groups on hard segments.

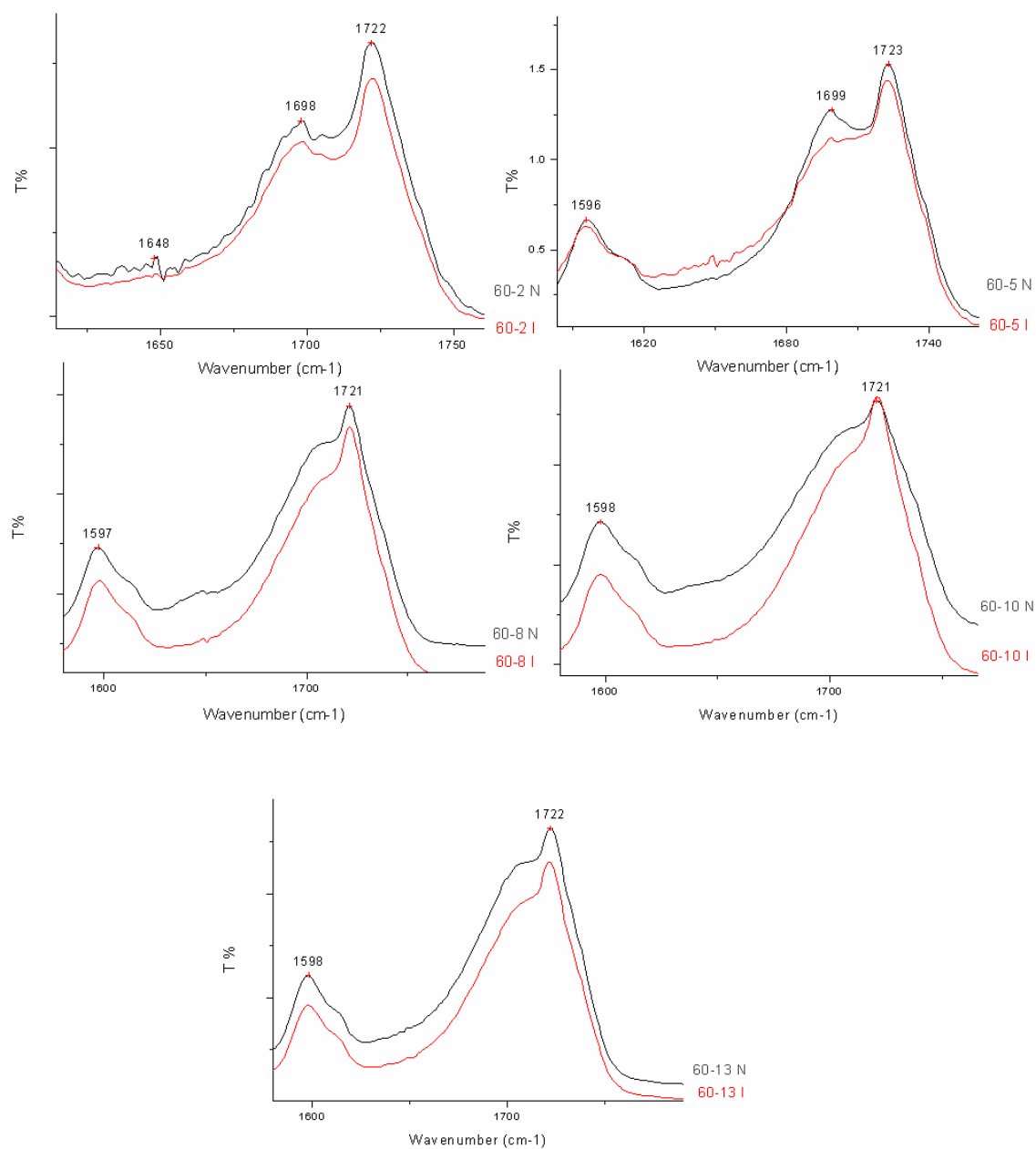


Figure 5.14 Comparison of IR spectrum between PU non-ionomers and ionomers

5.2.4 Cyclic thermo-mechanical investigation

The shape memory effect of ionic groups within hard segments of segmented polyurethane could be studied with cyclic tensile test as shown in Figure 4.2, in which the cyclic hardening, caused by the orientations of PU segments during extension, can be observed. This cyclic hardening and even the shape of stress-strain curve is mostly confined to the first several cycles and no significant variation is observed with further cycles[5]. Figure 5.15 shows the stress at 100% elongation at the second tensile cycle of PU non-ionomers and ionomers.

From the analysis in the study with DMA and FTIR, it was found that the introduction of asymmetrical extender caused the disruption of the order of hard domain, which is usually considered as the physical crossing link structure in the two phase morphology and contributed to the thermal stimulated deformation recovery [5, 47, 77, 104, 106]. Therefore, the shape memory effect of PU non-ionomer and ionomer series is supposed to be affected by the ionic group content.

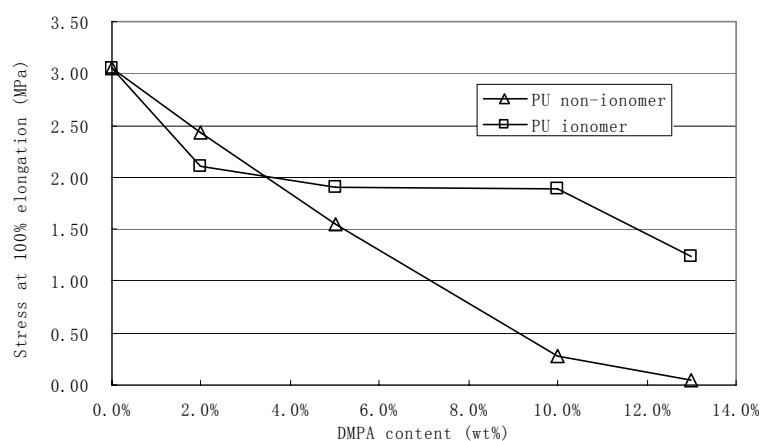


Figure 5.15 Comparison of stress at 100% elongation of second tensile cycle between PU non-ionomers and ionomers

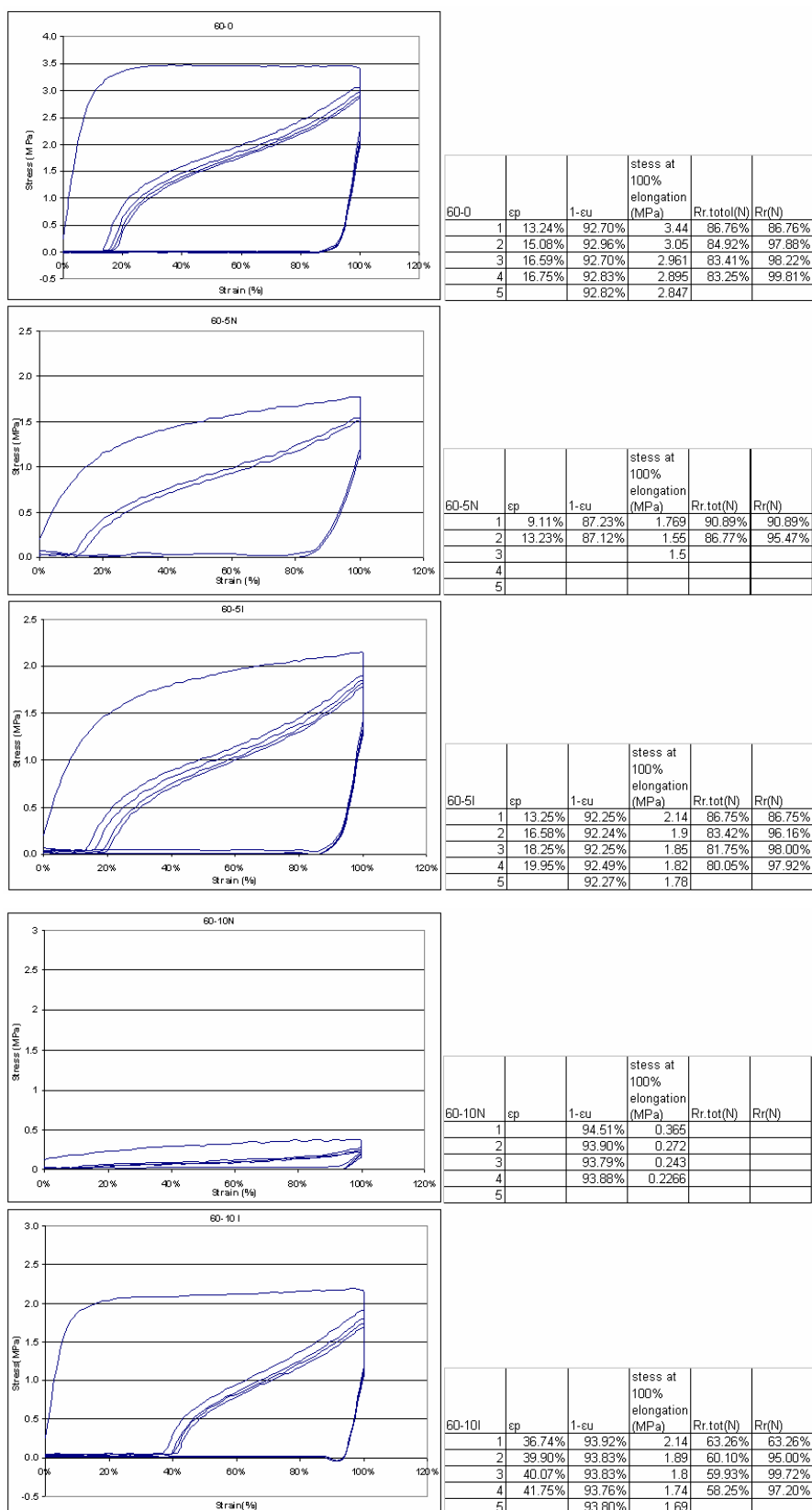


Figure 5.16 Cyclic tensile test of PU non-ionomers and ionomers

From Figure 5.15 and Figure 5.16 , it could be observed that the stress at 100% elongation of PU non-ionomer series at high temperature (60 °C) is decreased sharply with the increase of DMPA content; instead, that value of PU ionomer series is relative steady. This result was in agreement with the analysis above: the introduction of DMPA could disrupt the order of hard domain, which offers the physical crosslink in fixed phase; meanwhile charged ionic groups could enhance the cohesion between hard segments which has been characterized by DMA. With the increase of charged ionic groups in ionomer series, especially for PU ionomers with DMPA content higher than 10 wt %, the total strain recovery ratio ($R_{r.tot}$) decreases greatly from 83.4% (sample 60-2I: 2 wt % DMPA content at the first cycle test) to 61.6% (sample 60-13I: 13 wt % DMPA content at the first cycle test) and the recovery fixity ratio (R_f) could be kept in a high level at around 93% that might stem from the strong crystallibility of ionomer series as shown in DSC cooling scan in Figure 5.8. For all the specimen studied, the strain recovery ratio $R_r(N)$, reflecting the strain recovered in the following shape memory transition, could reach high level such as 97% or more after 3 or 4 testing cycle, which will be useful for some application area .

Deformation recovery property of PU non-ionomer and ionomer series could be investigated by strain recovery test as shown in Figure 4.3. In this study, the specimens for this test was prepared with cyclic tensile test in which the film is stretched to 100% elongation ratio at 60 °C, then cooled to room temperature (20 °C) and kept under strain constraint for a fixed time long (900s) so as to fix the deformation. When the stretched specimen was released from the strain constrain at room temperature, the relaxation without any constrain at room

temperature was conducted for different long time in order to investigate the relaxation time dependence of strain recovery property. In this test, only one sample 60-0 was tested and the resulting data was shown in Figure 5.17. From this figure, it elucidates that the deformation could be recovered sharply when the temperature is increased to switching temperature and most deformation recovery is finished in a narrow temperature range; besides, the switching temperature is shifted to high temperature with the increase of relaxation time and the strain recovery curves are almost superposed when the relaxation time is long enough such as 48 hour or more; the recovery ratio of the samples with different relaxation time is nearly same. Therefore, it could be concluded that, with the relaxation time, the switching temperature is increased to a steady status and the recovery ratio is not changed significantly.

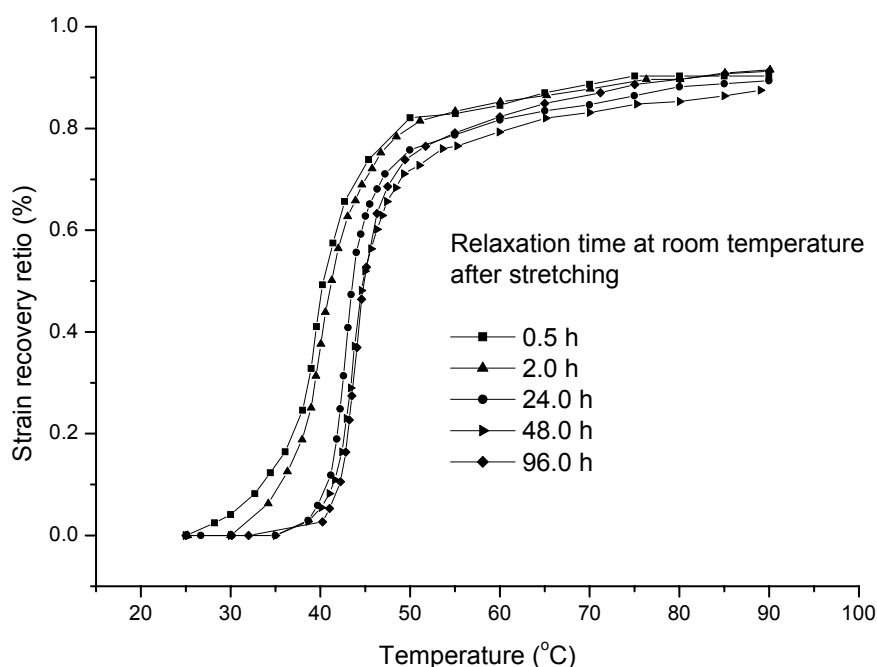


Figure 5.17 Relaxation time dependence of strain recovery property of sample 60-0

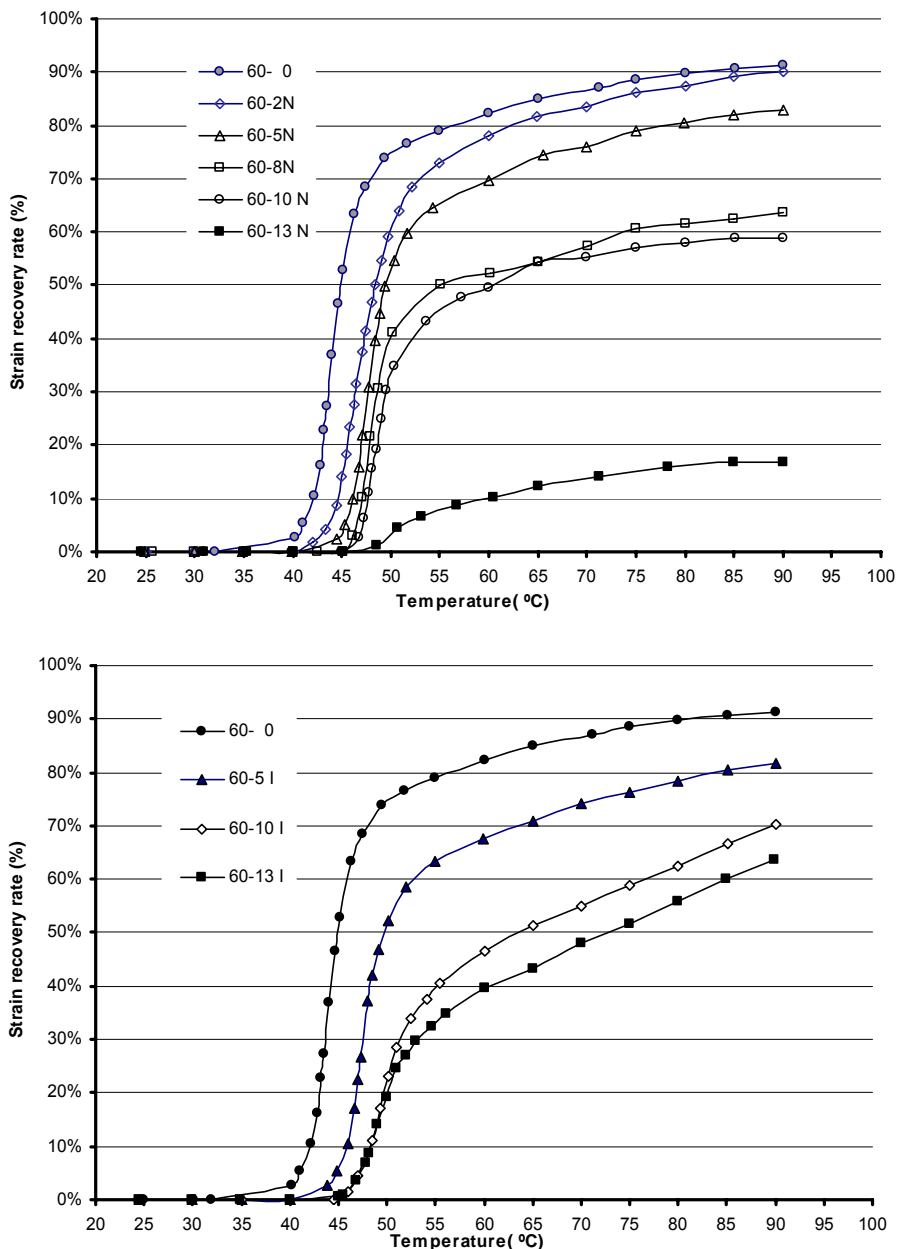


Figure 5.18 Strain recovery test of PU non-ionomers and ionomers

Based on the result above, the stretched samples for this test were all kept for a long time beyond 100 hour so as to reach the steady status after sufficient relaxation. Such measurement might be close to the application situation in some cases. Strain recovery curve is exhibited in Figure 5.18 in which it could be found that the switching temperature is increased evidently with the increase of DMPA content for PU non-ionomers and ionomers; the recovery ratio is

decreased sharply for non-ionomers but slightly lowered for ionomers as shown in Figure 5.19. The increase of switching temperature can be explained by the increase of T_m of soft segments. In samples with high DMPA content, the hysteresis effect could be observed. After heating up to switching temperature, the samples, especially for 60-10I and 60-13I, still could undergo strain recovery to some extent until the highest temperature is reached. This hysteresis effect might be related to the disruption of the order of hard domain and the enhanced cohesion between hard segments.

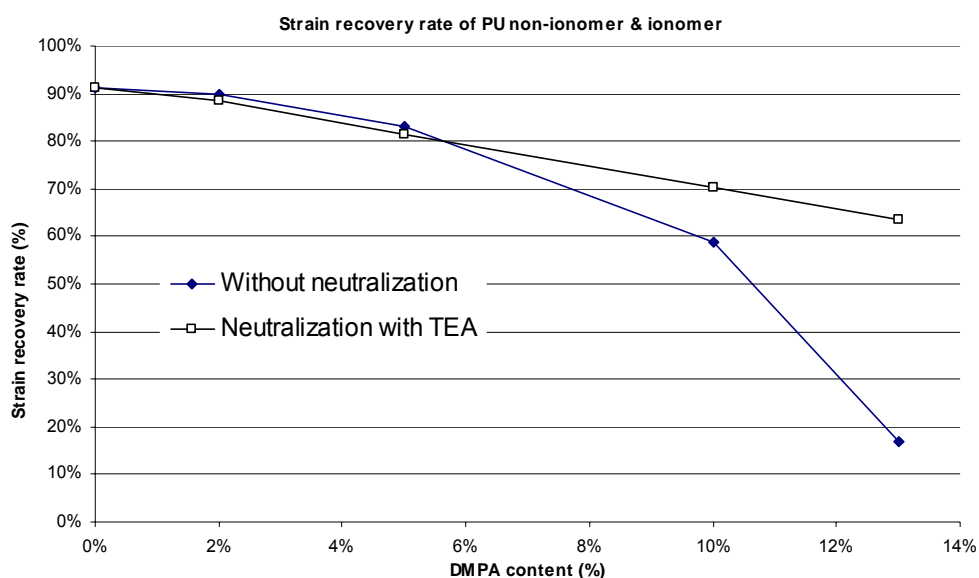


Figure 5.19 Strain recovery ratio of PU non-ionomers and ionomers

CHAPTER 6 STRUCTURE AND SME of SMPU CATIONOMERS

6.1 Crystallization and melting behavior of crystallizable soft-segments in SMPU cationomers

In the study of effect of crystallization and melting behaviour of crystallisable soft segments in SMPU cationomers, the series of SMPU cationomers shown in Table 3.4 were measured with DSC heating and cooling scan. Isothermal crystallization method under the similar high and low temperature point as the cyclic tensile testing condition were conducted so as to investigate the effect of cationic groups within hard segments on soft segments crystallization properties. The specific recipe design and synthesis routine have been described in the part 3.3.2.2.

6.1.1 Differential scanning calorimetry measurement

The thermograms of all the SMPU ionomers studied showed the exothermic crystallization peak of the soft segment in the cooling scan and the endothermic melting peak of the soft segment in the reheating (the second heating) scan as shown in Figure 6.1 and Figure 6.2. All the crystallization and melting behavior of hard segments cannot be detected in this testing cycle, which is due to the relative low hard segment content. The thermal properties data have been shown in details in Table 6.1. It was observed that T_{cs} in cooling scan (crystallization temperature of soft segments) increased significantly with increasing ionic group content and ΔH_{cs} (the enthalpy of crystallization of soft segments) in four SMPU

ionomer specimens is quite similar, but higher than that of the control sample 75-0. Generally, the enthalpy of crystallization in cooling scan can be used to investigate the crystallizability of specimen. Therefore, the resultant data of cooling scan suggests that the soft segment of SMPU ionomers have relatively stronger crystallizability. Accordingly, it can be observed that, in the reheating scan, T_{ms} (the melting point of soft segments) and ΔH_{ms} (the melting enthalpy of soft segments) of these two series SMPU ionomers (neutralization reagent is HAc or C8I respectively) is higher than 75-0. The crystallinity of soft segments in segmented polyurethane ionomer samples was calculated from the enthalpy of 100% crystalline PCL, 32.4cal/g, given by Crescenzi et al[97]. In that, it can be concluded that, in comparison with the control sample, the crystallinity of soft segments in segmented polyurethane is significantly raised with the existence of ionic groups within hard segments. According to the mechanism of shape memory effect proposed for segmented copolymers reported in previous studies[5-7], the crystallizable soft segment is responsible for the fixity of deformation. Therefore, it is expected that the higher crystallinity of soft segments might facilitate the temporary deformation fixity, potentially improve the fixity ratio. Besides, it is worth noting that there are dual-melting features in all the DSC reheating thermograms shown in Figure 6.2. Similar signature was also observed on the 30/70 DGEBA/PCL blend[124], binary blends of solution-chlorinated polyethylenes (CPE) with polycaprolactone (PCL), and blends of poly(hydroxyl ether of bisphenol A) (Phenoxy) with polycaprolactone (PCL)[125, 130], PCL/SAN investigated by Peter B[126]. In the study of Phenoxy/PCL by Defieuw[125], the isothermal crystallization process was interrupted after different time intervals and the DSC melting trace was immediately recorded.

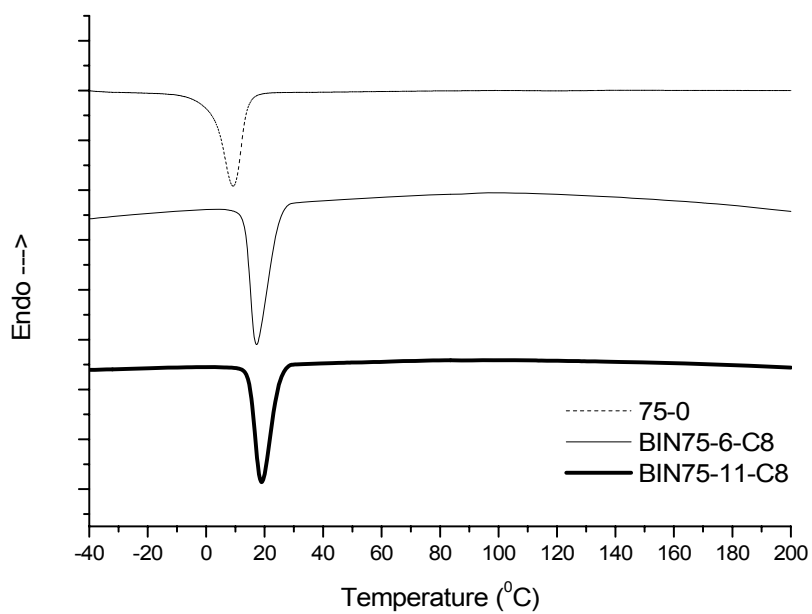
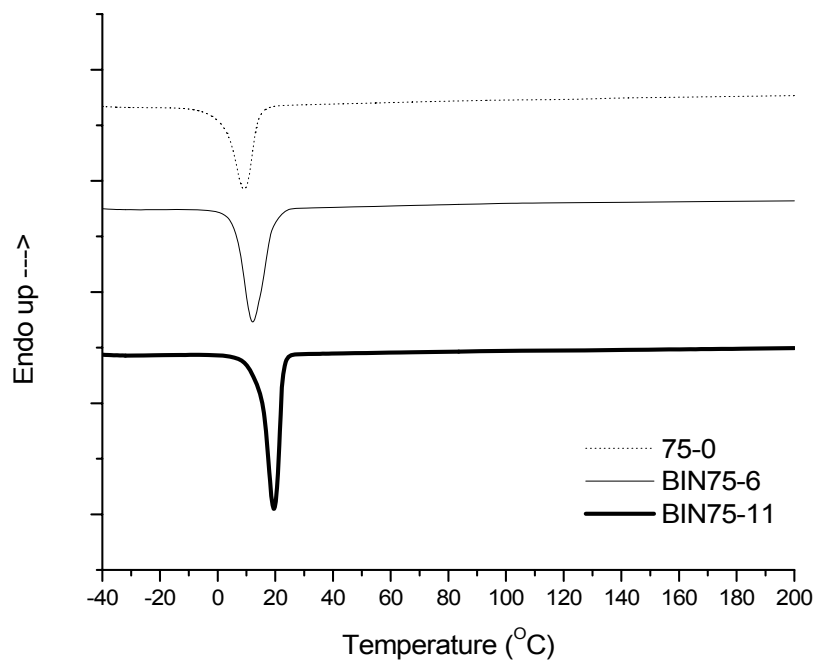


Figure 6.1 DSC cooling scan for SMPU ionomers

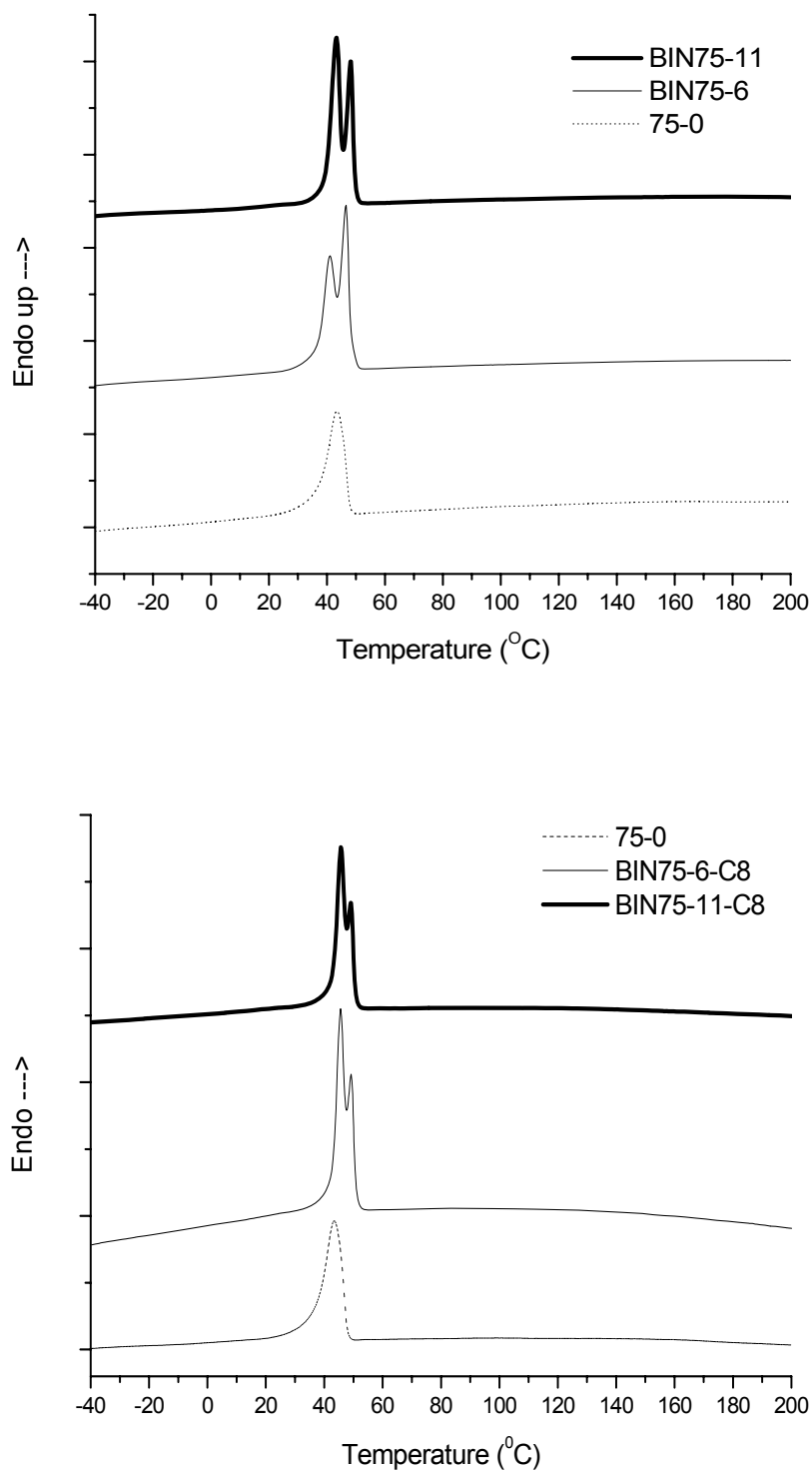


Figure 6.2 DSC heating scan for SMPU ionomers

Table 6.1 Thermal properties of SMPU ionomers

Sample Code	First heating at 10 °C/min			Second heating at 10 °C/min			Cooling at 10 °C/min	
	T_{ms} (°C)	ΔH_{ms} (J/g)	Crystallinity (%)*	T_{ms} (°C)	ΔH_{ms} (J/g)	Crystallinity (%)*	T_{cs} (°C)	ΔH_{cs} (J/g)
75-0	49.20	39.37	38.6%	43.46	35.62	34.9%	9.17	32.33
BIN75-6	46.94	39.81	39.0%	46.63(41.09)	50.60	49.6%	12.14	44.87
BIN75-11	47.46	41.75	40.9%	48.50(43.29)	49.45	48.5%	19.59	43.97
BIN75-6-C8	53.05	52.67	51.61%	45.51(49.21)	46.12	45.19%	17.27	-44.50
BIN75-11-C8	53.21	52.75	51.69%	45.68(49.03)	42.07	41.22%	18.91	-41.48

* Calculated according to the enthalpy of fusion of 100% crystallization PCL: 32.4cal/g.

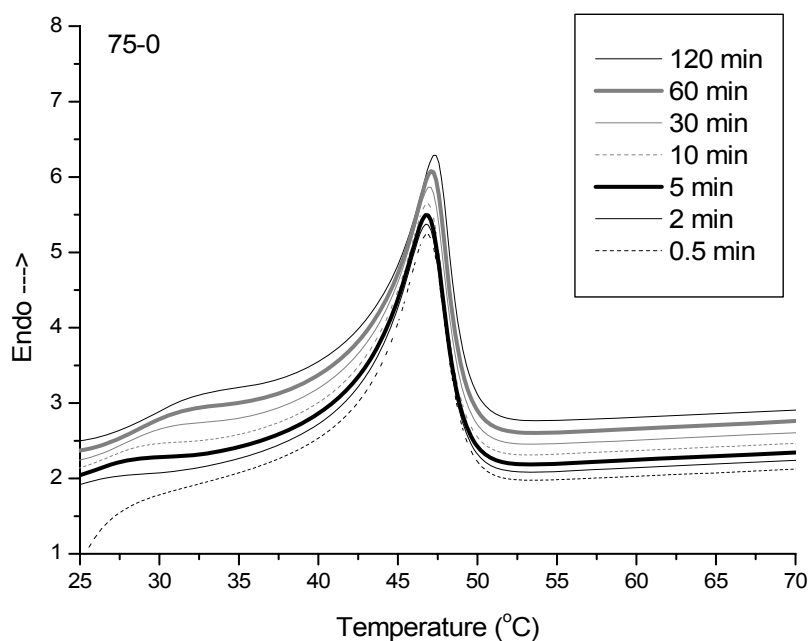


Figure 6.3 Heating scan after isothermal crystallization at 20°C for various time intervals for the sample 75-0

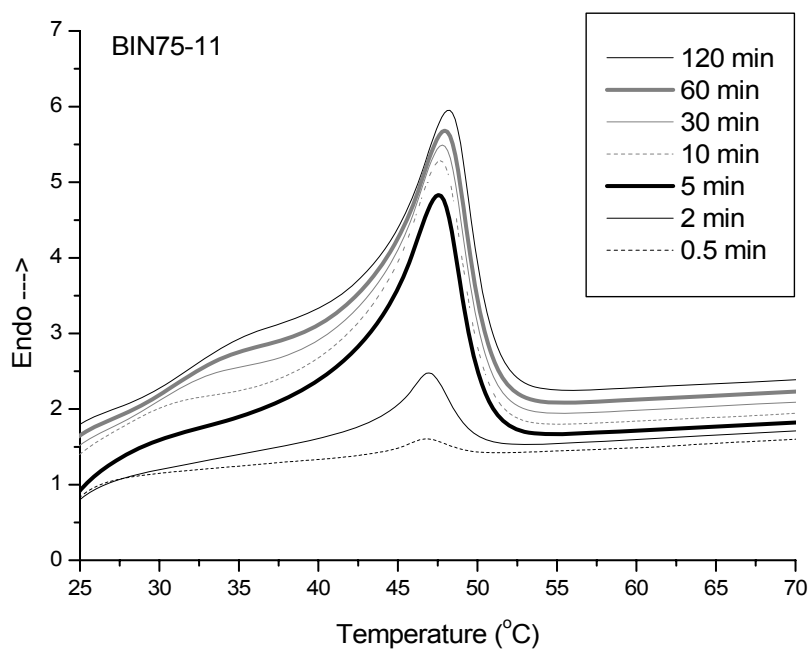
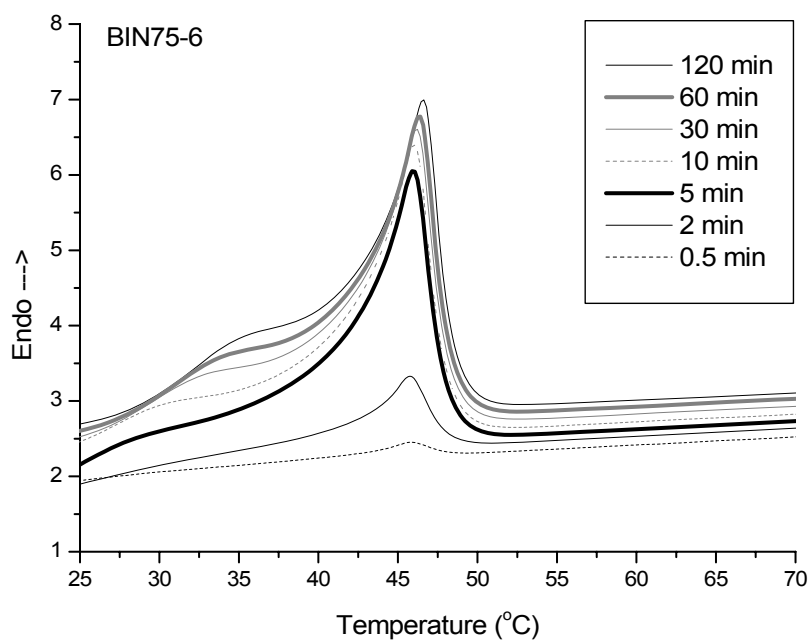


Figure 6.4 Heating scan after isothermal crystallization at 20°C for various time intervals for the sample BIN75-6 and BIN75-11

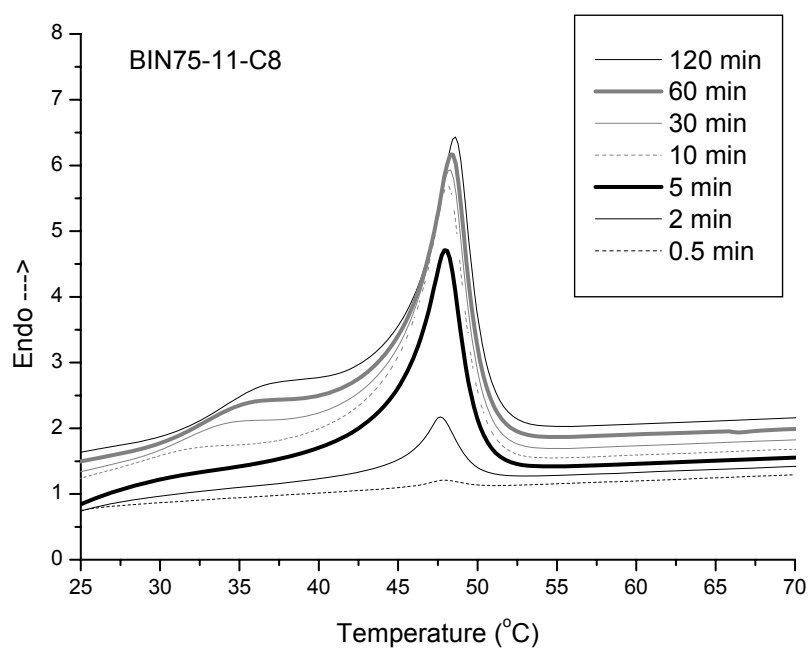
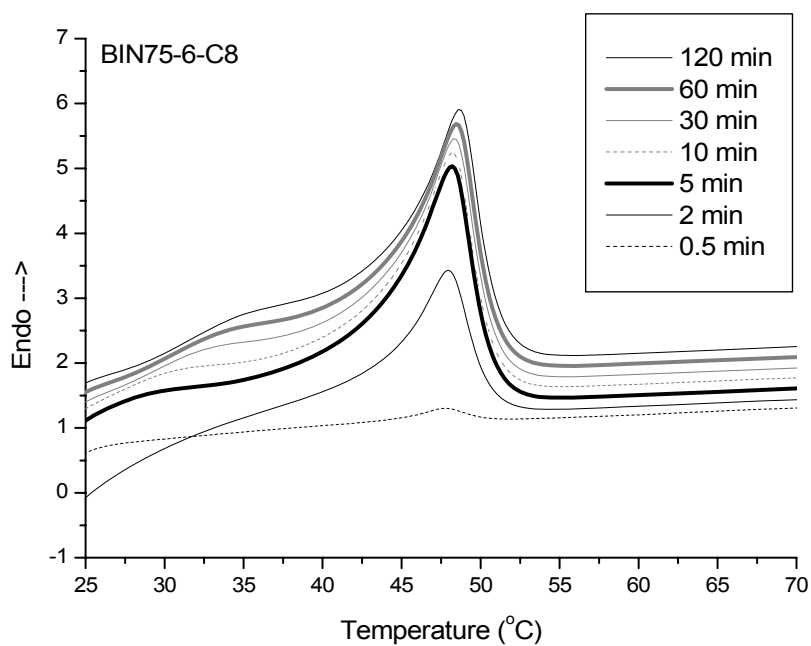
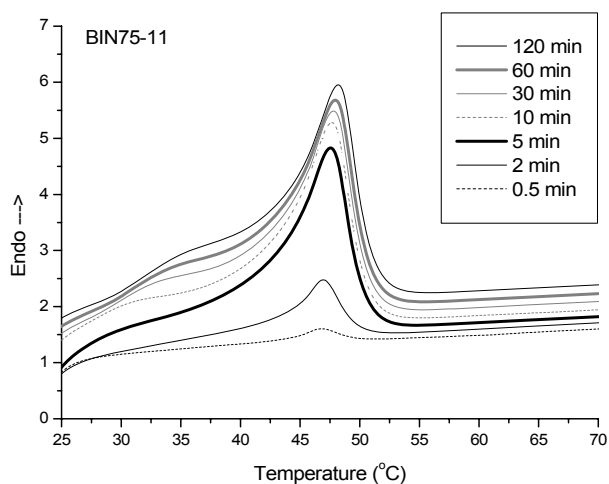
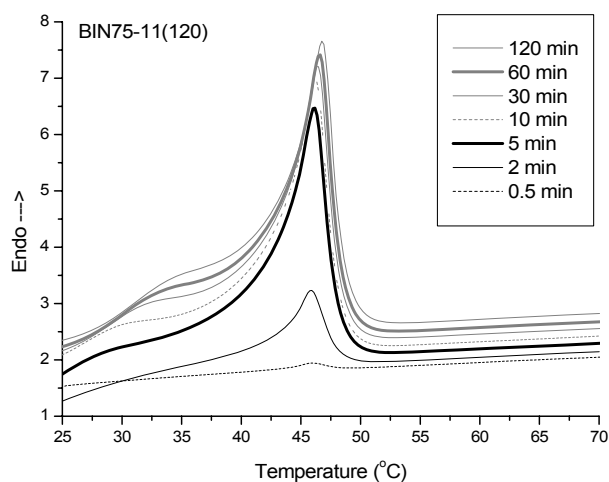


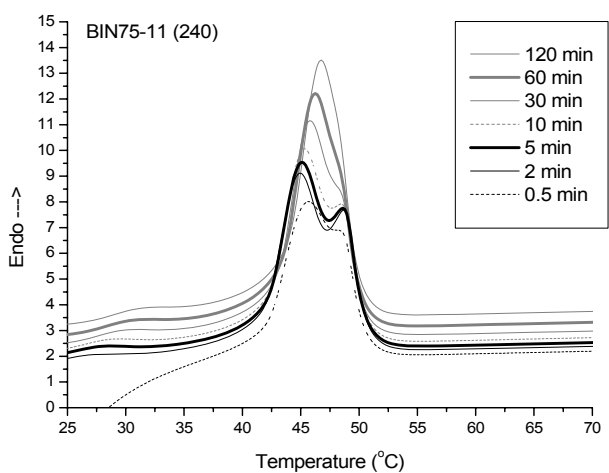
Figure 6.5 Heating scan after isothermal crystallization at 20°C for various time intervals for BIN75-6-C8 and BIN75-11-C8



(a)



(b)



(c)

Figure 6.6 Heating scan after isothermal crystallization at 20°C for various time intervals (In the first heating to remove the thermal history, the Maximum temperature is 70°C for BIN75-11(graph a), 120°C for BIN75-11(120)(graph b), 240°C for BIN75-11(240)(graph c) respectively)

The higher melting endotherm is of a fixed temperature after short isothermal crystallization times (primary crystallization), while the lower melting peak only appears after much longer crystallization times (secondary crystallization). The secondary crystallization is supposed to occur in the amorphous phase segregated during the primary crystallization of PCL, resulting in a slower crystallization process as this happens in the presence of a higher Phenoxy concentration. In our study, the similar routine was used to investigate the dual melting behavior of SMPU ionomers. In order to remove the effect of recrystallization in cooling process, the sample was quenched to the T_c (isothermal crystallization temperature) from 70°C with the high cooling rate (60°C/min). The isothermal crystallization temperatures are 20°C as shown in Figure 6.3, Figure 6.4 and Figure 6.5.

In the routine applied above, the high temperature, 70°C, and the low temperature, 20°C, are corresponding to the deforming temperature and fixing temperature of shape memory function cycle respectively studied in the part 6.2 and reported previously by our group[131]. Just like the result in the investigation of Phenoxy/PCL blends studied by Defieux[125], from the Figure 6.3, Figure 6.4 and Figure 6.5, it can be observed that the highest melting endotherm resides in the a constant area and position from 45 to 50°C in the heating scan after isothermal crystallization for various time intervals, instead, the lower melting keeps moving upward with the increase of isothermal crystallization time from 0.5 min to 120 min. However, after the isothermal crystallization at $T_c=20^\circ\text{C}$, it can be observed that the main melting peak area is from the primary crystallization, which was not the completely same as the dual

melting peak behavior in heating scan after cooling at 10°C/min from 240°C as shown in Figure 6.2. Therefore, this investigation was repeated for the sample BIN75-11 under different thermal history as follows: (a). Isothermal crystallization at 20°C after quenching from 75°C; (b). Isothermal crystallization at 20°C after quenching from 120°C; (c). Isothermal crystallization at 20°C after quenching from 240°C. The result presented in Figure 6.6 suggested that the specimen quenched from 240°C showed significant dual melting peak after isothermal crystallization for short time such as 5 min, but for longer time, the single melting peak will appear, which might be from the overlapped two peaks. For the samples quenched from 75 and 120°C, the primary crystallization is still predominant after various isothermal crystallization time. Therefore, the influence of thermal history on soft segment crystallization and melting behaviour is quite huge especially when the specimen was heated up to 240°C.

6.1.2 Analysis of isothermal crystallization kinetics

The kinetics of the isothermal crystallization of crystallizable soft segments from the melt was analyzed by using the modified Avrami equation called the Ozawa equation. The specific calculation can be conducted according to the equation 5.1 and the linear equation 5.2. $X(t)$ represents the relative amount of crystallization plotted in Figure 6.7 and Figure 6.8 for different crystallization temperatures and in Figure 6.9 for SMPU ionomers with various ionic group content at 28°C. Therefore, if the crystallization rate can be compared according to the time to finish the isothermal crystallization, it can be observed that the higher the isothermal crystallization temperature, the lower the crystallization rate will be; the crystallization rate decrease with the increase of BIN content in the series

SMPU ionomers whether the neutralization agent is HAc or C8I. Also, the choice of neutralization agent has some influence on the crystallization rate.

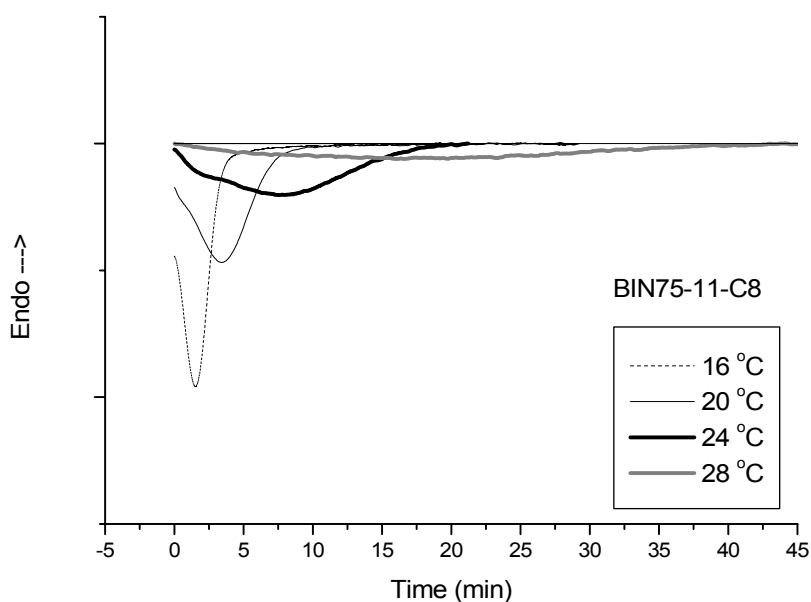
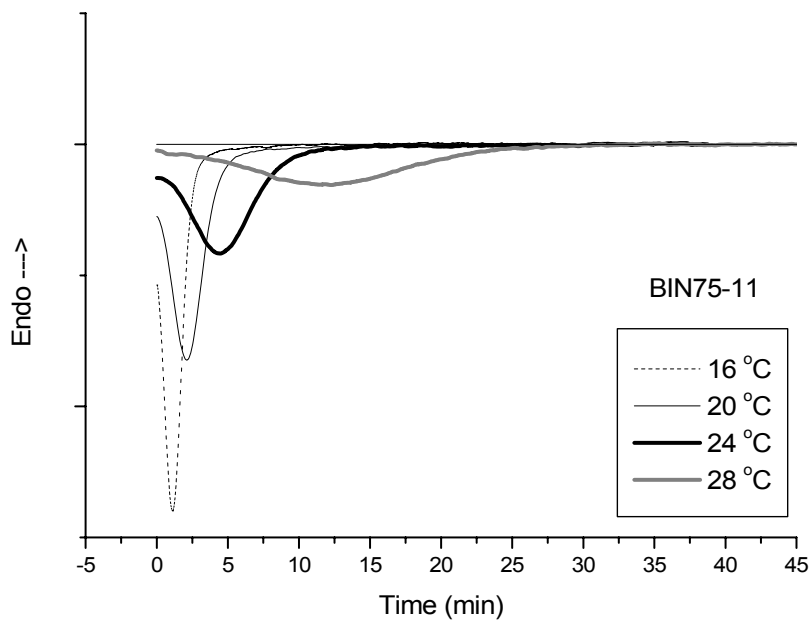


Figure 6.7 Exothermic curve for isothermal crystallization

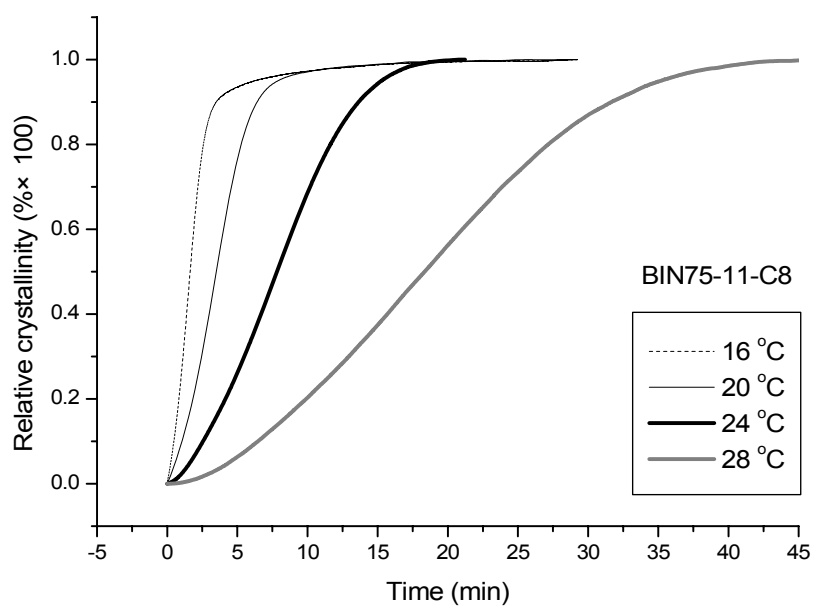
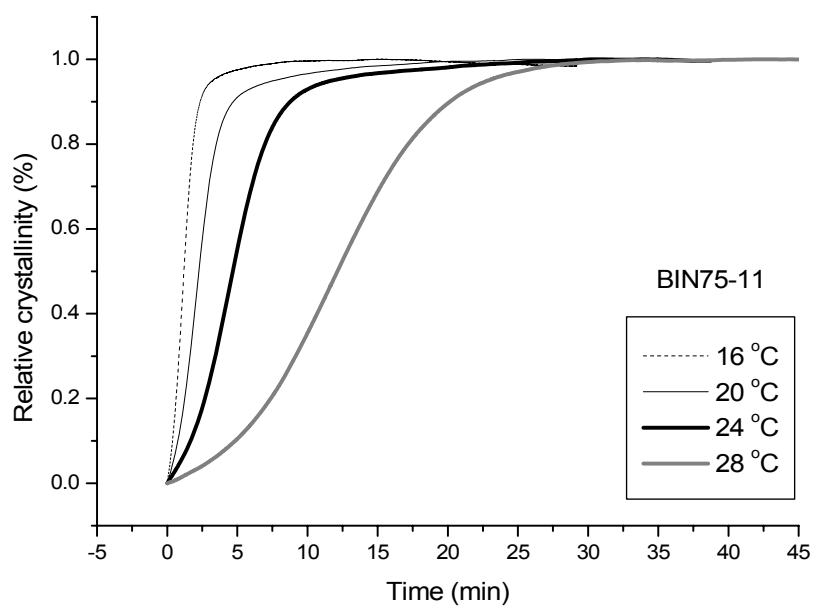


Figure 6.8 Relative crystallinity with time for isothermal crystallization

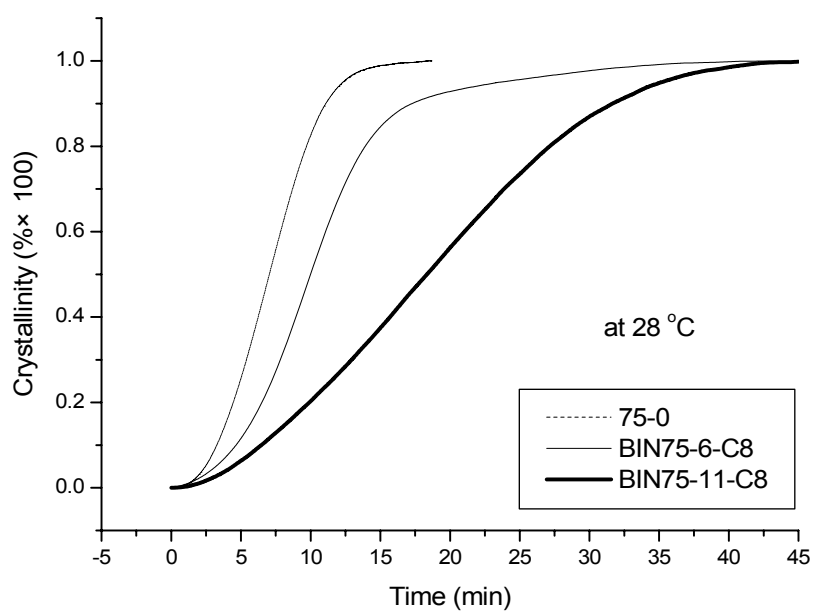
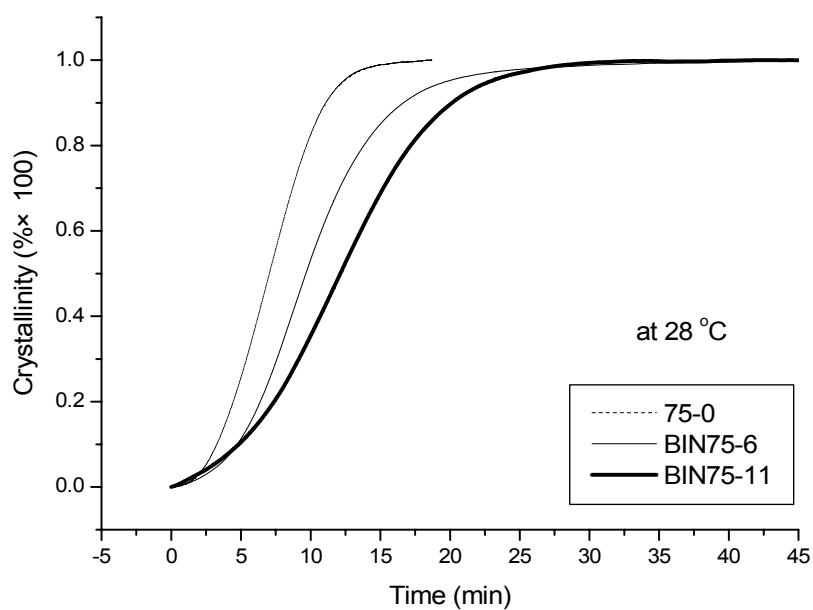


Figure 6.9 Relative crystallinity with various ionic group content for isothermal crystallization at 28 °C

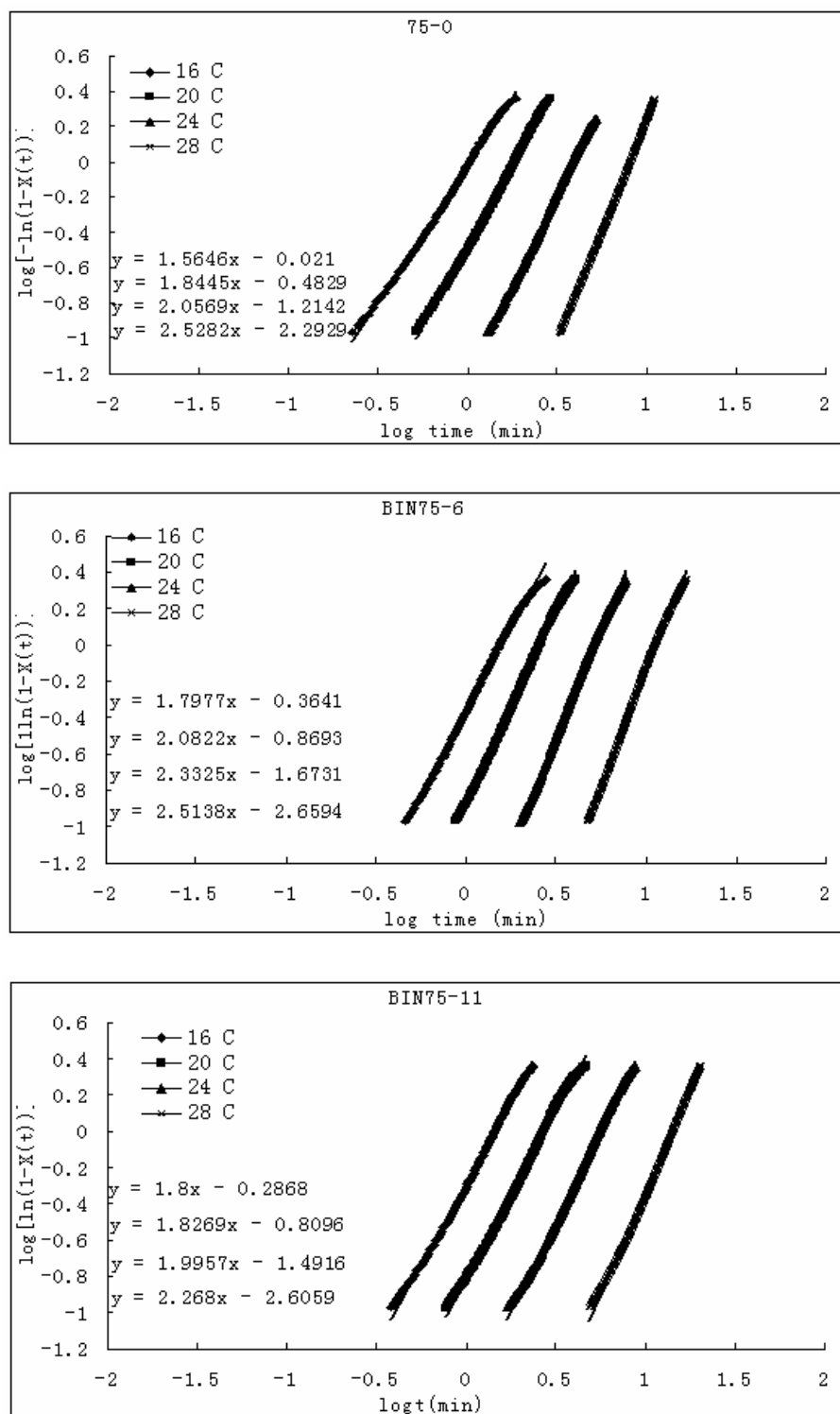


Figure 6.10 Plots of $\log[-\ln(1-X(t))]$ versus $\log t$ for isothermal crystallization for 75-0, BIN75-6, BIN75-11

Theoretically, if equation 5.2 can adequately follow the crystallization process, a plot of $\log[-\ln(1-X(t))]$ against $\log t$ should yield a straight line with slope n and intercept $\log K$. The double logarithmic plots of $\log[-\ln(1-X(t))]$ against $\log t$ for SMPU ionomers with various temperatures are shown in Figure 6.10 and Figure 6.11. Each plot represents a linear dependence of $\log[-\ln(1-X(t))]$ against $\log t$, but of slightly deviation from the prediction when both parameters are large, indicating the existence of a secondary crystallization of PCL which occurs consecutively with primary.

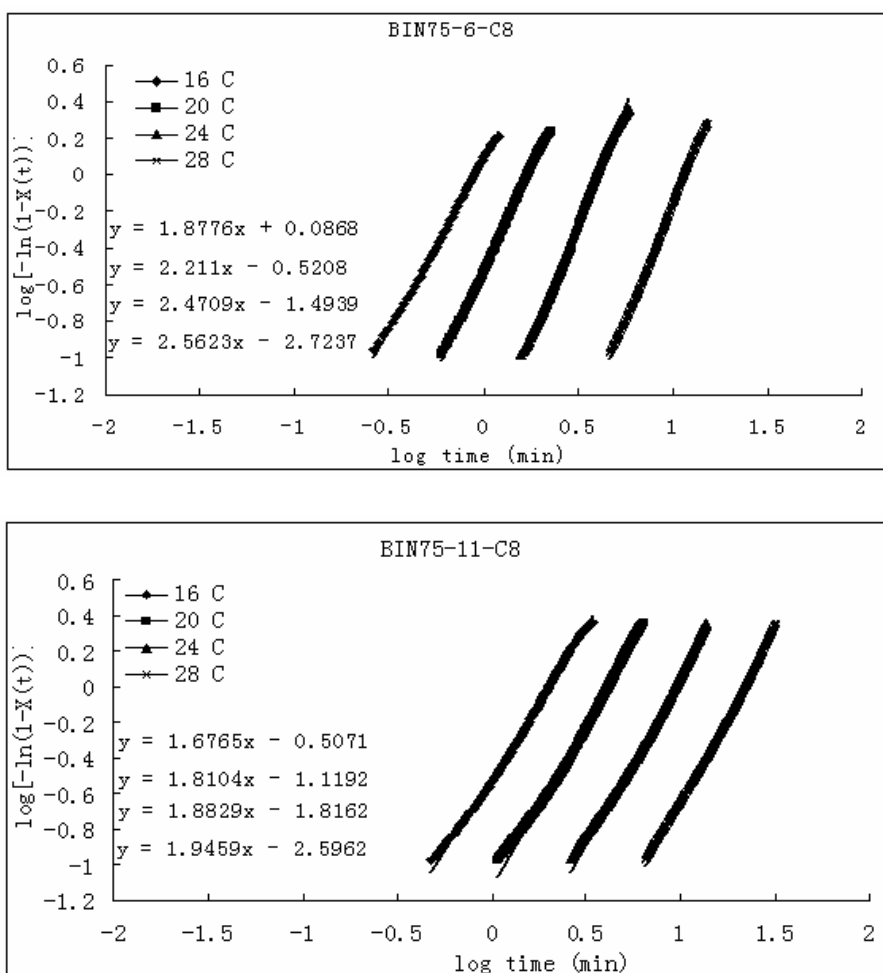


Figure 6.11 Plots of $\log[-\ln(1-X(t))]$ versus $\log t$ for isothermal crystallization

Table 6.2 Parameters of isothermal crystallization

Parameter Sample	T_c (°C)	T_c (K)	n	K	E (kJ/mol)	$t(0.5)$ (min)	$K=Ln2/[t(0.5)]^n$	T_e	T_m	Φ
75-0	16	289.15	1.56	9.53E-01	54.36	0.831	9.25E-01	54.1	45.77	0.23
	20	293.15	1.84	3.29E-01		1.52	3.21E-01		46.27	
	24	297.15	2.06	6.11E-02		3.25	6.11E-02		47.1	
	28	301.15	2.53	5.09E-03		7.04	4.97E-03		48.11	
BIN75-6	16	289.15	1.80	4.33E-01	51.83	1.27	4.51E-01	54.8	46.3	0.23
	20	293.15	2.08	1.35E-01		2.17	1.38E-01		46.79	
	24	297.15	2.33	2.12E-02		4.38	2.21E-02		47.63	
	28	301.15	2.51	2.19E-03		9.66	2.32E-03		48.63	
BIN75-11	16	289.15	1.80	5.17E-01	59.11	1.2	4.99E-01	52.9	46.11	0.19
	20	293.15	1.83	1.55E-01		2.27	1.55E-01		46.77	
	24	297.15	2.00	3.22E-02		4.68	3.16E-02		47.44	
	28	301.15	2.27	2.48E-03		12.13	2.40E-03		48.27	
BIN75-6 -C8	16	289.15	1.88	1.22E+00	66.87	0.74	1.22E+00	54.2	47.46	0.19
	20	293.15	2.21	3.02E-01		1.45	3.05E-01		47.79	
	24	297.15	2.47	3.21E-02		3.44	3.28E-02		48.45	
	28	301.15	2.56	1.89E-03		10	1.91E-03		49.29	
BIN75-11 -C8	16	289.15	1.68	3.11E-01	62.26	1.64	3.02E-01	54.1	46.6	0.21
	20	293.15	1.81	7.60E-02		3.5	7.18E-02		46.93	
	24	297.15	1.88	1.53E-02		7.83	1.44E-02		47.78	
	28	301.15	1.95	2.53E-03		18.35	2.41E-03		48.61	

The values of n and K for a particular sample can be determined from the initial linear portions of the double logarithmic plots shown in Figure 6.10 and Figure 6.11. The results for different samples are summarized in Table 6.2. The Avrami parameter n of the control sample and SMPU ionomers at 16~28 °C in this experiment is around 2.0 and present the slight increasing trend with the increase of temperature. This is a manifestation of the similar crystallization mechanism in the control sample and SMPU ionomers with various ionic group contents quenched from 70°C.

Table 6.2 summarizes the Avrami parameters for the soft segments of PU ionomers. The parameter K calculated from equation 5.3 agrees well with that obtained experimentally shown in Figure 6.10 and Figure 6.11. It suggests that the Avrami equation analysis is adequate to describe the crystallization mechanism of this series of SMPU ionomers[120]. The values of $t(0.5)$ for different samples are summarized in Table 6.2. It illustrates the fact that the crystallization rate decrease significantly with the introduction of asymmetrical chain extender, BIN. The more BIN weight content, the lower crystallization rate will be whether the neutralization agent is HAc or C8I. In comparison of BIN75-11 and BIN75-11-C8, it can be found that the crystallization rate is much higher in the former specimen, which can be judged from the shorter $t(0.5)$ for BIN75-11.

An understanding of the BIN wt% dependence of the Avrami parameters K is slightly more involved. Just like the previous study reported by Chen et al.[48], the incorporation of ionic component into hard segments can disrupt the order of the hard segments though the increased cohesion among ionic groups does exist in some specific case. Therefore, insertion of ionic groups in hard segments possibly can cause the more dissolved hard segments in soft segment domain, subsequently change the extent of phase mixing. Accordingly it influences the crystallization of crystallizable soft segments through varying the order of hard domain. In that, under the isothermal crystallization testing routine cooled from 70°C to room temperature such as 20°C, the presence of BIN ionic groups slows down the crystallization process significantly though the crystallization mechanism has not obvious changes. In practical viewpoint, it is supposed to

have huge influence on shape memory function under specific programming condition in this kind of SMPU ionomers and this relation between structure and shape memory properties will be further discussed in the part 6.2 and 7.1.

6.1.3 Equilibrium melting temperature

In Figure 6.12, it clearly reveals that T_m increases linearly with T_c . The experimental data can be fitted well by the Hoffman-Weeks equation[121]. The Φ in equation 5.6 can have values between 0 and 1 ($\Phi=0$ and $T_m=T_e$, whereas $\Phi=1$ and $T_m=T_c$). The crystal are most stable for $\Phi=0$ and unstable for $\Phi=1$. T_e can be calculated from the intersection point between plots of T_m against T_c and lines of $T_m=T_c$.

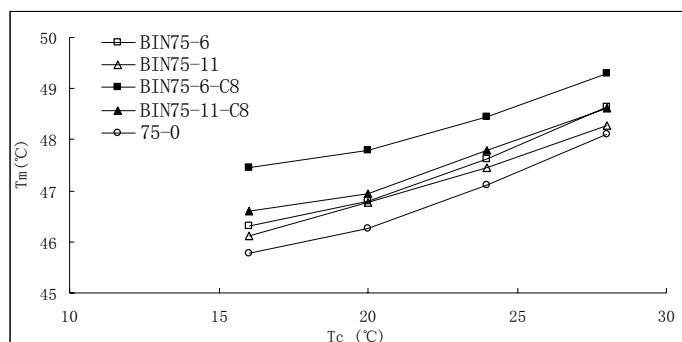


Figure 6.12 Plots of the observed melting temperature T_m against T_c for SMPU ionomers

As shown in Figure 6.12, the melting temperature T_m for SMPU ionomers increases with the crystallization temperature T_c as result studied in the part 5.1.5. The extrapolation of the observed melting temperatures to the line $T_m=T_c$ has been widely employed to calculate the T_e of different copolymers and homopolymers[107]. However, in this case, the similar phenomenon appears as that mentioned in the part 5.1.5: The extrapolation method fails to describe the

relations between the T_m and T_c . Due to the two possible reasons mentioned in the part 5.1.5, the lower T_c will cause the increase of T_m . Therefore, in our investigation of T_e of SMPU ionomers, the equilibrium melting temperature is calculated from the crystallization temperatures range above 20 °C.

Table 6.2 summarizes the values of equilibrium melting temperature (T_e) of this series of samples. It is interesting to note that the T_e values of SMPU ionomer samples are quite similar to that of the control sample, 75-0. After introduction of ionic groups within hard segments, the stability parameter Φ varies within 0.19 to 0.23 in SMPU ionomer samples, suggesting that the formation of crystals in SMPU ionomer samples is rather stable. The Φ values of PU ionomer samples are generally smaller than the control sample, 75-0, providing evidence that the ionic groups in hard segments improve the stability of the crystallization in soft segments.

6.2 Effect of cationic group content on SME in segmented PU cationomers

To investigate the effect of cationic group content on shape memory effect in segmented polyurethane cationomers, the series of SMPU cationomers as shown in Table 3.5 and Table 3.6 were prepared. In synthesis, the parameters, including synthesis temperature, specific procedures, soft segment length and soft segment contents, were adjusted to be consistent with the control sample 75-0, so as to solely investigate the effect of ionic group content. Cyclic tensile testing detailed in the part 4.6 was used to quantify the shape memory effect.

6.2.1 Thermal Properties

The thermograms of this series of SMPU cationomers showed the exothermic crystallization peak of the soft segment in the cooling scan and the endothermic melting peak of the soft segment in the reheating (the second heating) scan as shown in Figure 6.13 and Figure 6.14. The crystallization and melting behavior of hard segments cannot be detected. The thermal properties data have been shown in details in Table 6.3. In NMDA and BIN series of SMPU cationomers, it was observed that T_{cs} (crystallization temperature of soft segments) and ΔH_{cs} (the enthalpy of crystallization of soft segments) increased significantly with increasing ionic group content. Generally, the enthalpy of crystallization in cooling scan can be used to investigate the crystallizability of specimen[96]. Therefore, the resultant data of cooling scan suggests that the soft segment of SMPU cationomers with high ionic group content possesses relatively strong crystallizability. Moreover, the value of T_{cs} and ΔH_{cs} of NMDA series are lower than that of BIN series, indicating that the crystallizability of soft segments in NMDA series is weaker than that in BIN series. Accordingly, it can be observed that, in the reheating scan, T_{ms} (the melting point of soft segments) and ΔH_{ms} (the melting enthalpy of soft segments) of these two series increased with increasing ionic group content within hard segments. The crystallinity of segmented polyurethane ionomer samples was calculated from the enthalpy of 100% crystalline PCL, 32.4cal/g, given by Crescenzi et al[97, 132]. In that, it can be concluded that the crystallinity of soft segments in segmented polyurethane is significantly raised with the existence of ionic groups within hard segments. Generally speaking, the more ionic groups within hard segments, the higher crystallinity of soft segments can be achieved.

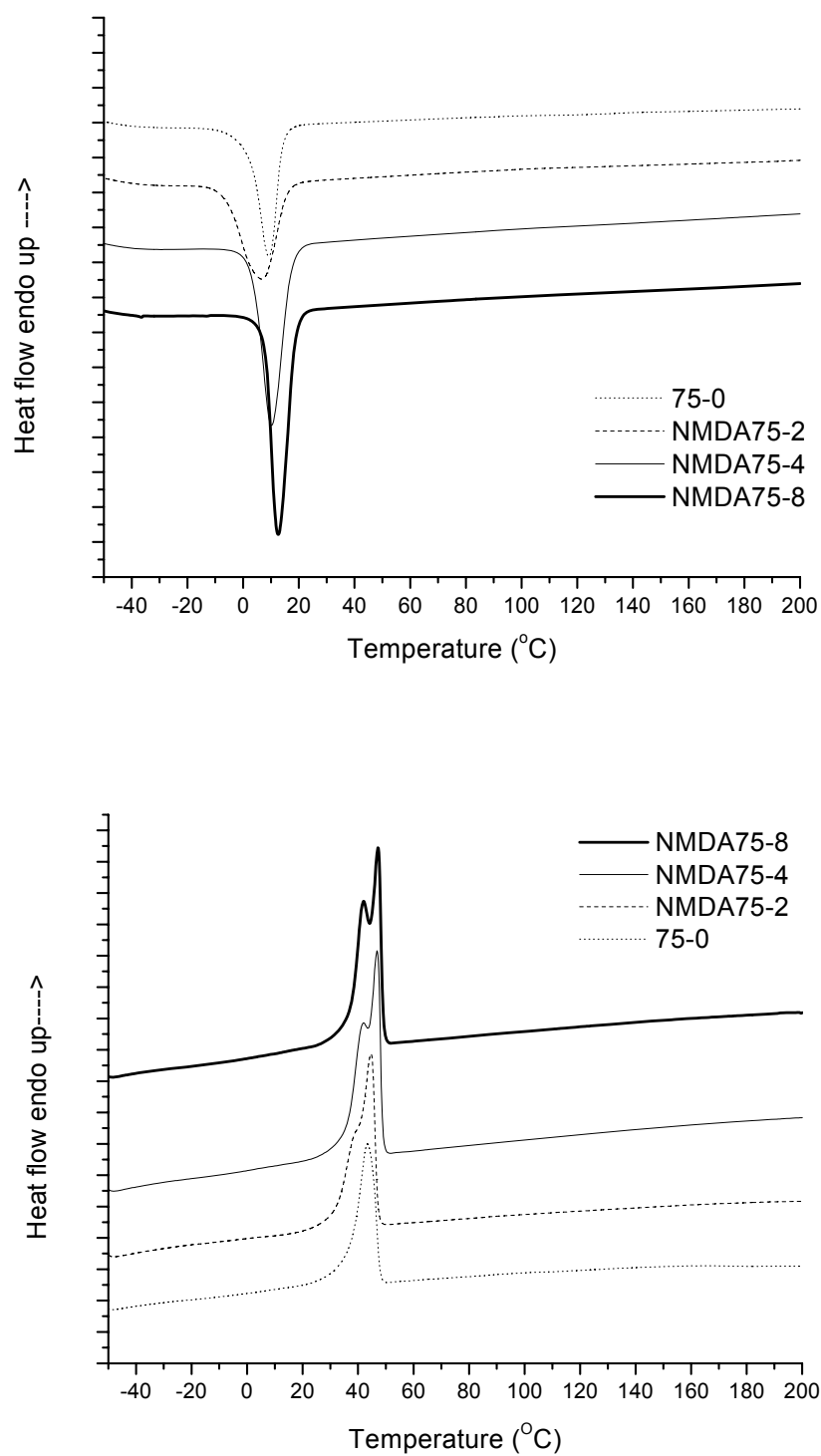


Figure 6.13 Cooling scan (upper) and reheating scan (lower) of NMDA series SMPU cationomers

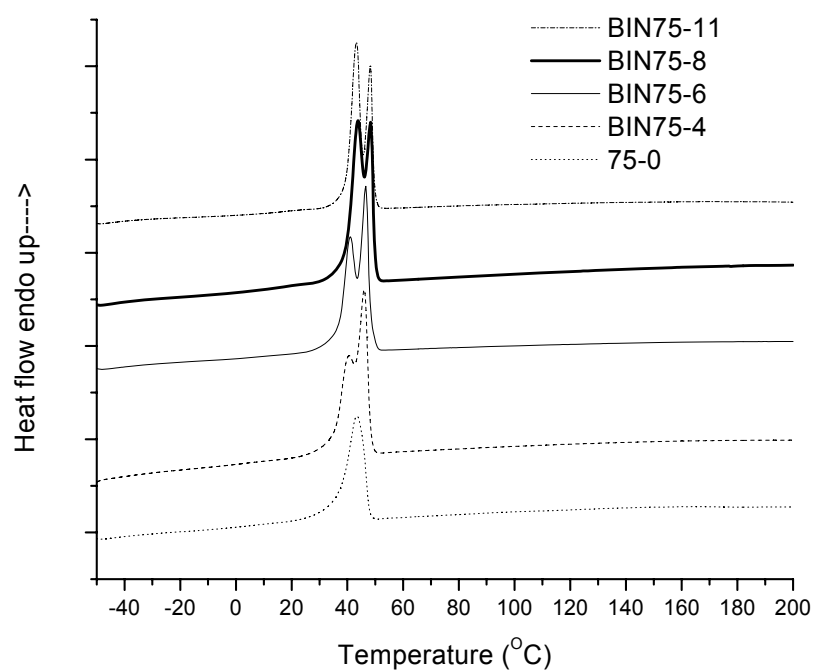
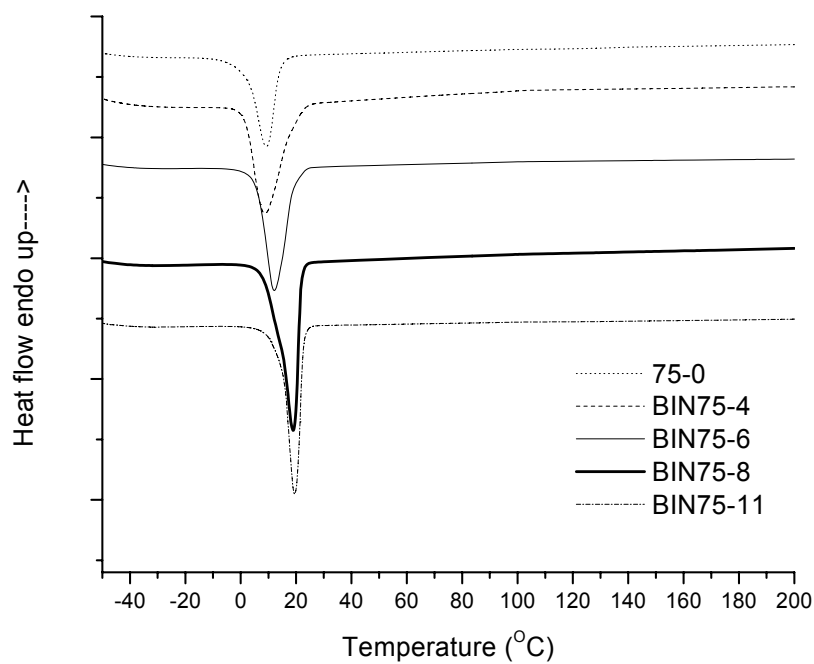


Figure 6.14 Cooling scan (left) and reheating scan (right) of BIN series SMPU cationomers

Table 6.3 Thermal properties of SMPU cationomers

Sample NO	First heating at 10 °C/min			Second heating at 10 °C/min			Cooling at 10 °C/min	
	T_{ms} (°C)	ΔH_{ms} (J/g)	Crystallinity (%)*	T_{ms} (°C)	ΔH_{ms} (J/g)	Crystallinity (%)*	T_{cs} (°C)	ΔH_{cs} (J/g)
75-0	49.20	39.37	38.6%	43.46	35.62	34.9%	9.17	32.33
NMDA75-2	51.82	48.15	47.2%	44.66	45.36	44.4%	6.75	38.97
NMDA75-4	52.12	49.73	48.7%	46.81 (41.97)	46.86	45.9%	10.18	42.59
NMDA75-8	50.43	52.72	51.7%	47.14 (41.96)	46.59	45.6%	12.65	43.61
BIN75-4	50.16	43.80	42.9%	45.99 (40.75)	48.93	47.9%	8.74	46.56
BIN75-6	46.94	39.81	39.0%	46.63 (41.09)	50.60	49.6%	12.14	44.87
BIN75-8	50.01	44.94	44.0%	48.13 (43.79)	51.37	50.3%	18.93	46.24
BIN75-11	47.46	41.75	40.9%	48.50 (43.29)	49.45	48.5%	19.59	43.97

* Calculated according to the enthalpy of fusion of 100% crystallization PCL: 32.4cal/g.

According to the mechanism of shape memory effect proposed for segmented copolymers reported in previous studies[5-7], the crystalline soft segment is responsible for the fixity of deformation. Therefore, it is expected that the higher crystallinity of soft segments might facilitate the temporary deformation fixity, possibly improve the fixity ratio.

6.2.2 Dynamic Mechanical Analysis

Figure 6.15 shows the storage modulus (E') from dynamic mechanical analysis of NMDA and BIN series. The result suggests that there is a main difference in the storage modulus in the temperature range from 40 to 50 °C within which a sharp transition is rendered to the SMPU cationomers. This transition is attributed to the melting of crystallization of soft segments according to the result of DSC aforementioned. Below the melting point of soft segments (T_{ms}), the crystalline state of soft domain together with the glass state of amorphous hard

domain ensures a high modulus of the film[5]. However, when the temperature is above T_{ms} , the entropic elasticity of the molecular chain and physical cross linking among hard segments jointly contribute the rubbery state modulus[5, 7, 56, 96].

Table 6.4 T_{gh} of hard segments of BIN series detected from the peak of loss tangent ($\tan\delta$)

Sample Code	BIN75-4	BIN75-6	BIN75-8	BIN75-11
T_{gh}	158.87	136.15	130.52	132.87

For hard segment rich phase, although the formation of hard domains can not be characterized in DSC, the DMA offers the indirect evidence with the temperature dependence of dynamic modulus[96]. The E' of all SMPU ionomers is nearly 1×10^9 MPa at room temperature range. After the melting of soft segments, the rubbery plateau of E' is located in 1×10^7 MPa around, indicating the existence of physical crosslinks in SMPU ionomers. It is also observed that the rubbery plateau of E' at temperature above T_{ms} trends to be shorter and lower with increasing ionic group content, when asymmetric extender is incorporated into hard segments, showing the decrease of the packing extent of hard domains in NMDA series. Different scenario observed in BIN series is that the E' plateau is shortened and lowered with the increase of BIN content when BIN content is increased up to 8 wt%, but tends to be longer and higher subsequently when the BIN content rises above 8 wt%. Such a turning point of the variation of E' with the increase of ionic group content also can be observed in segmented polyurethane anionomers in chapter 5 and our previous study[133]. It suggests that the charged ionic groups could enhance the cohesion among hard segments especially in high ionic group content. Figure 6.16 illustrates the dependence of E' on ionic groups content detected with DMA at 20°C and 70°C respectively, in

which the E' of two series PU ionomers increase slightly with the ionic group content at 20°C, whereas decrease significantly with the ionic group content at 70°C. Substantially, the turning point at 8 wt% BIN also can be found clearly just like aforementioned. Therefore, it can be concluded that the modulus ratio that was defined as $E'_{\text{at } 20^{\circ}\text{C}}/E'_{\text{at } 70^{\circ}\text{C}}$ increased with the increase of ionic group content. The slight increase of elastic modulus at 20°C with ionic group content in constant soft segment content specimen is due to the greater soft segment crystallization induced by ionic groups within hard segments. The immense depression of elastic modulus at 70°C with ionic group content should be attributed to the disruption effect of ionic groups on the extent of the order of hard domain.

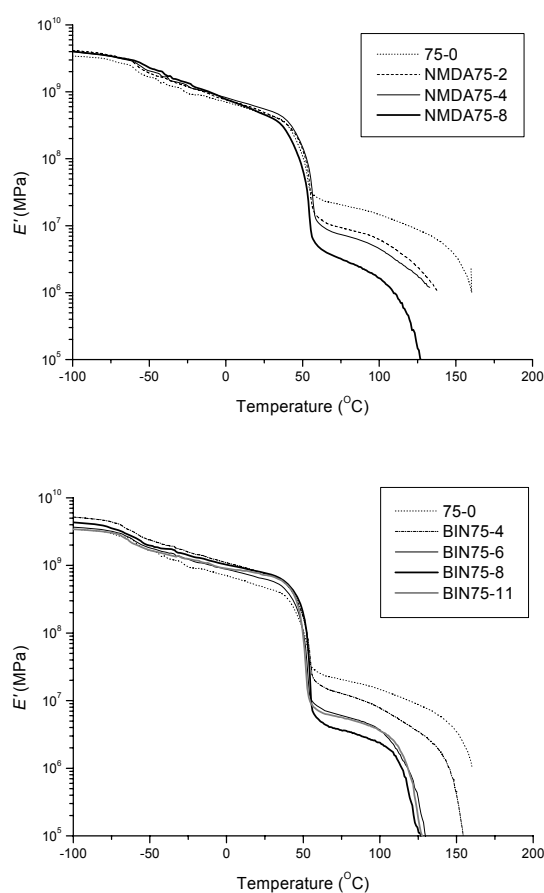


Figure 6.15 Storage modulus (E') of NMDA and BIN series SMPU cationomers

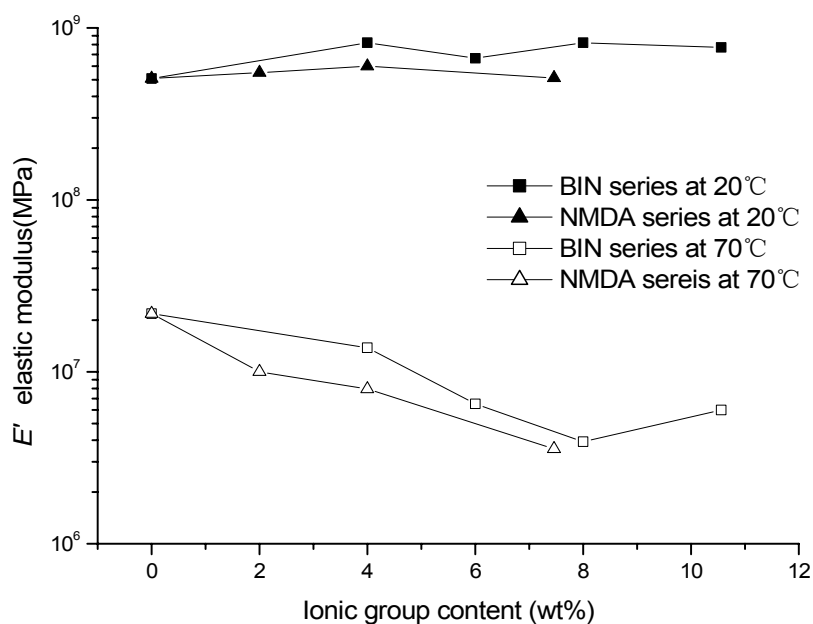


Figure 6.16 Elastic modulus of NMDA and BIN series SMPU cationomers at 20°C and 70°C

As shown in Figure 6.17 in comparison between SMPU cationomers and the corresponding non-cationomers, the SMPU cationomers all have longer and higher rubbery plateau than that of the corresponding non-cationomers, illustrating the existence of Coulombic Force among cationic groups and the increased cohesion among hard segments after ionization.

Considering the importance of the formation of hard segment domains as a structural characteristic for shape memory function, the deep study about the influence of ionic groups within hard segments on hard domain is necessary. The glass transition temperature of hard segments, MDI-BDO, in polyurethane was ever reported to be located at around 125°C [134]. The melting point of MDI-BDO crystal is in the range of 200-240°C [135]. Although the DSC can not

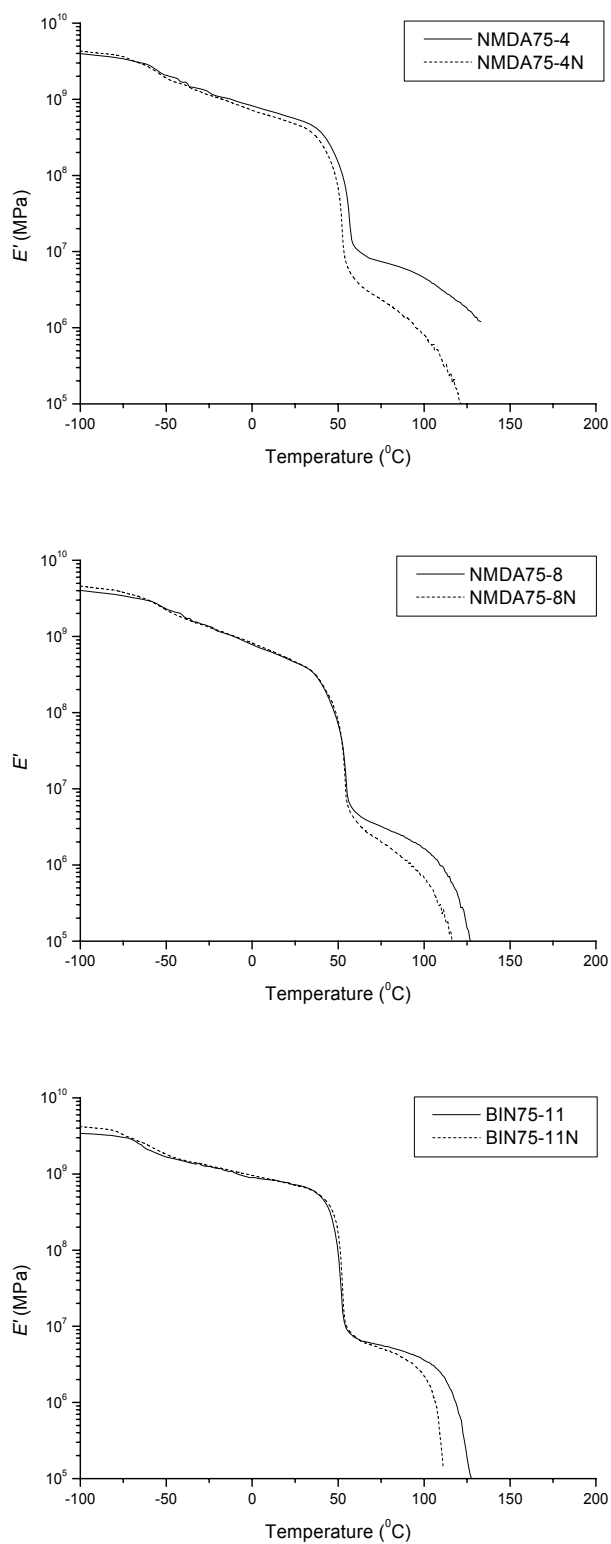
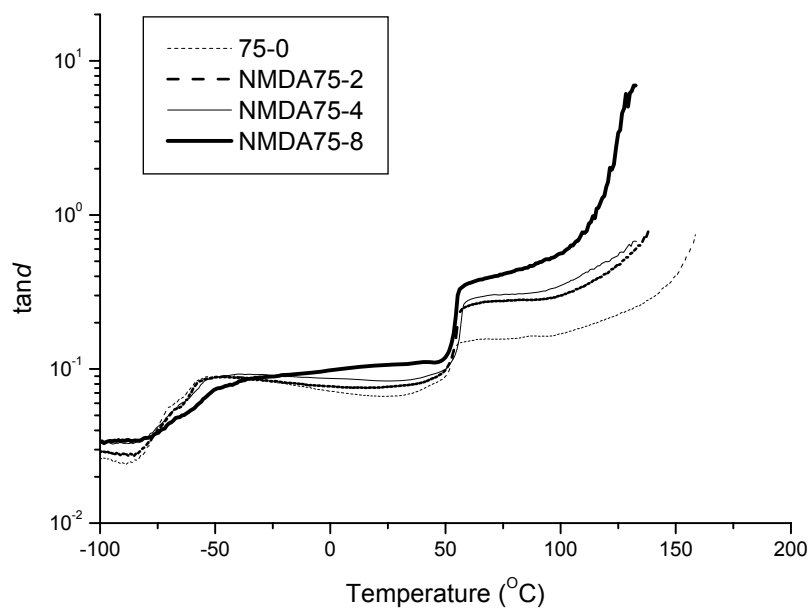
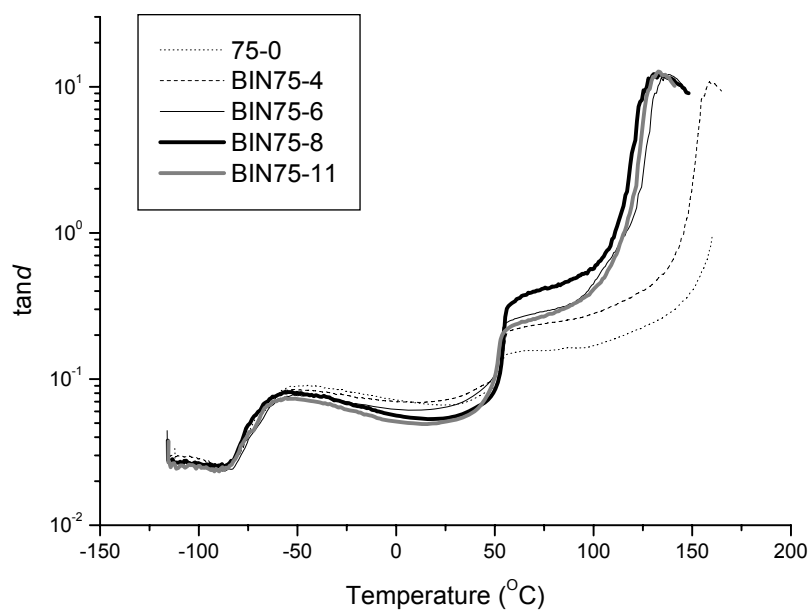


Figure 6.17 Comparison of E' between SMPU cationomers and the corresponding non-cationomers



(a)



(b)

Figure 6.18 Loss tangent ($\tan\delta$) of NMDA (a) and BIN (b) series SMPU cationomers

provide the information about the transition of hard segments, we still can detect the T_{gh} together with the various transition of soft segments with DMA. Figure 6.18 shows the dependence of loss tangent ($\tan\delta$) on temperature of NMDA and BIN series SMPU ionomers. The peak locating in -60°C around belongs to the glass transition temperature of soft segments(T_{gs}); the sharp rise at 50°C is attributed to the melting of soft segment crystallization; the peak appearing at the temperature above 100°C shown in (b) of Figure 6.18 is attributed to the glass transition of hard segment rich phase(T_{gh})[48-50]. Since $\tan\delta$ reflects the strain energy of dissipated by viscous friction, the larger $\tan\delta$ suggests the materials is more viscous and far from elastic[5]. Therefore, when heated above the melting point of soft segments (T_{ms}), generally the SMPU ionomers with high ionic group content having the higher $\tan\delta$ is more viscous than the specimen with low ionic group content. For BIN series, as shown in Figure 6.18 (b) and Table 6.4, the T_{gh} is monotonously depressed from 158.87 to 130.52°C with the increase of BIN weight content in hard segments from 4% to 8%, which indicates the insertion of ionic groups increase the disorder of hard domain, disrupt the order of the hard domain and lower the packing extent of hard domains. When the increase of ionic group content persists to the maximum allowable value, 10.56 wt% from 8 wt%, the T_{gh} can be move upward to 132.87°C from 130.52°C . This trend is quite similar with the result of the study on TDI series polyurethane cationomers reported by Chen et al.[48]. In that research, T_{gh} first decreases and then increases with increasing ionic content. The fall and rise of T_{gh} was explained by an increased extent of disordering due to disruption by ionization and an overcompensation of the increased cohesion due to the increased extent of ionization. Therefore, it is believed that the dependence of T_{gh} on ionic group

content is caused by the two opposite effects: disruption of hard domain by insertion of ionic groups and the increased cohesion among hard segments. When BIN content is high enough, such as in BIN75-11, the increased cohesion caused by Coulombic force among ionic groups is dominant compared with the sample BIN75-8, which also can be observed from the comparison of $\tan\delta$ value in rubbery plateau range, in which the BIN-11 is more elastic than BIN75-8, judging from the relative low $\tan\delta$ value of BIN-11.

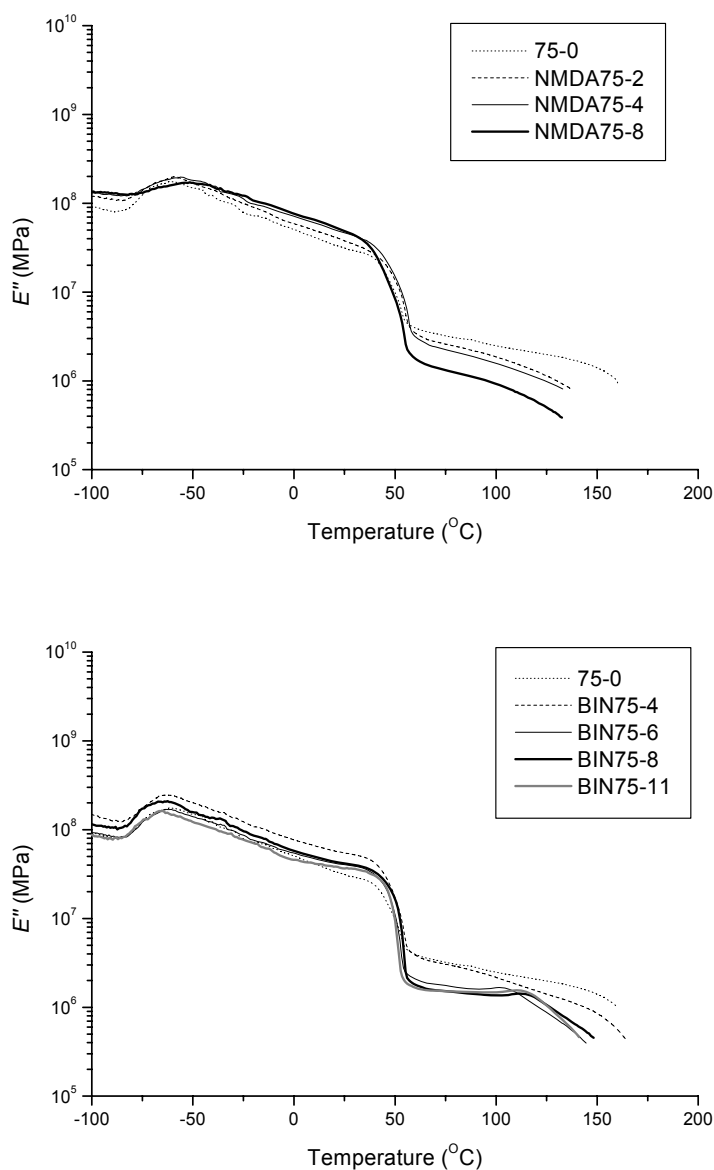


Figure 6.19 Loss modulus (E'') of NMDA and BIN series SMPU cationomer

Besides, the disruption effect of ionic groups on the order of hard domain could be manifested by the decrease of rubbery region extension with increasing ionic group content as shown in Figure 6.15. The short rubbery plateau region is due to the insufficient reinforcing effects from the hard segments. In addition, the first decrease and the subsequent increase trends in E' rubbery plateau shown in Figure 6.15 (b) aforementioned in BIN series might be also due to the disruption effect induced by ionization and the compensation of the increased cohesion caused by Coulombic force. In NMDA series, the E' plateau continuously decrease with the increase of ionic group content. Therefore, it illustrates that the disruption of the order of hard domain induced by ionic component insertion within hard segments should be predominant in this case.

6.2.3 Cyclic thermo-mechanical investigation

Shape memory effect of segmented PU films with ionic groups within hard segments can be studied with cyclic tensile test. The stress-strain relationship of the segmented PU film becomes stable after the several cycles and with no significant variation in further cycles as reported before [5, 27, 46, 47, 59]. It can be explained with the destruction of weak netpoints in the initial several cycles in deformation process, and the subsequent formation of ideal elastic network[1].

Chen and his coworkers have reported the incorporation of ionic extender during synthesis, to some extent, disrupts the order of hard domain[48], which also can be observed from the resulting data of DMA in this study. Whereas the hard domain is usually considered as having a physical cross linking structure in the two phase morphology, contributing the overall thermal stimulated deformation

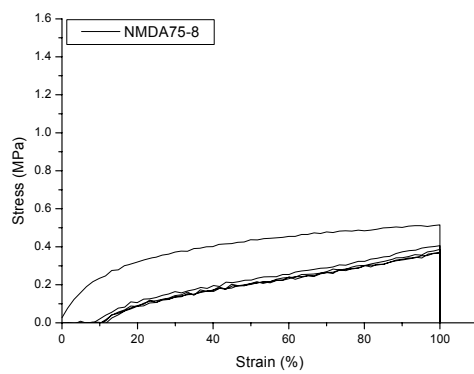
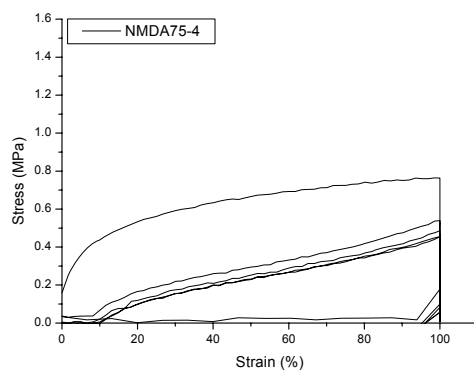
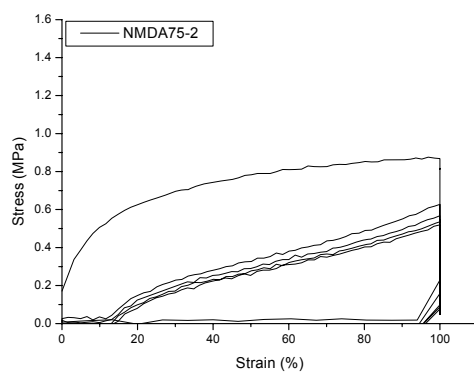
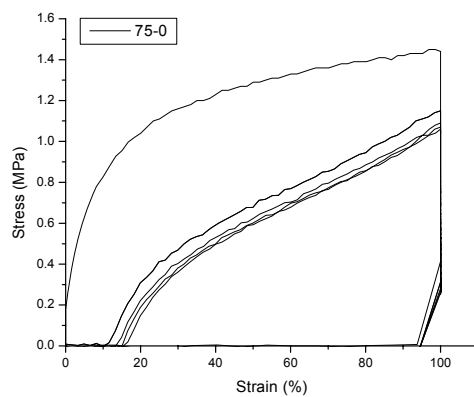


Figure 6.20 Cyclic tensile behavior of NMDA series SMPU cationomers

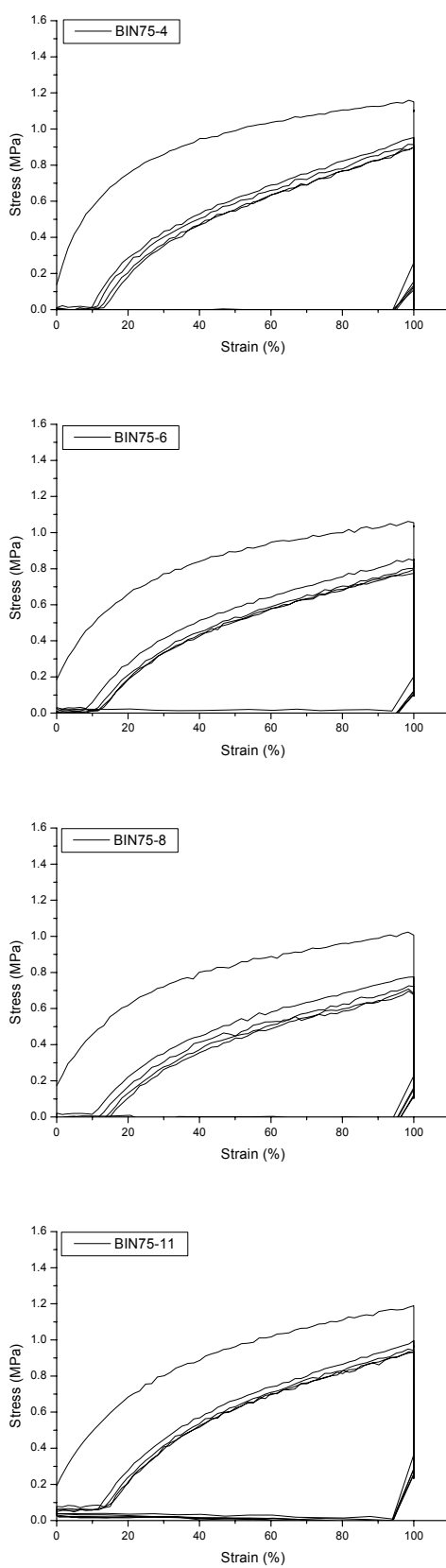


Figure 6.21 Cyclic tensile behavior of BIN series SMPU cationomers

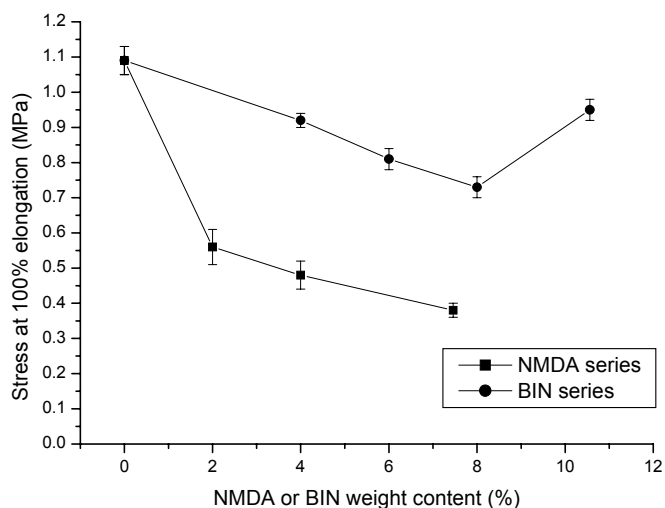


Figure 6.22 Stress at 100% elongation in the tensile cycle of NMDA and BIN series

recovery process as fixed phase [5, 47, 77, 104, 106]. Therefore, the insertion of ionic groups in hard segments possibly has the huge influence on the shape memory function. Moreover, the Coulombic force among ionic groups might partly compensate the loss of physical cross links among hard segments caused by disruption effect of ionization. Based on the analysis by DMA and DSC for the two series of SMPU cationomers, the effect of ionic group content on the shape memory property in segmented Polyurethane cationomers might be illustrated as follows: Figure 6.20 and Figure 6.21 demonstrate the cyclic stress-strain behavior of the NMDA and BIN series. The characteristics of shape memory properties on segmented polyurethane ever reported by other researchers [5, 45], such as strain hardening, insensitivity of cyclic property with cycle number can also observed in our investigation. According to the feature of cyclic thermal tensile test on shape memory polymer, the stress-strain relations can be seen in the first several cycles. The quantitative comparison of shape memory effect in this study was made solely by averaging parameters of the 2nd

cycle to 5th cycle and the parameters such as stress at 100% elongation, recovery ratio (R_r) and fixity ratio (R_f) in these cycles reflect the effect of ionic group content on shape memory properties. The error bar represents the standard variation of the relevant parameters.

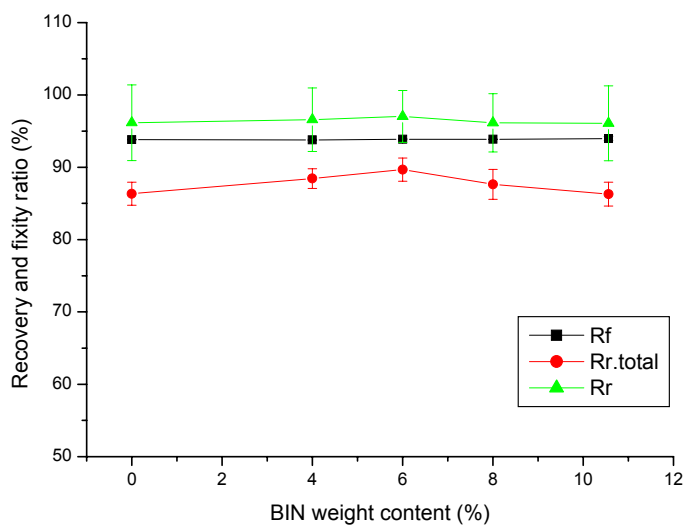
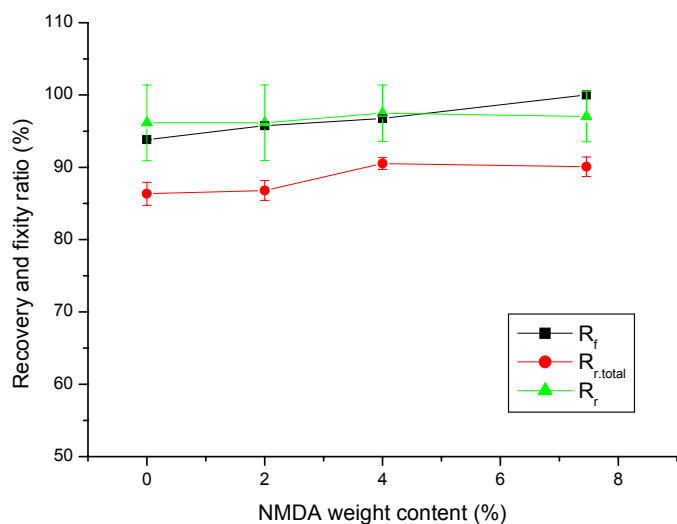


Figure 6.23 Fixity ratio and recovery ratio in the tensile cycle of NMDA and BIN series

Firstly, we can observe that the ionic group content has large influence on the stress at 100 % elongation for the two series. Figure 6.22 shows the effect of variation of ionic group content on stress at 100% elongation in the tensile cycles, illustrating that the stress in BIN series was decreased significantly with BIN content initially, and subsequently increased, which is consistent with the variation trends of E' at rubbery plateau in DMA analysis. For NMDA series, the stress values decrease with increasing NMDA content monotonously. In general, the stress in NMDA family is lower than that of BIN family, suggesting the presence of neutralized NMDA into hard segments offers more adverse effect to the order of hard domain in comparison with that from BIN. Therefore, the BIN series SMPU cationomers can withstand higher tensile force in deforming process, whereas in NMDA series, samples are readily deformed at higher temperature.

Figure 6.23 shows the dependency of fixity ratio and recovery ratio on the NMDA and BIN contents in SMPU cationomers in the 2nd to 5th tensile testing cycles. In the NMDA series, the fixity ability of specimens to temporary deformation can be improved effectively with incorporation of ionic groups. Increasing NMDA content from 0 % to the maximum allowable value causes the fixity ratio increases from 93.87 % to 100 %, meanwhile facilitate the recovery ability. On the other hand, for BIN series, the fixity ratio was not affected significantly by the BIN content, although the presence of neutralized BIN can give rise to a higher crystallinity of soft segments (as shown in Table 6.3). The total recovery ratio in BIN family was initially increased from 88.43 % to 91.76

% and subsequently decreased to 88.43 %. However, the variation in the recovery ratio in this series is not significant.

Comparison between the result of cyclic tensile test of the NMDA and BIN families suggests that the categories, together with the content of ionic groups have huge influence on the shape memory properties of SMPU cationomers. In the BIN series, just like NMDA series, the cationic groups should be formed from the quaternization of amine groups in backbone of macromolecule chain regardless of the presence of pyridine ring in BIN, because the base strength of R_3N ($K_b=6.31\times 10^{-5}$ for trimethylamine; $K_b=5.25\times 10^{-4}$ for triethylamine; $K_b=4.57\times 10^{-4}$ for tripropylamine) is much stronger than that of pyridine ($K_b=1.48\times 10^{-9}$). In specimens studied, the cationic moiety in NMDA series seem to decrease the extent of the order of the hard domain and cause the more loss of the elastic modulus of the sample at the temperature higher than T_{ms} detected with DMA. Coming back to the BIN series, in addition to the physical cross linking points, the Coulombic force induced by the cationic groups might be strong enough to compensate the loss of the cohesion owing to the disruption effect of ionization aforementioned, and then withstands the relative high load in the cyclic test. However, it is hard to give an explicit explanation about the variation of fixity ratio in BIN series SMPU ionomers compared with that of NMDA series. Usually the crystallization of soft segments is regarded as being responsible for memorizing the temporary deformation. In NMDA series of SMPU ionomers, the fixity ratio substantially increased with NMDA content owing to the higher crystallinity as shown in Table 6.3. Therefore, in BIN series, the higher crystallinity induced by ionic groups was expected to give rise

to higher fixity ratio for the temporary deformation. Nevertheless, the fixity ratio is almost unchanged when BIN weight content increased from 0% to the maximum allowable value. Actually, from the reported literature about the molecular mechanism of the shape memory effect of polymer, we can know that, if the thermal transition chosen to fix the deformation is the melting temperature of soft segments, the crystallization of soft segments can be initiated by cooling process[1]. After deformation, the crystallite of soft segments prevents the immediate recovery to the coil-like structure or the permanent shape defined by the net points of fixed phase. Therefore, the fixity and recovery ability usually called 'memory effect' is closely related to not only the crystallinity of soft segments, but the trends to the return to the original shape as well. In our two series SMPU ionomers, though the crystallinity of soft segments is increased significantly with ionic groups, the effect of ionic groups within hard segments on the cohesion among hard segments is not neglectable. Because the stronger cohesion among hard segments possibly causes the higher recovery ability, meanwhile leads to more difficulty in fixing the temporary deformation. Therefore, in the case of BIN, the fixity ratio is not improved significantly even the crystallinity of soft segment is enhanced. So, it is noticeable that the physical cross linking among hard segments has deep influence on the fixity ability.

CHAPTER 7 APPLICATION OF SMPU IONOMERS

7.1 SMPU ionomers with substrate bonding antibacterial activity

7.1.1 Crystallization and melting behavior

In this part, SMPU ionomers with antibacterial activity was synthesized according to the recipe listed in Table 3.7 mentioned in the part 3.3.2.3. The crystallization and melting behavior have been studied in the part 6.1.1 and the specific resulting data about the crystallinity and melting point of soft segments in this series of samples were presented in Table 6.1, Figure 6.1 and Figure 6.2, in which it can be found the sample BIN75-6-C8 and BIN75-11-C8 possess relative high crystallinity and melting point in soft segments compared to the control sample 75-0. Therefore, it can be supposed that the soft segments in BIN75-6-C8 and BIN75-11-C8 can offer the fixity ability in shape memory function. Considering the effect of ionic groups within hard segments on micro phase separation, the ionic group content will be a potential mean to control shape memory properties. Besides, the ionic groups neutralized with C8I were designed to impart the antibacterial activity into this series of SMPU ionomers. It will make these materials be a good candidate biomaterials used in immobilization usage.

7.1.2 Dynamic mechanical analysis

In Figure 7.1, it can be observed that a large difference of elastic modulus is located in the melting point of soft segments ($T_m \approx 50^\circ\text{C}$), which has been characterized with DSC. When the soft segment in SMPU ionomers is melt, the

elastic modulus can decrease at the 1~2 order magnitude. Moreover, the ratio of elastic modulus below and above the transition temperature was increased with the introduction of BIN ionic groups within hard segments, which usually means the deformation in high temperature will be made easily while the resistance for deforming at low temperature is quite good[5]. In SMPU ionomers with high ionic group content such as in BIN75-11-C8, the high modulus at temperature below the melting point of soft segments is caused by the relative high crystallinity, while the low modulus at temperature above the melting point of soft segments should be result from the weakened physical crosslink with packing extent decreased by the insertion of ionic groups. The plateau of elastic modulus at high temperature such as 70 °C is the indirect evidence of the existence of hard segment physical crosslink[96].

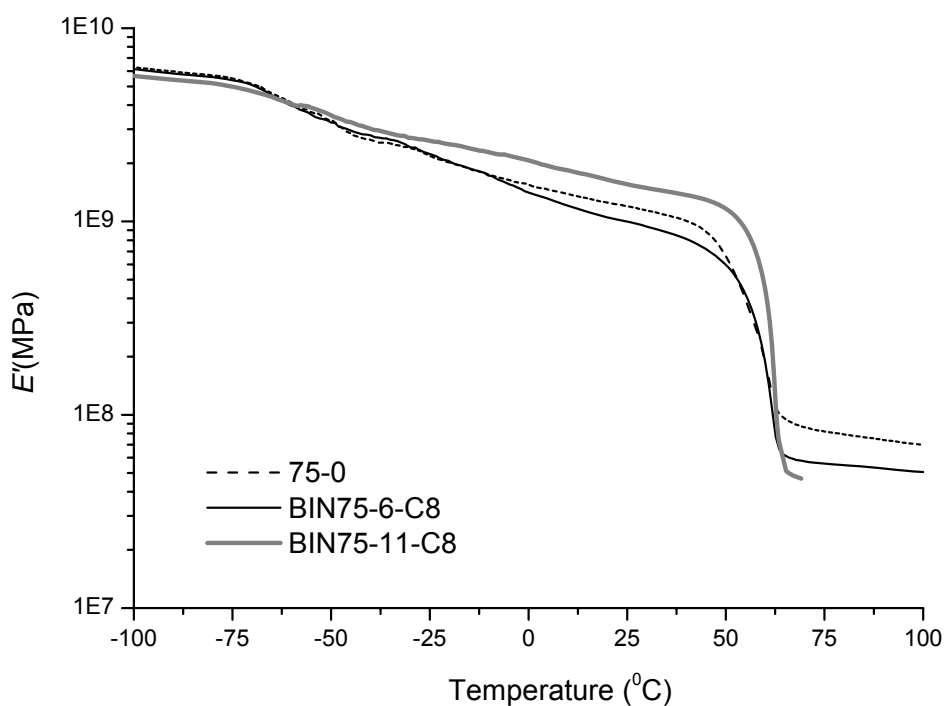


Figure 7.1 Elastic modulus (E') of SMPU ionomers with antibacterial activity detected with DMA

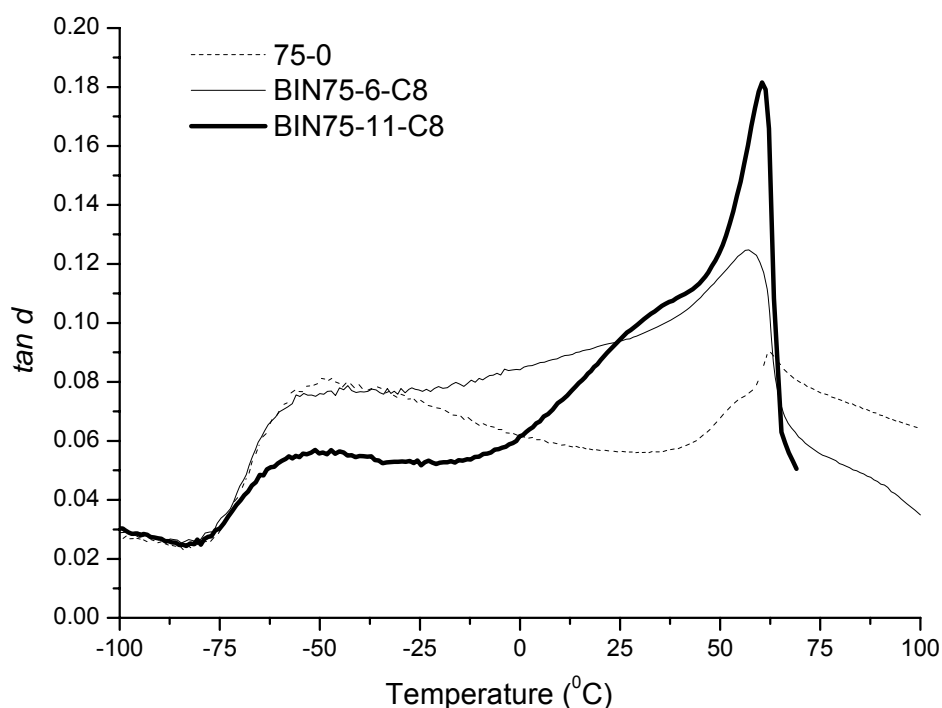


Figure 7.2 Loss tangent for SMPU ionomers

Figure 7.2 illustrates that there are two main transition determined from the peaks of loss tangent. The peak at near -50°C can be attributed to the glass transition of soft segments and the peak at near 50°C is taken as the melting point of the soft segments. For the $\tan\delta$ is corresponding to the strain energy dissipated by viscous friction, the high $\tan\delta$ value means the materials is more likely viscous than elastic. Therefore, $\tan\delta$ can be used to reflect the damping properties of materials. In this series SMPU ionomers, the damping property largely depends on the two factors: micro phase mixing and crystallization of soft segments. In low temperature range, the higher ionic group content can cause

lower $\tan\delta$ value. While temperature is increased to the melting point of soft segments, the $\tan\delta$ increases significantly, which is due to melting of crystal of soft segments. Therefore, it can be found that the SMPU ionomers is more likely elastic in the relative low temperature range and viscous in the temperature around T_{ms} .

7.1.3 IR analysis

From the scheme of molecular structure shown in Figure 3.1, it can be found that the chain extension is conducted with adding N, N-Bis(2-hydroxyethyl)-isonicotinamide and the N in pyridine cycle is supposed to be neutralized with 1-Iodooctane[82, 136, 137]. Therefore, FTIR is used to prove the neutralized ammonium structure in the molecular chain and study the evolution of hydrogen bonding between amine groups and carbonyl groups or ether oxygens.

In the spectra of FTIR about SMPU ionomers and the corresponding non-ionomers in Figure 7.3, it can be observed that the characteristic peaks of 3300~3400 cm^{-1} belong to urethane $>\text{NH}$ groups; the broad peaks at 1732 cm^{-1} mean $>\text{C}=\text{O}$ stretching at urethane linkage and ester linkage; the symmetric and asymmetric stretching of the $-\text{CH}_2-$ of PCL can be found in 2750~3000 cm^{-1} ; the intensity of the band at 1600 cm^{-1} can be attributed to the $>\text{C}=\text{C}<$ stretching of aromatic groups; the peaks at 1100 cm^{-1} arises from the stretching of $\text{C}-\text{O}-\text{C}$ of PCL; The peak at 1540 cm^{-1} is due to $\text{C}-\text{N}$ stretching and $\text{N}-\text{H}$ deformation; The polyurethane cationomers show a new peak at 1640 cm^{-1} as studied by other researchers without more discussion[136, 137], which is specifically due to quaternization of heterocyclic nitrogen. It can be found that in the samples 75-0

and BIN75-11N containing no ionic groups, the peak at 1640 cm^{-1} does not exist. Also, the peak located at 2273 cm^{-1} , which is from the absorption of isocyanate groups, can not be found in all samples, demonstrating that the NCO group can react completely[102]. In the sample BIN75-11-C8, the peak at 1640 cm^{-1} can be observed clearly, which means the neutralization reaction can be conducted in the synthesis conditions.

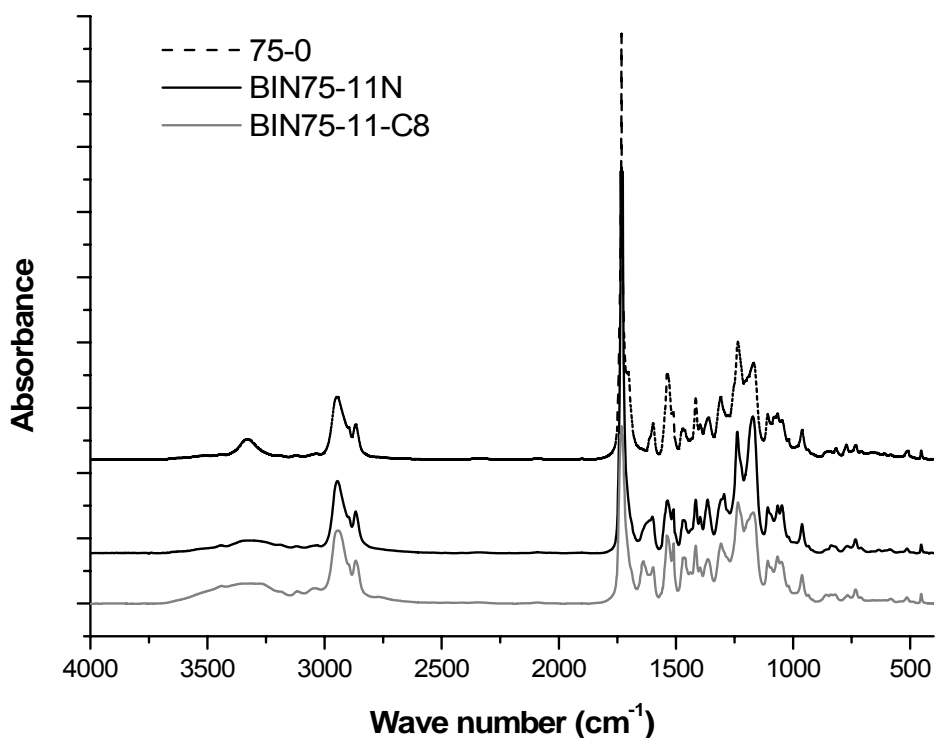


Figure 7.3 FTIR spectra of SMPU ionomers and non-ionomers

In the comparison of the samples 75-0, BIN75-6-C8 and BIN75-11-C8, the peaks at 1640 cm^{-1} illustrate the increasing trend when the BIN wt% increases from 0 wt% to 10.56 wt%, suggesting the ionic group content in SMPU ionomers can be controlled with adjusting the BIN weight content in synthesis process. Moreover, from Figure 7.4, the peaks of $3300\sim 3400\text{ cm}^{-1}$ belonging to urethane $>\text{NH}$ groups

show the trend that the peak area was broaden when more ionic groups were introduced into hard segments and the absorbance was increased with the increase of BIN weight content. Especially BIN75-11-C8 has a wide distribution

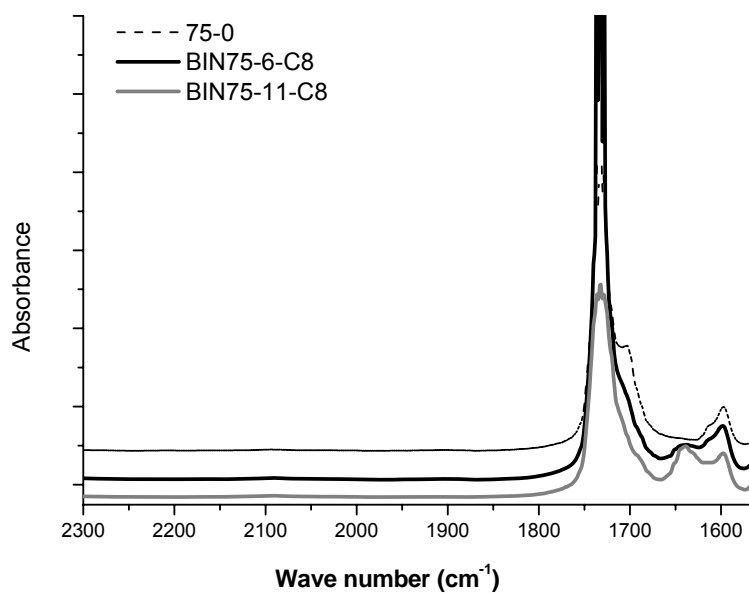
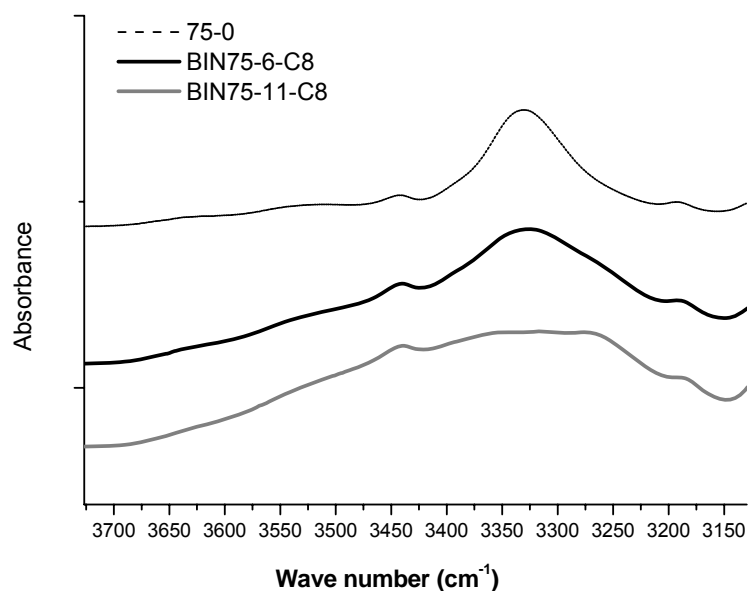


Figure 7.4 FTIR spectra of SMPU ionomers with BIN weight content: 0 wt%, 6 wt%, 10.56 wt%

on the high frequency side and the peak at 3450 cm^{-1} shows an increasing trend. For the peak area in the range of $1700\text{-}1730\text{ cm}^{-1}$, in the control sample 75-0 without ionic groups in hard segments, there is an obvious shoulder absorbance in low frequency side, which should rise from the overlap of the peak in 1732 cm^{-1} and 1730 cm^{-1} . Instead, in the sample BIN75-11-C8, the shoulder disappears and only the peak at 1732 cm^{-1} remains. Based on the literature about the attribution of urethane $>\text{NH}$ groups and $>\text{C}=\text{O}$ [128, 138-144], the NH hydrogen bonded to carbonyl or ether oxygens and carbonyl bonded to NH groups will give rise to the shift to low frequency side. Therefore, it can be concluded that the amount of free NH groups and free carbonyl groups are increased with the insertion of neutralized BIN groups. It might be due to the steric hindrance of long alkyl chain counter-ions and the disruption effect of insertion of ionic groups within hard segments, which possibly affect the forming of hydrogen bonding[48, 145].

7.1.4 Shape memory properties

Based on our previous research in the part 6.1.2, it can be observed that the cooling induced crystallization of crystalline soft segments in SMPU ionomers is of time dependence. Moreover, with the introduction of ionic groups BIN into hard segments, the crystallization rate is dropped significantly. However, from the Table 6.1 in the part 6.1.1, the crystallinity of soft segments in SMPU ionomers is increased obviously in comparison with the control sample 75-0, which is expected to be favor to the increase of fixity ability. In that, in this series sample, the cyclic tensile test routine was designed to be done with various cooling time such as 30s, 150s, 300s, and 900s respectively in order to

investigate the effect of cooling time on shape fixity ability. Others parameters such as heating time, T_{low} and T_{high} were fixed in this testing.

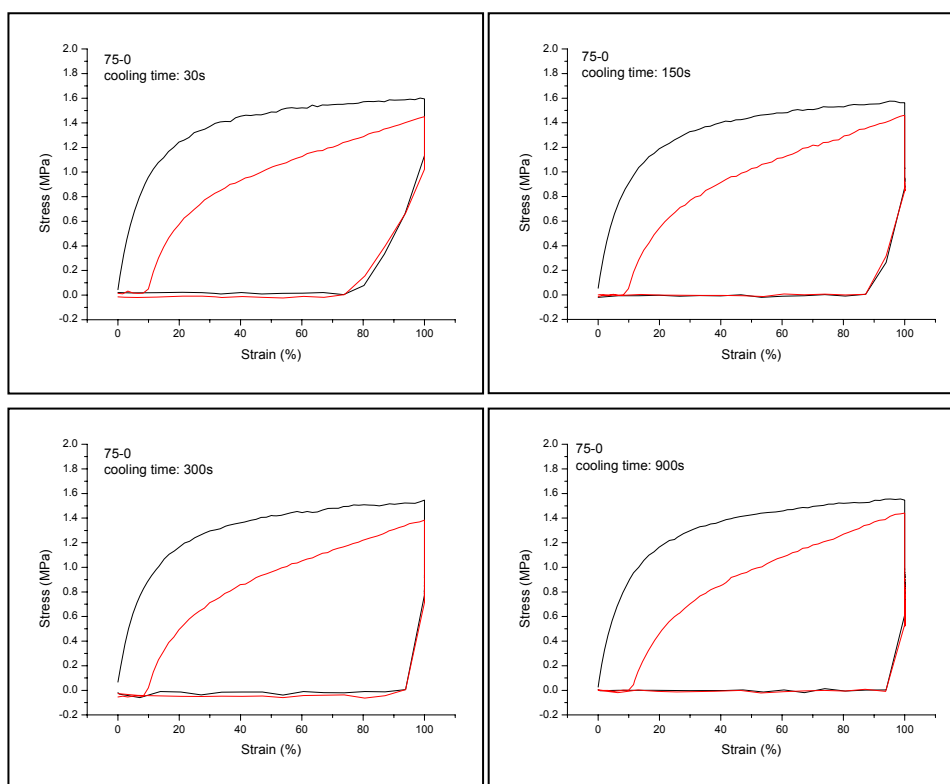


Figure 7.5 Cyclic tensile test for 75-0

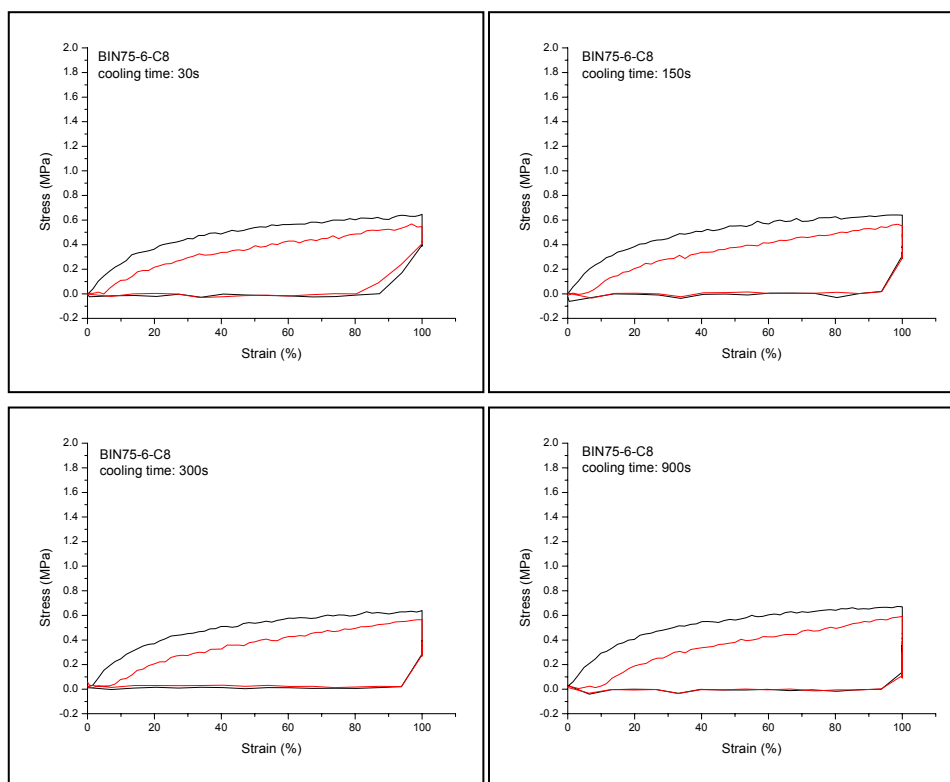


Figure 7.6 Cyclic tensile test for BIN75-6-C8

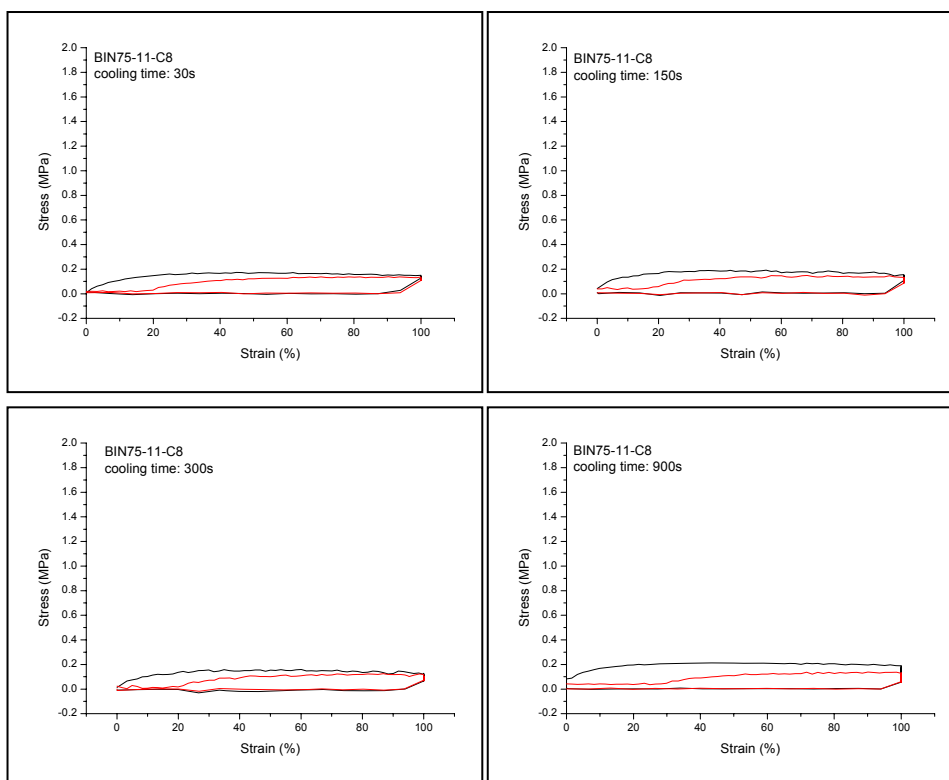


Figure 7.7 Cyclic tensile test for BIN75-11-C8

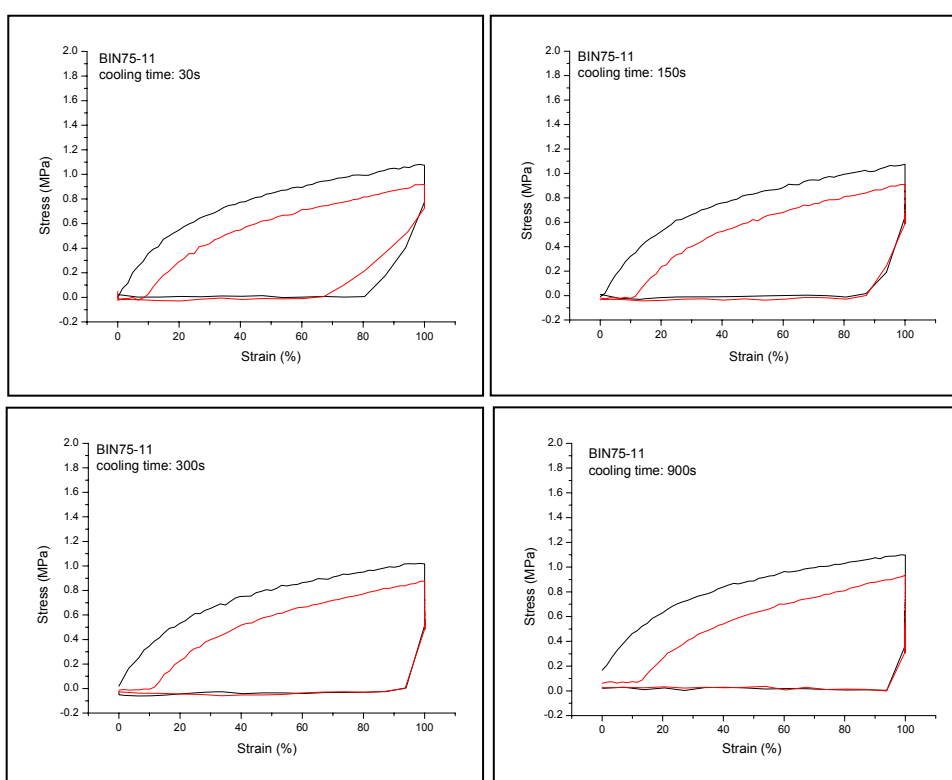


Figure 7.8 Cyclic tensile test for BIN75-11

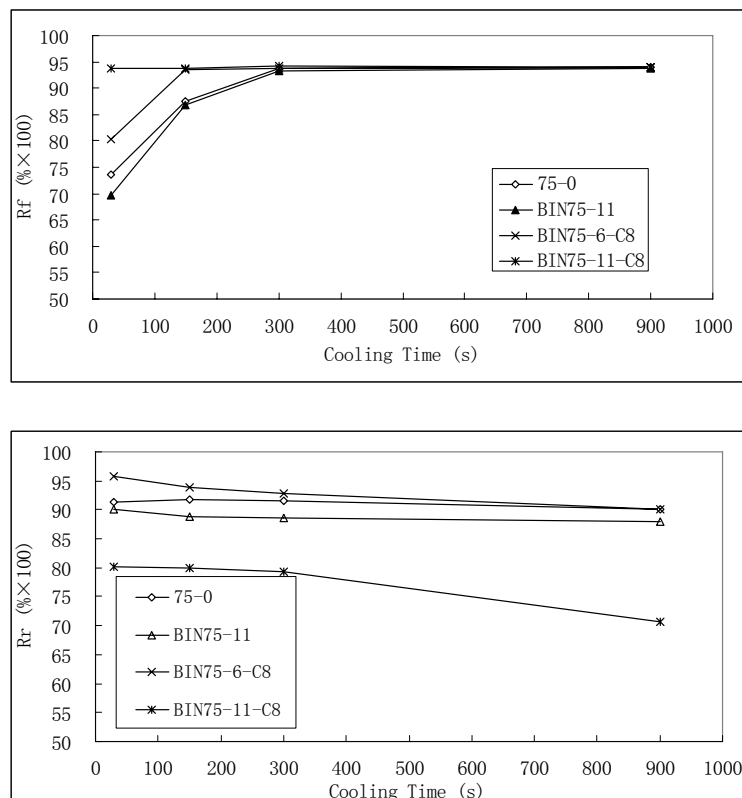


Figure 7.9 Dependence of fixity ratio (R_f) and recovery ratio (R_r) on cooling time

Figure 7.5 ~ 7.8 shows the resultant data about fixity ratio and recovery ratio are dependent on cooling time. The fixity ratio and recovery ratio for all samples have been summarized in Figure 7.9. For all samples, the dependence of fixity ratio on cooling time can be observed: the fixity ratio can be increased with the increase of cooling time, which should be due to the time dependence of crystallinity of soft segments; the fixity ratio can reach a stable value after enough long cooling time. For the control sample 75-0, the recovery ratio can remain in a similar value in different cooling time. For BIN75-11, the trend similar to that in 75-0 can be observed. The only difference is the lower fixity ratio at 30s cooling time and slight lower recovery ratio. This observance can be explained by the relative slow crystallization procedures aforementioned compared with 75-0. So, in this case, the effect of crystallization rate might be

predominant. But, for BIN75-11-C8, it can be found that the fixity ratio can reach rather high value even in the very short period, though the crystallization rate of BIN75-11-C8 is lowest one among 75-0, BIN75-11, BIN75-6-C8 and BIN75-11-C8. Moreover, the recovery ratio of BIN75-11-C8 is much lower than other samples and gradually decreases with the increase of cooling time. Just like the mentioned influence of insertion of ionic groups in hard segments, in this case, the order of hard segment domain was disrupted and the packing extent of hard segments decreased accordingly. That means the physical cross link offering the recovery force from temporary deformation to original shape was weakened with the insertion of ionic groups within hard segments, which is quite consistent to the lowering trend of the stress at 100% elongation ratio and the initial tensile modulus in cyclic tensile testing shown in Figure 7.10 ~ 7.11, in which the deformation temperature is 70°C. In that, the crystallization rate of soft segments has less effect on shape fixity ability when the physical cross link was weakened. With the extension of cooling time, the deformed hard segments possessing more disorder of hard domain in BIN75-11-C8 will relax more orientation structure, and then causes the low recovery ability. On the other hand, though the fixity ability of BIN75-11 and BIN75-11-C8 is quite different in relative short cooling time (30s), the final shape fixity ratio after enough long cooling time (900s) can be the same to the control sample 75-0. Therefore, we conclude that the crystallization of crystallizable soft segments together with the physical cross link of hard domain in SMPU ionomers all have substantial influence on shape fixity and shape recovery. When physical cross link is strong enough, the crystallization rate is a predominant factor determining the shape fixity ratio for various cooling time. Instead, when physical cross link is

weakening more; the shape fixity can be achieved in a very short period (30s) and the influence of crystallization rate is much less.

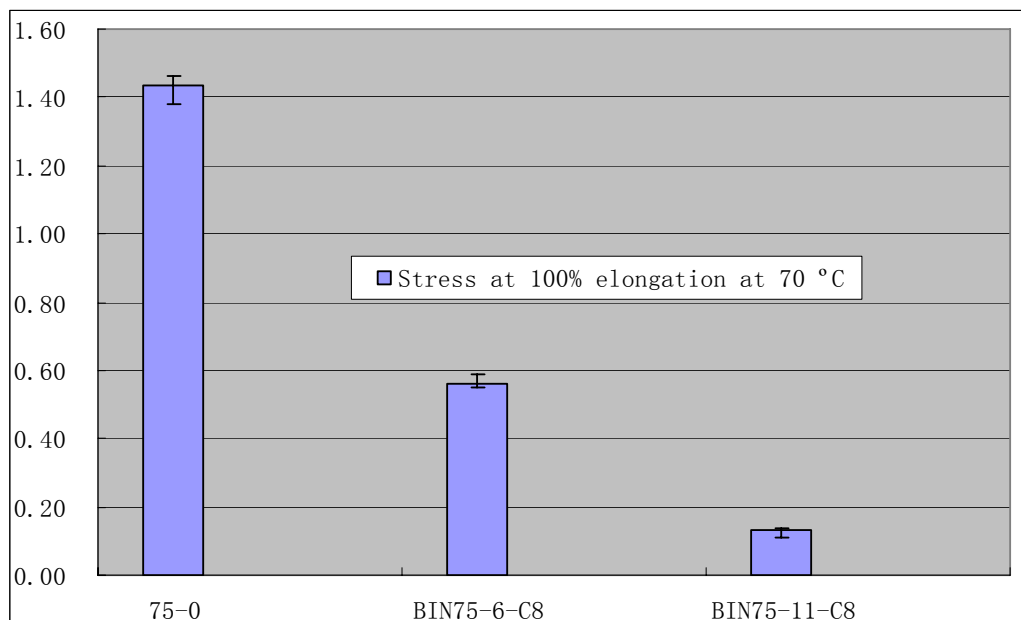


Figure 7. 10 Stress of SMPU ionomers at 100% elongation at 70 °C

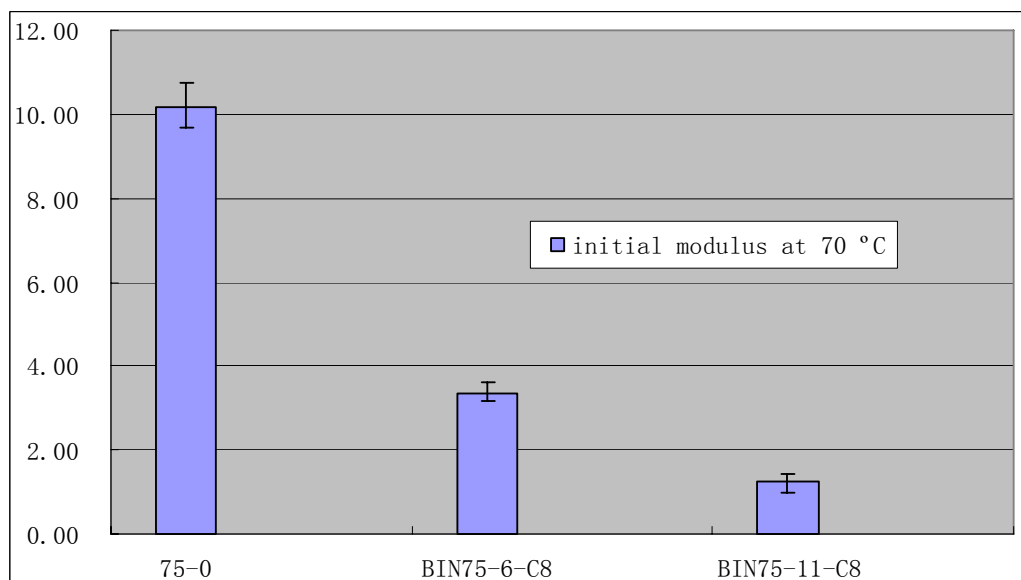


Figure 7. 11 Initial tensile modulus of SMPU ionomers at 70°C

For the shape memory properties, including shape memory recovery ratio, shape memory fixity ratio, the stress at 100% elongation ratio and the initial modulus,

the statistic analysis was conducted to investigate the significance of the resultant data. In our experimental design, there are two factors, cooling time and BIN wt%, affecting the sample responses including R_r , R_f , the stress at 100% elongation ratio and the initial modulus. Therefore, the graphs of true response of samples were drawn in Figure 7. 12, in which, we can observe how changes in the level of one factor such as BIN wt% depend on the level of the other factor such as the cooling time.

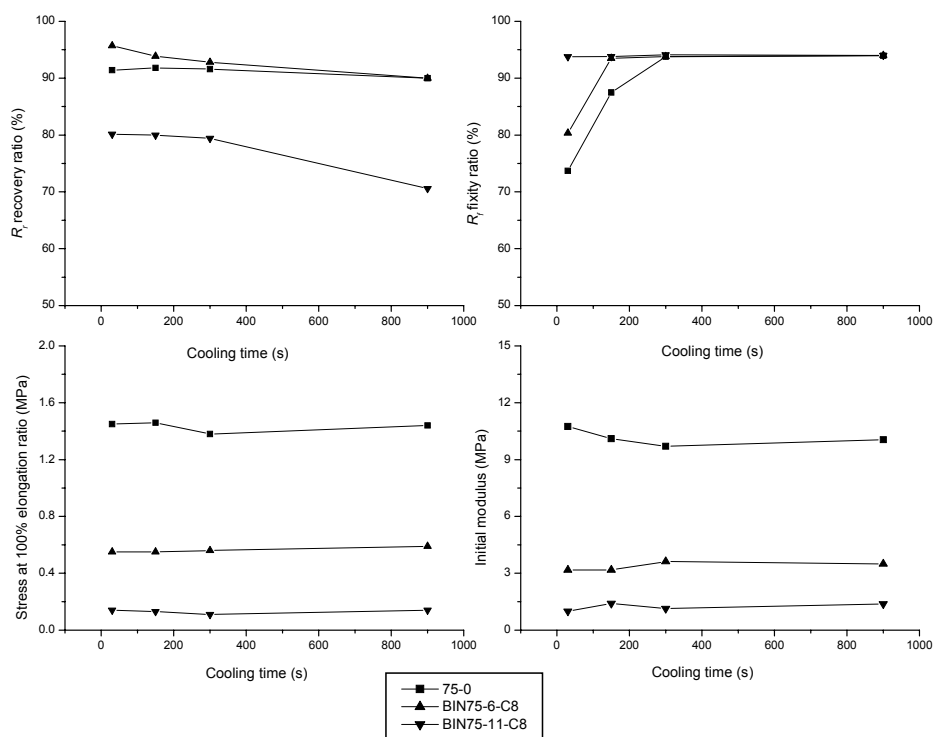


Figure 7. 12 Effect of cooling time and BIN wt% on R_r , R_f , the stress and the initial modulus

It can be found, for R_r and R_f , the interaction between the two factors, the cooling time and BIN wt%, does exist in these samples. Just as mentioned above, the disruption of the order of hard segments causes the lower recovery ratio in BIN75-11-C8 compared with 75-0 and the extension of cooling time make the

more disruption of weak net points. Besides, the fixity ratio is related to the crystallization process of soft segments, which is dependent on the cooling time in this cyclic tensile testing. Therefore, the interaction between these two factors for R_f might arise from the difference of crystallization properties among these SMPU ionomer specimens. So, the study about the shape fixity and shape recovery ability of SMPU ionomers was performed based on the analysis about the effect of ionic groups on the structure and crystallization properties. For the properties, the stress at 100% elongation ratio and the initial modulus, the interaction is hardly presented theoretically. Moreover, the change curves of true response dependent on the cooling time for samples are almost parallel, as in the lower figures in Figure 7. 12. Then we conclude that there is no interaction between the two factors according to related literatures[146]. In that, we choose the Two-Factor ANOVA without interaction to analyze the significance of the influence of the cooling time and BIN wt% on the stress at 100% elongation ratio and the initial modulus.

Table 7. 1 The stress at 100% elongation ratio of SMPU ionomers

Sample Code Cooling time(s)	75-0	BIN75-6-C8	BIN75-11-C8
30	1.45	0.55	0.14
150	1.46	0.55	0.13
300	1.38	0.56	0.11
900	1.44	0.59	0.14

Table 7. 2 ANOVA table of two-factor experiment for the stress

Source of Variation	df	Sum of Squares	Mean Square	F
A: cooling time	3	0.0027	0.0009	$F_A=1.58$
B: BIN wt%	2	3.5206	1.7603	$F_B=3088.26$
E: Error	5	0.0028	0.0006	
Total	11	3.5262		

Table 7.1 shows the resultant data of the stress at 100% elongation ratio in the 2nd tensile cycle for SMPU ionomers. ANOVA table for the above data is given in Table 7.2. Based on the aforementioned analysis, assuming that there is no interaction between cooling time and BIN wt%, let's test at level 0.05 for the presence of separate factor A, cooling time and factor B, BIN wt%. Computations are typically summarized in an ANOVA table, as shown in Table 7.2. There are two-factor ANOVA hypotheses and testes as follows:

1. H_0 : There are no factor A main effects.

H_1 : H_0 is not true.

$$\text{Test statistic: } F_A = \frac{\text{Meansquare(A)} / \text{df(A)}}{\text{Mean square(E)} / \text{df(E)}}, \text{ based on df(A)=3 and df(E)=5.}$$

2. H_0 : There are no factor B main effects.

H_1 : H_0 is not true.

$$\text{Test statistic: } F_B = \frac{\text{Meansquare(B)} / \text{df(B)}}{\text{Mean square(E)} / \text{df(E)}}, \text{ based on df(B)=2 and df(E)=5.}$$

The appendix table VII in the reference[146] suggests the smallest value at level 0.05 for df(A)=3 and df(E)=5 is 5.41. So, the P-value for $F_A=1.58$, based on df(A)=3 and df(E)=5 is more than 0.05. We therefore accept H_0 and conclude that there are no main effect of factor A, cooling time on the stress. The smallest value at level 0.05 for df(B)=2 and df(E)=5 is 5.79. The P-value for $F_B=3088.26$ is lower than 0.05. So, H_0 was rejected and it confirm that the stress does depend on the factor B, BIN wt%.

Table 7. 3 The initial modulus of SMPU ionomers

Sample Code Cooling time(s)	75-0	BIN75-6-C8	BIN75-11-C8
30	10.75	3.17	1
150	10.1	3.17	1.41
300	9.7	3.62	1.13
900	10.05	3.49	1.38

Table 7. 4 ANOVA table of two-factor experiment for the initial modulus

Source of Variation	df	Sum of Squares	Mean Square	F
cooling time	3	0.0508	0.0169	0.11
BIN wt%	2	173.5788	86.7894	543.35
Error	5	0.7986	0.1597	
Total	11	174.4283		

The similar analysis was conducted to check the significance of the effect of cooling time and BIN wt% on the initial modulus. For the factor, BIN wt%, P values is lower than 0.05 according to the test statistic aforementioned, instead, P value for the cooling time is higher than 0.05. Therefore, it can be concluded that the initial modulus does depend on the BIN wt% and the cooling time has not main effect on this result.

7.1.5 Substrate bonding antibacterial activity

Anti bacterial activity against both Gram-positive (*Staphylococcus aureus*) and Gram-negative bacteria (*Klebsiella pneumoniae*) was tested by using American Association of Textile Chemist and Colorist (AATCC147) test, because it is a relatively quick and easily executed qualitative method to determine antibacterial activity of diffusible antimicrobial agents on treated surface. A zone of inhibition occurs as a result of the diffusion of an antimicrobial agent from the specimen. After incubation, a clear area of interrupted growth underneath and

along the sides of the test material indicates antibacterial activity of the specimens.

Table 7.5 Antibacterial activity testing result according to AATCC 147

Sample code	Test microorganism	Culture type	Width of clear zone of inhibition (mm)	Colony forming on specimen surface	Comments
75-0	<i>Staphylococcus aureus</i>	Gram positive	0	Yes	Not acceptable
	<i>Klebsiella pneumoniae</i>	Gram negative	0	Yes	Not acceptable
BIN 75-6-C8	<i>Staphylococcus aureus</i>	Gram positive	0	No	Acceptable, but not significant
	<i>Klebsiella pneumoniae</i>	Gram negative	0	No	Acceptable, but not significant
BIN 75-11-C8	<i>Staphylococcus aureus</i>	Gram positive	0	No	Acceptable, but not significant
	<i>Klebsiella pneumoniae</i>	Gram negative	0	No	Acceptable, but not significant

Table 7.5 and Figure 7.13 shows the results for 75-0, BIN75-6-C8 and BIN75-11-C8. In all samples, no clear zone of inhibition can be observed with naked eyes, suggesting there are little diffusible antibacterial agent in all these samples. However, it can be observed that the colony can be formed on the surface of 75-0. Therefore, the comment for this sample is ‘not acceptable’. For BIN75-6-C8 and BIN75-11-C8, the colony on the surface can not exist after incubation, because biocidal quaternized pyridine moieties incorporated into hard segments through the chain extender of SMPU ionomers can kill the bacteria with the long alkyl chain neutralization agent[147].

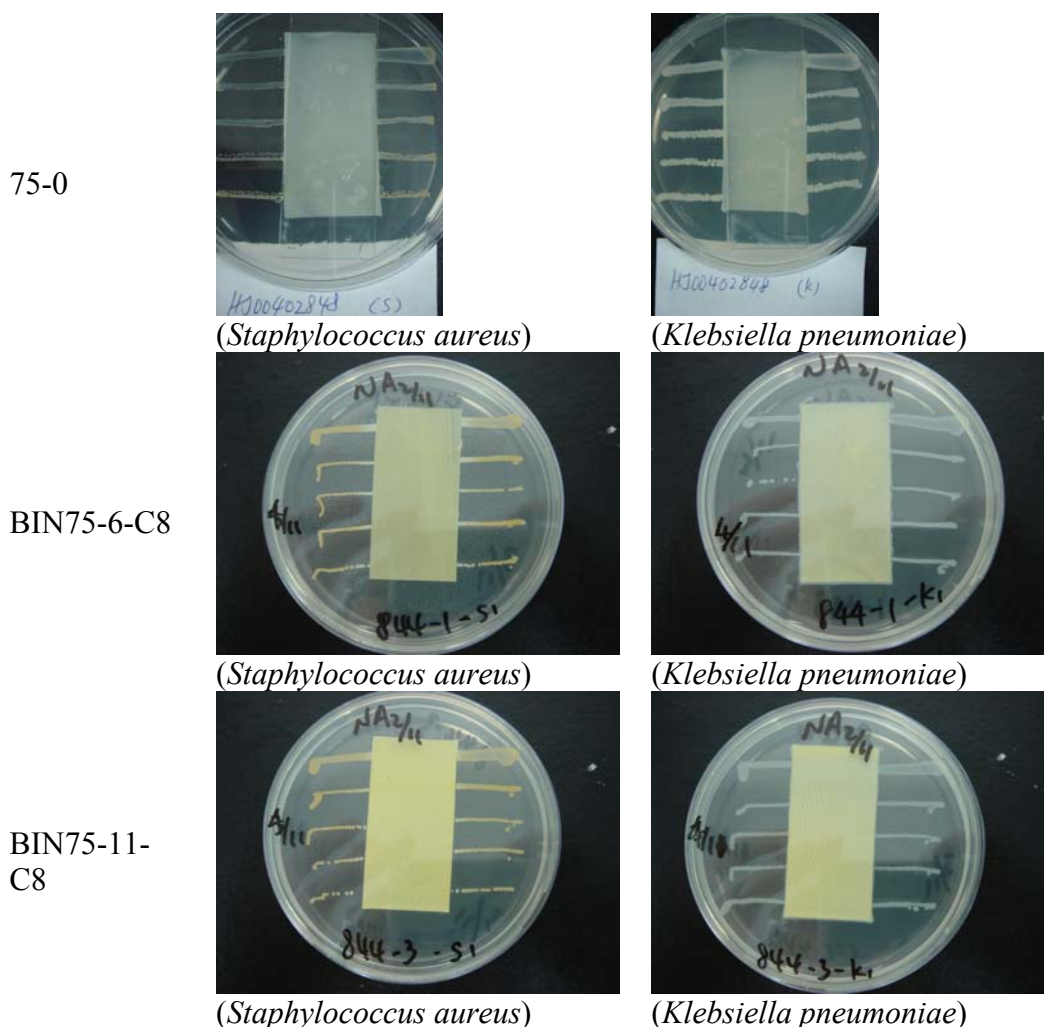


Figure 7.13 Zone of inhibition and bacterial growth under specimens in AATCC 147

Considering the test method such as AATCC 147 that are directly dependent on diffusion of antimicrobial agent are not appropriate for evaluating immobilized antibacterial activity, the other testing method was chosen to quantitatively determine the antimicrobial activity of SMPU ionomers. ASTM E2149 is designed to evaluate the resistance of non-leaching antimicrobial treated specimens to the growth of microbes under dynamic contact conditions. In this way, the antimicrobial activity of substrate bound antimicrobial is dependent on direct contact of microbes with specimens. The samples were shaken in concentrated bacterial suspension for a one-hour contact time and the percent

reduction is calculated based on initial counts. The result was listed in Table 7.6, suggesting that for the control sample 75-0, the antibacterial activity to Gram-positive bacteria (*Staphylococcus aureus*) is not acceptable and that to Gram-negative bacteria (*Klebsiella pneumoniae*) is insignificant; for SMPU ionomers (BIN75-6-C8 and BIN75-11-C8), the antibacterial activity to Gram-positive bacteria (*Staphylococcus aureus*) is significant and the reduction rate of bacteria even is 100%; the antibacterial activity to Gram-negative bacteria (*Klebsiella pneumoniae*) is lower than that to Gram-positive bacteria (*Staphylococcus aureus*) in SMPU ionomers studied, which is quite consistent with the result reported by Cooper et al[82]. The reduction of bacteria of BIN75-6-C8 to Gram-negative bacteria (*Klebsiella pneumoniae*) is 83.6%. In Cooper's interpretation for the lower antibacterial activity of quaternary ammonium to Gram-negative bacteria compared to the activity to Gram-positive bacteria, the difference in the structure of the cell envelope of the organisms is a predominant factor. The substrate bound biocide in SMPU ionomers is in favor to destroy the cell cytoplasmic membrane in Gram-positive bacteria (*Staphylococcus aureus*) with simple envelope structure. However, for the multilayered Gram-negative bacteria (*Klebsiella pneumoniae*), this effect is lowered. So, the comment based on our testing result for the antibacterial activity of SMPU ionomers to Gram-negative bacteria (*Klebsiella pneumoniae*) is only acceptable. In addition, it can be observed that the antibacterial activity of SMPU ionomers to Gram-negative bacteria (*Klebsiella pneumoniae*) increased with the increase of BIN content. When the BIN content is 10.56 wt% in BIN75-11-C8, the reduction rate of bacteria is 90.7%.

Table 7.6 Antibacterial activity testing result according to ASTM E2149

Sample code	Standard	Test microorganism	Culture type	Percent reduction of bacteria(%)	Comments
75-0	ASTM E2149	<i>Staphylococcus aureus</i>	Gram positive	0	Not acceptable
		<i>Klebsiella pneumoniae</i>	Gram negative	42.5%	Insignificant
BIN 75-6-C8	ASTM E2149	<i>Staphylococcus aureus</i>	Gram positive	100%	Acceptable and significant
		<i>Klebsiella pneumoniae</i>	Gram negative	83.6%	Acceptable
BIN 75-11-C8	ASTM E2149	<i>Staphylococcus aureus</i>	Gram positive	100%	Acceptable and significant
		<i>Klebsiella pneumoniae</i>	Gram negative	90.7%	Acceptable

7.2 SMPU fibers with ionic groups within hard segments

In our previous study about shape memory polyurethane fibers, some samples have been prepared and studied systematically[28, 58]. In shape memory polyurethane fiber study, PBA with the molecular weight of 600 was chosen to be the soft segment and the hard segment content was adjusted in the range between 42 wt% and 66 wt% so as to control the T_g of soft segments around room temperature. The T_g of soft segments decreases with the decrease of hard segment content and is in the range between 5°C and 64°C. The fiber was made by wet spinning process as shown in Figure 3.2. In comparison between shape memory polyurethane fibers and other man made fibers, the stress-strain curve of SMPU fibers with hard segment content of 55 wt% and 66 wt% is located between the high modulus fibers such as nylon and the high elasticity fibers such as Lycra. As shown in Figure 7.14, the data from DMA illustrate that the major difference between SMPU fibers and conventional man-made fibers is the variation of E' in normal using temperature range (around room temperature). For SMPU fibers, the variation of E' is very significant. Namely, when the

temperature was increased above the T_g , the E' will sharply decrease and the rubbery state plateau will appear and be extended to above 180°C. However, for other types of man-made fibers such as polyester and Lycra, though in the entire heating scan range, there are sharp transition area of E' , such as -40°C for Lycra[148], 100-105°C for Polyester fibers and yarns[100], the elastic modulus is almost the constant and changes little with the increase of temperature in room temperature range. Therefore, this transition point imparts the heating responsive shape memory properties to the SMPU fibers in normal using temperature just as reported T_g used as the switch temperature in the shape memory polyurethane film.

Considering the thermal responsive property of shape memory polyurethane fibers studied, there might be inter-stress produced in the spinning process, which will cause a large amount of shrinkage in heating, subsequently lead to the dimensional instability. Therefore, it is necessary to quantitatively investigate the thermal shrinkage extent of various fibers in heating process. So, Dynamic Mechanical Analyzer was used to measure the average strain of the fiber subject to periodic dynamic tensile stress at increasing temperature, then to characterize the extent of heating shrinkage. For post treatment, the thermal setting on the hot rollers and high pressure steaming were studied respectively. In former treatment, the thermal setting at 120°C hot rollers will give rise to the lower modulus and tenacity and the higher maximum elongation ratio in comparison with the untreated fiber and the SMPU fiber treated at 90°C; the thermal setting at 120°C can significantly eliminate the internal stress stored in SMPU fibers, subsequently decrease the shrinkage ratio at heating process as shown in Figure

7.15. Besides, thermal setting at lower temperature such as 90°C has less extent of elimination of internal stress compared with that with higher temperature. As for other traditional fibers, such as polyester, Nylon6 and Lycra, the dimensional stability is sufficient in the range from 0 to 100°C, which could be characterized from the average deformation under periodic stress. The average shrinkage ratio of these fibers is all below 5%.

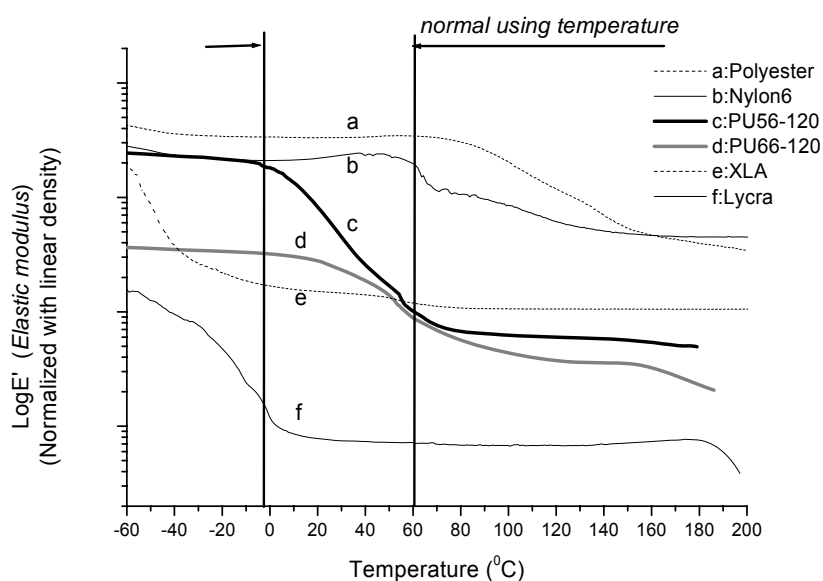


Figure 7.14 Comparison of elastic modulus between SMPU fibers and various man-made fibers (PU56-120: 56wt% hard segment content; thermal setting at 120°C; PU66-120: 66wt% hard segment content; thermal setting at 120°C)[28]

In the comparison between untreated SMPU fibers and SMPU fibers treated with high pressure steaming, shrinkage ratio as a function of increasing temperature for original and steamed SMPU fibers was detected by DMA and the resulting data is shown in Figure 7.16 (a) and (b). For original fibers, when the temperature increased beyond 50°C, the shrinkage ratio increase abruptly. For SMPU42-O, the shrinkage ratio even reached 40% or more at 100°C. For SMPU64-O, this value was also 20% around. It also can be observed from

Figure 7.16(a) that the onset temperature of thermal shrinkage is around 30 °C and the higher the hard segment content in fibers, the higher onset temperature of shrinkage will be. According to the mechanism of shape memory effect in polymer, below the transition temperature, almost all macroscopical deformation can be frozen. In addition, the internal stress storied in untreated fibers is closely relevant to various molecular orientation patterns, including soft segment orientation, hard domain orientation and hard segment orientation[149]. Moreover, the degree of orientation is much dependent on the drawing ratio, rate and operating temperature in stretching process. S. L. Cooper et al. ever reported the mode of hard segment orientation was found to be a function primarily of hard segment length, instead, the soft segment orientation is little affected by changes in polymer composition[150]. So, the mechanism of the storage of internal stress is quite complicated. In this experiment, generally, the thermal shrinkage ratio in fibers with lower hard segment content is higher, which can be roughly interpreted as follows: T_g of the BDO-MDI hard segment is 90-100°C[151] and much higher than stretching temperature (60°C). Therefore, the orientation of soft segments in fibers with low hard segment content (SMPU42-O) might be much more than that with high hard segment content (SMPU64-O). Subsequently, in heating scan of DMA, increased temperature beyond T_g of soft segments in SMPU42-O causes more reforming coil-like structure from orientation state. In the light of our previous study[28], other commercial man-made fibers possess 5% or below shrinkage ratio under this testing condition at 100°C. Therefore, for untreated SMPU fibers, it is necessary to remove the internal stress so as to improve the dimensional stability to meet the practical requirement. The thermal shrinkage ratio of treated SMPU fibers shown in

Figure 7.16 (b) remained at a very small value even at 100°C, which was similar to other man-made fibers. So, the post-treatment: high pressure steaming is an effective way to remove the internal stress and improve the dimensional stability for SMPU fibers.

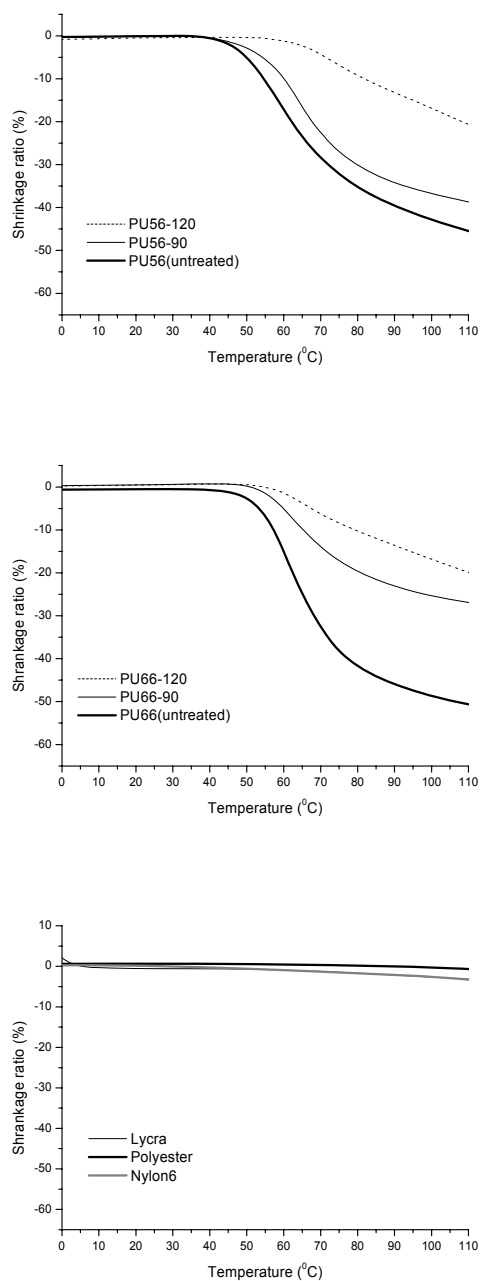


Figure 7.15 Thermal shrinkage ratio under periodic stress detected by DMA (PU XX-YY: XX wt% hard segment content with thermal setting at YY°C, such as PU66-120: 66wt% hard segment content; thermal setting at 120°C)[28]

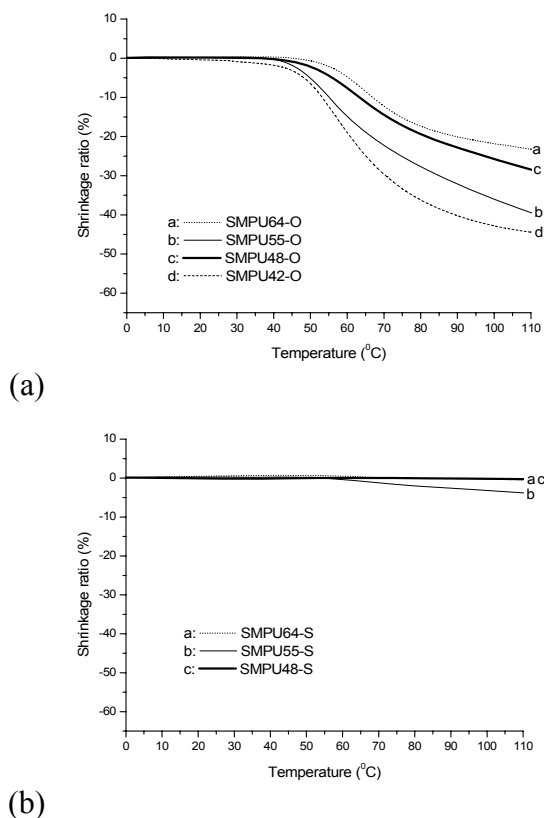


Figure 7.16 Thermal shrinkage ratio of original fibers (a) and treated fibers (b) under periodic stress detected by DMA (SMPU XX-O: XX wt% hard segment content without steaming; SMPU XX-S: XXwt% hard segment content with steaming treatment)[58]

T_{gs} (glass transition temperature of soft segments) in SMPU fibers moves forward to high temperature side when the hard segment content increases in untreated or steamed series of fibers, which can be detected from the peak point of $\text{Tan}\delta$ shown in Figure 7.17. The hard segment content dependence of T_{gs} is quite similar to that from DSC whether in untreated SMPU fibers and steamed fibers. Moreover, the influence of high pressure steaming on T_{gs} of fibers with high hard segment content such as SMPU64-O/SMPU64-S is larger than that on T_{gs} of those with low hard segment content such as SMPU48-O/SMPU48-S.

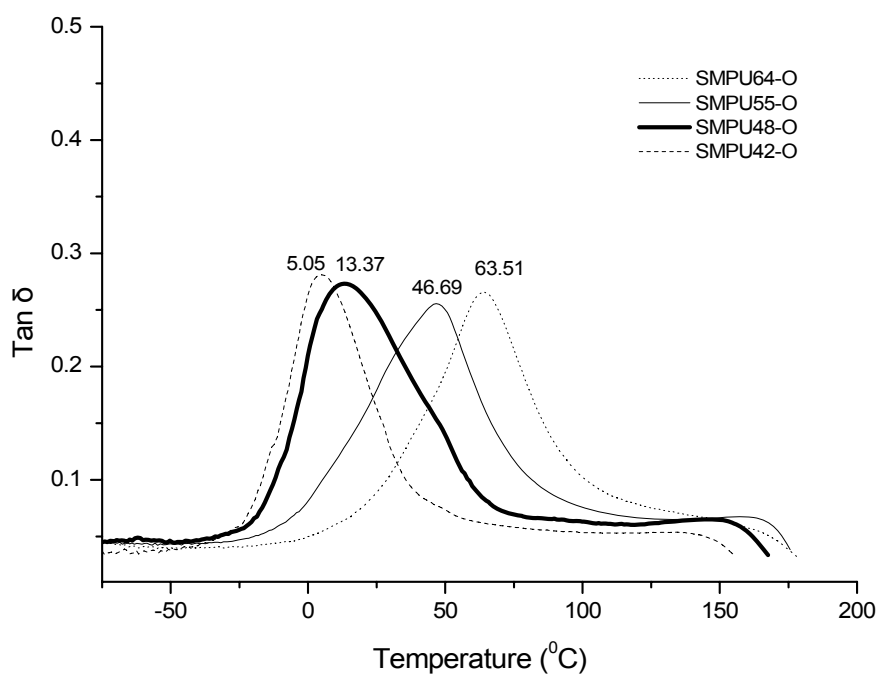
Among the investigation of shape memory effect of SMPU film, the cyclic tensile test as shown in Figure 4.2 is the commonly used one according to the literature reported[1, 5, 22, 27, 70]. Moreover, based on the research result about the shape memory effect of SMPU film, it can be found that the existence of irreversible strain and recovery trend offered by hard segment network give rise to the shape recovery ratio and shape fixity ratio, which are quantities determined to describe the shape memory properties of the materials. The irreversible strain ϵ_p observed from the initial point of the following tensile cycle is interpreted as the destruction of weak net-points followed by an increasing formation of an ideal elastic network[1]. However, for SMPU fibers, it is worth noting that the internal stress stored in fibers will cause the thermal shrinkage, which will lead to the decrease of the original length of fiber samples in heating process. So, in the cyclic tensile test procedures, the effect of thermal shrinkage on the shape recovery of SMPU fibers might be opposite to the effect of irreversible strain. In addition, in the cyclic tensile programming, the deformation is usually conducted at temperature higher than the switching temperature and then the deformation can be fixed in the cooling process. The advantage of deformation at higher temperature was explained by the fact that the SMPU film will possess lower elastic modulus and be readily shaped at higher temperature. But, if the switching temperature is higher than room temperature, with respect to the practical application such as the produce of wrinkle or the diminution of crease of the cloth, the fiber might be deformed at the temperature lower than the switching temperature. In this study, with respect to the practical application the SMPU fibers were all deformed at T_{low} (22°C) and recovered when heated up to T_{high} (75°C) with cyclic tensile method to quantitatively evaluate the shape

memory effect. According to the aforementioned, in heating process, there will be two opposite trends: irreversible strain caused by incomplete shape recovery and thermal shrinkage induced by internal stress. The extent of shrinkage ratio in heating process was quite different in original and treated SMPU fibers as shown in Figure 7.16 (a) and (b). Therefore, it is expected that the irreversible strain will be counteracted with different extend, subsequently influence the shape memory properties. Figure 7.18 demonstrates the stress-strain behavior in cyclic tensile test for original SMPU fibers, together with the cyclic dependence. Just like testing result of SMPU film in reported literatures[5, 47, 73], the stress-strain curve is mostly confined to the first several cycles and no more obvious changes can be observed in the further cycles. From Figure 7.18, it can be observed that after the first cycle, the length of original fibers decrease immensely and even is shorter than the original length, suggesting the thermal shrinkage is the predominant factor to thermal responsive shape recovery in this case. For SMPU55-O and SMPU48-O, the start point even move to -30% around after the first cycle. Also, it is noticeable that the stress at 50% elongation generally decreases with the decrease of hard segment content. The fixity ratio of shape memory effect can be calculated with the fixed strain after deformation: ε_u , as shown in Figure 4.2. Therefore, in original SMPU fibers, it can be found that fixity ratio of SMPU64-O is around 65~70% and the fixity ratio decrease with the decrease of hard segment content. The shape memory effect of SMPU fibers treated with high pressure steaming was demonstrated in Figure 7.19, in which we can observed that the length of fibers basically remain stable after heating recovery process. In this case, the irreversible strain can be found from the ε_p value (shown in Figure 4.2) for each specimen: for SMPU64-S, the recovery

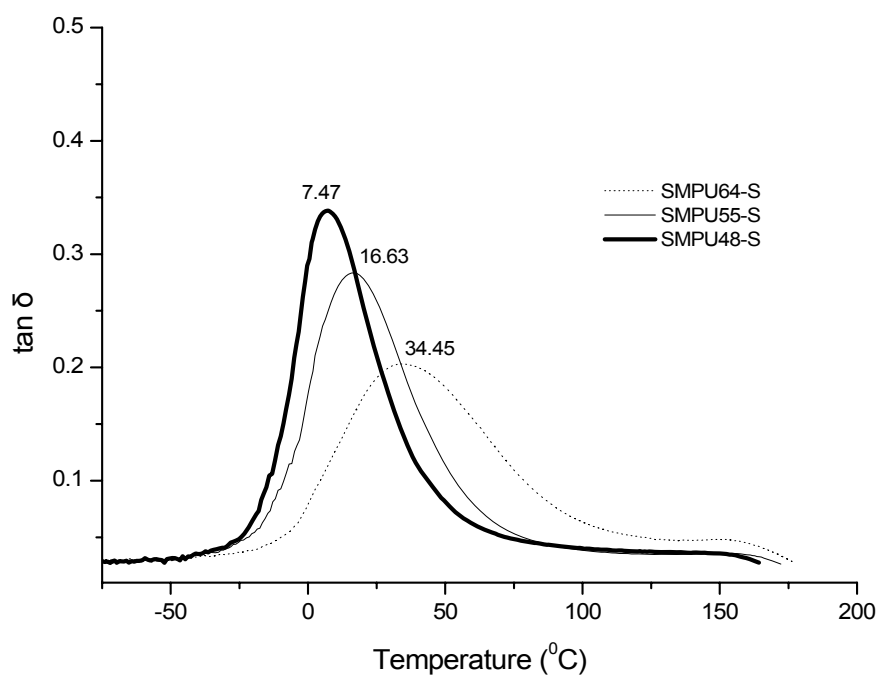
ratio is 90~95%; for SMPU55-S and SMPU48-S, the recovery is almost complete. Also, the fixity ratio decrease significantly with the decrease of hard segment content. It might be due to the influence of variation of transition temperature. If the transition temperature is much higher than fixing temperature, then the fixity ratio of shape memory materials will be higher according to our previous study[59]. For SMPU55-S and SMPU48-S, the T_{gs} is lower than fixing temperature (22°C). Therefore they are in rubbery status and possess immediate elasticity just like the stress-strain behavior of elastic fibers such as Lycra. As for the stress of treated fibers, similarly, the stress at 50% elongation of treated fibers decreases with the lowering of hard segment content.

All in all, after high pressure steaming, internal stress is released immensely and the dimensional stability of SMPU fibers can be improved more effectively in comparison with SMPU fibers treated with hot roller at used temperature. Meanwhile, the transition temperature was lowered with different extent. The counteraction effect between irreversible strain and thermal shrinkage also has a huge influence on thermal responsive recovery ability of SMPU fibers and then will be used in the further study of SMPU fibers and weaving process.

Therefore, in the study about SMPU ionomer fibers, the ionic groups were introduced into SMPU with different hard segment content (64 wt% and 55 wt %). Accordingly, the properties of untreated and steamed SMPU ionomers fibers were studied so as to illustrate the effect of tiny ionic groups on mechanical property, thermal property and shape memory function.



(a)



(b)

Figure 7.17 $\text{Tan } \delta$ value detected by DMA for original (a) and treated SMPU fibers (b)

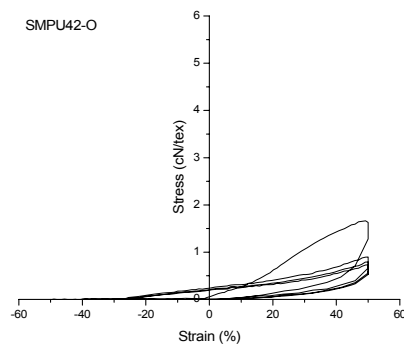
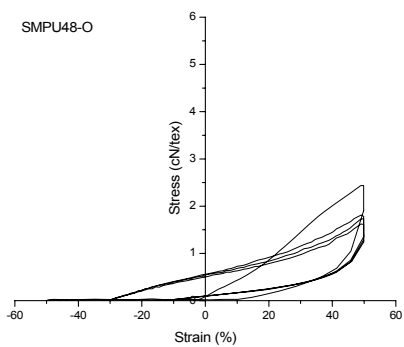
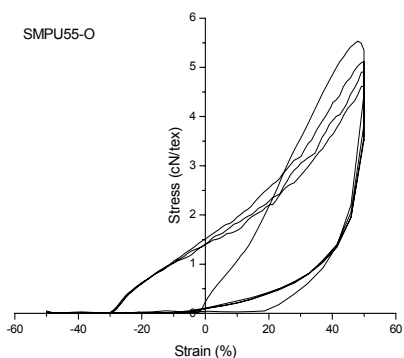
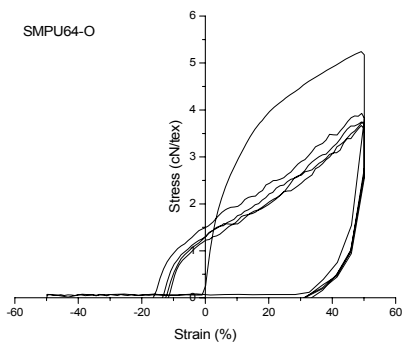


Figure 7.18 Cyclic tensile test for original SMPU fibers

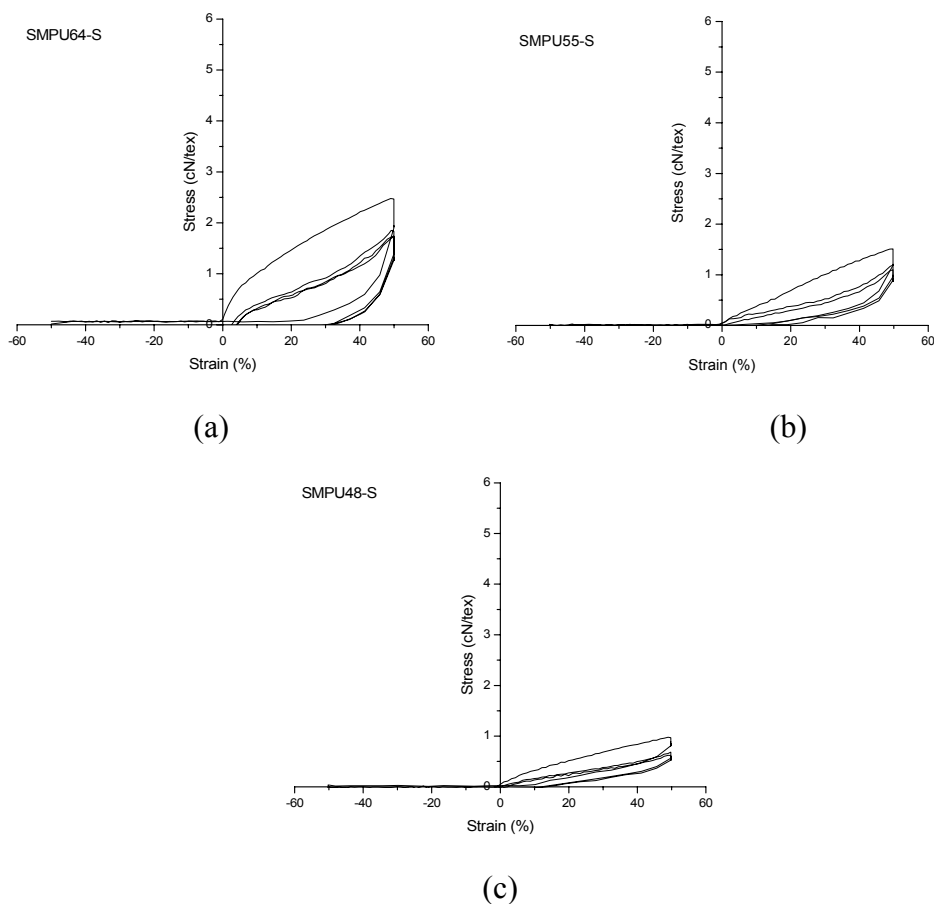


Figure 7.19 Cyclic tensile test for treated SMPU fibers

7.2.1 Mechanical and dynamic mechanical properties of SMPU ionomer fibers

Figure 7.20~7.23 demonstrate the temperature dependence of $\text{Tan}\delta$ and Storage modulus E' of SMPU ionomer fibers. The T_{gs} s were listed in Table 7.7. From the resulting data of DMA, it can be found that the ionic groups within hard segments in SMPU with different hard segment content will have different effect. In untreated specimens with 64.1 wt% hard segment content, 2wt% NMDA will cause increase of glass transition of soft segments from 63.5 °C to 70.6 °C. However, in specimens with 54.7 wt% hard segment content, the trend is reverse.

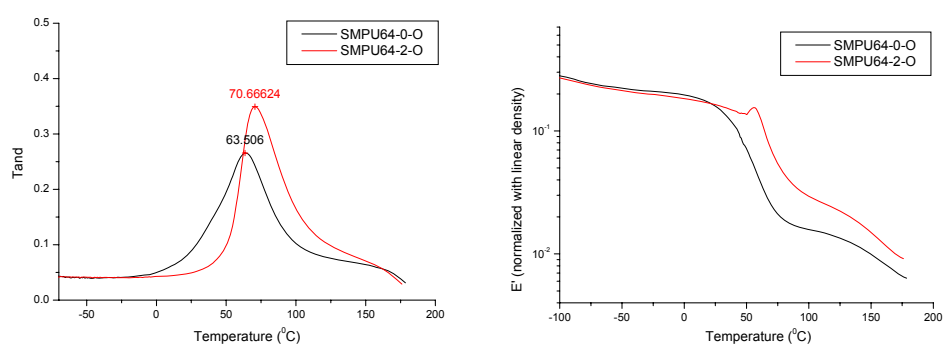


Figure 7.20 $Tan\delta$ and Storage modulus E' of SMPU ionomer original fibers with 64 wt% hard segment content

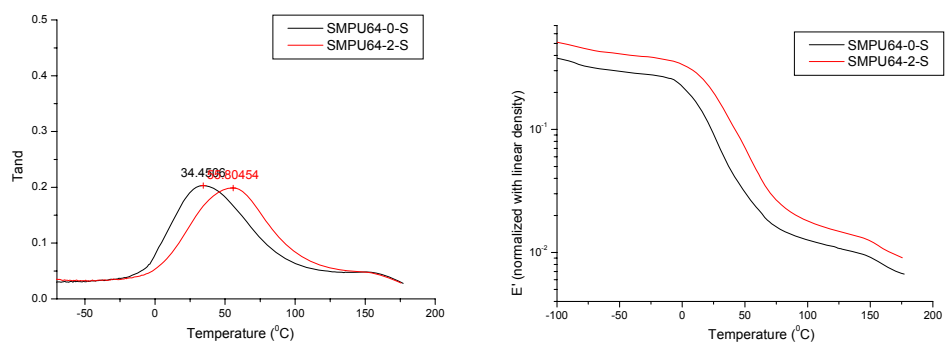


Figure 7.21 $Tan\delta$ and Storage modulus E' of SMPU ionomer steamed fibers with 64wt% hard segment content:

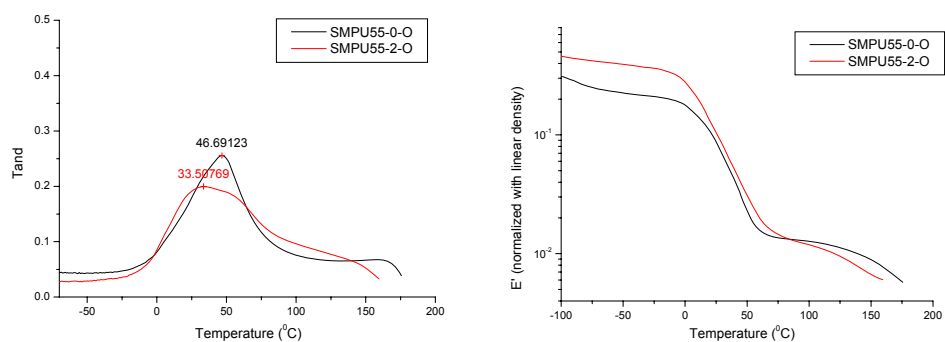


Figure 7.22 $Tan\delta$ and Storage modulus E' of SMPU ionomer original fibers with 55wt% hard segment content

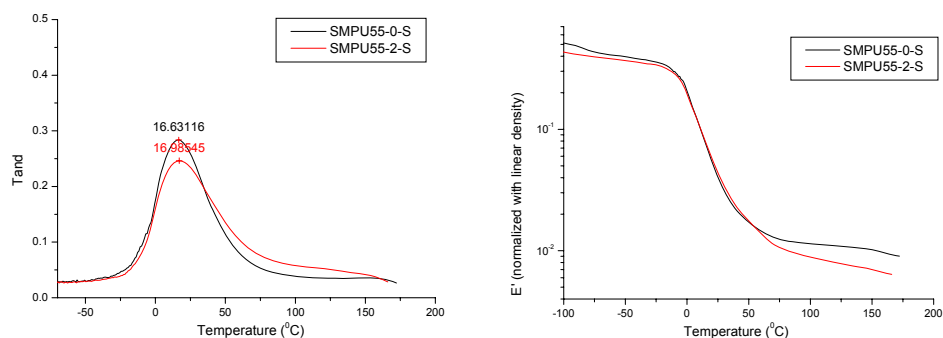


Figure 7.23 $Tan\delta$ and Storage modulus E' of SMPU ionomer steamed fibers with 55wt% hard segment content

Table 7.7 The samples were listed in the following table

Sample code	Hard segment content (wt%)	NMDA content (wt%)	Post treatment	Linear density (tex)	Maximum strain (%)	Tenacity (cN/tex)	T_{gs} (From the peak of $Tan\delta$ with DMA)($^{\circ}C$)
SMPU64-0-O	64.1	0	Non	7.62	80.2	9.7	63.51
SMPU64-2-O	64.1	2	Non	5.89	42	11.02	70.67
SMPU55-0-O	54.7	0	Non	8.47	67.5	14.2	46.69
SMPU55-2-O	54.7	2	Non	8.21	153.5	9.37	33.5
SMPU64-0-S	64.1	0	steaming	7.18	147	7.4	34.45
SMPU64-2-S	64.1	2	steaming	5.89	106.1	8.34	55.8
SMPU55-0-S	54.7	0	steaming	5.28	172.4	7.5	16.63
SMPU55-2-S	54.7	2	steaming	7.62	342.7	6.67	16.99

Compared with SMPU55-0-O, SMPU55-0-S possesses higher elongation ratio at break and lower T_{gs} . Generally, the steaming treatment can give rise to increase of elongation ratio and decrease of tenacity in all samples. Meanwhile, in heating scan of DMA, almost one order magnitude of decrease in elastic modulus can be observed in the glass transition temperature range, which offers the switch effect of the recovery ability from temporary shape to permanent shape in shape memory fibers. The plateau of elastic modulus from the glass transition

temperature of soft segments to 150°C or more shows the existence of physical crosslink of hard segments. In this temperature range, the immediate elasticity of the fibers can be observed. This elasticity imparts the shape memory system to memorize the original shape and to recover the original shape with the stimulus of heating.

The reported literature indicates that the ionic groups within the hard segments can influence the transition temperature, hard domain cohesion and phase mixing in the segmented polyurethane-block copolymer system[47]. The location of T_g is sometimes used as indicators of phase purity in multi-block polyurethanes. If the copolymer is assumed to behave like a blend of homopolymers, the T_g of the phases in the blend could be compared to those of the neat components to determine the degree of hard/soft segment mixing [109, 127]. However, in our study, when tiny ionic groups were introduced into hard segments, there are two opposing trends: the increased T_gs of SMPU64-2-O compared with SMPU64-0-O; the decreased T_gs of SMPU55-2-O compared with SMPU55-0-O. In their study of segmented polyurethane ionomer, Kim and Chen et al observed there are dual effect of ion insertion within hard segments on micro-phase separation morphology[47, 48]. When the hard segment content increase monotonously, the morphology of segmented PU will evolve from no hard segment domains, isolated hard segment domains, inter-connected hard segment domains and finally to a continuous hard segment phase[8, 152]. Therefore, the effect of ion insertion into different hard segments is likely to be based on the hard segment content and this might be one reason for the above two opposing trends in T_gs. Further investigation of the influence of tiny ions on the morphology of

segmented PU, which may offer a means to realize a designed shape memory function is needed.

7.2.2 Thermal properties

From the DSC shown in Figure 7.24, the comparison between SMPU ionomers with 55wt% HSC and 64wt% HSC can be made. It can be found the crystallization of hard segments in SMPU with 64wt% HSC is stronger than the sample with 55wt% HSC. Moreover, the steaming for only 10min under 180kPa saturated water vapor pressure can effectively induce the enhancement of hard segment crystallization. In addition, adding almost 2wt% ionic extender has little effect on hard segment crystallization in steamed specimens. It can be judged from the similar melting enthalpy between SMPU64-0-S/SMPU64-2-S or SMPU55-0-S/SMPU55-2-S. Crystallinity of hard segments in SMPU fibers shown in Table 7.8 was calculated by using the endothermic peak area located at 150°C to 200°C, hard segment content and a value of 36 cal/g for the heat of fusion of MDI/BDO segments determined by Kajiyama and MacKnight[98]. Therefore, it can be found the ionic groups have more influence on hard segment crystallization in original fibers compared to the steamed fibers. In steamed fibers, the influence of ionic groups on the crystallinity of hard segments is less.

In the original series of SMPU ionomer fibers, the fiber containing only 2wt% (SMPU64-2-O and SMPU55-2-O) has higher crystallinity of hard segments than the corresponding control samples (SMPU64-0-O and SMPU55-0-O). But, after steaming post-treatment, the difference trends to be not significant. Therefore, the effect of steaming on morphology of hard segments should be considered.

MacKnight et al reported that annealing at 150 °C for 90 min can give rise to the disappearance of the transition at 94 and 135 °C, simultaneously raise the melting endotherm at 202 °C in MDI-BDO model compounds[151]. Apparently, the non-crystalline domain structure converts to the crystalline state during annealing. It can be concluded that the short range ordering of hard segments (MDI-BDO) can be improved by annealing and the corresponding endotherm moves upward from relative low temperature. For our samples, the greater degree of microcrystallinity in steamed fibers can be reflected in the higher enthalpy values. Basically, this endothermic activity observed in DSC for SMPU fibers should be ascribed to morphological effects. Various amounts of short- and long- range order may co-exist and are caused by the distribution of the hard segment lengths. Cooper *et al* studied the effect of annealing on MDI-BDO hard segments in polyurethane with various hard segment contents[153]. Their results also suggest sufficient annealing can facilitate the forming of hard segment microcrystallines. However, when annealing is not sufficient or the hard segments are not long enough to form the perfect morphology of hard segments with well-defined high temperature transition, it can be supposed that only increased enthalpy values can be observed and the maximum temperature attainable probably is lowered. Steaming for only 10 min can be regarded as an insufficient annealing procedure in comparison with annealing at 150°C for 90 min. This might be the reason for the lower T_{mhs} of steamed fibers than the unsteamed ones. The similar phenomenon was observed in polyurethane with 24 wt% diisocyanate content (sample code: ES-24-1) by Cooper et al[153].

Table 7.8 DSC data for the heating scan of SMPU fibers

Sample Code	Hard Segment Content (wt%)	Post treatment	NMDA weight content (wt%)	(First heating at 20 °C/min)			
				T_{gs} (°C)	T_{mh} (°C)	ΔH_h (J/g)	Hard segment Crystallinity* (%)
SMPU64-0-O	64%	Non	0	39.35	171.3	8.58	8.85%
SMPU64-2-O	64%	Non	2		169.9	17.3	17.85%
SMPU55-0-O	54.7%	Non	0	6.62	166.5	3.8	4.59%
SMPU55-2-O	54.7%	Non	2		165.35	7.3	8.83%
SMPU64-0-S	64%	Steaming	0	2.33	153.1	20.08	20.72%
SMPU64-2-S	64%	Steaming	2		153.9	20.3	20.95%
SMPU55-0-S	54.7%	Steaming	0	-6.41	153.1	11.58	14.00%
SMPU55-2-S	54.7%	Steaming	2	-9.7	153.5	10.8	13.06%

* Hard segment crystallinity calculated from the value of 36 cal/g of the heat of fusion of MDI/BDO determined by Kajiyama and MacKnight[98].

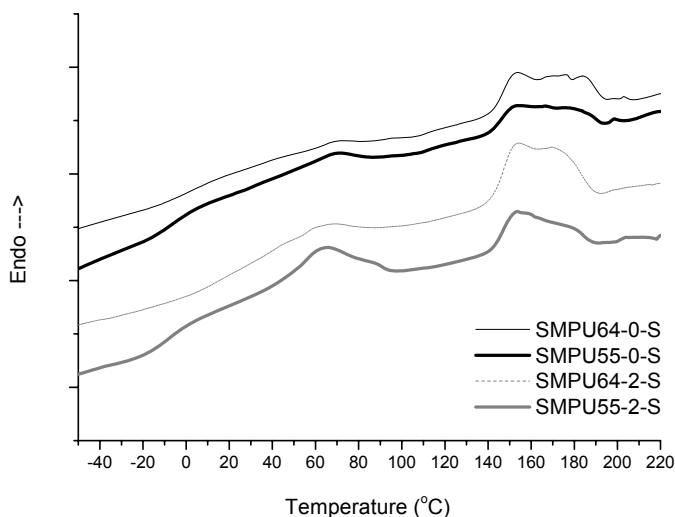


Figure 7.24 DSC heating scan for steamed SMPU ionomer fibers

7.2.3 Shape memory properties of SMPU ionomer fibers

As for shape memory properties, it can be found in Figure 7.25 that the effect of steaming on shape memory properties is similar with previous result mentioned above, such as lowering the stress at 100% elongation ratio, eliminating the thermal shrinkage in heating process. In Table 7.9, the data about shape fixity

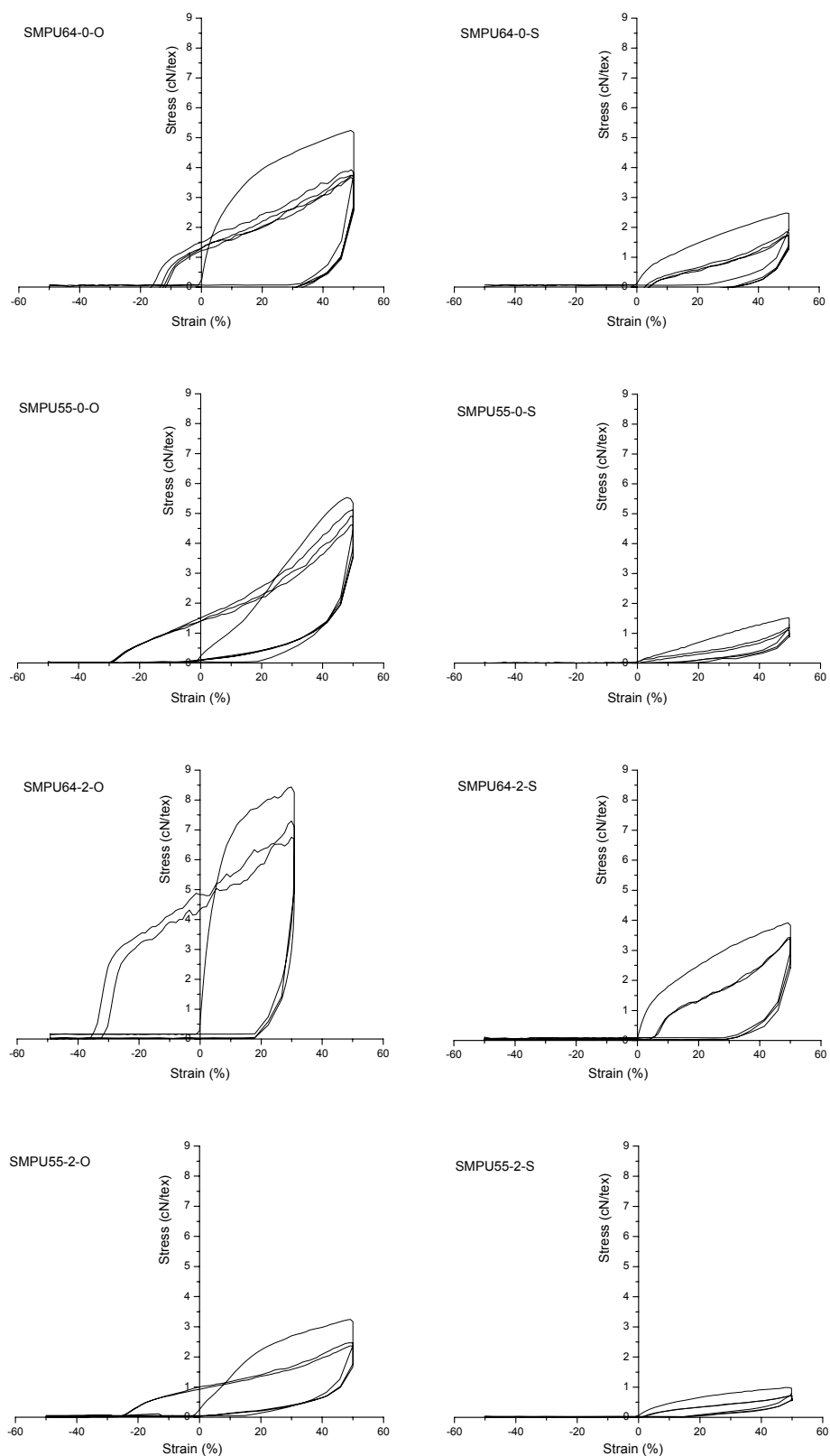


Figure 7.25 Cyclic tensile test for SMPU ionomer fibers

ratio and recovery ratio were summarized. For untreated fibers, the existence of thermal shrinkage causes the length of fibers to be shorter than the original length in the 2nd and following tensile cycles. Therefore, the shape recovery ratio can not be given in details. Besides, compared with the effect of hard segment content, the steaming has little influence on R_f . For steamed fibers, it can be observed that the fixity ratio decrease with the decrease of hard segment content and the introduction of ionic groups can lead to the lowering trend of R_r . It might arise from the disruption effect of ionic groups on the order of hard segments, because the physical cross link of hard segments is believed to be responsible for the fixity of permanent shape in shape memory function[1].

Table 7.9 Summary of shape fixity ratio (R_f) and shape recovery ratio (R_r)

Sample NO	Hard Segment Content (wt%)	NMDA content (wt%)	R_f (%)	R_r (%)
SMPU64-0-O	64%	0	65.0	--
SMPU64-2-O	64%	2	59.6	--
SMPU55-0-O	54.7%	0	--	--
SMPU55-2-O	54.7%	2	30.0	--
SMPU64-0-S	64.1%	0	67.0	91.1
SMPU64-2-S	64%	2	58.1	87.6
SMPU55-0-S	54.7%	0	--	100.0
SMPU55-2-S	54.7%	2	31.2	95.3

CHAPTER 8 CONCLUSIONS AND SUGGESTIONS

FOR FUTURE RESEARCH

According to the above chapters about studies of the structure and shape memory effect of segmented polyurethane ionomers, some conclusions were drawn as follows. Such investigations enable ones to have the overall understanding about the relations between the structure and shape memory effect in such kinds of smart polymer materials, so as to open the way to design the tailor made SMPU ionomers with specific properties. In the second part of this chapter, some meaningful subject matters about SMPU ionomers were suggested on the basis of the previous literatures and results obtained in this project.

8.1 Conclusions

8.1.1 Effect of ionic groups on the crystallization of soft segments

PCL-4000 based segmented PU non-ionomers and corresponding ionomers with different total molecular weight, 80% soft segment content, 5% DMPA content and similar molecule structure were synthesized and characterized by GPC, DSC and POM. The crystallization kinetics of the above samples and PCL-4000 were studied, suggesting that ionic groups in hard segments play different roles on the crystallization of soft segments in segmented PU samples with different molecular weights. In PU samples with low molecular weight, Coulombic force mostly enhances the restriction of molecule chain, which causes the decrease of Avrami parameter n and the increase of K . Instead, in PU with high molecular weight, Coulombic force mainly induce the high level of micro phase separation,

which results in the increase of Avrami parameter n and the decrease of K . Meanwhile, the crystallization rate is lowered down in segmented PU with low M_n , instead speeded up in PU with high M_n . The crystallization, which is affected obviously by Coulombic force according to the result, potentially has some influence on shape memory effect of such kind of polyurethane.

The investigation of the isothermal crystallization kinetics of PCL-10000 based SMPU cationomers with 75% soft segment content was carried out by differential scanning calorimetry. With the usage of Avrami equation, the crystallization mechanism of SMPU cationomers and the control sample was analyzed. The result suggests that the n values of PCL-10000 based SMPU cationomers and the control sample are all around 2.0. The difference is the crystallization rate parameter K . After the introduction of ionic groups within hard segments by chain-extension with BIN, the crystallization rate decreases significantly and the more BIN wt% in hard segments, the lower crystallization rate would be. Moreover, neutralization agents also have some influence on the crystallization rate. In the melting behavior study, it was revealed that, in heating scan after isothermal crystallization at 20 °C, the melting peak of SMPU ionomers quenched from 70 °C or 120 °C will be mostly attributed to the primary crystallization, but SMPU ionomers quenched from 240 °C showed significant dual melting peak after isothermal crystallization for short time such as 5 min, but for longer time, the single melting peak will appear which was from the overlapped two peaks.

8.1.2 Effect of ionic groups within hard segments on SME

For the study of SMPU anionomers, the PCL-4000 based segmented non-ionomers and ionomers series with 60% soft segment content were synthesized. These two series segmented PU samples all exhibit the increased phase mixing with the DMPA content and the charged ionic groups within hard segments could enhance the cohesion among hard domain and phase separation compared with the corresponding non-ionomers, which was examined by FTIR, DMA. The ionic groups on hard segments play two-fold effect: the effect of disruption of the order of hard domain; the effect of enhancing the cohesion among hard segments. When the DMPA content is moderate such as 5 wt%, the former effect is predominant; when the ionic group content is high enough, the cohesion among hard segments will be increased greatly and the later effect will be dominant. Therefore, the PU non-ionomer and ionomer series samples possess different shape memory properties: with the introduction of asymmetrical extender, the stress at 100% elongation of two series are decreased, especially lowered sharply for non-ionomer series because of disruption effect for the order of hard domain, which usually is regarded as physical crosslink point of fixed phase in shape memory segmented PU; the Coulombic Force in neutralized samples enhances the cohesion between hard segments, to some extent, supplementing the physical crosslink point of fixed phase; the fixity ratio of ionomer series is not affected; the total recovery ratio of ionomer series is decreased greatly; after sufficient relaxation for stretched samples studied, the switching temperature is increased, whereas the recovery ratio is decreased with increased DMPA content. Thereby, in the molecular design of shape memory polyurethane ionomers, the complicated effect of ionic groups on shape memory

effect and morphology of this kind of functional materials should be considered carefully.

For the series of SMPU cationomers, PCL-10000 based segmented PU cationomer series were synthesized to study the effect of cationic groups within hard segments on the shape memory effect, with emphasis being on the shape recovery and fixity ability of the segmented PU cationomer films. DMA and DSC results suggest that the segmented PU cationomers exhibits improved crystallizability by the presence of cationic groups; on the other hand, the cationic groups on hard segments enhance the cohesion among them through the Coulombic force compared with the corresponding PU non-cationomers. The cationic groups on hard segments play the two-fold effect: (i) the disruption of the order of hard domain, and (ii) the enhancement of cohesion among hard segments. The effect of cationic groups on the hard segments is manifested by the reduction of the stress in sample at 100% elongation at high temperature and the depression of the overall rubbery state modulus. Cyclic tensile test result suggests that when the cationic groups in the NMDA series, both the fixity ratio and recovery ratio can be improved simultaneously. However, in the BIN series, cationic groups have less effect on the fixity ratio and shape recovery ratio. This study demonstrates that the content and category of cationic groups have deep influence on the shape memory effect in segmented PU cationomers.

8.1.3 SMPU ionomers with substrate antibacterial activity

For the introduction of novel function into SMPU, ionic groups were incorporated into hard segments of PCL-10000 based SMPU ionomers with

constant 75% soft segment content. The neutralization agent is 1-Iodooctane. BIN weight content was used to control the ionic group content in this series of SMPU ionomers. The resultant data from the testing according to AATCC 147 and ASTM E2149 demonstrates that the synthesized SMPU ionomers possesses substrate bonding antibacterial activity against the testing cultures including Gram positive organism *Staphylococcus aureus* and Gram negative organism *Klebsiella pneumoniae*. Moreover, it is observed that the antibacterial activity in SMPU ionomers to Gram-position bacteria (*Staphylococcus aureus*) is significant and the reduction rate of bacteria even is 100%; the antibacterial activity to Gram-negative bacteria (*Klebsiella pneumoniae*) is lower than that to Gram-positive bacteria (*Staphylococcus aureus*) and increases with the increase of ionic groups content. In addition, SMPU ionomers neutralized with C8I presents the rapid fixity ability for temporary deformation compared with the control sample. The fixity ratio of this series of SMPU ionomers after enough long cooling time is similar to the control sample. These characteristic performances are due to the combination of effects from the decreased crystallization rate and the weakened physical cross links among hard segments. In the case of BIN75-11-C8, weakened physical cross link is a predominant factor determining the shape fixity ratio for various cooling time.

8.1.4 SMPU ionomers used as shape memory fiber materials

Ionic groups can be incorporated into hard segments of SMPU by using NMDA as a part of chain extender. Only 2 wt% NMDA can change the glass transition temperature of soft segment phase significantly whether in SMPU fibers with high or low HSC. DSC shows that the ionic group within hard segments can

facilitate the crystallization of hard segments in untreated SMPU ionomers fibers. But for steamed fiber specimens, this effect is insignificant. From DMA, it can be observed that the ionic groups within hard segments in SMPU with different hard segment content will have different effect. In untreated SMPU fibers with 64 wt% hard segment content, 2wt% NMDA will cause the increase of glass transition of soft segments from 63.5°C to 70.6°C. However, in fibers with 55 wt% hard segment content, the T_g is lowered from 46.7°C to 33.5°C. The post treatment—high pressure steaming is an effective way to remove the internal stress so as to improve the dimensional stability of SMPU ionomer fibers. Also, in steamed SMPU fibers, the introduction of ionic groups gives rise to the decrease of recovery ratio and the lowering of hard segment content cause the depression of fixity ratio significantly.

8.2 Future work suggested

8.2.1 Influence of chemical structure of ionic groups on SMPU ionomers

AL-SALAH et al. ever studied the influence of mono and divalent nontransition and transition metals on the glass transition and mechanical properties of PCL based polyurethane anionomers[154]. It is concluded that the mechanical properties are influenced by the type of the counter-ion. For monovalent and nontransition metals, the mechanical properties of the anionomers were improved by increasing the ionic potential; transition metals containing anionomers exhibited good mechanical properties but no relation between the mechanical properties and ionic potential was observed. Yang et al.[50] ever observed that small angle x-ray scattering patterns of ionic polyuretehanes exhibit two peaks,

one characteristic of scattering between the hard and soft domains and the other reflecting scattering from aggregates of ionic groups residing within the hard domain. In this case, the ionic aggregation can be the primary driving force for phase separation though the morphology is much close to non-ionic polyurethanes. Therefore, it can be found that the chemical structure of ionic groups including counter-ion category has huge influence on not only mechanical property, thermal property, but the micro phase structure as well. In this thesis, the influence of ionic group content with SMPU ionomers on thermal properties, dynamic mechanical properties and SME were investigated systematically in several series of specimens. But, the further overall research of chemical structure of ionic groups on SME is worthy being conducted. And it is expected to facilitate the research on novel shape memory polymeric materials to satisfy various application areas.

8.2.2 Effect of ionic groups within soft segments on SMPU ionomers

Present research result illustrates that the shape memory function is quite relevant to the micro phase separation in segmented polyurethane. Therefore, the most of research about these materials were focused on the influence on the hard and soft segment on shape memory effect. With the introduction of ionic moiety into molecular chain, a new control means for micro phase separation and SME were opened up. Thereby, the ionic groups were inserted into the hard segments as a part or all of chain extender in polymerization. In this way, the ionic group usually can be inserted into hard segments. As for the PU ionomers with ionic groups within soft segments, XIN WEI et al[155] reported a series of polyether (PTMO, PEO) polyurethane ionomers having different contents of sodium

sulfonate groups in the soft segments can be synthesized with the reaction of transesterification to incorporate the sodium sulfonate groups in the polyether. In their findings, the compatibility of the hard and soft segments increased with the increase of ionization level and the T_g of soft segments increased significantly in this case. Therefore, the influence mechanism of ionic groups with soft segments on morphology and SME in SMPU ionomers might be different with the specimens studied in this thesis and is believed to be potential for designing new species of shape memory molecules.

8.2.3 Crystallization process and SME in SMPU ionomers

In this research, it is observed that cooling time in deformation fixing process has huge influence on the shape fixity ratio and shape recovery ratio. Also, considering the time dependence of cooling induced crystallization process, the crystallization rate was studied with isothermal crystallization method. The result of the part 7.1.4 reveals that the crystallization process is one of primary control factors for fixing deformation during different cooling time: the longer the cooling time, the higher the fixity ratio will be during a short fixing time. In this part, the cooling induced crystallization of crystallizable soft segments of SMPU ionomers was analyzed systematically. However, the strain induced crystallization was tentatively ignored for the limit of effective measurement. Li et al[156] ever used in-situ small- and wide-angle X-ray scattering to demonstrate the bundles with smectic ordering produced by a step shear in a supercooled isotactic polypropylene melt. That research offers an effective way to obtain the on-line observation for shear/strain induced crystallization process.

It is expected to facilitate disclosing the mechanism of the fixity process in T_m type SMPU.

8.2.4 SMPU ionomers with improved SME

In previous research, chemical crosslink structure was introduced into hard segments with multi functional chain extender or the excess of diisocyanate[27, 55] so as to improve shape memory function and mechanical properties in shape memory segmented polyurethane. However, just as mentioned in the part of the literature review, the processing advantage of thermal plastic polymer was lost with the forming of chemical crosslink. For polyurethane ionomers, the molding process can be done with the neutralization process simultaneously such as film casting as reported by Sriram et al[136, 137], in which the polyurethanes were converted to crosslinking PU cationomers by neutralization reaction. Therefore, such kinds of SMPU ionomers might be a potential candidate to fabricate the novel species of shape memory polymer with both improved molecular networks and the easy processing advantage.

8.2.5 Other novel function introduced into SMPU with ionic groups

Since the polymer ionomer was reported by Rees et al in 1965[157], it has been developed wildly for its characteristics such as improving the phase compatibility in copolymer system, increasing the conductivity in specific molecular system, changing the hydrophilic property and so on. In this thesis, the substrate bonding antibacterial activity was imparted to SMPU ionomers with pyridinium-type cationomers. Some other novel functions also are expected to be introduced into

shape memory polymer system with the ionic moiety. It will broaden the application area of this kind of smart functional polymeric materials.

8.2.6 Effect of molecular orientation on SME in SMPU fibers

Based on the previously reported literature, it can be found that the molecular orientation including the soft segment, hard segment and domain orientation has huge influence on properties of polyurethane fibers[149, 158]. Moreover, the spinning process and chemical composition can give rise to the significant difference in orientation function of various functional groups, which can be detected from the birefringence measurement[149]. Considering the characteristic molecular structure of SMPU fibers, the transition temperature of soft segments is usually higher than using temperature, therefore, the influence of soft segment and hard segment orientation might be different from that in traditional PU fibers on properties including dimensional/thermal stability and recovery ability[28]. The relevant research is expected to reveal the relation between properties and various patterns of orientation structure, so as to optimize the manufacture process of such kinds of smart functional fibers.

References

- [1] A. Lendlein and S. Kelch, "Shape-Memory Polymers," *Angewandte Chemie-International Edition*, vol. 41, pp. 2034 - 2057, 2002.
- [2] Z. G. Wei, R. Sandstrom, and S. Miyazaki, "Review: Shape-memory materials and hybrid composites for smart systems," *Journal of Materials Science*, vol. 33, pp. 3743-3762, 1998.
- [3] C. Liu, S. B. Chun, P. T. Mather, L. Zheng, E. H. Haley, and E. B. Coughlin, "Chemically cross-linked polycyclooctene: Synthesis, characterization, and shape memory behavior," *Macromolecules*, vol. 35, pp. 9868-9874, 2002.
- [4] C. liang, C. A. Rogers, and E. Malafeew, "Investigation of shape memory polymers and their hybrid composites," *Journal of intelligent material systems and structures*, vol. 8, pp. 380-386, 1997.
- [5] B. K. Kim, S. Y. Lee, and M. Xu, "Polyurethane having shape memory effects," *Polymer*, vol. 37, pp. 5781-5793, 1996.
- [6] J. A. Hou, X. Q. Ma, X. L. Luo, D. Z. Ma, X. Zhang, W. Zhu, and M. Xu, "Thermally Simulated Shape Recovery Effect of Segmented Polyurethane," in *The International Symposium on Polymer Alloys and Composites*, C. L. Choy and F. G. Shin, Eds. Hong Kong Polytechnic University, Hong Kong: Hong Kong Polytechnic University, 1992, pp. 211.
- [7] F. K. Li, X. Zhang, J. N. Hou, M. Xu, X. L. Luo, D. Z. Ma, and B. K. KIM, "Studies on Thermally Stimulated Shape Memory Effect of Segmented Polyurethanes," *Journal of Applied Polymer Science*, vol. 64, pp. 1511-1516, 1997.
- [8] J. R. Lin and L. W. Chen, "Study on Shape-Memory Behavior of Polyether-Based Polyurethanes. I. Influence of the Hard-Segment Content," *Journal of Applied Polymer Science*, vol. 69, pp. 1563-1574, 1998.
- [9] J. R. Lin and L. W. Chen, "Study on Shape-Memory Behavior of Polyether-Based Polyurethanes. II. Influence of Soft-Segment Molecular Weight," *Journal of Applied Polymer Science*, vol. 69, pp. 1575-1586, 1998.
- [10] B. S. Lee, B. C. Chun, Y. C. Chung, K. I. Sul, and J. W. Cho, "Structure and Thermomechanical Properties of Polyurethane Block Copolymers with Shape Memory Effect," *Macromolecules*, vol. 34, pp. 6431-6437, 2001.
- [11] J. H. Yang, B. C. Chun, Y. C. Chung, and J. H. Cho, "Comparison of thermal/mechanical properties and shape memory effect of polyurethane block-copolymers with planar or bent shape of hard segment," *Polymer*, vol. 44, pp. 3251-3258, 2003.

- [12] J. W. Cho, Y. C. Jung, Y.-C. Chung, and B. C. Chun, "Improved Mechanical Properties of Shape-Memory Polyurethane Block Copolymers through the Control of the Soft-Segment Arrangement," *Journal of Applied Polymer Science*, vol. 93, pp. 2410-2415, 2004.
- [13] A. Lendlein, H. Jiang, O. Junger, and R. Langer, "Light-induced shape-memory polymers," *Nature*, vol. 434, pp. 879-882, 2005.
- [14] B. Yang, W. M. Huang, C. Li, and J. H. Chor, "Effects of moisture on the glass transition temperature of polyurethane shape memory polymer filled with nano-carbon powder," *European Polymer Journal*, vol. 41, pp. 1123-1128, 2005.
- [15] B. Yang, W. M. Huang, C. Li, C. M. Lee, and L. Li, "On the effects of moisture in a polyurethane shape memory polymer," *Smart Materials and Structures*, vol. 13, pp. 191-195, 2004.
- [16] W. M. Huang, B. Yang, L. An, C. Li, and Y. S. Chan, "Water-driven programmable polyurethane shape memory polymer: Demonstration and mechanism," *Applied Physics Letters*, vol. 86, pp. 114105-1~114105-3, 2005.
- [17] B. Yang, W. M. Huang, C. Li, and L. Li, "Effects of moisture on the thermalmechanical properties of a polyurethane shape memory polymer," *Polymer*, vol. 47, pp. 1348-1356, 2006.
- [18] Y. C. JUNG, H. H. SO, and J. W. CHO, "Water-Responsive Shape Memory Polyurethane Block Copolymer Modified with Polyhedral Oligomeric Silsesquioxane," *Journal of Macromolecular Science. Part B: Physics*, vol. 45, pp. 453-461, 2006.
- [19] J. W. Cho, J. W. Kim, Y. C. Jung, and N. S. Goo, "Electroactive Shape-Memory Polyurethane Composites Incorporating Carbon Nanotubes," *Macromolecular Rapid Communications*, vol. 26, pp. 412-416, 2005.
- [20] A. M. Schmidt, "Electromagnetic Activation of Shape Memory Polymer Networks Containing Magnetic Nanoparticles," *Macromolecular Rapid Communications*, vol. 27, pp. 1168-1172, 2006.
- [21] H. Koerner, G. Price, N. A. Pearce, M. Alexander, and R. A. Vaia, "Remotely actuated polymer nanocomposites-stress-recovery of carbon-nanotube-filled thermoplastic elastomers," *Nature Materials*, vol. 25, pp. 115-120, 2004.
- [22] H. Tobushi, H. Hara, E. Yamada, and S. Hayashi, "Thermomechanical properties in a thin film of shape memory polymer of polyurethane series," *Smart Materials and Structures*, vol. 5, pp. 483-491, 1996.
- [23] S. Hayashi and N. Ishikawa, "High Moisture Permeability Polyurethane for Textile Application," *Journal of Coated Fabrics*, vol. 23, pp. 74-83, 1993.
- [24] J. L. Hu, X. M. Ding, X. M. Tao, and J. M. Yu, "Shape Memory Polymers and Their Applications to Smart Textile Products," *Journal of Dong Hua University (Eng Ed)*, vol. 19, pp. 89, 2002.

- [25] Y. M. Zeng, J. L. Hu, and H. J. Yan, "Temperature Dependency of Water Vapor Permeability of Shape Memory Polyurethane," *Journal of Dong Hua University (Eng Ed)*, vol. 19, pp. 53, 2002.
- [26] J. L. Hu and S. Mondal, "Structural characterization and mass transfer properties of segmented polyurethane: influence of block length of hydrophilic segments," *Polymer International*, vol. 54, pp. 764-771, 2005.
- [27] J. L. Hu, Z. H. Yang, L. Y. Yeung, F. L. Ji, and Y. Q. Liu, "Crosslinked polyurethanes with shape memory properties," *Polymer International*, vol. 54, pp. 854-859, 2005.
- [28] Y. Zhu, J. L. Hu, L. Y. Yeung, Y. Liu, F. L. Ji, and K. W. Yeung, "Development of Shape Memory Polyurethane Fiber with Complete Shape Recoverability," *Smart Materials & Structures*, vol. 15, pp. 1385-1394, 2006.
- [29] S. Mondal, J. L. Hu, and Y. Zhu, "Free volume and water vapor permeability of dense segmented polyurethane membrane," *Journal of Membrane Science*, vol. 280, pp. 427-432, 2006.
- [30] Y. Q. Liu, J. L. Hu, Y. Zhu, and Z. H. Yang, "Surface modification of cotton fabric by grafting of polyurethane," *Carbohydrate Polymers*, vol. 61, pp. 276-280, 2005.
- [31] F. L. Ji, Y. Zhu, J. L. Hu, Y. Liu, L.-Y. Yeung, and G. D. Ye, "Smart polymer fibers with shape memory effects," *Smart Materials and Structures*, vol. 15, pp. 1547-1554, 2006.
- [32] J. L. Hu, "Shape memory textiles," in *Shape Memory Polymers and Textiles*. Cambridge: Woodhead Publishing Limited, 2007.
- [33] S. Mondal, "Studies of structure and water vapor transport properties of shape memory segmented polyurethanes for breathable textiles, PhD thesis," in *Institute of Textiles and Clothing*, vol. PhD thesis. Hong Kong: The Hong Kong Polytechnic University, 2006.
- [34] X. Ding, "Microstructure and water vapor transport properties of temperature sensitive polyurethanes, PhD thesis," in *Institute and Textiles and Clothing*, vol. PhD thesis. Hong Kong: The Hong Kong Polytechnic University, 2004.
- [35] J. L. Hu, Y. M. Zeng, and H. J. Yan, "Influence of Processing Conditions on the Microstructure and Properties of Shape Memory Polyurethane Membranes," *Textile Research Journal*, vol. 73, pp. 172-178, 2003.
- [36] X. M. Ding, J. L. Hu, and X. M. Tao, "Effect of Crystal Melting on Water Vapor Permeability of Shape-Memory Polyurethane Film," *Textile Research Journal*, vol. 74, pp. 39-43, 2004.
- [37] A. Lendlein and R. Langer, "Biodegradable, Elastic Shape-Memory Polymers for Potential Biomedical Applications," *Science*, vol. 296, pp. 1673-1676, 2002.

- [38] D. G. Anderson, J. A. Burdick, and R. Langer, "Smart Biomaterials," *Science*, vol. 305, pp. 1923-1924, 2004.
- [39] A. Alteheld, Y. Feng, S. Kelch, and A. Lendlein, "Biodegradable, Amorphous Copolyester-urethane Networks Having Shape-Memory Properties," *Angew Chem International Edition*, vol. 44, pp. 1188-1192, 2005.
- [40] R. Langer and D. A. Tirrell, "Designing materials for biology and medicine," *Nature*, vol. 428, pp. 487-492, 2004.
- [41] A. Lendlein, S. A. M, and R. Langer, "AB-polymer networks based on oligo(ϵ -caprolactone) segments showing shape-memory properties.," *Proceedings of the National Academy of Sciences of the United States of America*, vol. 98, pp. 842-847, 2001.
- [42] R. P. Kusy and J. Q. Whitley, "Thermal characterization of shape memory polymer blends for biomedical implantations," *Thermochimica Acta*, vol. 243, pp. 253-263, 1994.
- [43] G. Baer, T. S. Wilson, D. L. Matthews, and D. J. Maitland, "Shape-Memory Behavior of Thermally Stimulated Polyurethane for Medical Application," *Journal of Applied Polymer Science*, vol. 103, pp. 3882-3892, 2007.
- [44] J. Jagur-Grodzinski, "Polymers for tissue engineering, medical devices, and regenerative medicine. Concise general review of recent studies," *Polymers for Advanced Technologies*, vol. 17, pp. 395-418, 2006.
- [45] H. M. Jeong, B. K. Ahn, S. M. Cho, and B. K. Kim, "Water Vapor Permeability of Shape Memory Polyurethane with Amorphous Reversible Phase," *Journal of Polymer Science: Part B: Polymer Physics*, vol. 38, pp. 3009-3017, 2000.
- [46] H. M. Jeong, B. K. Ahn, and B. K. Kim, "Temperature sensitive water vapour permeability and shape memory effect of polyurethane with crystalline reversible phase and hydrophilic segments," *Polymer International*, vol. 49, pp. 1714-1721, 2000.
- [47] B. K. Kim, S. Y. Lee, J. S. Lee, S. H. Baek, Y. J. Choi, J. O. Lee, and M. Xu, "Polyurethane ionomers having shape memory effects," *Polymer*, vol. 39, pp. 2803-2808, 1998.
- [48] S. A. Chen and W. C. Chan, "Polyurethane Cationomers. I. Structure-Property Relationships," *Journal of Polymer Science: Part B: Polymer Physics*, vol. 28, pp. 1499-1514, 1990.
- [49] B. K. Kim and J. C. Lee, "Polyurethane ionomer dispersions from poly(neopentylene phthalate) glycol and isophorone diisocyanate," *Polymer*, vol. 37, pp. 469-475, 1996.

- [50] C. Z. Yang, T. G. Grasel, J. L. Bell, R. A. Register, and S. L. Cooper, "Carboxylate-Containing Chain-Extended Polyurethanes," *Journal of Polymer Science: Part B: Polymer Physics*, vol. 29, pp. 581-588, 1991.
- [51] H. A. AL-SALAH, H. X. XIAO, J. A. McLEAN, J., and K. C. FRISCH, "Polyurethane Cationomers. I. Structure-Properties Relationships," *Journal of Polymer Science: Part A: Polymer Chemistry*, vol. 26, pp. 1609-1620, 1988.
- [52] C. P. Chwang, C. L. Wang, Y. M. Kuo, S. N. Lee, A. Chao, and D. Y. Chao, "On the Study of Polyurethane Ionomer-Part I," *Polymers for Advanced Technologies*, vol. 13, pp. 285-292, 2002.
- [53] C. P. Chwang, S. N. Lee, Y. M. Kuo, S. Chao, and D. Y. Chao, "On the Study of Polyurethane Ionomer-Part II," *Polymers for Advanced Technologies*, vol. 13, pp. 293-300, 2002.
- [54] H. G. Jeon, P. T. Mather, and T. S. Haddad, *Polymer International*, vol. 49, pp. 453, 2000.
- [55] S. H. Lee, J. W. Kim, and B. K. Kim, "Shape memory polyurethanes having crosslinks in soft and hard segments," *Smart Materials and Structures*, vol. 13, pp. 1345-1350, 2004.
- [56] F. K. Li, L. Y. Qi, J. P. Yang, M. Xu, X. L. Luo, and D. Z. Ma, "Polyurethane/Conducting Carbon Black Composites: Structure, Electric Conductivity, Strain Recovery Behavior, and Their Relationships," *Journal of Applied Polymer Science*, vol. 75, pp. 68-77, 2000.
- [57] J. Hazziza-Laskar, N. Nurdin, G. Helary, and G. Sauvet, "Biocidal Polymers Active by Contact. I. Synthesis of Polybutadiene with Pendant Quaternary Ammonium Groups," *Journal of Applied Polymer Science*, vol. 50, pp. 651-662, 1993.
- [58] Y. Zhu, J. L. Hu, L. Y. Yeung, J. Lu, Q. H. Meng, S. J. Chen, and K. W. Yeung, "Effect of steaming on shape memory polyurethane fibers with various hard segment contents," *Smart Materials & Structures*, vol. 16, pp. 969-981, 2007.
- [59] J. L. Hu, F. L. Ji, and Y. W. Wong, "Dependency of the shape memory properties of a polyurethane upon thermomechanical cyclic conditions," *Polymer International*, vol. 54, pp. 600-605, 2005.
- [60] T. Ohki, Q. Q. Ni, N. Ohsako, and M. Iwamoto, "Mechanical and shape memory behavior of composites with shape memory polymer," *Composites Part A: applied science and manufacturing*, vol. 35, pp. 1065-1073, 2004.
- [61] F. K. Li, Y. Chen, W. Zhu, X. Zhang, and M. Xu, "Shape memory effect of polyethylene/nylon6 graft copolymers," *Polymer*, vol. 39, pp. 6929-6934, 1998.
- [62] S. R. Chowdhury, J. K. Mishra, and C. K. Das, "Structure, shrinkability and thermal property correlations of ethylene vinyl acetate(EVA)/carboxylated

nitrile rubber(XNBR) polymer blends," *Polymer Degradation and Stability*, vol. 70, pp. 199-204, 2000.

[63] S. Ota, "Current Status of Irradiated Heat-Shrinkable Tubing in Japan," *Radiation Physics and Chemistry*, vol. 18, pp. 81-87, 1981.

[64] W. Chen, K. Xing, and L. Sun, "The Heat Shrinking Mechanism of Polyethylene Film," *Radiation Physics and Chemistry*, vol. 22, pp. 593-601, 1983.

[65] K. Sakurai and T. Takahashi, "Strain-induced crystallization in polynorbornene," *Journal of Applied Polymer Science*, vol. 38, pp. 1191-1194, 1989.

[66] K. Sakurai, T. Kashiwagi, and T. Takahashi, "Crystal structure of polynorbornene," *Journal of Applied Polymer Science*, vol. 47, pp. 937-940, 1993.

[67] K. Sakurai, Y. Shirakawa, T. Kashiwagi, and T. Takahashi, *Polymer*, vol. 35, 1994.

[68] F. K. Li, W. Zhu, X. Zhang, C. T. Zhao, and M. Xu, "Shape Memory Effect of Ethylene-Vinyl Acetate Copolymers," *Journal of Applied Polymer Science*, vol. 71, pp. 1063-1070, 1999.

[69] X. Luo, X. Zhang, M. Wang, and D. Ma, "Thermally Stimulated Recovery of Ethylene Oxide-Ethylene Terephthalate Segmented Copolymers," *Journal of China University of Science and Technology*, vol. 27, pp. 103-108, 1997.

[70] T. Takahashi, N. Hayashi, and S. Hayashi, "Structure and Properties of Shape-Memory Polyurethane Block Copolymers," *Journal of Applied Polymer Science*, vol. 60, pp. 1061-1069, 1996.

[71] K. Gall, M. L. Dunn, Y. Liu, D. Finch, M. Lake, and N. A. Munshi, "Shape memory polymer nanocomposites," *Acta Materialia*, vol. 50, pp. 5115-5126, 2002.

[72] A. Lendlein and S. Kelch, "Shape-Memory Polymers," *Angew Chem International Edition*, vol. 41, pp. 2035-2057, 2002.

[73] H. Tobushi, T. Hashimoto, N. Ito, S. Hayashi, and E. Yamada, "Shape Fixity and Shape Recovery in a Film of Shape Memory Polymer of Polyurethane Series," *Journal of Intelligent Material Systems and Structures*, vol. 9, pp. 127-136, 1998.

[74] H. Tobushi, T. Hashimoto, S. Hayashi, and E. Yamada, "Thermomechanical Constitutive Modeling in Shape Memory Polymer of Polyurethane Series," *Journal of Intelligent Material Systems and Structures*, vol. 8, pp. 711-718, 1997.

- [75] Kobayashi, Kazuyuki, Hayashi, and Shunichi, "Woven fabric made of shape memory polymer," vol. USA5,128,197, J. Mitsubishi Jukogyo Kabushiki Kaisha (Tokyo, Ed. United States Patent, 1989.
- [76] D. I. Cha, H. Y. Kim, K. H. Lee, Y. C. June, J. W. Cho, and B. C. Chun, "Electrospun Nonwovens of Shape-Memory Polyurethane Block Copolymers," *Journal of Applied Polymer Science*, vol. 96, pp. 460-465, 2005.
- [77] F. K. Li, X. Zhang, J. A. Hou, W. Zhu, and M. Xu, "Thermoplastics segmented polyurethanes with shape memory properties," *ACTA POLYMERICA SINICA*, vol. 4, pp. 462, 1996.
- [78] C. R. Arciola, L. Radina, P. Alvergnà, E. Cennib, and A. Pizzoferrato, "Heparin surface treatment of poly(methylmethacrylate) alters adhesion of a *Staphylococcus aureus* strain: utility of bacterial fatty acid analysis," *Biomaterials*, vol. 14, pp. 1161-1164, 1993.
- [79] J.-E. Yang, J.-S. Kong, S.-W. Park, D.-J. Lee, and H.-D. Kim, "Preparation and Properties of Waterborne Polyurethane-Urea Anionomers. I. The Influence of the Degree of Neutralization and Counterion," *Journal of Applied Polymer Science*, vol. 86, pp. 2375-2383, 2002.
- [80] T. J. Franklin and G. A. Snow, *Biochemistry of antimicrobial action*, 3rd ed. London, New York: Chapman and Hall, 1981.
- [81] N. Kawabata and M. Nishiguchi, "Antibacterial Activity of Soluble Pyridinium-Type Polymers," *Applied and Environmental Microbiology*, vol. 54, pp. 2532-2535, 1988.
- [82] J. A. Grapski and S. L. Cooper, "Synthesis and characterization of non-leaching biocidal polyurethanes," *Biomaterials*, vol. 22, pp. 2239-2246, 2001.
- [83] Kobayashi, Kazuyuki, Hayashi, and Shunichi, "Woven fabric made of shape memory polymer." United States Patent 5, 128, 197: Mitsubishi Jukogyo Kabushiki Kaisha (Tokyo, JP), 1992.
- [84] C. Oertel, *Polyurethane Handbook*. New York: Hanser Publisher, 1985.
- [85] N. M. K. Lamba, K. A. Woodhouse, and S. L. Cooper, *Polyurethanes in Biomedical Applications*. New York: CRC press, 1997.
- [86] Z. Wirpsza, *Polyurethanes: Chemistry, Technology and Applications*. New York: Ellis Horwood, 1993.
- [87] M. Li, "Concise Handbook of Chemical Data." Beijing: Chemical Industry Press, 2003, pp. 152.
- [88] S. Song, G. Zhuang, and Z. Wang, "Physical Chemistry," The 3rd ed. Tianjin: Higher Education Press, 1994, pp. 279-285.
- [89] W. M. Groenewoud, *Characterisation of polymers by thermal analysis*, 1st ed. Amsterdam; New York: Elsevier, 2001.

- [90] D. Campbell, R. A. Pethrick, and J. R. White, *Polymer characterization: physical techniques*, 2nd ed: Cheltenham [England]: Stanley Thornes, c2000, 2000.
- [91] B. Stuart, *Polymer analysis*. Chichester; New York: John Wiley & Sons, 2002.
- [92] J. Ma, D. Ma, Y. Li, and M. Xu, "Spherulite formation of hard segments and compatibility between soft and hard segments in polyurethanes," *ACTA POLYMERICA SINICA*, pp. 426-431, 2000.
- [93] N. Luo, D. Wang, S. Ying, Y. Qian, and Z. Zhu, "DSC study of Microphase Separation in RIM Polyurethane Elastomers," *Chemical Journal of Chinese University*, pp. 1076-1080, 1994.
- [94] Y. Guo, Z. Zhuang, S. Ying, Q. Ye, Z. Yuan, and Y. Gao, "Effects of Hard Segment Content on Morphology and Properties of Polyester-Based Polyurethane Elastomer," *China Synthetic Rubber Industry*, vol. 18, pp. 19-22, 1995.
- [95] W. Jia-min, J. Zhi-guo, Z. Chun-yu, and Z. Heng-jin, "Influence of the hard-segment content on the shape-memory performance of thermally stimulated shape-memory polyurethane," *Journal of Beijing University of Chemical Technology*, vol. 30, pp. 89-91, 2003.
- [96] F. K. Li, J. A. Hou, W. Zhu, X. Zhang, M. Xu, X. L. Luo, D. Z. Ma, and B. K. Kim, "Crystallinity and Morphology of Segmented Polyurethanes with Different Soft-Segment Length," *Journal of Applied Polymer Science*, vol. 62, pp. 631-638, 1996.
- [97] V. Crescenzi, G. Manzini, G. Calzolari, and C. Borri, "Thermodynamics of fusion of poly- β -propiolactone and poly- ϵ -caprolactone. comparative analysis of the melting of aliphatic polylactone and polyester chains," *European Polymer Journal*, vol. 8, pp. 449-463, 1972.
- [98] T. Kajiyama and W. J. MacKnight, "Thermal Properties of Polyurethanes. Enthalpies and Entropies of Fusion," *Polymer Journal*, vol. 1, pp. 548-554, 1970.
- [99] M. He, W. Chen, and X. Dong, *Polymer Physics*, 2nd ed. Shang Hai: Fudan University Publishing House, 1991.
- [100] A. M. Manich, T. Bosch, J. Carilla, M. H. Ussman, J. Maillo, and J. Gacén, "Thermal Analysis and Differential Solubility of Polyester Fiber and Yarns," *Textile Research Journal*, vol. 73, pp. 333-338, 2003.
- [101] N. Luo, D.-N. Wang, and S.-K. Ying, "Hydrogen-Bonding Properties of Segmented Polyether Poly(urethane urea) Copolymer," *Macromolecules*, vol. 30, pp. 4405-4409, 1997.
- [102] D. Jia, X. Wang, Y. Luo, and X. Wu, "Formation Reaction Kinetics of Simultaneous Interpenetration Networks by FTIR Spectroscopy," *Journal of South China University of Technology (Nature Science)*, vol. 22, pp. 1-7, 1994.

- [103] H. Liu, J.-S. Guo, H.-Q. Xie, B. Wang, S.-Q. Li, and S.-J. Wang, "Characterization of Crosslinked Poly(ether urethane) and Study of Its Transitions and Free-Volume Properties with Position Annihilation," *Chemical Journal of Chinese Universities*, vol. 15, pp. 603-607, 1994.
- [104] H. M. Jeong, B. K. Ahn, and B. K. Kim, "Miscibility and shape memory effect of thermoplastic polyurethane blends with phenoxy resin," *European Polymer Journal*, vol. 37, pp. 2245-2252, 2001.
- [105] J.-h. WU and W.-d. YU, "The Elasticity and Clothing Pressure of Knitted Fabrics," *Journal of Wu Han University of Science and Engineering*, vol. 19, pp. 21-25, 2006.
- [106] X. L. Luo, X. Y. Zhang, M. T. Wang, D. Z. Ma, M. Xu, and F. K. Li, "Thermally Stimulated Shape-Memory Behavior of Ethylene Oxide-Ethylene Terephthalate Segmented Copolymer," *Journal of Applied Polymer Science*, vol. 64, pp. 2433-2440, 1997.
- [107] Y. Liu and C. Pan, "Relationship between phase structure and mechanical properties of polyurethane prepared from copoly(ppo-THF) diols," *European Polymer Journal*, vol. 34, pp. 621-624, 1998.
- [108] M. S. Sanchez-Adsuar, "Influence of the composition on the crystallization and adhesion properties of thermoplastic polyurethane elastomers," *International Journal of Adhesion & Adhesives*, vol. 20, pp. 291-298, 2000.
- [109] J. T. Garrett, R. Xu, J. Cho, and J. Runt, "Phase separation of diamine chain-extended poly(urethane) copolymers: FTIR spectroscopy and phase transitions," *Polymer*, vol. 44, pp. 2711-2719, 2003.
- [110] H.-L. Chen, L.-J. Li, W.-C. Ou-Yang, J. C. Hwang, and W.-Y. Wong, "Spherulitic Crystallization Behavior of Poly(ϵ -caprolactone) with a Wide Range of Molecular Weight," *Macromolecules*, vol. 30, pp. 1718-1722, 1997.
- [111] M. Avrami, "Kinetics of Phase Change. I," *Journal of Chemical Physics*, vol. 7, pp. 1103-1112, 1939.
- [112] S. Liu, Y. Yu, Y. Cui, H. Zhang, and Z. Mo, "Isothermal and Nonisothermal Crystallization Kinetics of Nylon-11," *Journal of Applied Polymer Science*, vol. 70, pp. 2371-2380, 1998.
- [113] C. Li, G. Tian, Y. Zhang, and Y. Zhang, "Crystallization behavior of polypropylene/polycarbonate blends," *Polymer Testing*, vol. 21, pp. 919-926, 2002.
- [114] S. H. Kim, S. H. Ahn, and T. Hirai, "Crystallization kinetics and nucleation activity of silica nanoparticle-filled poly(ethylene 2,6-naphthalate)," *Polymer*, vol. 44, pp. 5625-5634, 2003.

- [115] A. A. Alwattari and D. R. Lloyd, "Isothermally crystallization of isotactic polypropylene-hexamethylbenzene blends: kinetics analysis," *Polymer*, vol. 39, pp. 1129-1137, 1998.
- [116] C. C. Lin, "The Rate of Crystallization of Poly(Ethylene Terephthalate) by Differential Scanning Calorimetry," *Polymer Engineering and Science*, vol. 23, pp. 113-116, 1983.
- [117] P. Cebe and S.-D. Hong, "Crystallization behavior of poly(ether-ether-ketone)," *Polymer*, vol. 27, pp. 1183-1192, 1986.
- [118] S. W. Kuo, S. C. Chan, and F. C. Chang, "Crystallization Kinetics and Morphology of Binary Phenolic/Poly(ϵ -caprolactone) Blends," *Journal of Applied Polymer Science*, vol. 42, pp. 117-128, 2004.
- [119] B. Bogdanow, V. Toncheva, E. Schacht, L. Finelli, B. Sarti, and M. Scandola, "Physical properties of poly(ester-urethane) prepared from different molar mass polycaprolactone-diols," *Polymer*, vol. 40, pp. 3171-3182, 1999.
- [120] J. Li, C. X. Zhou, G. Wang, Y. Tao, Q. Liu, and Y. Li, "Isothermal and nonisothermal crystallization kinetics of elastomeric polypropylene," *Polymer Testing*, vol. 21, pp. 583-589, 2002.
- [121] J. D. Hoffman and J. J. Weeks, "Rate of Spherulitic Crystallization with Chain Folds in Polychlorotrifluoroethylene," *Journal of Chemical Physics*, vol. 37, pp. 1723-1741, 1962.
- [122] R. G. Alamo, B. D. Viers, and L. Mandelkern, "A Re-examination of the Relation between the Melting Temperature and the Crystallization Temperature: Linear Polyethylene," *Macromolecules*, vol. 28, pp. 3205-3213, 1995.
- [123] R. G. Alamo, E. K. M. Chan, and L. Mandelkern, "Influence of Molecular Weight on the Melting and Phase Structure of Random Copolymers of Ethylene," *Macromolecules*, vol. 25, pp. 6381-6394, 1992.
- [124] Q. Guo and G. Groeninckx, "Crystallization kinetics of poly(ϵ -caprolactone) in miscible thermosetting polymer blends of epoxy resin and poly(ϵ -caprolactone)," *Polymer*, vol. 42, pp. 8647-8655, 2001.
- [125] G. Defieux, G. Groeninckx, and H. Reynaers, "Miscibility, crystallization and melting behavior, and semicrystalline morphology of binary blends of polycaprolactone with poly (hydroxyl ether of bisphenol A)," *Polymer*, vol. 30, pp. 2164-2169, 1989.
- [126] P. B. Rim and J. P. Runt, "Melting Behavior of Crystalline/Compatible Polymer Blends: Poly(ϵ -caprolactone)/Poly(styrene-*co*-acrylonitrile)," *Macromolecules*, vol. 16, pp. 762-768, 1983.
- [127] C. S. P. Sung, C. B. Hu, and C. S. Wu, "Properties of Segmented Poly(urethaneureas) Based on 2, 4-Toluene Diisocyanate. 1. Thermal Transitions, X-ray Studies, and Comparison with Segmented Poly(urethane)," *Macromolecules*, vol. 13, pp. 111-116, 1980.

- [128] F. F. Xiao, D. Y. Shen, X. Zhang, S. R. Hu, and M. Xu, "Studies on the morphology of blends of poly(vinyl chloride) and segmented polyurethane," *Polymer*, vol. 28, pp. 2335-2345, 1987.
- [129] T.-C. Wen, M.-S. Wu, and C.-H. Yang, "Spectroscopic Investigation of Poly(oxypropylene)glycol-Based Waterborne Polyurethane Doped with Lithium Perchlorate," vol. 32, pp. 2712-2720, 1999.
- [130] G. Defieuw, G. Groeninckx, and H. Reynaers, "Miscibility and morphology of binary polymer blends of polycaprolactone with solution-chlorinated polyethylenes," *Polymer*, vol. 30, pp. 595-603, 1989.
- [131] Y. Zhu, J. L. Hu, K. W. Yeung, K. F. Choi, Y. Q. Liu, and H. M. Liem, "Effect of Cationic Group Content on Shape Memory Effect in Segmented Polyurethane Cationomer," *Journal of Applied Polymer Science*, vol. 103, pp. 545-556, 2007.
- [132] P. Ping, W. Wang, X. Chen, and X. Jing, "Poly(caprolactone) Polyurethane and Its Shape-Memory Property," *Biomacromolecules*, vol. 6, pp. 587-592, 2005.
- [133] Y. Zhu, J. L. Hu, K. W. Yeung, H. J. Fan, and Y. Q. Liu, "Shape Memory Effect of PU Ionomer With Ionic Group on Hard-segment," *Chinese Journal of Polymer Science*, vol. 24, pp. 173-186, 2006.
- [134] C. G. Seefried, J. V. Koleske, and F. E. Critchfield, *Journal of Applied Polymer Science*, vol. 19, pp. 2493, 1975.
- [135] R. M. Briber and E. L. Thomas, "Investigation of Two Crystal Forms in MDI/BDO-Based Polyurethanes," *Journal Of Macromolecular Science-Physics*, vol. 22, pp. 509-528, 1983.
- [136] V. Sriram and G. Radhakrishnan, "Novel Short-chain Crosslinked Cationomeric Polyurethanes," *Polymer Bulletin*, vol. 55, pp. 165-172, 2005.
- [137] V. Sriram, G. N. Mahesh, R. G. Jeevan, and G. Radhakrishnan, "Comparative studies on short-chain and long-chain crosslinking in polyurethane networks," *Macromolecular Chemistry and Physics*, vol. 201, pp. 2799-2803, 2000.
- [138] H. S. Lee, Y. K. Wang, and S. L. Hsu, "Spectroscopic Analysis of Phase Separation Behavior of Model Polyurethanes," *Macromolecules*, vol. 20, pp. 2089-2095, 1987.
- [139] C. S. P. Sung, T. W. Smith, and N. H. Sung, "Properties of Segmented Polyether Poly(urethaneureas) Based on 2, 4-Toluene Diisocyanate. 2. Infrared and Mechanical Studies," *Macromolecules*, vol. 13, pp. 117-121, 1980.
- [140] C. S. P. Sung and N. S. Schneider, "Temperature Dependence of Hydrogen Bonding in Toluene Diisocyanate Based Polyurethane," *Macromolecules*, vol. 10, pp. 452-458, 1977.

- [141] C. B. Wang and S. L. Cooper, "Morphology and Properties of Segmented Polyether Polyurethaneureas," *Macromolecules*, vol. 16, pp. 775-786, 1983.
- [142] Z. Li and D. Li, "The Application of FTIR in Polyurethane Chemistry," *Elastomer (China)*, vol. 7, pp. 28-33, 1997.
- [143] N. Luo, D. Wang, and S. Ying, "Infrared Spectral Analysis of Hydrogen Bonding in Polyurethane," *China Synthetic Rubber Industry*, vol. 18, pp. 200-203, 1995.
- [144] Z. Chen, J. Cheng, W. P. Yang, and C. W. Macosko, "The Study of Important Spectrum Bands of Polyurethane and Polyurea by Transmission Spectra of Fourier Transform Infrared Spectroscopy," *Journal of Yantai University (Nature Science and Engineering)*, pp. 41-45, 1994.
- [145] M. Awkal, A. Jonquieres, R. Clement, and P. Lochon, "Synthesis and characterization of film-forming poly(urethaneimide) cationomers containing quaternary ammonium groups," *Polymer*, vol. 47, pp. 5724-5735, 2006.
- [146] R. Peck, C. Olsen, and J. Devore, *Introduction of Statistics and Data Analysis*. Calif.: Duxbury: Thomson Learning, 2001.
- [147] N. Nurdin, G. Helary, and G. Sauvet, "Biocidal Polymers Active by Contact. II. Biological Evaluation of Polyurethane Coatings with Pendant Quaternary Ammonium Salt," *Journal of Applied Polymer Science*, vol. 50, pp. 663-670, 1993.
- [148] R. V. Meyer, E. Haug, and G. Spilgies, "Sources of stretch," *Textile Asia*, pp. 40-45, 1994.
- [149] H. S. Lee, J. H. Ko, K. S. Song, and K. H. Choi, "Segmental and Chain Orientational Behavior of Spandex Fibers," *Journal of Polymer Science: Part B: Polymer Physics*, vol. 35, pp. 1821-1832, 1997.
- [150] R. W. Seymour, A. E. Allegrezza, Jr., and S. L. Cooper, "Segmental Orientation Studies of Block Polymers. I. Hydrogen Bonded Polyurethanes," *Macromolecules*, vol. 6, pp. 896-902, 1973.
- [151] C. M. Brunette, S. L. Hsu, and W. J. MacKnight, "Hydrogen-Bonding Properties of Hard-Segment Model Compounds in Polyurethane Block Copolymers," *Macromolecules*, vol. 15, pp. 71-77, 1982.
- [152] F. L. Ji, J. L. Hu, T. C. Li, and Y. W. Wong, "Morphology and shape memory effect of segmented polyurethanes. Part I: With crystalline reversible phase," *Polymer*, vol. 48, pp. 5133-5145, 2007.
- [153] R. W. Seymour and S. L. Cooper, "Thermal Analysis of Polyurethane Block Polymers," *Macromolecules*, vol. 16, pp. 48-53, 1973.
- [154] H. A. AL-SALAH, K. C. FRISCH, H. X. XIAO, J. A. McLEAN, and JR., "Polyurethane Aniomomers. I. Structure Properties of Polyurethane

Anionomers," *Journal of Polymer Science: Part A: Polymer Chemistry*, vol. 25, pp. 2127-2137, 1987.

[155] X. Wei and X. H. Yu, "Synthesis and Properties of Sulfonated Polyurethane Ionomers with Anions in the Polyether Soft Segments," *Journal of Polymer Science: Part B: Polymer Physics*, vol. 35, pp. 225-232, 1997.

[156] L. Li and W. H. d. Jeu, "Shear-Induced Smectic Ordering as a Precursor of Crystallization in Isotactic Polypropylene," *Macromolecules*, vol. 36, pp. 4862-4867, 2003.

[157] R. W. Rees and D. J. Vaughan, ""SURLYN" A IONOMERS. I. THE EFFECT OF IONIC BONDING ON POLYMER STRUCTURE," *Polymeric Preprints (American Chemical Society, Division of Polymer Chemistry)*, vol. 4, pp. 287-295, 1965.

[158] T. F. Yang, D. J. Chen, and Y. J. Li, "Structure and Property of Melt-Spinning Spandex," *Journal of Textile Research*, vol. 21, pp. 29-31, 2000.